An investigation of the combined stable isotopic composition of methane emissions from northern wetlands

Thesis

An Investigation of the Combined Stable Isotopic Composition of Methane Emissions from Northern Wetlands

by

Sarah May Jackson B.Sc.(Hons.), M.Sc.

A thesis submitted for the degree of

Doctor of Philosophy

September 1998

Planetary Sciences Research Institute

The Open University

Abstract

Methane is a radiatively active, naturally occurring atmospheric trace gas which is thought to account for as much as 19% of the enhanced greenhouse effect. Ice core studies have shown that the atmospheric concentration has more than doubled since pre-industrial times. Wetlands are the largest natural source of atmospheric methane, contributing around 21% of the annual global flux. The magnitude of various sources of methane is still poorly defined. Stable isotope measurements are increasingly being used to constrain global budgets of atmospheric trace gases because isotopic analysis provides a much clearer picture of global atmospheric chemistry than CH_4 concentration measurements alone. Conventional analytical techniques for studying dual stable isotopic composition of methane ($\delta^{13}C$ and δD) require prohibitively large quantities of CH_4 for analysis.

At the Planetary Sciences Research Institute of the Open University, a highly sensitive static mass spectrometer has been developed which uniquely uses CH_4 as the analyte. The method requires only 8 ng of CH_4 for analysis (<10 ml ambient air), making replicated measurements of the isotopic composition of CH_4 emissions from wetlands feasible for the first time.

Methane emissions from an ombrotrophic mire in Snowdonia have been measured over 2 years, (1995-1997) and analysed for $\delta^{17}M$. Parallel laboratory studies have also been conducted, to constrain the effects of environmental variables such as peat temperature and water table depth. The presence of vascular plants enhanced methane flux. In the field, methane flux showed seasonal variation. Peat temperature and water table depth could account for 68% of this variation.

The isotopic composition of methane flux from the ombrotrophic mire also exhibited seasonal variation, with $\delta^{17}M$ ranging from -34 to -17‰. The lowest values were observed in summer and the highest in winter. Variations in the isotopic composition of peat water are unlikely to account for more than a 2‰ shift in $\delta^{17}M$. Although there was a strong correlation between peat temperature and methane isotopic composition in the field, peat temperature is thought to be an indirect effect, because in laboratory studies this relationship was absent. There was no relationship between water table depth and $\delta^{17}M$. It was concluded that the seasonal variation in the isotopic composition of methane emission is linked to the plant growth cycle. Comparison of $\delta^{17}M$ values determined for methane emissions in Snowdonia with published $\delta^{13}C$ and δD data leads to the conclusion that methane is produced mainly by CO_2 reduction.

Contrasting terrains in a palsa mire in the Arctic region of Finland exhibited methane emissions with distinct $\delta^{17}M$ values: lakes, +4.8 ±1.2‰; pools, -3.9 ±0.1‰ and hummocks, -28.6 ±5.8‰. From these isotope data it was concluded that in pool and lake sediments the methanogenic pathway is acetate fermentation, while in hummocks methane is produced by CO_2 reduction.

This study is the first investigation of the stable isotopic composition of methane emissions from wetlands in the UK. The data collected in Snowdonia, and in Finland, show the need for systematic, year round isotopic analysis of methane emissions, if isotope data are to be used in constraining the global methane budget.

Acknowledgements

First and foremost, I wish to express my gratitude to Prof. Colin Pillinger, for providing the opportunity to do this research within the Planetary Sciences Research Institute. Thanks also to my other supervisor, Dr. Nancy Dise, for her input into this work.

I am indebted to Dr. Geraint Morgan and Dr. Andy Morse for the benefit of their wisdom, their infinite patience, encouragement and unstinting advice, especially in the laboratory. Thanks also to Dr. Anna Butterworth for instructing me in the ways of MIRANDA.

Thanks must also go to the following people:
Prof. Lee and Dr. Press for permitting me to use the University of Sheffield field site at the Migneint,
Prof. David Fowler and Dr. Ken Hargreaves for allowing me to join their field trip to Jänkäjärvi, Finland in June 1997, and
Dr. Phil Ineson and Mr. Dylan Williams for access to laboratory facilities at ITE, Merlewood; and for bringing their mobile laboratory to the Migneint.

I must also thank Prof. Tony Fallick and Dr. Andrew Bristow, who both kindly analysed samples for me.

I am most grateful to the following people who braved the elements at the Migneint to be my field assistant. Some got soaked, others froze or were blown away and just one got sunburnt!

Simeon Barber	David Beesley	Iain Berry	Clare Dickinson
Nancy Dise	Vince Gauci	Rhino George	Olive & David Hardy
Michelle Higgins	Sophie Jowett	Liz Kennedy	Adam Mac
Taff Morgan	Andy Morse	Tubbs Thornton	Jane Wares

and last, but by no means least, my mum!

The NERC TIGER programme is gratefully acknowledged for funding the studentship, and for providing extra funding for the fieldwork campaigns.

And finally, I must express my sincere gratitude to Michelle and Jackie who, out of the kindness of their hearts, proof-read the final draft of this thesis.

Rain

It rained and it rained and rained and rained
The average fall was well maintained
And when the tracks were simply bogs
It started raining cats and dogs.

After a drought of half an hour
We had a most refreshing shower
And then the most curious thing of all
A gentle rain began to fall.

Next day was also fairly dry
Save for the deluge from the sky
Which wetted the party to the skin
After that the rain set in.

Anon.

The anonymous writer of this poem was clearly
familiar with my field site at the Migneint in Snowdonia!

Contents

Chapter Two

Analysis Techniques for Determining the Size and Isotopic Composition of Methane Emissions 49

Chapter Three

Combined Isotopic Composition of Methane Emissions from an Ombrotrophic Mire 83

Chapter Four

Chapter Five

List of Figures

List of Tables

Atmospheric Methane in the Global Context

1. Introduction

The presence of methane in the Earth's atmosphere was first identified from infrared absorption features in the solar spectrum (Migeotte, 1948). Methane is a radiatively active atmospheric trace gas that plays an important rôle in the "enhanced greenhouse effect" and the oxidative capacity of the troposphere (Logan *et al.*, 1981).

Air extracted from ice-cores clearly show that the concentration of methane in the atmosphere has doubled since pre-industrial times (Etheridge *et al.*, 1988). The present atmospheric burden of CH_4 is estimated to be 4900 Tg (1 Tg = 10^{12} g), or 1.73 ppmV (IPCC, 1994).

There are many varied sources of methane, both natural and anthropogenic. About 510 Tg of methane is added to the atmosphere each year. Approximately 22%

of this is believed to come from wetland sources (Prather *et al.*, 1995). Methane is produced in wetlands by microbial activity under anaerobic conditions. It is the terminal step of organic matter degradation. Uncertainties exist in the estimates of methane emissions due to a lack of understanding of the processes involved in methane production, consumption and transport through the ecosystem.

There are a number of techniques available for measuring the flux rates from wetlands, ranging in scale from meters to hundreds of kilometres. Increasingly, stable isotopes are being used to help distinguish between the sources of methane, and to determine the specific processes involved.

1.1 The Earth's Atmosphere

1.1.1 The Greenhouse Effect

The radiation balance of the Earth's atmosphere is determined by comparing the incoming solar radiation and the outgoing thermal radiation. Incoming solar radiation averages about 343 Wm^{-2} (IPCC, 1994). Some of this energy is reflected by the surface and by the atmosphere. The Earth also radiates thermal energy itself. The incoming and outgoing radiation fluxes must balance if the Earth's temperature is to remain constant. Assuming for simplicity that the atmosphere did not absorb any energy, the radiation balance would result in a mean surface temperature of -17 °C. As the average surface temperature is about 15 °C, the atmosphere is clearly having a warming effect (Wayne, 1992).

The radiation budget for the atmosphere is given in Figure 1.1, demonstrating how incoming flux is balanced by outgoing flux. It is clear that any changes in the atmosphere that affect the balance of the solar energy cycle may also cause changes in the Earth's temperature and climate.

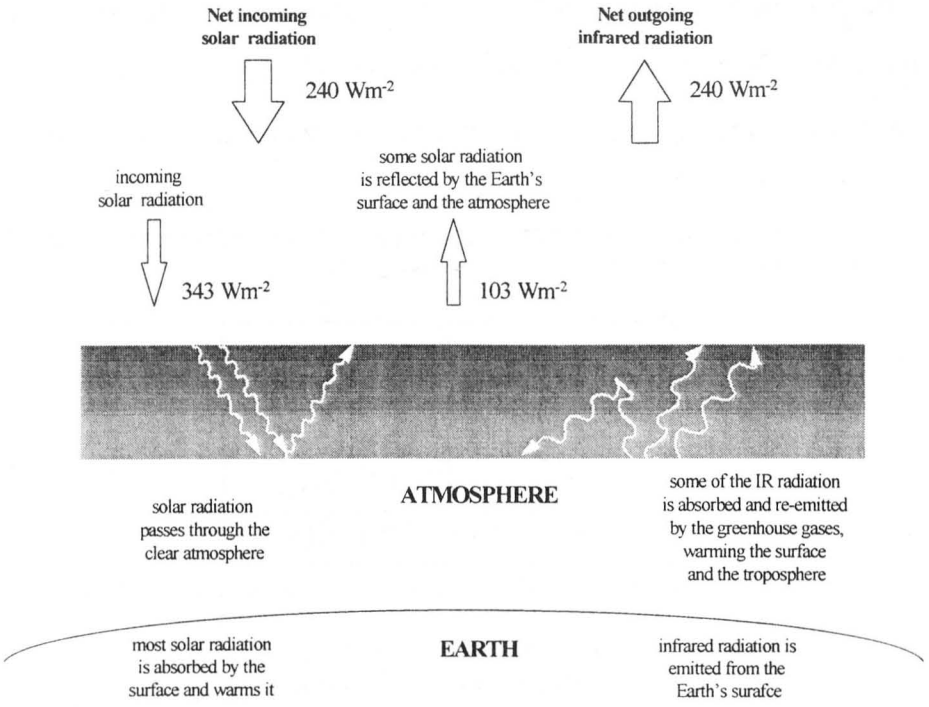

Figure 1.1 Radiation budget for the Earth's atmosphere (IPCC, 1994).

1.1.2 The Enhanced Greenhouse Effect

The natural greenhouse effect is primarily due to the gaseous water and carbon dioxide present in the atmosphere at their natural abundance. The amount of water vapour in the troposphere depends mainly on the temperature of the surface of the ocean and is not influenced directly by human activity.

The concentration of CO_2 in the atmosphere, on the other hand has changed substantially since the Industrial Revolution, due to anthropogenic activity. Analysis of air trapped in ice cores shows that the pre-industrial atmospheric concentration of CO_2 was 280 ppmV (Neftel *et al.*, 1985; Friedli *et al.*, 1986; Pearman *et al.*, 1986). Modern day levels are now 356 ppmV (IPCC, 1994) and rising. The radiative forcing due to this increase is estimated to be 1.56 Wm^{-2} (IPCC, 1994). It is also estimated that without controls on anthropogenic emissions of carbon dioxide, levels could double in the next 100 years. Exactly what the resultant climate change effect will be is a subject of intense debate and will be addressed in Section 1.1.3.

The greenhouse gases which are directly influenced by human activities are carbon dioxide, methane, the chlorofluorocarbons (CFCs), nitrous oxide, NO_x gases and ozone. The concentrations of some greenhouse gases are given in Table 1.1.

Table 1.1 Greenhouse gases and their concentrations in the atmosphere (IPCC, 1992).

Gas	Atmospheric concentration
CO_2	356 ppmV
CH_4	1.72 ppmV
N_2O	310 ppbV

It is clear from the global monitoring of the atmosphere and its constituents by the National Oceanic and Atmospheric Administration (NOAA) network that there is a continued rise in the concentrations of CO_2, CH_4 and N_2O (IPCC, 1995; Simmonds *et al.*, 1996). This is cause for some concern due to the impact the gases might have on the global climate in the long term. However, with the exception of CFC-12 (dichlorofluoromethane), all the major man-made halocarbons have stopped increasing in the atmosphere and are now steadily declining (Simmonds *et al.*, 1996). This is a direct consequence of a reductions in emissions due to the Montreal Protocol and its amendments (World Meteorological Organisation, 1988).

1.1.3 Climate Change Models

Increasing levels of greenhouse gases in the atmosphere will result in increased absorption of infrared (IR) radiation, and subsequent disruption of the Earth's thermal radiative balance. Development of numerical models of the global climate gives rise to better understanding and greater accuracy in the prediction of future climate changes. Such models incorporate mathematical representations of the interactions of all climate system components, (atmosphere, ocean, sea ice, continental and ice surfaces (IPCC, 1992)). Most advanced is the atmospheric part of these global

models, the so-called general circulation model (GCM) of the atmosphere. Early work on GCMs started in the late 1950s and there are now 30 to 40 models being worked on around the world. These are being used for a range of climate studies and are increasingly being systematically compared. However there is still debate how much climate change we can expect in the future, and which parts of the world will be most affected.

It has been claimed that global warming in the past century is beyond dispute, although the precise amount is not (Parker *et al.*, 1994). However, actual warming doesn't follow the pattern predicted by climate change models (Michaels, 1990); and models are unable to simulate the *current* climate of Antarctica particularly well (Genthon, 1994). Discrepancies between reality and climate change models may occur for a number of reasons:

- it has been suggested that development of the models is limited by computing power (Trenberth, 1997),
- there is a lack of observational data to use in the models (Genthon, 1994), and
- there may be lack of understanding of the importance of some parameters. For example, the effects of change in land use have been omitted from models; and there is great uncertainty in the treatment of clouds (Trenberth, 1997). Revision of the United Kingdom Meteorological Office (UKMO) model to use a more realistic cloud parameterisation had a profound effect on the outcome of the model. The projected mean global warming that would be caused by a doubling of the atmospheric CO_2 concentration then dropped from 5.5 to 2.7 °C (Mitchell, 1989).

1.2 Methane

1.2.1 Chemistry of Methane in the Atmosphere

a) Contribution to Global Warming

Although the atmospheric concentration of methane is much lower than that of carbon dioxide (1.7 ppmV compared to 350 ppmV for CO_2), it accounts for a large proportion of enhanced global warming. Most researchers agree that CH_4 is the most important greenhouse gas after CO_2 and water vapour. It is thought to account for <3% of the total greenhouse effect (Lelieveld *et al.*, 1993) and between 15 to 19% of the enhanced greenhouse effect (Bouwman, 1990; Badr *et al.*, 1991a; Prather *et al.*, 1995).

b) Global Warming Potential

The first Intergovernmental Panel on Climate Change (IPCC) Scientific Assessment highlighted the need for providing policymakers with an index which defines the warming effect of each greenhouse gas relative to that of carbon dioxide (Derwent, 1994). This is known as the global warming potential (GWP). The contribution of a trace gas to global warming will depend on a number of factors such as its IR absorption properties, its lifetime in the atmosphere, the change in its atmospheric concentration, and its influence on the concentrations of other greenhouse gases.

There is some dispute over the global warming potential of methane. Lelieveld *et al.* (1993) showed, using a hemispherical 1-D model, that methane has a global warming potential (GWP) of 7.5 times that of carbon dioxide mole for mole over a 100 year integration. However, over a 10 year integration period the GWP for methane is actually 26.9 times greater than CO_2. It is claimed that this difference arises from the fact that the life time of CH_4 in the atmosphere is between 5-20 times shorter than that of CO_2.

In light of the uncertainties in the atmospheric life spans of the major greenhouse gases, Harvey (1993) proposed an alternative GWP index which is tied to investment decision. Derwent (1994) acknowledged the shortcomings of the original GWP formulation and proposed a modified calculation which takes into account a sustained emission scenario over a 100 year life time. Methane has a GWP of 17 by this new estimation, compared to 11 by the earlier method. The IPCC 1994 report considered both direct and indirect effects of methane releases and gives the following GWPs: 7.5 over 500 years, 24.5 over 100 years and 62 over 20 years, (that is: CH_4 has 62 times the global warming potential of CO_2 molecule for molecule). Badr *et al.* (1991a) gave a more comprehensive list of GWP estimates for CH_4.

c) Life Time of Methane in the Atmosphere

Some of the discrepancy in the GWP arises from the uncertainty in the lifetime of methane in the atmosphere. The IPCC report (IPCC, 1994) now chooses to take into account the effect of the methane pulse during its own lifetime, giving an adjustment time of 14.5 ± 2.5 years. Other estimates of the lifetime of CH_4 in the atmosphere only consider the direct effects of methane and are therefore lower, ranging from 7 to 11 years (Cicerone and Oremland, 1988; Pearman and Fraser, 1988; Lelieveld and Crutzen, 1993; Derwent, 1994).

d) Atmospheric Chemistry

About half the contribution of methane to the greenhouse effect is due to its ability to absorb long-wave radiation emitted from the Earth's surface in the 4-100 μm atmospheric window, directly affecting the atmospheric temperature (Lacis *et al.*, 1981; Hansen *et al.*, 1988; Ramanathan, 1988). The other half arises because of its rôle in the overall chemistry of the atmosphere.

Methane influences the abundance of ozone in both the troposphere and the stratosphere (Johnston, 1984) and it has long been known that CH_4 oxidation is a major source of stratospheric water (Nicolet, 1964; Pollock *et al.*, 1980), thus

indirectly affecting the temperature through its chemical reactions. Once in the atmosphere, most methane is destroyed by reaction with the hydroxyl radical ($OH^{\bullet}$) but ~ 10% enters the stratosphere where it can undergo several destructive reactions (Cicerone and Oremland, 1988). It is through its reaction with $OH^{\bullet}$ that methane affects the tropospheric concentration of O_3, $OH^{\bullet}$ and CO.

The hydroxyl radical required to initiate the oxidation of CH_4 is produced *via* the photolysis of ozone by short wave length (< 310 nm) solar UV radiation.

$$O_3 + h\nu \rightarrow O^*(^1D) + O_2 \qquad \text{Equation 1.1}$$

The resulting excited oxygen atom then reacts with water vapour to form the $OH^{\bullet}$:

$$O^*(^1D) + H_2O \rightarrow 2OH^{\bullet} \qquad \text{Equation 1.2}$$

The exact progression of methane oxidation by the hydroxyl radical depends upon the environmental conditions; the sequence of reactions are different at high and low atmospheric NO_x concentrations:

$$CH_4 + OH^{\bullet} \rightarrow CH_3^{\bullet} + H_2O \qquad \text{Equation 1.3}$$

$$CH_3^{\bullet} + O_2 + M \rightarrow CH_3O_2^{\bullet} + M \qquad \text{Equation 1.4}$$

High NO concentration (> 10 ppt NO):

$$CH_3O_2^{\bullet} + NO \rightarrow CH_3O^{\bullet} + NO_2 \qquad \text{Equation 1.5}$$

$$CH_3O^{\bullet} + O_2 \rightarrow HCHO + HO_2^{\bullet} \qquad \text{Equation 1.6}$$

$$HO_2^{\bullet} + NO \rightarrow OH^{\bullet} + NO_2 \qquad \text{Equation 1.7}$$

$$2[NO_2 + h\nu \rightarrow NO + O^{\bullet}] \qquad \text{Equation 1.8}$$

$$2[O^{\bullet} + O_2 + M \rightarrow O_3 + M] \qquad \text{Equation 1.9}$$

$$\textit{net}: \; CH_4 + 4O_2 \rightarrow HCHO + 2O_3 + H_2O \qquad \text{Equation 1.10}$$

Low NO concentration (< 10 ppt NO):

$$CH_3O_2\bullet + HO_2^{\bullet} \rightarrow CH_3O_2H + O_2 \qquad \text{Equation 1.11}$$

$$CH_3O_2H + h\nu \rightarrow CH_3O^{\bullet} + OH^{\bullet} \qquad \text{Equation 1.12}$$

$$CH_3O^{\bullet} + O_2 \rightarrow HCHO + HO_2^{\bullet} \qquad \text{Equation 1.13}$$

$$\textit{net}: \; CH_4 + O_2 \rightarrow HCHO + H_2O \qquad \text{Equation 1.14}$$

The next stage of the reaction, the oxidation of HCHO is the same regardless of NO concentration:

$$HCHO + h\nu \rightarrow H^{\bullet} + HCO^{\bullet} \qquad \text{Equation 1.15}$$

$$H^{\bullet} + O_2 + M \rightarrow HO_2^{\bullet} \qquad \text{Equation 1.16}$$

or:
$$HCHO + OH^{\bullet} \rightarrow H_2O + HCO^{\bullet} \qquad \text{Equation 1.17}$$

then:
$$HCO^{\bullet} + O_2 \rightarrow CO + HO_2^{\bullet} \qquad \text{Equation 1.18}$$

Thus, it can be seen that the oxidation of methane constitutes an important source of atmospheric carbon monoxide. As much as 46% of atmospheric CO may derive from the destruction of methane in the atmosphere (Wofsy, 1976). Carbon monoxide is subsequently oxidised to carbon dioxide, initially by reaction with the $OH^{\bullet}$ radical:

$$CO + OH^{\bullet} \rightarrow CO_2 + H^{\bullet} \qquad \text{Equation 1.19}$$

Hence, in regions containing high levels of NO_x, *e.g.* around industrial centres, the overall oxidation of CH_4 *via* CO to CO_2 results in a *net production* of ozone and OH radicals. In the absence of NO_x, *e.g.* over the tropics, away from anthropogenic pollution sources, a *net loss* of ozone and $OH^{\bullet}$ may occur. Ozone in the troposphere absorbs IR radiation and thus contributes to the enhanced greenhouse effect.

In the stratosphere methane can react with Cl atoms as follows:

$$CH_4 + Cl^{\bullet} \rightarrow {}^{\bullet}CH_3 + HCl \qquad \text{Equation 1.20}$$

which is important because it sequesters Cl atoms that would otherwise destroy stratospheric ozone, converting them to HCl which is inactive towards ozone (Cicerone and Oremland, 1988). In the stratosphere, ozone absorbs UV radiation.

A more comprehensive account of the atmospheric chemistry of methane can be found in Crutzen (1995), Crutzen (1993), Badr *et al.* (1992a), Wayne (1992), Bouwman (1990) and Wofsy (1976).

1.2.2 Global Budgets

The current (1996) global average atmospheric methane concentration is 1.73 ppmV (Dlugokencky, NOAA, *pers. comm.*), which represents an atmospheric reservoir of about 4900 Tg. Analysis of gases trapped in dated ice-cores shows that atmospheric methane has more than doubled in the last 200 years (Craig and Chou, 1982; Rasmussen and Khalil, 1984; Pearman *et al.*, 1986) (Figure 1.2). The concentration of atmospheric CH_4 ranged between 0.6 and 0.8 ppmV over the previous 3,000 years (Cicerone and Oremland, 1988; Chappellaz *et al.*, 1994). In the last one hundred years the increase in the atmospheric concentration has been highly correlated with global human population (Houghton, 1994). Rinsland (1985) and Zander (1989) have used infrared solar spectra to show that the atmospheric concentration of methane has increased by about 30% in the last 40 years.

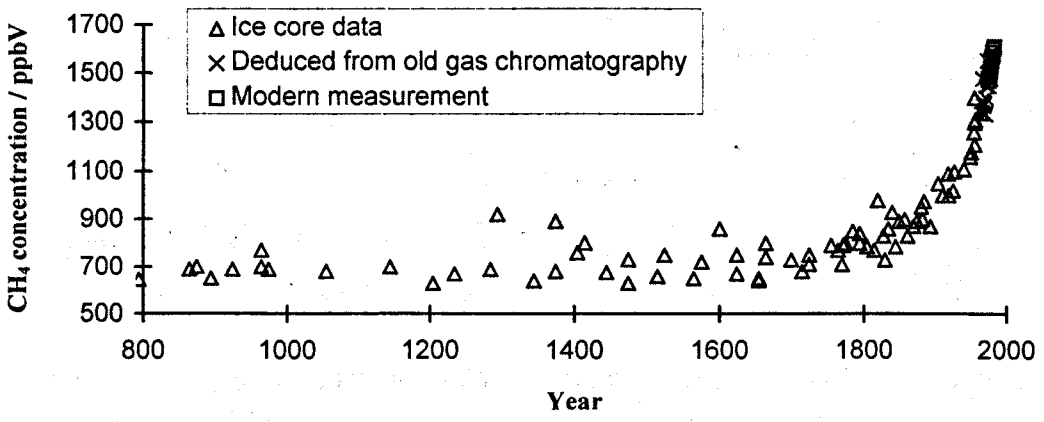

Figure 1.2 Methane concentration in the atmosphere from dated ice cores and modern measurements (data from Badr *et al.*, 1992a).

Direct measurements of atmospheric concentrations of CH_4 began in 1978 when the global average value was 1.51 ppmV (Rasmussen and Khalil, 1981). Since that time the National Oceanic and Atmospheric Administration/Climate Monitoring and Diagnostics Laboratory (NOAA/CMDL) co-operative air sampling network has been extended to cover 35 remote locations around the globe, ranging from 82 °N to 90 °S. A comprehensive data set for the years 1985 to 1992 for individual sites is given in Dlugokencky *et al.* (1994a). Corresponding data for global average values is given in Dlugokencky *et al.* (1994b). Data are also available on the NOAA/CMDL website: www.cmdl.noaa.gov .

The global average methane concentration in the atmosphere increased from 1.51 ppmV in 1978 to 1.73 in 1996, but this increase has not been uniform. From 1978 to 1980 there were large annual increases of 2 to 3% (Rasmussen and Khalil, 1981; Blake *et al.*, 1982). The annual rate of increase throughout the 1980s was reported to be between 1.2 and 1.4% (Fraser *et al.*, 1984; Blake and Rowland, 1986; Blake and Rowland, 1988). Shorter term analysis showed that for 1983-5 the growth rate was only 0.78% (Steele *et al.*, 1987).

Although the atmospheric CH_4 burden continues to grow, the overall rate of increase has slowed. The average increase has been estimated to be about 0.5% yr^{-1} for 1984-1996 (Dlugokencky *et al.*, 1998). However, this average masks a sudden decline in the rate of increase seen in 1992 (Dlugokencky *et al.*, 1994c). Current estimates predict that the concentration of CH_4 in the atmosphere will stabilise in the next two decades (Steele *et al.*, 1992; Dlugokencky, 1998).

Closer to home, Simmonds *et al.* (1996) report data collected from Mace Head in Ireland (a NOAA/CMDL sampling network site) from 1987 to 1994. Over the 8 year period, the level of methane increased by 7.2 ppbV yr^{-1}, or less than 0.5 % annually. The overall trend of global decline in growth rates remains an issue of some conjecture. Suggestions include:

- a decrease in CH_4 emissions from fossils fuels in Eastern Europe and the former Soviet Union and improved environmental controls on existing fuel use, transport and waste products (Dlugokencky *et al.*, 1994c; Rudolph, 1994);
- decreased methane emissions from temperature-dependent northern wetlands due to surface temperature decreases associated with the eruption of Mount Pinatubo in 1991 (Dlugokencky *et al.*, 1994c), although this can't account for the slowing of the growth rate in the late 1980s;
- a reduction in biomass burning (Lowe *et al.*, 1994; Rudolph, 1994) and
- an increase in the $OH^{\bullet}$ radical concentration because of increased UV radiation (Bekki *et al.*, 1994) as a result of ozone depletion (Gleason *et al.*, 1993). Isotopic data and model calculations indicate this last suggestion, however, is unlikely (Gupta *et al.*, 1996).

It is important to understand the driving force behind these trends because it is unlikely that control strategies would be able to guarantee such a rapid reduction in growth rate as that seen here without the benefit of legislative intervention (Khalil and Rasmussen, 1994).

a) Inter-hemispheric Difference and Seasonal Cycles.

The methane concentration in the atmosphere varies strongly with latitude, being the highest in the northern half (above about 50 ^{o}N) of the Northern Hemisphere, and lowest in the Antarctic. This latitudinal gradient is now well documented (Khalil and Rasmussen, 1983; Rasmussen and Khalil, 1984; Steele *et al.*, 1987; Blake and Rowland, 1988; Steele *et al.*, 1992; Dlugokencky *et al.*, 1994d). There is an annual mean difference of about 140 ppbV between the northernmost and southernmost sampling sites in the NOAA/CMDL co-operative air-sampling network. This arises because the major methane sources are predominantly in the Northern Hemisphere. The tropics are also a major source of atmospheric CH_4, but the production of $OH^{\bullet}$, which destroys methane, is also high in that region. Northern

sources are less balanced by sinks so the net effect is a build-up of methane in high northern latitudes, with a strong southward transfer. Figure 1.3 shows the global distribution of methane where seasonal cycles are also apparent.

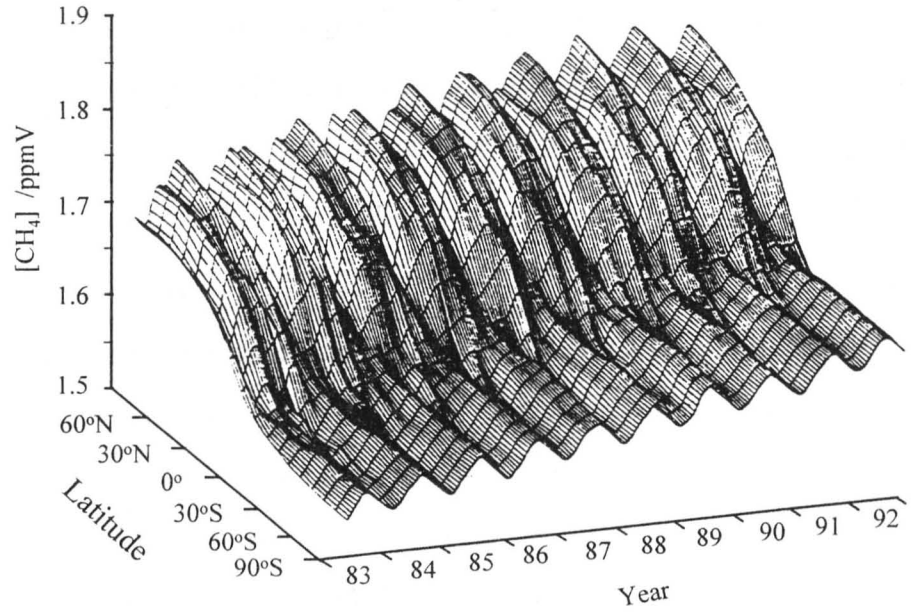

Figure 1.3 Global distribution of methane in the marine boundary layer (smoothed and zonally averaged, grid spacing is 10° latitude by 2 weeks) (adapted from Dlugokencky *et al.*, 1994d).

Methane levels exhibit a strong seasonal fluctuation. Comprehensive data sets for many sampling sites in the NOAA air sampling network show these trends clearly (Steele *et al.*, 1987; Dlugokencky *et al.*, 1994a).

Khalil and Rasmussen (1983) found 25-34 ppbV less CH_4 in the atmosphere of the Northern Hemisphere during the summer compared to the rest of the year, and that the methane concentration rapidly rose to an annual maximum in the autumn. The lowest point of the Southern Hemisphere seasonal cycle was seen in late Australian summer and autumn, 14 ppbV lower than the rest of the year. They concluded that the rapid rise of CH_4 concentration during the autumn in the Northern Hemisphere was the result of a large autumnal source at latitudes above 30°N; and the rest of the observed seasonal cycle was consistent with the seasonal cycle of $OH^{\bullet}$.

These findings are in keeping with the more recent work of Dlugokencky et al. (1994d), who found a relatively simple seasonal cycle in the high southern latitudes, with a minimum in the late summer-early autumn, which they believed to be dominated by the seasonal cycle of the photochemical destruction of CH_4. They do however report a seasonal cycle amplitude of about 30 ppbV, and twice that in the high north. They speculated that seasonal cycles at sites in the Northern Hemisphere are more complex than those in the Southern Hemisphere due to the interaction between CH_4 sources, sinks and atmospheric transport (see Table 1.2).

Figure 1.4 shows the seasonal cycle in atmospheric methane at Mace Head in Ireland, which is the closest NOAA sampling site to the location of the work carried out in this project.

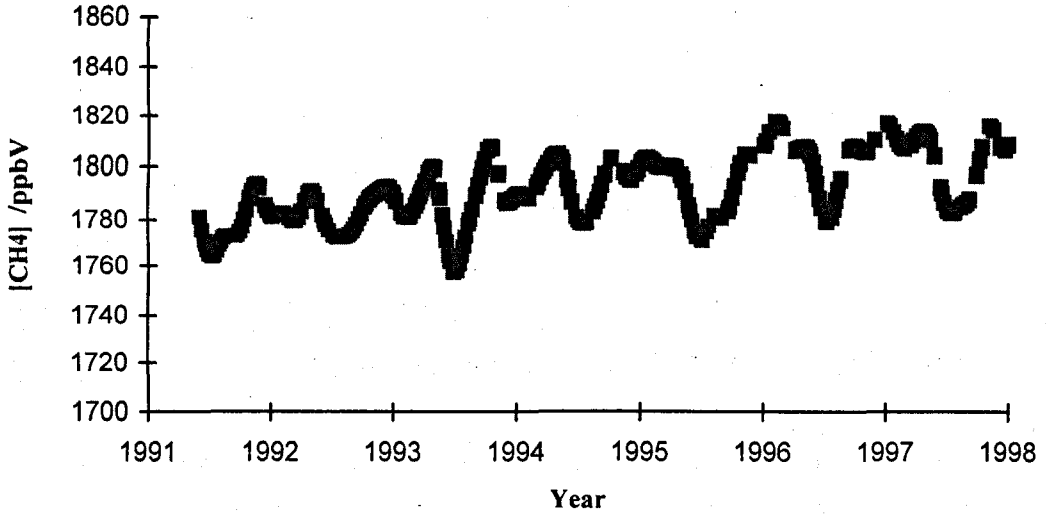

Figure 1.4 The seasonal cycle of methane in the atmosphere at Mace Head in Ireland (data from the NOAA/CMDL co-operative air sampling network Dlugokencky, *pers. comm.*, 1998).

b) Sources

The increase in atmospheric methane concentration is believed to derive from an anthropogenic increase in terrestrial production of CH_4 (IPCC, 1992). Houghton (1994) stated that unless anthropogenic emissions are reduced the atmospheric CH_4

concentration will continue to rise in tandem with increases in the world population. He argued that as United Nations estimates show that the world population will double in the next century, we can also expect to see a doubling of the enhanced greenhouse effect due to CH_4.

As methane has a short life time in the atmosphere, MacKenzie (1994) claimed that cutting current methane emissions by 10% would stabilise atmospheric CH_4 at present concentrations. This supports the view of Lelieveld and Crutzen (1993); although Badr *et al.* (1992a) estimated that a reduction of 20% of anthropogenic emissions is needed. In contrast, the IPCC (1995) summary for policymakers estimated that an 8% reduction in anthropogenic sources would stabilise atmospheric CH_4 concentrations at today's levels. These differences of opinion presumably arise due to uncertainties in the life time of methane in the atmosphere, and the relative contributions of the various global sources. In view of the slowing down of the growth rate of methane in the atmosphere, the IPCC estimate is possibly the more realistic in terms of policy-making.

There is still great uncertainty regarding methane source strengths, because figures are often obtained by extrapolating a few site-specific methane flux measurements up to global scales (Quay *et al.*, 1991). In recent years, however, there have been research and monitoring campaigns conducted on a global scale which should give a clearer picture in the future.

Two of the earliest determinations of the global source strengths came from Sheppard *et al.* (1982) and Khalil and Rasmussen, (1983). Their results are given in Table 1.2, along with other estimates. Sheppard and his co-workers suggested a total annual global methane emission of 1210 Tg. In the light of subsequent work, it appears that this was an over-estimation, probably arising from an over-estimate in CH_4 emissions from natural wetlands. Khalil and Rasmussen estimated a total global emission of 553 Tg for 1978. This figure is supported by studies on the sinks of methane. If the magnitude of the methane sink in the atmosphere is known, and the

increase in the atmospheric burden is known, the size of the emissions can be calculated. (Section 1.2.3.)

Table 1.2 Major global sources of methane. (Figures are in Tg CH_4 yr^{-1}, numbers in brackets indicate the possible range of the flux).

Source	Sheppard *et al.* (1982)	Khalil & Rasmussen (1983)	Cicerone & Oremland (1988)	IPCC (1992)	Lelieveld & Crutzen (1993)
Natural Wetlands	772	162	115 (100-200)	115 (100-200)	125 ±70
Rice Paddies	39	95	110 (60-170)	110 (25-170)	70 ±50
Enteric Fermentation	70	120	80 (65-100)	80 (65-100)	80 ±20
Fossil Fuel Production	100	-	80 (50-95)	80 (44-100)	115 ±35
Biomass Burning	60	25	55 (50-100)	40 (20-80)	30 ±15
Termites	-	-	40 (10-100)	40 (10-100)	30 ±30
Landfills	50	-	40 (30-70)	40 (20-70)	40 ±25
Oceans & Freshwater	54	23	15 (6-45)	15 (6-45)	15 ±10
CH_4 Hydrate Destabilisation	-	-	5 (0-100)	5 (0-100)	5 ±5
Other	65	128	-	-	50 ±10
TOTAL	1210	553	540 (400-640)	525 (400-600)	560 ±90

Graedel et al. (1993) provided a comprehensive list of published global methane inventories. The IPCC (1992) report is most often quoted, as the numbers in that data set are drawn from many expert sources. Each source still has a large uncertainty attached to it (Table 1.2). Much of this uncertainty arises from the extrapolation of small scale flux measurements into global estimates. Whilst, however, the extrapolation of "flower pot" experiments to global estimates is not highly accurate, it does at least provide order-of-magnitude estimates (Aselmann, 1989). In fact, the global budgets of methane presented in the literature have greater

uncertainty ranges than allowed by the constraints on its global cycle (Kandlikar and McRae, 1995).

If the world human population continues to grow, there will be an corresponding increase in methane emissions from such sources as rice paddies, and enteric fermentation by domestic animals. If standards of living improve globally, emissions from landfills may also increase. Socio-economic factors, therefore, also play a part in global methane emissions. Badr *et al.* (1991b) estimated that 50% of present sources are controlled by man. More recently, Lelieveld and Crutzen (1993) estimated that about 70% of total methane emissions are due to anthropogenic activities. Uncertainties in source strengths are the most likely cause of these differences of opinion.

Despite the uncertainties in the global methane budget, it is likely that about 50% of the emissions come from wetlands, rice paddies and animals. The methane is produced by specialised bacteria during anaerobic fermentation. Bacterial methane is also released by landfills and termites. Non-bacterial methane is released in the production and transportation of fossil fuels (gas drilling and coal mining), and also from incomplete combustion during biomass burning.

Natural wetlands are probably the single largest source of methane, accounting for almost 22% of global emissions, or 115 Tg CH_4 yr^{-1}. Two studies have made estimates of the area of wetlands around the world, Matthews and Fung (1987) and Aselmann and Crutzen (1989). Although both agreed on the total flux, there are a number of differences in their calculations (see Section 1.3.1 for a detailed analysis).

Rice paddies are a further large source of methane. Estimates range from 25 - 70 Tg CH_4 yr^{-1} (Cicerone and Shetter, 1981; Holzapfel-Pschorn *et al.*, 1985; Yagi *et al.*, 1996). Mudge and Adger (1995) estimated emissions of about 96 Tg CH_4 yr^{-1}, based on 1991 rice production data. Minami (1994) gave an excellent review of published data on methane emissions from rice paddies. Dlugokencky *et al.* (1993) used a 3-D atmospheric chemistry model to analyse data from weekly air samples

collected at Tae-ahn Peninsula, Korea; the relative maximum CH_4 mixing ratio in May and June constrains the global methane emission from rice cultivation to ~ 100 Tg yr^{-1}. A major difficulty in obtaining accurate estimates arises from the fact that 90% of rice paddies are in Asia, and detailed data are sparse. As rice production is an anthropogenic source, various suggestions have been put forward for potential mitigation strategies (Minami, 1994; Mudge and Adger, 1995). Emissions from rice paddies depend on several factors, including water management practices, application of fertilisers and manure, soil properties and time of season.

Enteric fermentation in ruminant animals yields a global CH_4 flux of about 80 Tg yr^{-1} (IPCC, 1992). Methane emissions depend upon animal population sizes and the nature of their diet. Although numbers of domestic animals have increased over the last century in line with population increases, this is partly off set by the decrease in wild ruminants.

Termites as a source of methane has been under investigation for many years (Zimmerman *et al.*, 1982). Current flux estimates range from 10 to 100 Tg CH_4 yr^{-1}. There are great difficulties associated with the methodology involved in laboratory experiments because of changes in metabolic rate (Tyler, 1989). Species and diet play a part in the size of the methane flux. It is also difficult to estimate the global termite population.

Using isotope mass balance calculations, ($\delta^{13}C$ and ^{14}C) (Section 1.3) biomass burning has been estimated to account for about 11% of total methane release (Quay *et al.*, 1991). This broadly agrees with other estimates of biomass burning, *e.g.* Cicerone and Oremland (1988).

Early estimates suggest that less than 10% of global CH_4 emissions derive from a fossil methane source (Sheppard *et al.*, 1982). More recent studies use carbon-14 to assess the contribution of fossil fuel methane to the global budget. Fossil CH_4 from gas drilling, coal mining and, possibly, seepage of natural gas is free of ^{14}C, while bacterial methane contains more or less contemporary ^{14}C. Wahlen *et al.*

(1989) made calculations of source partitioning based on ^{14}C, CH_4 concentrations and $\delta^{13}C$ which indicated that, in 1987, 21 (±3)% of atmospheric CH_4 came from fossil carbon. Quay *et al.* (1991) estimated the figure to be about 16% (~90 Tg CH_4 yr^{-1}).

The disposal of refuse in landfills by wealthy nations generates large amounts of CH_4. IPCC (1992) estimated that between 20 and 70 Tg CH_4 yr^{-1} are produced from landfills. However, it is hard to determine an accurate figure. Investigations have shown that there is great variation in landfill gas production between different sites. Also, more modern sites are now designed in such a way as to either recover the landfill gas and utilise it as an energy source, or to minimise its emission. Landfills are extremely heterogeneous environments, characterised by high solids content. Badr *et al.* (1991b) presented a comprehensive review of the national estimates of many countries for mass of refuse dumped and conversion factors. Sheppard *et al.* (1982) calculated that the total CH_4 production from landfills in the U.S.A. is 8.4 Tg yr^{-1}. If the global population is 20 times that of the U.S.A., the global figure would be 170 Tg CH_4 yr^{-1}. However, this is clearly an over-estimate as many nations have a far lower standard of living than the U.S.A. and consequently produce much less solid waste, and so they estimated that the actual global annual flux from landfill is 50 Tg CH_4 yr^{-1}.

Piccot *et al.* (1996) reported estimated methane fluxes from an wide variety of minor anthropogenic sources such as fuel combustion, industrial waste treatment, manufacturing processes and charcoal production, none of which are considered in the main global methane budgets. Although each source in itself is small, together they amount to about 40 Tg CH_4 yr^{-1}, or about 8% of the total methane flux. Piccot *et al.* also suggested that half of this derives from residential fossil and bio-fuel burning.

The global flux of gas seepage through the seabed of the continental shelves has been estimated to be approximately 8 to 65 Tg CH_4 yr^{-1} (Hovland *et al.*, 1993).

Even though much of this will be oxidised before reaching the atmosphere, oceans could represent a significantly greater source of methane flux than previously thought. As much of this methane is ^{14}C depleted, Hovland *et al.* (1993) claimed it would partially account for the shortfall of fossil methane in current atmospheric budgets. In contrast are the findings of Bates *et al.* (1996). They studied the open ocean as a source of methane to the atmosphere, taking measurements in the Pacific Ocean from 1987 to 1994. They reported a total global ocean-to-atmosphere flux of 0.4 Tg CH_4 yr^{-1}. Despite an uncertainty factor of 2, this is still an order of magnitude less than previous estimates (IPCC, 1992). The differences in the two studies mentioned could arise from the different approaches used to make the estimates. Bates *et al.* (1996) made measurements in the atmosphere over one ocean, whereas Hovland *et al.* (1993) used data and anecdotal evidence provided by the petroleum industry, of seepage from the floors of many oceans. The IPCC report (1992) acknowledges that the estimate given for oceans is based on a limited and out-dated data set.

It is evident that there is still much uncertainty surrounding the global methane budget and further work is required to constrain the data more accurately.

c) Sinks

There are three main sinks of methane: reaction with the $OH^{\bullet}$, oxidation by soils and escape to the stratosphere. The budgets for methane sinks are on the whole better constrained than for the sources. Some recent estimates are given in Table 1.3.

Approximately 85-90% of tropospheric methane is destroyed by reaction with the $OH^{\bullet}$ (Section 1.2.1). The reaction with $OH^{\bullet}$ is the rate-determining step in the chain of reactions leading to complete oxidation:

$$CH_4 + OH^{\bullet} \rightarrow H_2O + CH_3^{\bullet} \qquad \text{Equation 1.21}$$

The amount of hydroxyl radical available for this reaction in the clean background atmosphere also depends upon the concentration of CO, which completes with CH_4 for the $OH^{\bullet}$.

Table 1.3 Sinks of methane. (Figures in brackets indicate range of estimates, numbers are Tg CH_4 yr^{-1}).

Sink	Cicerone and Oremland (1988)	IPCC (1992)	Lelieveld and Crutzen (1993)
destruction by $OH^{\bullet}$	500 (405-595)	500 (400-600)	500 ±60
soils	-	30 (15-45)	30 ±25
escape to stratosphere	55 (50-60)	-	-

Understanding the sinks of methane and the rate of increase of atmospheric CH_4 allows an accurate estimate of emissions to the atmosphere to be made. It is virtually impossible to distinguish between increasing levels of CH_4 and decreasing levels of $OH^{\bullet}$. As $OH^{\bullet}$ has a very short lifetime (1-2 seconds) it is very difficult to derive a global average concentration from individual measurements. However, it can be estimated by means of model calculations, which are then validated against measurements on methylchloroform (Prinn *et al.*, 1987; Lelieveld and Crutzen, 1993). This is a man-made compound of known emission rate and known sinks. The models can then be used along with the rate coefficient of the reaction of CH_4 with the hydroxyl radical (Vaghjiani and Ravishankara, 1991) to estimate the strength of the CH_4 sink in the atmosphere, and thus the size of total methane emissions. This method is contradicted by Slania and Warneck (1994), who stated that the $OH^{\bullet}$ sink has an uncertainty of 40% or more and therefore cannot be used to evaluate the quality of methane emission data.

It is reported that 10 to 20% of tropospheric methane is lost to the stratosphere where it reacts with $OH^{\bullet}$, $O^*(^1D)$ and Cl (Cicerone and Oremland, 1988).

Soils also provide a small sink for atmospheric methane. Direct uptake and consumption of atmospheric methane on dry, aerated soils has been observed by Keller *et al.* (1983), Seiler *et al.* (1984) and Striegl *et al.* (1992). Bacterial oxidation of methane also occurs in aerobic conditions above anaerobic CH_4 production zones in wet environments (Keller *et al.*, 1983; King *et al.*, 1989). Galchenko *et al.* (1989) stated that it is necessary to conceptually separate these two types of bacterial sinks: the sink of methane inside the ecosystem (or biofilter) and the soil sink of atmospheric methane. Details of methane oxidation are discussed further in Section 1.3.6. Schütz *et al.* (1990) calculated the soil sink to be 23 to 56 Tg CH_4 yr^{-1}, (7 to 8% of the total CH_4 decomposition). However, this figure is speculative due a lack of information regarding the rôle of large potential CH_4-oxidising land areas, (*e.g.* deserts, savannahs).

The rate of CH_4 uptake in temperate and boreal forest soils may decrease by as much as 33% as a result of nitrogen fertiliser applications (Steudler *et al.*, 1989). Thus, nitrogen fertilisation may significantly reduce this methane sink. In New England, nitrogen enrichment from acid precipitation as well as fertiliser use has been found to suppress the rate of CH_4 decomposition (Badr *et al.*, 1992b).

d) Climate Change Implications

Early estimates predicted that if the atmospheric CH_4 concentration continued to rise at the rate of 2% yr^{-1}, it would result in a warming of 0.2 to 0.4K in the Earth's surface temperature by the year 2020 (Rasmussen and Khalil, 1981). A decade later Badr *et al.* (1991a) suggested that if there is no control policy and anthropogenic emissions of methane continue to increase, then the atmospheric concentration of CH_4 may reach 4 ppmV by the year 2100, causing the Earth's surface temperature to rise by 0.5 °C. However, it is now predicted that if CH_4 sources and $OH^{\bullet}$ concentration remain at 1996 levels, the global average atmospheric CH_4 concentration will stabilise at 1.8 ppmV in the next two decades (Dlugokencky *et al.*,

1998). These differences of opinion arise from the fact that the annual growth rate in atmospheric CH_4 concentration has decreased over the past 20 years.

In the event of global warming scenarios, Blake and Rowland (1986) estimated that bacterial methane emissions could increase by up to 20% for every 1 °C rise in temperature, (see Chapter 6 for a detailed discussion of the effect of temperature on methane flux). However, this is critically tied to water levels. Generally, warmer and wetter results in increased CH_4 flux while warmer and drier may result in a decrease in CH_4 emissions due to increased CH_4 oxidation.

A further cause for concern in the event of warming in the Earth's atmosphere is the melting of permafrost. This may result in a feedback effect: globally every meter depth of permafrost contains about 40 Tg of trapped methane, which may be released if the permafrost melts. Moraes and Khalil (1993) developed a heat and gas transfer model which showed that the permafrost is likely to contribute less than 10 Tg CH_4 yr^{-1} to the global methane budget. However, they also concluded that if the permafrost does melt, it could convert to wetlands which may then become a significant source of methane. Nisbet (1989) also modelled the potential feedback of permafrost thaw, and concluded that the effect would be small but noted there was large uncertainty.

Potential feedback between wetlands and climate change have been studied by Christensen (1991), and Bridgham *et al.* (1995). Both studies examined in detail the effect of increasing temperature, and also wetter or drier conditions. The conclusion in both studies was that the complexity of the ecosystem and the CH_4 cycle prevent any definitive statement on whether or not there would be a positive feedback, re-iterating the need for more research into the processes controlling methane fluxes from wetlands. Preliminary modelling of the sensitivity of methane emissions from northern wetlands by Harriss *et al.* (1993), however, indicated that any potential feedbacks are unlikely to significantly influence rates of climate change in the event of global warming.

1.2.3 Isotopes

The advantage of isotopic information in atmospheric chemistry arises from the fact that the relative proportions of isotopes for an element in a molecular species are not evenly distributed throughout the atmosphere. The distribution of isotopes is the result of deterministic chemical, biological and physical processes. For stable isotopes such as ^{13}C and ^{2}H (or D), isotopic distributions are largely controlled by the isotopic composition of precursor molecules, isotopic fractionation and the kinetics of production and removal of the particular species.

a) Isotopes Explained

As methane consists of carbon and hydrogen, it is necessary to consider the isotopes of both elements. The stable isotopes of carbon are ^{12}C and ^{13}C. The stable isotopes of hydrogen are hydrogen, H and deuterium, ^{2}H or D. The average natural abundance ratio of $^{13}C/^{12}C$ is 0.011 (Craig, 1957) and for D/H it is 156×10^{-6} (Hagemann *et al.*, 1970). Both carbon and hydrogen also have radioactive isotopes; ^{14}C and tritium, ^{3}H. Radiocarbon is produced cosmogenically, mainly in the stratosphere, and has a half life of 5730 years. If radiocarbon is sequestered within the Earth's crust over millions of years, the methane in natural gas, oil and coal deposits that are eventually released into the atmosphere will be virtually free of ^{14}C as will any atmospheric oxidation products. The methane emitted from peat bogs and tundra is also depleted in ^{14}C compared to contemporary atmospheres because large amounts of C are stored in the ecosystem; and decomposition and cycling is slow (Wahlen *et al.*, 1989). Tritium is also produced cosmogenically; however anthropogenic production *via* nuclear power-reactors or bomb-testing appears to exceed cosmogenic production. The half life of ^{3}H is relatively short, 12.26 years.

b) Delta Notation

The measured isotopic ratio of a sample is always compared to that of an internationally agreed standard: this is to compensate for possible instrumental

effects and thus allows inter-laboratory comparison of data. This convention is known as the delta notation and was first introduced by Urey (1948).

$$\delta^{H}X = ([({}^{H}X/{}^{L}X)_{sam}/({}^{H}X/{}^{L}X)_{ref}] - 1) \times 1000 \text{ ‰} \qquad \text{Equation 1.22}$$

where $({}^{H}X/{}^{L}X)_{sam}$ and $({}^{H}X/{}^{L}X)_{ref}$ are the ratio of heavy to light isotopes of the sample and reference standard, respectively. Results are expressed in parts per thousand, or per mil; ‰.

Thus, for the stable isotopes of carbon, the delta notation is :

$$\delta^{13}C = ([({}^{13}C/{}^{12}C)_{sam}/({}^{13}C/{}^{12}C)_{ref}] - 1) \times 1000 \text{ ‰} \qquad \text{Equation 1.23}$$

and for δD:

$$\delta D = ([(D/H)_{sam}/(D/H)_{ref}] - 1) \times 1000 \text{ ‰} \qquad \text{Equation 1.24}$$

The main isotopomers of methane are:

$^{12}C^{1}H_4$ $^{13}C^{1}H_4$ $^{12}C^{1}H_3{}^{2}H$ $^{13}C^{1}H_3{}^{2}H$

The work carried out in this project utilised the combined isotopes of methane, that is the ratio of mass 17/mass 16. Further details of this concept, and of the international reference standards used are given in Chapter 2.

c) Isotopic Fractionation

Fractionation effects fall into two categories: a) those caused by physical effects and mass dependence, and b) those controlled by chemical bonds.

For sources of atmospheric trace gases, fractionation is controlled by differences in nuclear mass. Kinetic isotopic effects (KIEs) occur because rate coefficients involving isotopically heavier molecules are exponentially dependent on the vibrational energy between the reactants and the transition state (Kaye, 1987). Generally, rate coefficients are larger for isotopically lighter molecules and therefore

reactions are faster, as seen for example in the first step in the oxidation of atmospheric methane (asterisk denotes heavier molecule):

$$^{13}CH_4 + OH^{\bullet} \xrightarrow{k^*} {}^{13}CH_3^{\bullet} + H_2O \qquad \text{Equation 1.25}$$

$$^{12}CH_4 + OH^{\bullet} \xrightarrow{k} {}^{12}CH_3^{\bullet} + H_2O \qquad \text{Equation 1.26}$$

Since $k > k^*$, unreacted CH_4 in the atmosphere is ^{13}C-enriched relative to the $^{13}C/^{12}C$ ratio in the absence of fractionation.

The equilibrium effect may result in a product that is either isotopically enriched or depleted, depending on whether the rate constant for the forward or reverse reaction predominates (Kaye, 1987). Fractionation effects also appear during photolysis as well as chemical reactions. The overall result may be different rates of photolysis for isotopically different molecules, usually KIEs are very small.

The isotopic composition of methane is effected by the KIEs in chemical and enzymatic reactions, as well as isotopic equilibrium effects. The resulting fractionation effects can be measured using isotope ratio mass spectrometry. Thus stable isotopes can be used as tracers in the various biogeochemical cycles to study global source-sink relationships and mechanistic processes.

d) Using Isotopic Data in Mass Balance Calculations.

Control of methane emissions to the atmosphere demands a reliable characterisation of methane source-sink relationships. Stable isotope signatures of methane are potentially a powerful tool for resolving some of the uncertainties in the global methane budget. For this tool to be successful, however, there are some criteria that must be met. Firstly, the isotope signatures must be relatively distinct, diagnostic and measurable. Secondly, the processes leading to isotopic fractionation need to be known, or at least readily predictable at every stage of the pathway from formation to destruction. Finally, the implications regarding the uncertainty of flux

magnitudes should be considered; *i.e.* will changes in the different source strengths of methane cause a significant shift in the isotopic signature of atmospheric methane?

Early work (which had a geological emphasis) examined the isotopic composition of methane from natural gases from a variety of sources. Using the knowledge that different biogeochemical processes cause different fractionation effects, it was deduced that the methane under consideration was of biogenic, rather than abiogenic origin. A diagrammatic display ($\delta^{13}C$ vs. δD) of the methane isotopes was also presented, showing that the various source groups of natural gases can be defined more clearly in this way (Schoell, 1980). This work was later extended to distinguish between the metabolic pathways of bacterially-produced methane in geological natural gases (Schoell, 1988).

The concept of utilising the characteristic isotopic composition to distinguish between methane from various origins was expanded by Wahlen (1994) to incorporate all the major sources. He used the same concept of a $\delta^{13}C$ vs. δD diagram to present the data. This is shown in Figure 1.5, where it can be seen that the various sources of methane do indeed have a characteristic isotopic fingerprint.

An isotopic approach for resolving the methane budget by using $\delta^{13}C$ was first proposed by Stevens and Rust (1982), who stated that the mass-weighted average isotopic composition of all the sources should equal the mean $\delta^{13}C$ of atmospheric methane when corrected for the kinetic isotopic effect of $OH^{\bullet}$ destruction on CH_4:

$$\Sigma(\delta_{source} \cdot m_{source}) - \Sigma(\delta_{sink} \cdot m_{sink}) = \delta_{atm} \cdot m_{atm} \qquad \text{Equation 1.27}$$

where δ is the isotopic composition, and m is the mass, of methane in the atmosphere (Equation 1.27 is an approximation, but for the range of isotopic compositions of the methane sources and sinks in the atmosphere it is accurate to about 0.02‰).

This approach can be expanded further to include ^{14}C and deuterium in methane. There have been a number of studies that compare source-weighted

isotopic values of sources and sink processes to isotopic values in atmospheric CH_4 (*e.g.* Wahlen *et al.*, 1989; Quay *et al.*, 1991; Lassey *et al.*, 1993; Lowe *et al.*, 1994; Gupta *et al.*, 1996).

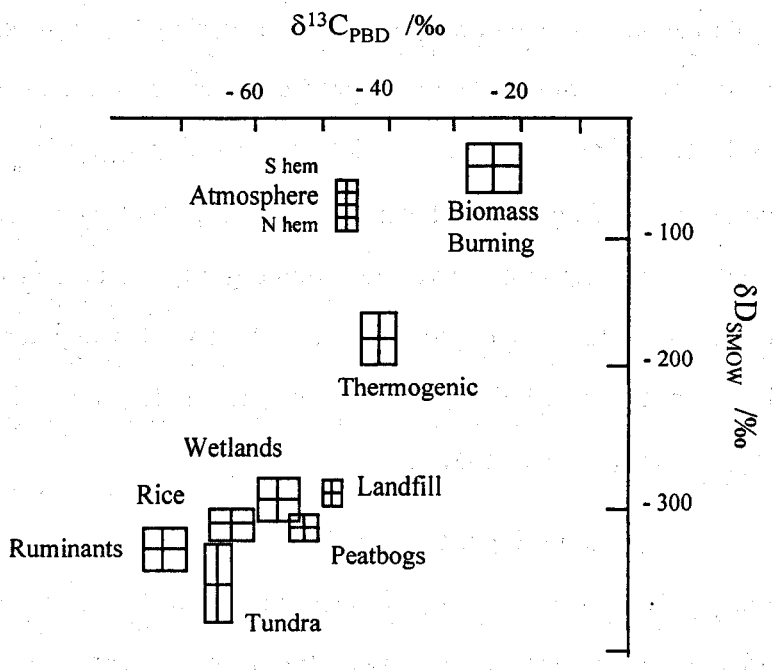

Figure 1.5 Diagram to show the stable isotopic composition of methane from various sources and atmospheric methane. Boxes show the mean values for sets of samples for ^{13}C and D in methane (adapted from Wahlen (1993)).

Long-term monitoring of atmospheric $\delta^{13}CH_4$ around the globe has shown an appreciable but variable seasonal cycle in $\delta^{13}CH_4$ at most sites, with less negative values (^{13}C-enriched) in summer and more negative values (^{13}C-depleted) in winter (Quay *et al.*, 1991; Thom *et al.*, 1993; Lowe *et al.*, 1994). A corresponding seasonal cycle in δD has been reported (Conny and Currie, 1996): maximum δD values (^2H enriched) occurred in summer and minimum δD values (^2H depleted) occurred later in the year.

i. Kinetic Isotope Effects for Methane Sinks

The usefulness of isotopic information for balancing the global CH_4 budget depends to a great extent on the accuracy of the sink fractionation factors. Estimates

for the carbon kinetic isotope effect (k_{12}/k_{13}) (Section 1.2.3.c) in the reaction of CH_4 with $OH^{\bullet}$ range from 1.003 (±0.001) to 1.010 (±0.003) (Rust and Stevens, 1980; Davidson *et al.*, 1987; Cantrell *et al.*, 1990; Lasaga and Gibbs, 1991). The differences may be explained in part by the different approaches used in determining the KIE. The accepted value is 1.0054 (Cantrell *et al.*, 1990).

Although uptake of methane by soils is a much smaller sink than the $OH^{\bullet}$ reaction, it has a larger fractionation effect. Estimates from field measurements by King *et al.* (1989) gave k_{12}/k_{13} values of 1.027 and 1.016. This is in good agreement with work done by Coleman *et al.* (1981) using laboratory cultures of methane-oxidising bacteria at 11.5 and 26 °C. The KIEs are reported as 1.0130 and 1.0244 respectively. More recent field studies by Tyler *et al.* (1994) determined k_{12}/k_{13} to be 1.022. All these reported values represent a large isotopic shift when atmospheric methane is oxidised by soil bacteria.

Quay *et al.* (1991) used mass and isotope balances with atmospheric data in an interhemispheric box model to determine the overall carbon kinetic fractionation effect of $OH^{\bullet}$ destruction and soil uptake. They report a value of 1.007 ± 0.002.

The kinetic isotope effects for hydrogen are much larger than those for carbon. This is seen in the wider range of δD values in source and atmospheric air measurements in comparison to $\delta^{13}C$ data. Earliest determinations of a KIE for CH_3D oxidation by $OH^{\bullet}$ gave a k_H/k_D value of 1.50 (Gordon and Mulac, 1975), which was much higher than that for $^{13}CH_4$. More recently, however, an estimate of KIE = 1.17 has been reported, a value based on the comparison of δD values for sources with those for ambient air (Wahlen *et al.*, 1990). A temperature dependence of the hydrogen KIE has been revealed by DeMore (1993) who reported a k_H/k_D value of 1.19 at 277K.

k_H/k_D values for the action of methane-oxidising soil bacteria of 1.297 at 26 °C and 1.103 at 11.5 °C have been reported (Coleman *et al.*, 1981), again higher than for the corresponding carbon KIEs.

By incorporating KIE values for methane sinks into a 2-D model it has been calculated that soil uptake enriches $\delta^{13}C$ in atmospheric methane by 1.18‰ in the Northern Hemisphere and 1.16‰ in the Southern Hemisphere (Gupta *et al.*, 1996), highlighting the importance of including this sink in global models. If the soil sink is substantially larger than previously thought this would have serious implications for the global budget models (Equation 1.27).

Stevens and Engelkemeir (1988) used Davidson's KIE value for methane oxidation by the OH radical of 1.010, and the average atmospheric methane $\delta^{13}C$ value of -47.7‰ to calculate that, in 1978, the average $\delta^{13}C$ value for the sources of methane was -55.3‰. Using information from polar ice cores (Craig *et al.*, 1988), Stevens and Wagner (1989) estimated the $\delta^{13}C$ for natural sources of methane to be -58.3‰ and for anthropogenic sources, -52.3‰. The calculated average value of $\delta^{13}C$ for natural sources of methane is heavier than most measured sources, possibly because the measured results are limited in number, are not very representative or there is an unknown CH_4 source which is isotopically heavier. Stevens and Engelkemeir also demonstrate the importance of fully understanding all the processes involved in the global methane cycle. If, for example, they had used Rust and Stevens KIE value of 1.003 in their calculations (instead of Davidson's value of 1.010), the average $\delta^{13}C$ for natural sources = -52.3‰; this is very significantly higher than measured values and would require a much greater source of heavier CH_4 for the budget to balance.

1.3 Wetlands and Peat Bogs

The Canadian Wetland Classification System defines wetlands as "land that has the water table at, near, or above the land surface or which is saturated for a long enough period to promote wetland or aquatic processes as indicated by hydric soil, hydrophytic vegetation and various kinds of biological activity that are adapted to the wet environment". A peatland is defined as " a wetland with more than 40 cm of

peat". A bog has the following description: "a peatland, generally with the water table near the surface. The bog surface, which maybe raised or level with the surrounding terrain, is virtually unaffected by nutrient-rich groundwater from the surrounding mineral soils and is thus generally acid and low in nutrients. The dominant materials are moderately to weakly decomposed *Sphagnum* and woody peat, underlain at times by sedge peat. The soils are mainly Fibrosols, Mesisols, and Organic Cyrosols[†] . Bogs maybe treed or treeless, and they are usually covered with *Sphagnum* spp. and ericaceous shrubs". Definitions for fens, marshes, swamps and shallow waters are given in Appendix A.

1.3.1 Global Distribution

In the past, wetlands have been poorly documented in land maps and statistics, as they represent only a small part of the total global land area and are of low economic value. Therefore, global estimates of CH_4 flux based on wetland area have been highly uncertain. Indeed, early global flux estimates were based on an outdated and inaccurate global wetland area of 2.6×10^{12} m^2, calculated in 1926 by Twenhofel (Matthews, 1993). An additional problem in estimating the flux of methane arises because the areal coverage of wetland habitats may vary during the year due to the seasonality of inundation periods.

Matthews and Fung (1987) integrated three global digital databases of vegetation, ponded soils and fractional inundation at a resolution of 1° latitude by 1° longitude to give a global wetland area of 5.3×10^{12} m^2. This is in excellent agreement with Aselmann and Crutzen (1989) who determined the global wetland area to be 5.7×10^{12} m^2, by compiling regional and local wetland reports at a 2.5° resolution. Both studies agreed that about 50% of the global wetland area lies between 50° and 70°N, a region characterised by highly seasonal emissions of methane, due to the temperature-dependent thaw season. They also agreed that about one third of the global area of wetlands is widely distributed across the latitudes 20°N

[†] see Appendix A for equivalent soils in the England and Wales Soil Classification System (Avery, 1980).

to 30°S. Again, these tropical wetlands undergo seasonal expansion and contraction due to the seasonal nature of the rainfall cycle, resulting in marked seasonality of the methane flux (Devol *et al.*, 1990; Wassmann *et al.*, 1992).

The largest discrepancy between these two studies lies in the area between the equator and 10°S. Matthews and Fung calculate that this region accounts for only 10% of the global total wetland area, while Aselmann and Crutzen estimate that about 20% of the total lies in this zone. This disagreement may arise because there are a number of large river systems in this part of the world, which have an associated large areal uncertainty (Matthews, 1993).

Despite the areal differences, using revised flux measurement data and the Matthews and Fungs' global wetland distribution data-set, Fung *et al.* (1991) calculate annual flux rates for each 10° latitude that are very similar to that compiled by Aselmann and Crutzen (1989) (Figure 1.6).

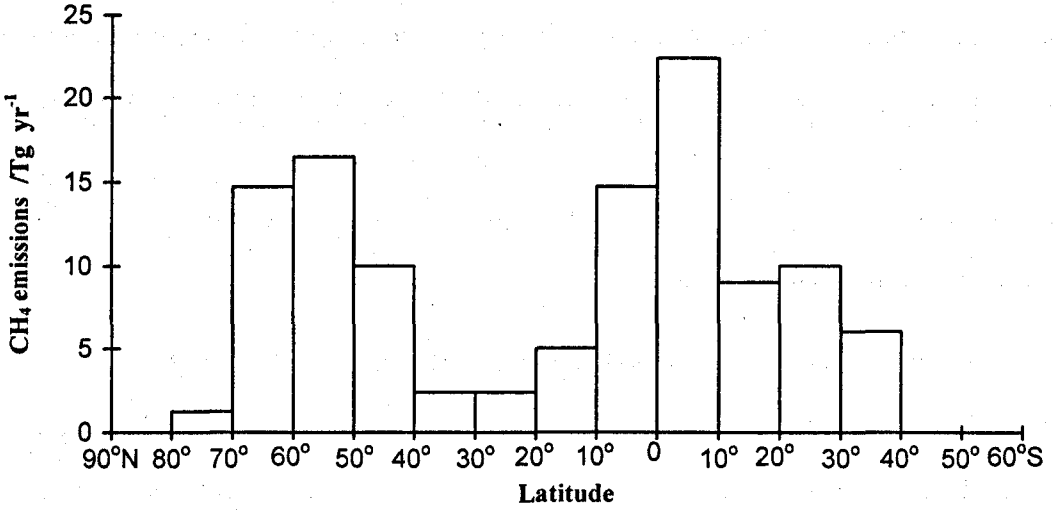

Figure 1.6 Latitudinal distribution of methane emission (from Fung *et al.*, 1991).

1.3.2 Peat Accumulation

Peat covers about 3% of the Earth's surface (Matthews and Fung, 1987). Peatlands that receive water wholly from precipitation are classified as ombrotrophic (from the Greek: rainstorm fed); those that receive water from neighbouring mineral

soils are minerotrophic. The former are bogs and are generally acid. The latter are fens and are sometimes calcareous and therefore alkaline.

Peat accumulates very slowly as follows: *Sphagnum* moss forms a porous mass, growing from the apex. New organic matter is added at the apex and topmost branches, which are green and photosynthetic. However, sunlight is unable to penetrate more than 2-4 cm. As a consequence, most of the plant dies below this depth and aerobic decay by fungi and bacteria begins. The gaseous product is CO_2. The apex continues to grow above, and the load, mainly capillary water, increases. Eventually the structure collapses. There is a four-fold increase in dry bulk density, and hydraulic conductivity decreases by about 250-fold. Most of the water now flows laterally, while only a small amount enters the underlying peat. This process keeps the peat waterlogged so long as precipitation exceeds evaporation and drainage. In the centimetre below the water table oxygen is utilised faster by microbial activity than it can be replaced by diffusion. Anoxia occurs, microbial activity becomes anaerobic and the decay process slows down. Under these conditions the gaseous products are CH_4 and CO_2. Detailed descriptions and models of the peat accumulation process can be found in Clymo (1984), Clymo (1987), Clymo (1991), Clymo (1992) and Francez and Vasander (1995).

The topography of a peatbog generally consists of hummocks, hollows and pools. Hummocks are slightly raised above the surrounding surface, while hollows are lower, and may fill periodically with water. Hollows have a complete vegetation cover, while pools do not. Over many years, the peat bog develops into two distinct layers. The acrotelm is the largely oxygenated surface layer with relatively high hydraulic conductivity and within which the water table fluctuates. The catotelm is the underlying, permanently saturated and mainly anoxic layer of lower hydraulic conductivity (Ingram, 1978).

1.3.3 Microbiology of Methane Production

Methane-producing bacteria are members of the domain Archaea, a taxonomic group that is distinct from the Bacteria, and the Eukaryotes (multi-celled organisms with a distinct nucleus). The distinction between archaea and bacteria is based on molecular phylogenetic evidence and many other features, including the structure of their ribosomal RNA and their lipid components. The characteristics which methanogens share with bacteria and eukaryotes likely developed early in the evolution of life on earth and studies of methanogens' biochemistry may help us understand how early life evolved.

Methanogenesis occurs as the terminal step in organic matter decomposition, (Figure 1.7). Each step of the organic matter breakdown is catalysed by a separate group of bacteria; however, as the processes occur simultaneously concentrations of the intermediate products are usually small.

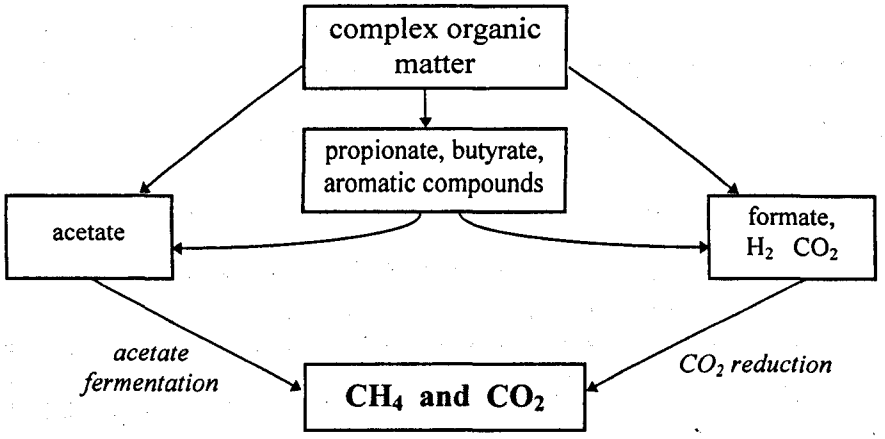

Figure 1.7 Decomposition of organic material in methanogenic ecosystems.

Methanogens are strict anaerobes requiring a redox potential of less than -330mV. They are also obligately methanogenic: methane synthesis is required for growth (Jones, 1991). Detailed description of the biochemistry of microbial methane production can be found for example in Zeikus (1977), DiMarco *et al.* (1990) and Knowles (1993). Methanogenesis only occurs when all other electron acceptors in the ecosystem have been used up. Methanogens can only metabolise a limited

number of substrates. They rely on other microbes to break down the complex organic matter into products they can use. In wetlands CH_4 is produced by two different microbial processes: acetate fermentation, and CO_2 reduction with H_2.

Acetate fermentation is given by:

$$*CH_3COOH \rightarrow *CH_4 + CO_2 \qquad \text{Equation 1.28}$$

and CO_2 reduction by:

$$CO_2 + 4H_2 \rightarrow CH_4 + 2H_2O \qquad \text{Equation 1.29}$$

Acetate fermentation refers to methanogenesis that involves the transfer of a methyl group from a simple organic substrate (*e.g.* acetate, methanol, methylated amines). Although the term 'acetate fermentation' is widely used in the literature, it is in fact a misnomer. A more accurate term for this process is acetoclastic methanogenesis. The metabolic pathway by which the methane is formed will have a direct influence upon the isotopic composition on the methane emission from the wetlands.

1.3.4 Metabolic Pathways of Methane Production and Isotopic Implications

Each of the two metabolic pathways produce methane with distinctive carbon and hydrogen stable isotopic composition (Alperin *et al.*, 1992; Blair and Carter, 1992; Sugimoto and Wada, 1993; Hornibrook *et al.*, 1997). The isotopic composition of the precursor organic matter will have some bearing on the composition of the methane produced, causing difficulty in making comparisons from region to region, or between areas covered with very different vegetation types.

During carbon dioxide reduction all four hydrogen atoms incorporated into the CH_4 come from ambient water (Daniels *et al.*, 1980). In the case of methane produced from acetate, it is thought that three hydrogen atoms originate from the methyl group and only one comes from the water (Pine and Barker, 1956; Smith and

Mah, 1980). However, Sugimoto and Wada (1995) claimed that there is isotopic evidence which suggests that in fact more than one hydrogen atom comes from the water because some of the hydrogen atoms in the acetate methyl group have exchanged with water. Since the δD value for rain water changes with latitude (becoming isotopically lighter the further from the equator you are), this also has implications for the isotopic composition of the methane produced by wetlands (Wahlen, 1994). Burke (1993) suggested that the wide range of δD values for methane from natural wetlands may be due to variations in hydrogen gas concentration.

There is isotopic evidence that the two metabolic pathways of methanogenesis result in different $\delta^{13}C$ and δD values for the methane. This is due to different kinetic isotope effects associated with each of the two pathways (Section 1.2.3c), and the differences in the isotopic composition of the methanogenic precursors. Whiticar *et al.* (1986) reported that $\delta^{13}C$ = -110 to -60‰ and δD = -250 to -170‰ for marine sediments. In freshwater environments, they found $\delta^{13}C$ = -65 to -50‰ and δD = -400‰ to -250‰. They concluded that CO_2 reduction was the predominant pathway in marine sediments, while acetate fermentation was the main pathway in freshwater environments. This was also the conclusion of Schütz and Seiler (1989). However, the more recent findings of Lansdown *et al.* (1992) suggested that CO_2 reduction accounts for all CH_4 production in freshwater wetlands and that acetate is not an important precursor. They reported a $\delta^{13}C$ value of -74 ±5‰ and a δD value for methane ebullition of -308 ±20‰. As the soil water δD was -65 ±3‰, this represented a large hydrogen isotope fractionation of around -240‰. Whiticar *et al.* (1986) reported a hydrogen isotope effect of -180 ±20‰ in marine sediments, where CO_2 reduction predominates. Incubation studies on paddy soils showed a hydrogen isotope fractionation of -317 ±20‰ for CO_2 reduction and -302 ±15‰ for acetate fermentation, although this was at elevated temperatures (Sugimoto and Wada, 1995).

The discrepancy between the findings of Whiticar *et al.* and Lansdown *et al.* may be due to the following reasons:

- Whiticar *et al.* investigated sediments, while Lansdown *et al.* studied a peat bog. The former contain no actively growing plants, while the latter does. This may have a bearing upon the metabolic pathway utilised by the microbes.
- There is evidence that the metabolic pathway depends upon substrate availability. This may be a more important factor than whether the ecosystem is marine or freshwater.
- Differences in pH. There is evidence that in some acidic environments methanogenesis by CO_2 reduction is inhibited, and thus acetate fermentation becomes the main metabolic pathway.

In a study using anoxic marine sediments, Alperin *et al.*, (1992) showed that when acetate levels were low, CO_2 reduction prevailed, with associated $\delta^{13}C$ values of -94 to -80‰. As the acetate concentration in the sediment increased, acetate fermentation predominated and $\delta^{13}C$ became enriched, $\delta^{13}C$ = -42‰. As the acetate concentration declined, CO_2 reduction was again the predominant pathway and $\delta^{13}C$ ranged from -58 to -46‰. Similarly, using incubated paddy soils, Sugimoto and Wada (1993) showed that initially CH_4 is produced by acetate fermentation, but after the acetate is depleted the pathway switches to CO_2 reduction. Again, it was isotope measurements that led to this conclusion. Hornibrook *et al.* (1997) used stable isotope techniques to examine the spatial distribution of the metabolic pathways in wetland soils. They determined that acetate fermentation is favoured in the shallow subsurface, where there is plenty of fresh decomposing organic matter; and CO_2 reduction is more predominant in older, less reactive peat at depth.

Whiticar *et al.* (1986) reported a carbon isotope fractionation ($CO_2 \rightarrow CH_4$) in freshwater environments of 1.04 to 1.06; and in marine sediments, 1.05 to 1.09. This is in good agreement with the work done on pure cultures of methanogens: the

$^{13}C/^{12}C$ fractionation factor for CO_2 to CH_4 is 1.021 to 1.061 (at elevated temperatures); acetate fermentation is assumed to have a similar fractionation effect (Games and Hayes, 1976; Games *et al.*, 1978; Gelwicks *et al.*, 1994).

1.3.5 Transport of Methane to the Atmosphere.

Work carried out by several groups in the Terrestrial Initiative in Global Environmental Research (TIGER) programme (see Section 1.5) showed that maximum methane production occurs in a 10 cm band, approximately 10 to 20 cm below the water table; and that this band moves with the water table (Clymo and Pearce, 1995; Nedwell and Watson, 1995; Thomas *et al.*, 1995; Benstead and Lloyd, 1996). There are three routes by which methane produced in peat can escape to the atmosphere: slow diffusion through the saturated peat; transport *via* vascular plants or by ebullition (bubbles) (Figure 1.8).

Ebullition occurs in highly productive ecosystems where the rate of CH_4 production exceeds the rate of diffusion. Methane accumulates until its partial pressure is greater than the ambient pressure, bubbles form and the gas leaves the peat very rapidly, avoiding re-oxidation by methanotrophs (Section 1.3.6). Diffusion of methane through the peat is controlled by Fick's law and is therefore proportional to the concentration gradient; and is affected by the temperature and the air-filled porosity of the peat. (Where the peat is saturated, diffusion is entirely in the water phase (Conrad, 1995)). If the diffusion path is long, then there is great potential for methane oxidation to occur on the way to the surface. CH_4 oxidation activity is usually concentrated in the oxic surface layer of the peat (if there is one). This layer may increase in depth during times of reduced rainfall, increasing the potential for methane oxidation. As discussed in Section 1.2.3c, isotopic fractionation occurs during microbial activity, lighter isotopes of methane being preferentially consumed. Thus the residual methane will be isotopically heavier (Oremland and Marais, 1983; Alperin *et al.*, 1988).

Vascular plants have been implicated in the transport of methane from wetlands for some time (*e.g.* Aselmann and Crutzen, 1989; Boon and Sorrell, 1995; Shannon *et al.*, 1996; Thomas *et al.*, 1996; Waddington *et al.*, 1996). The plant roots can trap gas bubbles temporarily. In addition, oxygen is transported from the shoots *via* the aerenchyma system to the roots for root respiration. Some O_2 may escape into the rhizosphere creating an anoxic-oxic interface within the anaerobic zone of the peat. The gas transport system that permits oxygen supply to the roots also provides an escape route for methane to the atmosphere. Hollow plants such as bog bean (*Menyanthes trifoliata*) and horsetails (*Equisetum* spp.) are particularly effective in transporting CH_4 to the atmosphere (Daulat and Clymo, 1998; MacDonald *et al.*, 1998).

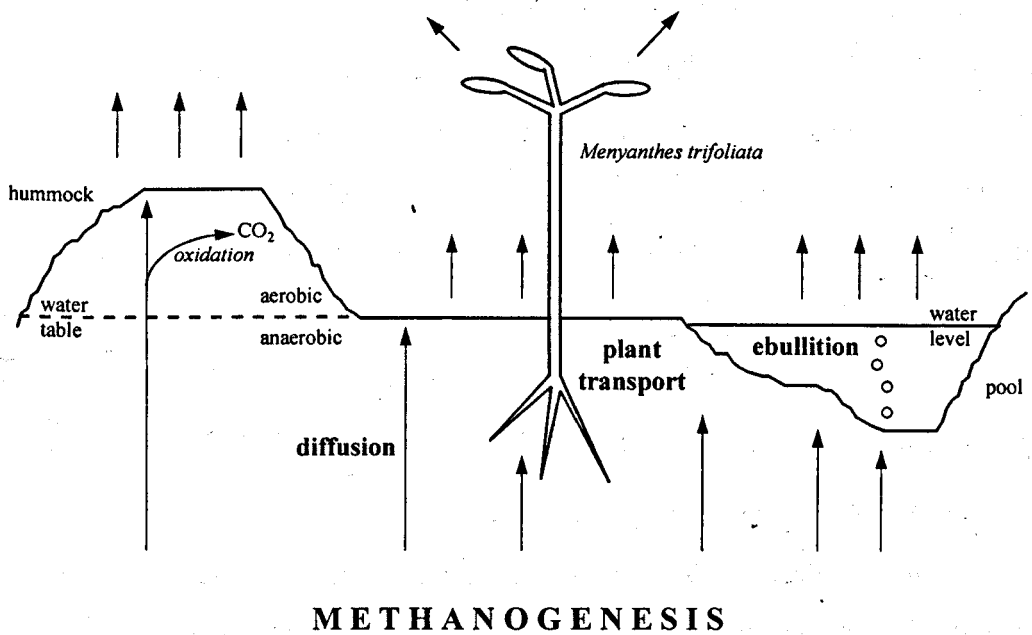

Figure 1.8 Transport mechanisms for the emission of methane from peatbogs.

The processes involved in methane emission from peatland and their relative contributions to the ecosystem have been modelled (Cao *et al.*, 1996; Watson *et al.*, 1997; Arah and Stephen, 1998; Stephen *et al.*, 1998). These models also include many of the environmental variables which influence the production of methane.

1.3.6 Methane Oxidation

Methane oxidation is an important component in the methane budget. Studies suggest that oxidation at or near a sediment surface may limit the methane flux to a fraction of the methane produced, sometimes <10% reaches the atmosphere (Holzapfel-Pschorn *et al.*, 1985; Schütz *et al.*, 1990; King, 1992). It has been estimated that, overall, 30% of CH_4 production is oxidised in high latitude wetlands before it reaches the atmosphere (Reeburgh *et al.*, 1993). Small decreases (10 to 20 cm) in wetland water table levels may be sufficient to balance CH_4 production and consumption globally (Roulet *et al.*, 1992).

Methane-oxidising bacteria are known as methanotrophs. Detailed descriptions of the biochemistry and physiology of methanotrophy can be found in, for example, O'Neill and Wilkinson (1977), Bédard and Knowles (1989), Bender and Conrad (1993), Duenas *et al.* (1994), King (1992), Knowles (1993) and Topp and Hanson (1991).

There are two different scenarios for methane oxidation: near the surface of wetland soils, as the methane produced at depth passes through on its way to the atmosphere; and in drier well-aerated soils, atmospheric methane filtering down from above can be consumed. It is thought that two different microbial populations are responsible for these activities (Knowles, 1993; Schimel *et al.*, 1993; Conrad, 1995). The methanotrophs active in aerated soils differ in their kinetics to those in wetlands soils. In aerated soils the bacteria are exposed to atmospheric concentrations of CH_4, while those in wetland soils are exposed to elevated levels of methane.

Methanotrophic bacteria obtain energy by oxidising CH_4. Methane is oxidised sequentially *via* methanol and formaldehyde, eventually forming carbon dioxide:

$$CH_4 \rightarrow CH_3OH \rightarrow HCOOH \rightarrow CO_2. \qquad \text{Equation 1.30}$$

The enzyme responsible for the first step, methane monooxygenase (MMO) requires molecular oxygen: all methanotrophs so far isolated are obligate aerobes. However,

some prefer O_2 concentrations below ambient, they occur close to the anoxic/oxic interface where the CH_4 and O_2 concentration gradients overlap. There is also evidence for anaerobic methane oxidation (Murase and Kimura, 1994). It is usually associated with regions of sulphate-depletion in marine sediments.

In comparison to methanogenesis (see next section), the temperature quotients (Q_{10}) for methane oxidation are lower (1.4 to 2.1), and activation energies are also lower (20 to 80 kJ mol^{-1}). Between 0 and 5°C there is still appreciable methanotrophic activity (Dunfield *et al.*, 1993), which will enhance any decrease in methane emissions at low temperatures. CH_4 consumption can occur in peat soils at pH values below 4.0 (Moore and Knowles, 1990).

Nitrifying bacteria and methanotrophs are both capable of oxidising CH_4 and NH_4^+, due to the structural similarity of these molecules and the low specificity of the monooxygenase enzymes (Bédard and Knowles, 1989). This raises the possibility of competitive inhibition of CH_4 consumption by NH_4^+. This may be reason for the inhibitory effect of nitrogen fertiliser additions on methane consumption (Keller *et al.*, 1983; Steudler *et al.*, 1989; Mosier *et al.*, 1991; Boeckx and Van Cleemput, 1996).

1.4 Flux Measurements.

Over the last two decades there have been numerous research studies carried out on wetlands, particularly in the region between 50 and 70 °N in North America. Some of this work is reviewed in detail by, for example, Schütz and Seiler (1989) and Bartlett and Harriss (1993). During the 1990s there has been a concerted effort to determine the rôle of U.K. wetlands in climate change, as part of the TIGER programme (Section 1.5).

Methane flux rates have been reported in the range of 2.5 to 5625 μmol m^{-2} hr^{-1} (Bartlett and Harriss, 1993) from a wide variety of wetland habitats. Generally, bogs produce an order of magnitude less methane than fens (Moore and Knowles, 1989;

Dise, 1993; Dise *et al.*, 1993), which may be related to the acidity of the peat. Methane emission from hummocks is less than from hollows, generally between one third and one tenth (Clymo and Pearce, 1995; Nedwell and Watson, 1995; Kettunen *et al.*, 1996; Waddington and Roulet, 1996; MacDonald *et al.*, 1998). Open water and floating vegetation mats can produce an order of magnitude more methane than vegetated wetlands, depending on the depth of water (Yavitt *et al.*, 1990; Moosavi *et al.*, 1996).

Researchers in North America report average fluxes of 99 to 521 μmol CH_4 m^{-2} hr^{-1} from wetlands over a geographically diverse area: Minnesota, West Virginia, Maryland, Alaska, Ontario and New Hampshire (Yavitt *et al.*, 1990; Bubier *et al.*, 1993; Dise, 1993; Melloh and Crill, 1996; Moosavi *et al.*, 1996). Methane emissions change from year to year at the same sites; for example Melloh and Crill (1996) reported average winter flux measurements from a New Hampshire fen of 52, 102, 138, 146 and 68 μmol CH_4 m^{-2} hr^{-1} for the winters of 1990, 1992, 1992, 1993 and 1994 respectively. Average methane flux varies tremendously from different regions, it is especially high in northern U.S. wetlands for reasons that are not entirely clear.

Using aircraft-based measurements, Gallagher *et al.*. (1994) reported fluxes of 205 (±100) μmol CH_4 m^{-2} hr^{-1} over northern Scotland. This is in agreement with the findings of Clymo and Pearce (1995), who reported flux rates of up to 200 (±64) μmol CH_4 m^{-2} hr^{-1} from Ellergower Moss in northern Scotland; and MacDonald *et al.* (1998) who reported an average flux of 129 (±114) μmol CH_4 m^{-2} hr^{-1}, from a blanket bog at Loch More in Caithness, northern Scotland. Flux measurements from peat monoliths (representative of hummocks or hollows) under controlled water table conditions but variable temperature (ambient) were similar (Nedwell and Watson, 1995; MacDonald *et al.*, 1998) (Table 1.4).

Hutchin et al. (1995) reported a summer maximum in methane flux rate of 396 μmol CH_4 m^{-2} h^{-1}, from an ombrotrophic bog in Snowdonia.

Table 1.4 Mean methane fluxes from peat monoliths in μmol m^{-2} hr^{-1}. The water table was at the surface for hollow and lawn monoliths, and at a depth of 15 or 17 cm for the hummocks, temperature was allowed to vary according to ambient conditions.

Terrain	MacDonald et *al.* (1998)	Nedwell and Watson (1995)
hollow/lawn	98.5 (n=69)	95.8 (n=3)
hummock	8.4 (n=33)	14 (n=3)

The large variability in methane fluxes from natural wetlands arises from the complex suite of environmental factors that effect the rate of methanogenesis, and the factors that affect the release of the methane to the atmosphere.

1.4.1 Factors Controlling Emission Rates

The net flux of methane from the surface of a peatland is equivalent to the methane produced minus the methane consumed in the peat:

$$\text{flux} = \text{production} - \text{oxidation}$$

This section will consider the environmental factors which determine the rate of methane emission. Most of the research on methane emissions from high latitude wetlands has looked for a link between flux and the main controlling environmental variables of water table and temperature.

Fluxes have been correlated with a number of individual ecological variables, and in general, no quantitative results can be applied to all wetland environments. There is some dispute over what is the most important or controlling variable. Dise (1993) used a statistical approach to determine the relative importance of water table and temperature in controlling methane fluxes from a series of wetland ecosystems with a gradient in wetness in northern Minnesota. The water table could account for 62% of the variability in the flux. Adding the annual soil temperature change into the regression equation resulted in accounting for 90% of the annual variability. However when specific sites were examined separately, soil temperature rather than

water table explained most of the variability. Dise and others (1993) concluded that temperature controls the short-term variation in flux at individual sites but hydrology distinguishes long-term between-site variability.

Studies by Yavitt *et al.* (1990) produced only a poor correlation between CH_4 flux and environmental variables including soil moisture and average temperature; the latter possibly because the peat temperatures under consideration were at 2 and 10 cm depth, which would vary with air temperature and are also above the main zone of methane production and therefore possibly not ideal parameters to use. Moore *et al.* (1994) reported a significant correlation between seasonal flux and mean position of the water table over a range of sites, noting that this emphasises the importance of hydrology. However, they found only a weak statistical relationship between daily flux and peat temperature & water table. Torn and Chapin (1993) reported that soil temperature and moisture account for 75% of variation in CH_4 flux across a range of vegetation types. Bubier *et al.* (1993) and Vourlitis *et al.* (1993) stated that most of the variation in methane flux can be explained by water table position; both study sites being in areas characterised by long, cold winters (when the ground is frozen) and short, cool summers. Moosavi *et al.* (1996) suggest that methane flux is turned on and off by changes in site hydrology: a large saturated zone creates high potential for methanogenesis; prolonged dry conditions which leave little saturated peat above the permafrost substantially reduce the potential for methanogenesis, effectively turning CH_4 fluxes off. In complete contrast to all other researchers, Kettunen *et al.* (1996) reported a negative correlation between methane flux and water table depth, possibly due to high levels of precipitation and persistently high water tables during the measurement period.

Ponds also have a large effect on total methane flux. Hamilton *et al.* (1994) reported fluxes from ponds between 3 and 30 times greater than from adjacent vegetated surfaces in the Hudson Bay wetlands. Fowler *et al.* (1995b) saw a

doubling of the flux rate when the area occupied by pools increased from 5 to 30%, in a micrometeorological fetch in a blanket bog in northern Scotland.

Temperature changes can account for much of the seasonal variation in methane flux. Increased temperature has been shown to result in increased CH_4 production rates (Crill *et al.*, 1988). Edwards *et al.* (1994) reported a strong relationship between daily average CH_4 flux and wet bog temperature at 20 cm; Lansdown *et al.* (1992) saw a linear relationship between flux and temperature at 30 cm in a temperate bog. Below about 15 cm depth, the peat temperature will be much less affected by short-term changes in air temperature. It may be possible to make a generalisation that CH_4 flux is correlated with peat temperature at all depths below a critical depth, say for example 15 cm.

Dunfield *et al.* (1993) reported that CH_4 production is dependent on temperature with an optimum between 25 and 30 °C. Moosavi *et al.* (1996) reported an exponential response to temperature, and a range of three orders of magnitude, depending on the type of vegetation present. Fowler *et al.* (1995b) reported a temperature response in flux of 4.9 μmol CH_4 m^{-2} h^{-1} $°C^{-1}$ between 6 and 12 °C. Whiting and Chanton (1993) claimed that temperature doesn't consistently predict CH_4 fluxes, due to changes in substrate availability. Production of methanogenic substrates may be more temperature limited than methane production itself (Conrad, 1989). Peat bog ecosystems are highly complex, and there are other environmental factors which affect the methane flux *e.g.* vegetation. The different responses to temperature reported in the literature may arise because of the interfering effect of other factors which have been overlooked or assumed to be negligible.

The differences of opinion as to whether temperature or water table is the most important factor may be due to climatic differences in the sites studied. There is a trend in that research which indicated water table was the most important environmental variable was conducted at northern field sites in areas characterised by long, cold winters and short, cool summers. The ground would be frozen for long

periods of time. In contrast, research which indicated that temperature is more important than water table was conducted in more temperate regions, where the ground is unlikely to be frozen for protracted periods, and temperatures would generally be higher. There would also be differences in day-length which has implications for the active growing season.

There are also differences of opinion regarding the effect of pH on methane emissions. Valentine *et al.* (1994) reported that methanogenesis is inhibited at low pH. On the other hand, Moore and Knowles (1989) reported highest fluxes from the most acidic samples, pH < 3.5. Generally, however, methanogens are thought to exhibit optimum growth at pH 7 or thereabouts (Conrad, 1989). The observations of Valentine *et al.* (1994) are deduced from field studies, while Conrad reported on laboratory studies. Populations of methanogens will undoubtedly comprise of a mixture of bacterial species, which may all have different responses to pH, so there will be a range of preferred pH conditions for methanogenic bacteria within peat bogs.

1.4.2 Methods of Flux Measurement

a) Headspace Chambers

Measurements of trace gas fluxes are frequently made using headspace chambers. Chambers can be permanently installed, but are generally portable. Size varies up to about 0.75 m^2. There are several advantages to using headspace chambers: their simplicity permits them to be readily transported and used in many ecosystems, rapid sampling is possible, measurements can be made throughout the year and the cost is minimal.

The presence of a chamber can, however, affect the rate of methane emission. The temperature of the soil surface may increase if the chamber is left in place for a protracted period, leading to over-estimates of CH_4 flux.

The spatial variability in natural ecosystems such as wetlands may cause large uncertainties when chamber measurements are used to estimate field scale flux rates.

b) Micrometeorological Methods

Micrometeorological methods integrate over areas of 10^4 to 10^5 m^2 and overcome the problems of spatial variability. A tunable diode laser spectrophotometer is used to determine CH_4 concentrations in the air; instrument sensitivity and rapid response time are sufficient to allow eddy covariance techniques to be employed for measuring CH_4 fluxes.

Micrometeorological methods are limited by the fetch requirement, that is the area of open ground over which the air passes immediately before sampling. Set-up is cumbersome but once running the instruments can be left for several days with minimal operator attention. Micrometeorological methods are described in Section 5.2.1.

c) Round Britain Flights

A Hercules C130 W Mk2 of the United Kingdom Meteorological Office has been adapted to allow the collection of air samples and meteorological data while in flight. Several flights have been deployed around the northern coastline of Britain on occasions when the prevailing wind direction and other weather conditions were favourable. The normal sampling altitude is approximately 150 m. Samples are also collected at four heights between 15 and 300 m to evaluate the CH_4 concentration profile at strategic points. The resulting profiles and up- and down-wind concentrations can be used with appropriate models to establish the major sources of methane flux (Beswick *et al.*, 1998).

1.5 Project Aims

This research was part of an extensive research programme, the Terrestrial Initiative in Global Environmental Research (TIGER) programme. TIGER was

established as a research programme of the Natural Environment Research Council (NERC) to study global environmental changes at the land surface. TIGER engaged 300 researchers at 60 different universities and research institutes over 5 years of activity at a cost to the tax-payer of over £20 million. Reports from TIGER II, the atmospheric trace gas section of TIGER, were recently published in a special edition of Atmospheric Environment, volume 32, issue 19.

TIGER has three broad thrusts:

- to investigate physical and biological processes through which the land surface influences climate,
- to predict the overall effects of climate change on the natural environment, and
- to understand the feedbacks from the land that may accelerate or slow climate change.

The research reported here is the main methane isotope work associated with the TIGER II programme. The main aim of the work was to use a recently developed, highly sensitive static mass spectrometer to make combined stable isotope measurements on methane emissions from wetlands. Stable isotope measurements were made regularly and repeatedly on methane fluxes from an ombrotrophic mire, for the first time in the U.K.. Seasonal changes in the isotopic composition were monitored over 21 months. These changes were correlated with such environmental variables as temperature, water table and isotopic composition of water in the peat. Methane fluxes were also recorded. Parallel laboratory studies were set up to determine the precise effects of temperature and oxidation on the isotopic composition of methane emissions.

A brief case-study was also conducted in a palsa mire in Finland. The topography of this mire was different to that of the ombrotrophic mire and provided an excellent contrast.

Analysis Techniques for Determining the Size and Isotopic Composition of Methane Emissions

2. Introduction

The main purpose of this research was to assess the use of the combined stable isotope ratio of methane as a tool in determining the spatial and temporal variability of methane fluxes from wetlands in the UK, and secondly to assist others in constraining the global methane budgets. Biological systems are notorious for their heterogeneity, which is traditionally counter-acted by high sample replication. To ensure a temporal continuity it was decided to sample on a monthly basis. Thus, it was necessary to find an analytical technique that combined ease of isotopic analysis with simplicity of sampling technique.

Details of the techniques used to obtain samples are given in Chapters 3, 4 and 5, whilst this chapter focuses on the laboratory techniques used to determine:

- the concentration of methane in air samples acquired from peat bogs or peat cores,
- the isotopic composition of the methane, and
- the isotopic composition of water samples taken from the peat bog.

Methane concentration and the isotopic composition of the water were measured using conventional methods of gas chromatography and mass spectrometry respectively. The stable isotopic composition of the methane, however, was determined using a novel mass spectrometry technique.

Details of manufacturers and suppliers are provided in Appendix B.

2.1 Gas Chromatography

2.1.1 Principles of Gas Chromatography

All chromatography techniques depend on the same basic principle: variation in the rate at which different components of a mixture migrate through a stationary phase under the influence of a mobile phase.

2.1.2 The Gas Chromatograph

The determination of the methane concentration of the samples collected in the field was performed using a commercial gas chromatograph (GC), fitted with a standard packed column.

The instrument used was a Chrompack CP9001 GC (Chrompack UK Ltd.). The GC was fitted with a Carbosphere (80/100 mesh) stainless steel packed column, 10 ft by $^1/_8$" o.d. (Alltech Associates Ltd.). This column was chosen because it readily separated out methane from the other components of air, and unlike molecular sieve columns, it was tolerant to the presence of water. The carrier gas was helium. The detector was a flame ionisation detector (FID). An FID detector

was chosen for methane because an electron capture detector (ECD) does not respond to methane and a thermal conductivity detector (TCD) is not sensitive enough. In addition to sensitivity an FID has the added advantage of an extensive linear response range.

a) Sample Inlet System

The GC was fitted with a sample inlet system similar to that on MIRANDA, (Section 2.3.2). Samples were introduced into the GC by way of a short vacuum line fitted with manual Nupro bellows valves (North London Valve and Fitting Company Ltd.). Samples were expanded statically into the sample loop (5 cm^3) of a 6-port, 2-way Valco valve (Chrompack UK Ltd.) . The sample vessel tap was left open for 30 seconds to achieve equilibrium. The pressure in the loop was recorded using an Edwards EPS10 pressure transducer (1050 to 1 mbar). An ice/salt cryotrap (-20 °C) was placed on the line before the loop to dry the sample. Between sample injections the line was evacuated by a rotary pump.

b) Operating Conditions

At the start of this research the carrier gas flow rate was set at 37 ml min^{-1}. Later the flow rate was dropped to 25 ml min^{-1} (because a capillary column was added to the GC for other work). Although this increased the retention volume for the methane peak, it did not affect the results, as standard gas mixtures were used daily to calibrate the instrument. The column head pressure at the start of the analysis was 50 psig.

Samples were analysed using a single temperature ramp programme. The initial temperature of 80 °C was held for 2 minutes. The temperature was then increased at a rate of 50 °C min^{-1}, to 200 °C. The final temperature was held for 2 minutes. The detector and the injector were both maintained isothermally at 250 °C.

c) Data Collection and Handling

Initially, data collection was performed by software written by Dr. G.H. Morgan. This was written in Turbo BASIC, and was able to integrate under the peaks of the chromatogram, following manual selection of the beginning and end of the peaks. Later, in February 1996, a Maestro chromatography data system (Chrompack UK Ltd.) was installed on the PC. Again, peak integration was a major feature of the software, however the system had the advantage of automated peak selection.

The retention time and the area under the peak were recorded from the computer. Comparison of retention time values ensured that the peak measured was in fact methane.

As the pressure of each sample injection differed, it was necessary to calculate the area per unit pressure (A/P) and use this to determine the methane concentration of the sample. This was done by direct comparison with a known standard gas:

$$[CH_4]_{sample} = [CH_4]_{std} \times \frac{(A/P)_{sample}}{(A/P)_{std}} \qquad \text{Equation 2.1}$$

d) Standard Gases

Within the concentration range of the samples, three standard gases were available: 2 ppmV (CK Gas Products Ltd), 11 ppmV and 102 ppmV (Aldrich Chemical Company). Tests using all three standards were undertaken to ensure linearity of response of the GC-FID. Firstly, each standard was repeatedly analysed across a range of sample loop pressures. Results are given in Figure 2.1. It is seen that the response of the GC-FID to each standard over a range of pressures is linear.

Secondly, these results are compared in Figure 2.2, showing linearity of response to methane concentration.

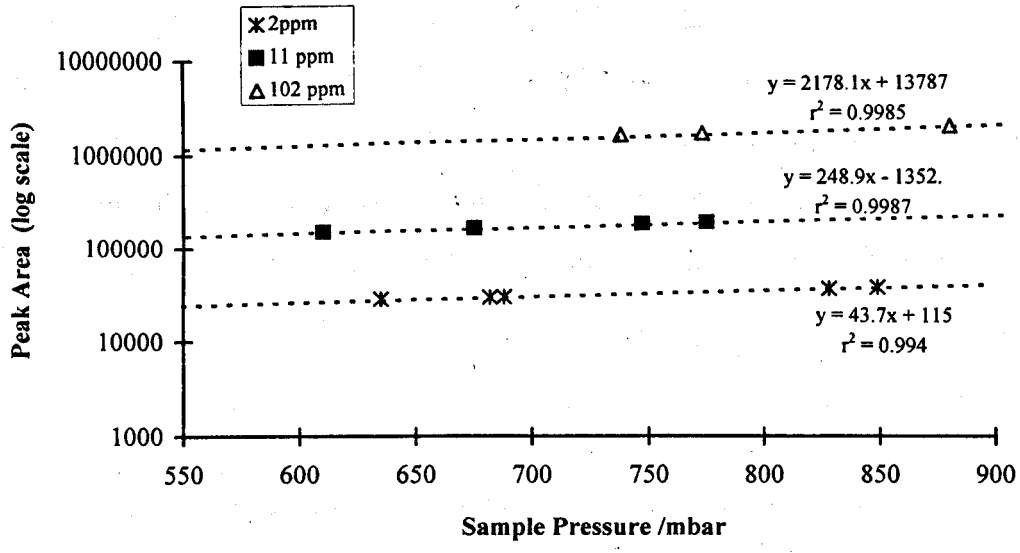

Figure 2.1 Linear response of GC-FID over a range of pressures.

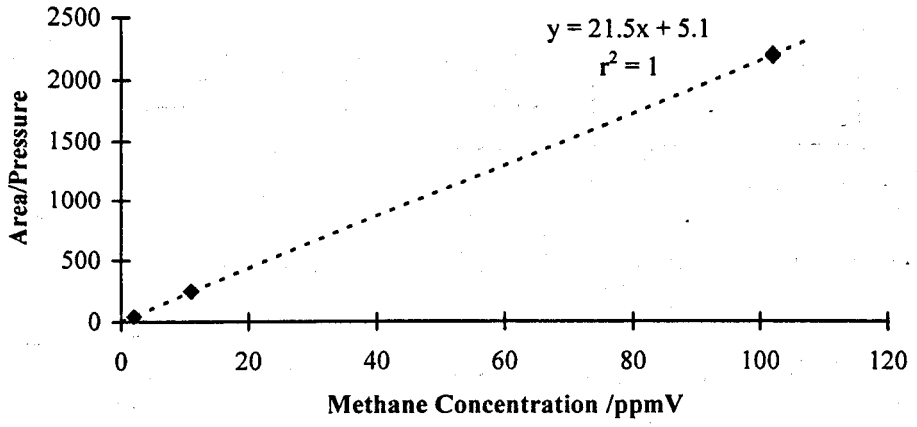

Figure 2.2 Linear response of GC-FID to methane concentration, (n=12, points from Figure 2.1).

2.2 Mass Spectrometry

Mass spectrometry is a technique for identifying complex molecules according to the manner in which they fragment when bombarded with high energy electrons. The bombardment produces many fragments carrying a charge which facilitates their separation and detection by electrical and magnetic means. It is potentially useful for measuring the ratio of the stable isotopes of a particular element (isotope ratio mass spectrometry).

The most popular instrument for stable isotope analysis is the magnetic sector mass spectrometer. It has the advantage of allowing simultaneous measurements of more than one isotope. The sector instrument is versatile, giving rise to a wide range of potential applications. A resolution of more than 10,000 can be attained by combinations of electrical and magnetic sectors (Johnson and Nier, 1953).

2.2.1 Theory of Operation

The essential components of a mass spectrometer include a sample inlet system, an ionisation source and acceleration chamber where samples are ionised, fragmented and accelerated into an analyser or separator, an ion detection and recording system and a high vacuum pumping system (Figure 2.3).

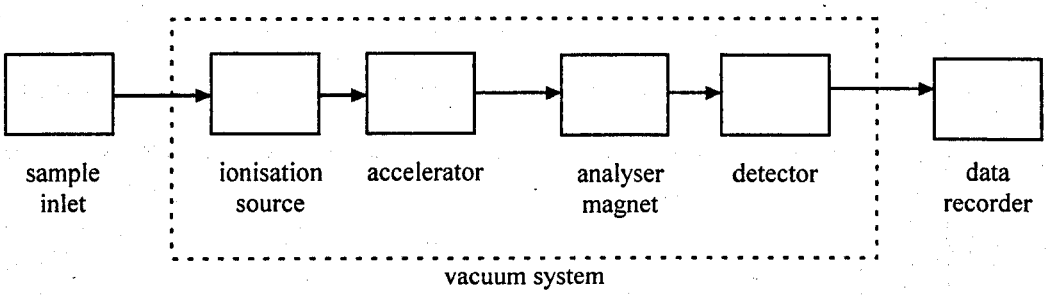

Figure 2.3 Simplified schematic diagram of a mass spectrometer.

In a sector mass spectrometer the gaseous sample is introduced through the sample inlet, usually at very low pressure (10^{-4} to 10^{-6} Nm^{-2}) to prevent loss of the charged fragments by collision with un-ionised molecules. Once in the ionising chamber, collision with thermally generated electrons results in ionisation. The resulting ions pass between two charged plates, where there is a difference of several thousand volts. In this region the ions are accelerated and pass through a slit into the magnetic field.

The separation by a magnetic analyser can be expressed in terms of the kinetic energy of the fragment ions, the accelerating voltage and the magnetic field. The

kinetic energy of fragments of mass m and charge e accelerated in a potential gradient V may be equated with the electrical force acting upon them:

$$^1/_2mv^2 = eV \qquad \text{Equation 2.2}$$

where v is the velocity of the fragments. The magnetic field, acting at right angles to the direction of motion, causes them to be deflected into a circular trajectory in which the centripetal force due to the magnet is balanced by the centrifugal force due to the kinetic energy. Thus:

$$Bev = mv^2/r \qquad \text{Equation 2.3}$$

where B is the magnetic field and r the radius of curvature of the trajectory. Eliminating v from Equation 2.2 and Equation 2.3 gives:

$$\frac{m}{e} = \frac{B^2r^2}{2V} \qquad \text{Equation 2.4}$$

For ions carrying a single positive charge, the radius of curvature is directly proportional to the square root of the mass. At a particular value of the accelerating voltage V, fragment ions of a given mass will pass along the analyser tube and through an exit slit to impinge on a collector plate. By continuously varying the accelerating voltage, fragment ions of different masses can be focused through the exit slit in turn and an entire mass spectrum recorded.

2.2.2 Typical Instrumentation Associated with a Mass Spectrometer

a) Sample Inlet System

Volatile or volatilizable compounds may be introduced into the spectrometer via a pinhole aperture or molecular leak which allows a steady stream of sample molecules into the ionisation area.

Electron impact ionisation is most commonly used for gaseous samples. A beam of electrons emitted from a hot metal filament is directed across the chamber

containing the sample gas. The electrons are given enough energy (~ 70 eV) to remove a further electron from the sample gas molecules by collision. Ions thus produced are removed through a slit in the chamber by an electric field and accelerated into the analyser.

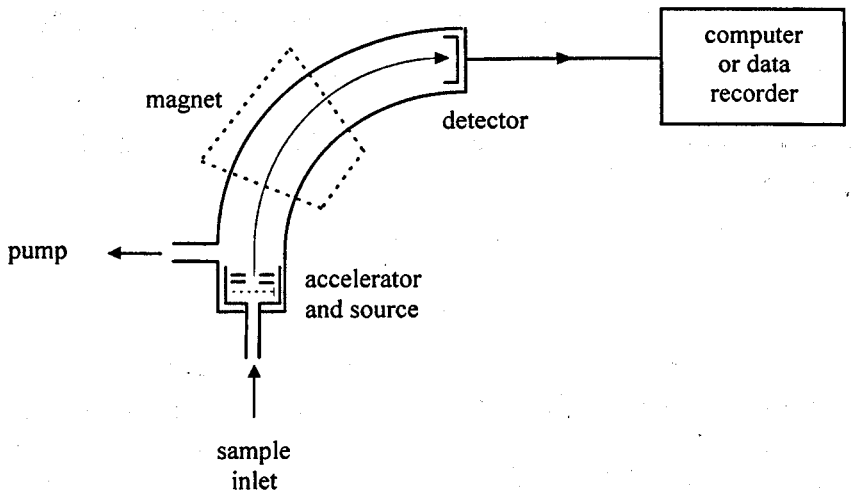

Figure 2.4 Schematic diagram of a magnetic sector mass spectrometer.

b) Analyser or Separator

After ionisation or fragmentation of the sample, positive fragment ions are accelerated into the analyser chamber by means of a potential gradient and slit system. The fragment ions are then separated in space by allowing them to move through a magnetic and/or an electrostatic field to a detector. A schematic diagram of a single magnetic analyser (sector analyser), the most widely used mass spectrometer, is shown in Figure 2.4. The trajectory of the ion is determined by its mass and the accelerating voltage (see Equation 2.4.).

c) Ion Detection and Recording System

Ions from the analyser pass through a slit and impinge on the detector. The most common ion detection system is the electron multiplier. The magnitude of the current produced is proportional to the intensity of the ion beam. The electron multiplier collector is used for low ion currents (~ 10^{-13} A). For beams of sufficient

intensity (> 10^{-12} A) simple Faraday cups can be used to collect the ion beams. Ions hitting the Faraday cup at ground potential produce a current which is then amplified by electrometer amplifiers.

The simplicity of Faraday cup collectors allows a number to be mounted close together to facilitate simultaneous collection of multiple ions beams. Defining slits are mounted above the collector cups, and are made slightly wider than the ion beams to be measured, so that small variations in trajectory of the ion beams does not affect the intensity of the detected signal. Mass spectrometers are usually interfaced with a dedicated computer to facilitate the processing and presentation of the very rapidly accumulated data and to make comparisons with library spectra.

The reliability of mass spectral data is ensured by frequent calibration of the instrument with a standard of known fragmentation pattern, or isotopic ratio.

2.2.3 The Development of Sector Mass Spectrometry for Stable Isotope Research.

The first purpose built stable isotope ratio mass spectrometer was described by Nier in 1940. Its specific purpose was the measurement of isotopes used as tracers in chemical and biochemical research. The most notable feature was the magnet which was smaller and required much less power than contemporary instruments. The cost was also greatly reduced. Dual collectors, allowing the simultaneous measurement of two isotopes of an element, were a subsequent improvement (Nier, 1947).

a) Dual-Inlet Mass Spectrometry

The inlet system was further improved by McKinney *et al* (1950), moving from a single capillary leak to a system which allowed many rapid sample-reference comparisons. This dual inlet arrangement consists of two reservoirs, one holding the sample gas and one holding a reference gas. Use of a change-over valve permits one gas to bleed into the mass spectrometer whilst the other vents to waste and *vice versa*. By matching the pressures of the two reservoirs, the ion beam intensities can

also be matched, thus improving the precision by allowing multiple comparisons between similar signals from a sample and reference gas.

The isotopic analysis of methane (CH_4) using this technique requires the conversion of CH_4 to carbon dioxide (CO_2) and water (H_2O). To avoid contamination the complete separation of the CH_4 from the CO_2 and H_2O initially present in the sample is essential. Nitrous Oxide (N_2O) must also be removed because of isobaric interference of mass 44, 45 and 46 with that of carbon dioxide. Off-line sample preparation is tedious and time-consuming which has limited the quantity of available data. A further complication is the memory effect of the water, necessitating large sample size. Generally, $\delta^{13}C$ has been measured to a precision of ± 0.04‰ and δD to a precision of ± 3‰ (Wahlen *et al.*, 1989; Lowe *et al.*, 1994). However, it remains the mainstay of modern day stable isotope ratio analysis for background air analyses.

b) Continuous Flow Isotope Ratio Mass Spectrometry

A variation on the traditional method of stable isotope analysis is continuous flow isotope ratio mass spectrometry. This uses only a capillary leak in to the mass spectrometer. Pulses of sample gas are carried past the inlet by a carrier gas, usually helium, where a proportion is diverted by an open-split interface into the mass spectrometer before the rest passes to waste; a similar system is employed for the reference gas. Sample preparation occurs on-line. Usually the inlet system is used in conjunction with gas chromatography, so on-line combustion of the components eluting from the GC may be necessary. This technique is readily automated which has revolutionised sample through-put times.

A comprehensive review of the development of this technique is given by Barrie (1991). Continuous flow IRMS is now a well established technique for measuring the stable isotopes of nitrogen and carbon in many solid and liquid samples. It has also been used with great success to measure C and N isotopes of

gaseous samples. Recent developments in continuous flow isotope ratio mass spectrometry have allowed $\delta^{13}C$ of methane, in 5 ml samples of ambient air, to be determined with a precision of 0.2‰ (Merritt *et al.*, 1995).

At present this method does not allow the determination of D/H ratios.

c) Static Vacuum Mass Spectrometry

Dynamic mass spectrometers such as those described above have the drawback that relatively large quantities of gas (> 0.25 mmol) are required. One of the reasons for this is that most of the gas entering the mass spectrometer flows to the pumps without being ionised. It has been estimated that only one molecule of sample gas in about ~16,000 is ionised and collected to contribute to the isotopic measurement (Prosser *et al.*, 1990). Static mass spectrometry of active gases developed out of the desire to investigate stable isotopes of extra-terrestrial samples (Gardiner and Pillinger, 1979). Obviously samples of meteorites, lunar and Martian materials are very small and precious, so there arose a need to reduce sample requirement from mmol to nmol or even pmol levels.

In static-vacuum isotope ratio mass spectrometry, the mass spectrometer is pumped to a high vacuum, then isolated from the pump. The entire sample is admitted to the mass spectrometer for measurement. Figure 2.5 shows a static vacuum mass spectrometer. In all other respects, static vacuum isotope ratio mass spectrometry is the same as conventional dynamic mass spectrometry.

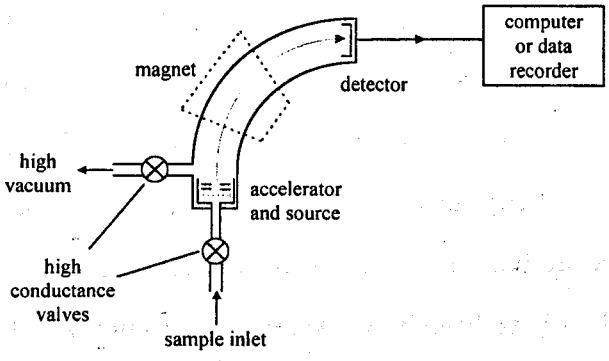

Figure 2.5 Static vacuum isotope ratio mass spectrometer (after Carr *et al.*, 1986).

d) Mass Spectrometer Performance

The following section is a glossary of the terms used to describe the performance of an isotope ratio mass spectrometer:

Linearity: Two parameters which are of importance for stable isotope mass spectrometers are ratio linearity and pressure linearity. Ratio linearity is the need for the measured ratio of isotopes of an element to be directly proportional to the true ratio over a sufficiently wide range of isotopic enrichment and depletion, otherwise accurate relative measurements would be impossible. Pressure linearity refers to the need for minimal change in measured ratio with change in sample amount.

Accuracy: Accuracy is a measure of how close to the 'true' value the measurement gets. For isotope ratio measurements this poses a problem, due to mass discrimination. However, one means of overcoming any difficulty is to measure against an internationally recognised standard. Thus, values are agreed, and all instruments measure on the same scale of enrichment.

Precision: This is a measure of the reproducibility of measurement. It is independent of accuracy. It is actually possible to obtain inaccurate measurement with a high level of precision, due to systematic error. Precision can be divided into two elements when discussing the performance of stable isotope mass spectrometers, internal and external. Internal precision gives an indication of the reproducibility of the mass spectrometer alone, while external precision provides the reproducibility of the whole system , including the sample preparation and the inlet system.

2.2.4 Alternative Approaches to Stable Isotope Research

Bergamaschi and his co-workers have recently developed an alternative to standard mass spectrometry techniques, using a tunable diode laser absorption spectrometer to measure both the $\delta^{13}C$ and the δD ratio of methane (Bergamaschi *et al.*, 1994). $\delta^{13}C$ values have been measured with an accuracy of ± 0.44‰, and δD to ± 5.1‰. However, the disadvantage of this method is the amount of sample

required. For direct measurements of $\delta^{13}C$, the minimum methane concentration of the sample needs to be 50 ppmV, (2 μmol CH_4) and for δD determination it requires 2000 ppmV, (80 μmol CH_4).

2.3 MIRANDA

A Methane Isotope Ratio Analyser (MIRANDA) was developed in two stages within the Planetary Sciences Research Institute at the Open University. Initially a static vacuum mass spectrometer was shown to be able to measure the $^{17}M/^{16}M$ ratio of nanomole aliquots of standard methane with a precision of ~1‰ (Morse, 1991). The initial application of this technique was the analysis of δD of water from extra-terrestrial samples. However, the potential was soon recognised for using this instrument for research into the isotopic composition of atmospheric methane samples.

An inlet apparatus was developed to quantitatively separate methane from air samples and transfer the gas to the existing mass spectrometer via a high vacuum inlet (Figure 2.6) (Morse *et al.*, 1996; Butterworth, 1997). Separating methane from air by packed column gas chromatography has been a standard procedure for two decades, and capillary columns are commonly used for sample preparation in dynamic mass spectrometry. The packed column gas chromatograph and the high vacuum inlet system were designed to provide purified, dry methane sample, removing all traces of the carrier gas. As the sample requirement for the mass spectrometer was 0.1 - 0.6 nmol CH_4, 10 ml of air sample provided sufficient methane at ambient concentration for isotopic analysis. Full details of the development of this instrument can be found in Butterworth (1997).

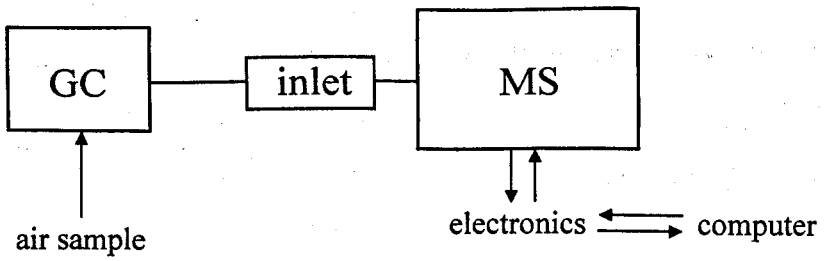

Figure 2.6 Schematic Layout of MIRANDA

2.3.1 Theory of the combined isotope composition ($\delta^{17}M$) of methane

Determination of the $\delta^{17}M$ of methane depends upon the measurement of the mass 17 and mass 16 ion beam intensities. The mass 17 peak of methane consists of two isotopomers, $^{13}CH_4$ and $^{12}CDH_3$, whereas the major contributor to the mass 16 peak is $^{12}CH_4$. The ratio of mass 17 to mass 16 for methane can thus be given by:

$$\frac{^{17}M}{^{16}M} = \frac{^{13}C}{^{12}C} + 4\,\frac{D}{H} \qquad \text{Equation 2.5}$$

where ^{17}M and ^{16}M are the mass 17 and mass 16 ion beam intensities, $^{13}C/^{12}C$ is the carbon isotope ratio and D/H is the hydrogen isotope ratio of the methane. Since methane consists of one carbon molecule and four hydrogen molecules, there is a need to incorporate a factor of four into Equation 2.5. The $\delta^{17}M$ value is calculated in the same fashion as $\delta^{13}C$, as explained in Section 1.2.3:

$$\delta^{17}M = \frac{(^{17}M/^{16}M)_{sample} - (^{17}M/^{16}M)_{reference}}{(^{17}M/^{16}M)_{reference}} \times 1000 \qquad \text{Equation 2.6}$$

The reference gas chosen was NGS#3 (Morse *et al.* , 1996), because it had the highest methane concentration, and its isotope ratios were most representative of the samples that would be analysed using this technique. It is defined as having a $\delta^{17}M$ value of 0‰; and a $^{17}M/^{16}M$ ratio of 0.0109351 (calculated from published data (Dumke *et al.*, 1989)).

By substitution of Equation 2.4 into Equation 2.5, $\delta^{17}M$ can related to $\delta^{13}C$ and δD in methane by:

$$\delta^{17}M = \left(\frac{4 \times (D/H)_{sample} + (^{13}C/^{12}C)_{sample}}{(^{17}M/^{16}M)_{reference}} - 1 \right) \qquad \text{Equation 2.7}$$

where $(D/H)_{sample} = (\delta D/1000 + 1) \times (D/H)_{SMOW}$

and $(^{13}C/^{12}C)_{sample} = (\delta^{13}C/1000 + 1) \times (^{13}C/^{12}C)_{PDB}$

SMOW = Standard Mean Ocean Water;

$(D/H)_{SMOW} = 1.5576 \times 10^{-4}$ (Hagemann *et al.*, 1970).

PDB = Pee Dee Belemite;

$(^{13}C/^{12}C)_{PDB} = 0.0112372$ (Craig, 1957).

By substituting all this information into Equation 2.7, it can be seen that $\delta^{17}M$ can be determined from $\delta^{13}C$ and δD measurements in the following way:

$$\delta^{17}M = (1.02893 \times \delta^{13}C) + (0.0569929 \times \delta D) + 84.9205 \qquad \text{Equation 2.8}$$

Thus, it is possible using Equation 2.8 to calculate a $\delta^{17}M$ value for methane if its carbon and hydrogen isotopic compositions are known. This has been done for the CH_4 sources reported by Wahlen (1994) (Section 1.2.3, Figure 1.5) and is shown in Figure 2.7.

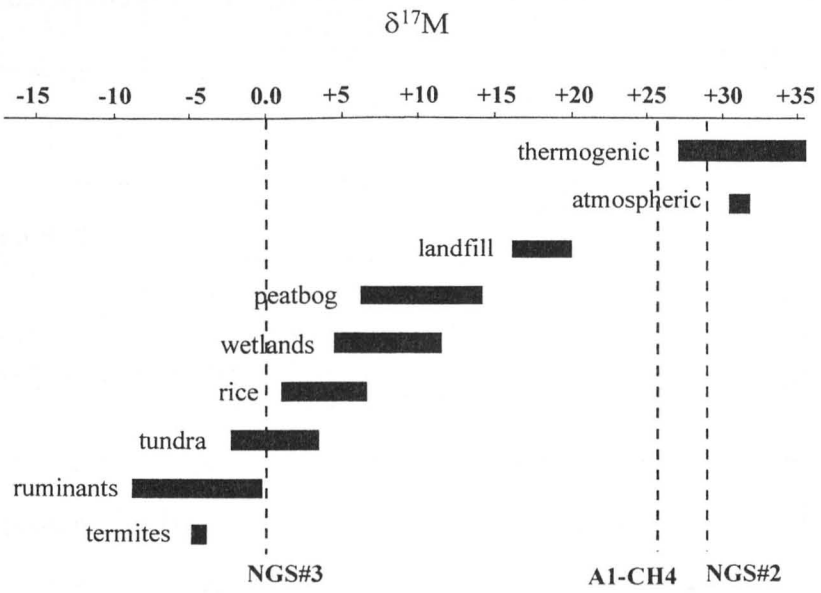

Figure 2.7 $\delta^{17}M$ values for various methane sources, calculated from data published by Wahlen (1994). Al-CH_4 is the working methane standard, NGS#1, NGS#2 and NGS#3 are international gas standards.

2.3.2 A Description of MIRANDA

As discussed earlier, a pseudo-GCMS system, colloquially known as MIRANDA, was used in this work. MIRANDA consists of a (dynamic) gas chromatograph linked *via* a high vacuum inlet system, to a static vacuum isotope ratio mass spectrometer, as shown in Figure 2.8. In this section the apparatus which constitutes MIRANDA is described in detail, including computer control and data acquisition. The operational procedures for analysing samples through MIRANDA are discussed in Section 2.2.3.

The general principle was to separate methane out from the other components of air and cryogenically trap all the eluted methane from the carrier flow. The helium and the last traces of nitrogen were removed in the inlet system and the methane transferred to the mass spectrometer.

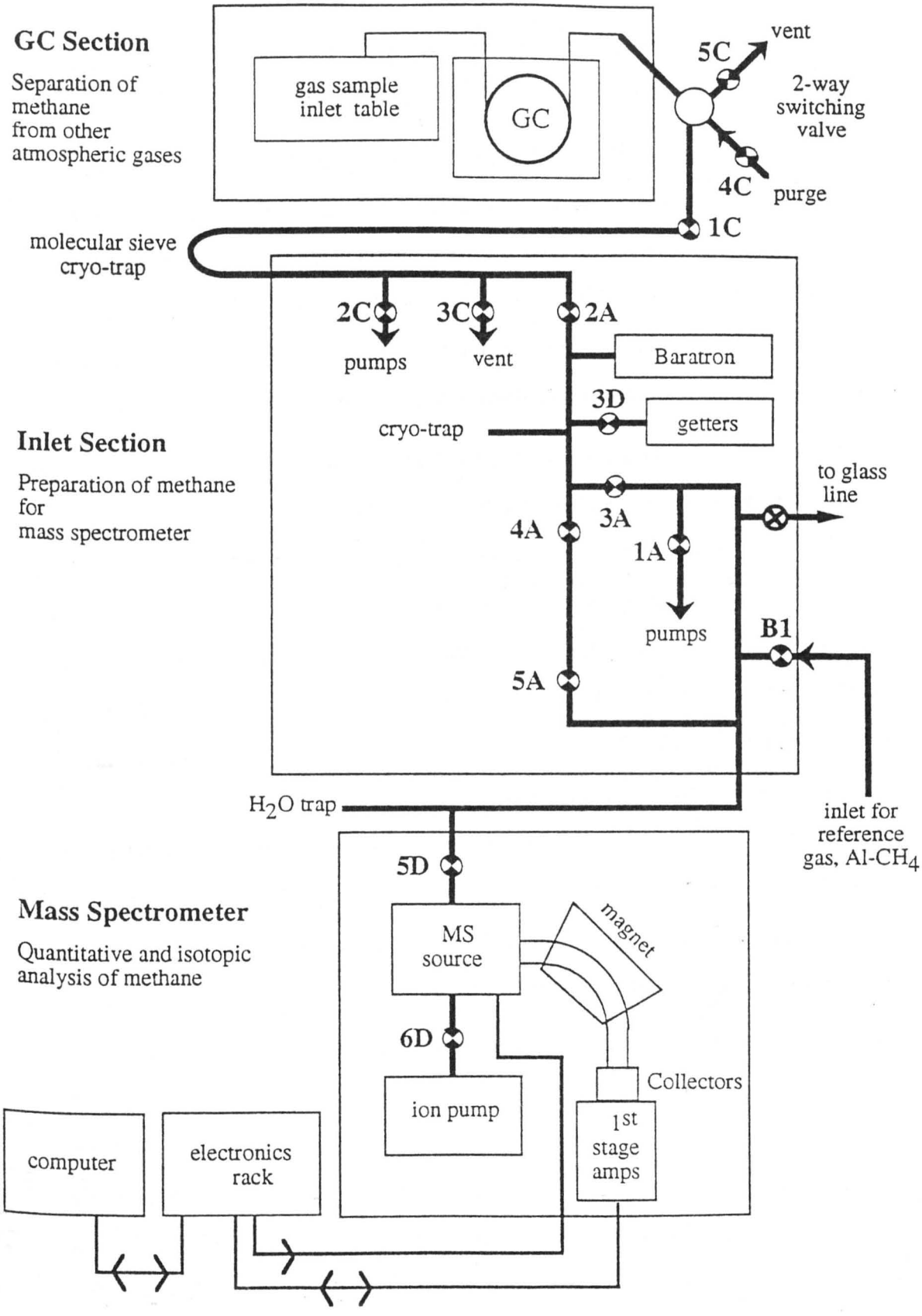

Figure 2.8 Schematic diagram to show MIRANDA (see Fig 2.9 for key to symbols).

a) Gas Chromatograph

The purpose of the gas chromatography was to separate the methane from the other constituents of air, *e.g.* nitrogen, oxygen, carbon dioxide, nitrous oxide.

Gas chromatograph: The gas chromatograph used was the same type that was used for methane concentration measurements: a Chrompack CP9001 GC, model 903A, fitted with a Carbosphere (80/100 mesh) stainless steel column, 10 ft by $^1/_8$" o.d.. (Alltech Associates Ltd.). The GC was run isothermally at 50 °C for sample analysis. The GC had been highly modified during the system development to such an extent that it was merely used as a constant temperature oven.

Sample Inlet: The small sample inlet vacuum line attached to the front end of the GC was made from thick walled stainless steel tubing. The inlet was connected to the GC *via* a Valco 6-port, 2-way gas sample injector (UWT series, Chrompack UK, Ltd.) and was pumped by a rotary pump (E2MS, Edwards High Vacuum International). Figure 2.9 shows the detail of the arrangement. The gas sample injector was fitted with a 10 ml sample loop. The sample was injected onto the column by flushing the loop with carrier gas. Samples were collected and stored in glass flasks which are described in detail in Section 3.1.1. The flasks had a $^1/_4$" o.d. side arm which fitted exactly into the Swagelok® T-piece in the sample inlet. The joint was rendered vacuum-tight by use of a standard Teflon® ferrule. The total volume of the sample inlet was 14 ml. The pressure in the inlet was recorded using an Edwards EPS10 pressure transducer (1050 to 1 mbar).

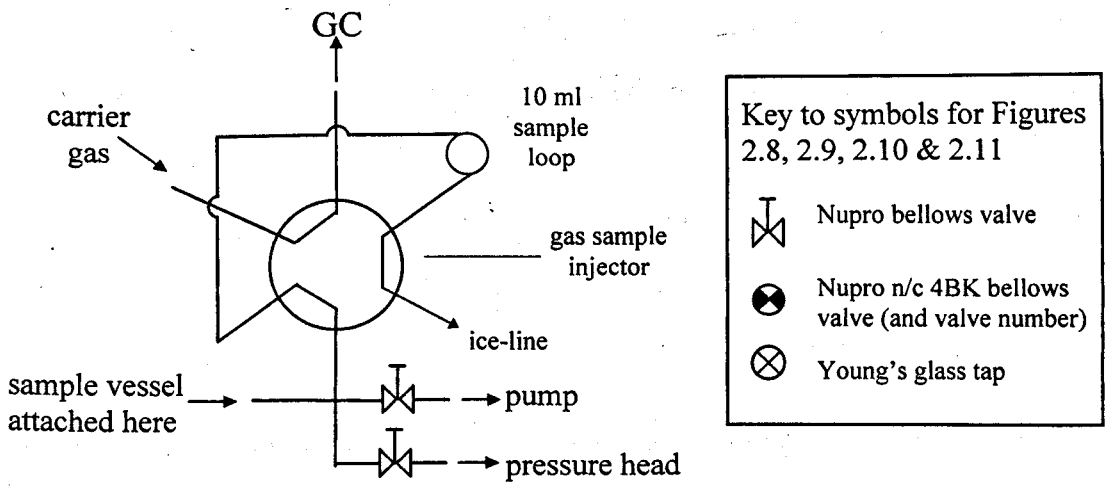

Figure 2.9 Sample inlet system in the load position. One valve port also allowed the introduction of samples from the independent sample preparation line used in the analysis of CH_4 trapped in ice cores.

Carrier Gas: High purity (grade 5.5) helium (Air Products, Speciality Gases) was used as a carrier gas. The helium was further purified using a molecular sieve trap (IMS-100, SGE (UK) Ltd.) to remove water and carbon dioxide, and an Oxy-trap (Alltech Associates Ltd.) to remove oxygen. A 13X molecular sieve (Phase Separation Ltd.) trap at 77K was used to remove nitrogen and hydrocarbons. The flow rate of carrier gas through the column was set at 20 ml/min by a needle valve.

b) Dynamic-Static Interface

The basic principle of this section was to transfer the methane eluting from a dynamic system into a static inlet. As the sample was passing through the GC, a second helium flow purged the cryogenic methane trap to prevent laboratory atmosphere back-flushing onto the trap. When the methane eluted from the column, carrier flow was switched through the cryotrap, by means of a 4-port, 2-way valco switching valve. Once the methane had been collected, the carrier flow was switched back to vent. The trap was closed off from the helium supply and from the vent so that the remaining non-condensable carrier gas could be pumped away. When sufficient vacuum had been attained the trap was heated, releasing the methane sample, which was then transferred to the main inlet of the mass spectrometer

through Valve 2A. It was important that all the methane from the sample was transferred to the mass spectrometer to avoid any possible fractionation effects from the GC.

Cryotrap: The trap contained 13X ungraded molecular sieve (Phase Separations Ltd.) and was cooled to 77K by immersion liquid nitrogen at the appropriate stage of sample analysis.

Switching Valve: A 4-port, 2-way Valco valve, (Alltech Associates Ltd.) was used to divert the carrier flow through the cryotrap as the methane was eluted.

c) High Vacuum Inlet System

The purpose of this section of the instrument was to further purify the methane sample before transporting it into the mass spectrometer. The methane was cryogenically trapped onto the "baratron finger" while any traces of condensables such as residual helium were pumped away. The methane was then desorbed by heating and the pressure recorded. If necessary, the sample was split at this point, to provide optimum sample size for analysis by the mass spectrometer. Any other active gases present, particularly nitrogen, were then removed by getters. The sample was finally passed *via* a cryogenic water trap into the mass spectrometer. Moving the gas around the inlet was achieved by the use of pneumatically operated Nupro valves.

Inlet: Metal pipework was utilised because the inlet needed to be bakeable in order to outgas adsorbed species, particularly water. A vacuum was maintained in the inlet at $\sim 4 \times 10^{-7}$ mbar by a Turbomolecular pump.

Valves: All the valves in the GC-MS interface section and the high vacuum inlet system were pneumatically operated, normally closed, stainless steel Nupro bellows valves, controlled by electronically activated solenoid valves, (SMC). Normally closed valves had been chosen so that in the event of a power failure the vacuum in the inlet would be protected.

Baratron Finger: This cryotrap contained 13X molecular sieve (Phase Separations Ltd.). It was attached to the main inlet *via* a $^1/_4$" Cajon® VCR® seal using a Cajon® frit flange (North London Valve and Fitting Company Ltd.) to prevent molecular sieve getting into the main inlet. The trap was cooled to 77K, by immersion in liquid nitrogen at the appropriate time in the sample analysis.

Baratron: This was a conductance manometer (Baratron, Chell Instruments Ltd.) giving a pressure reading which was used to estimate the quantity of methane in the inlet.

Getters: The getters used were non-evaporable, St172 (St172/OU/11-6.8/200, SAES Getters (GB) Ltd.). The getters were necessary because ~ 0.004% of the nitrogen from the air samples eluted through the GC column. The sample transferred to the inlet was thus about 10% methane in nitrogen, but it needed to be close to 100% methane for meaningful isotope measurements. The getters operated at 50 °C and were able to getter nitrogen from six air samples before being reactivated at 450 °C for ten minutes.

Water Trap: This glass trap was kept at 88K by warming it using heater tape, while it was immersed in liquid nitrogen. The purpose of this trap was to remove any trace of water from samples or reference gas before entering the mass spectrometer. Water would directly effect the m/e 17 beam intensity.

Automatic Aliquoter: An automated system had been developed based on an original design by Russell (1992) to provide aliquots of reference gas (Figure 2.10). Automation helps eliminate operator error and increases precision of measurement. A lecture bottle of methane (99%, Aldrich.) was used to fill a large reservoir with reference gas to about 15 bar. The rest of the aliquoter was continuously pumped through the backing line (B1 closed to the inlet, B2 and B3 open to the pump).

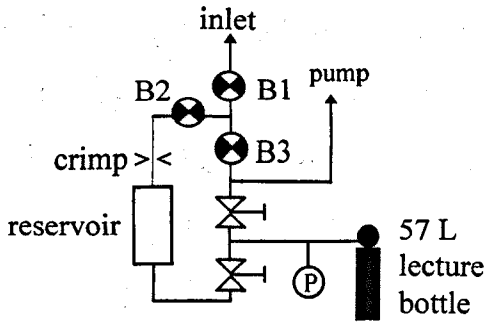

Figure 2.10 Schematic diagram of automated reference gas aliquoter, Al-CH_4.

d) Mass Spectrometer

This was a static mass spectrometer; which meant that all of the sample was expanded into the ionising source, remaining there, isolated from the pumps, throughout the analysis. The source, flight tube and the detectors were all pumped out between analyses by an ion pump, to below 10^{-11} mbar.

Source Control: Electron impact ionisation was used as the ionising source. A hot tungsten filament produced an electron beam at ~ 85 eV. The accelerating voltage was 3000V.

Mass Analyser: A modified Micromass 602E analyser (Vacuum Generators Isotopes Ltd.) was employed. It consisted of an open source, an extended geometry flight tube and Faraday collectors with high gain remote head amplifiers and housing. The analyser was continually pumped to ultra high vacuum (UHV).

Electronics and Data Acquisition: By increasing both the number of data collections per sample, and the speed of analysis, it is possible to counter the relatively short half life of the ion beams, which is imperative for high precision measurements on small samples of methane. Data acquisition was by almost simultaneous collection. The source conditions were controlled by the desktop computer *via* a digital-to-analogue converter (DAC). By scanning across a small range (80V) the correct accelerating voltage could be chosen. The beam intensity

data were then collected and relayed back to the computer *via* high gain amplifiers and the ADC unit.

e) Computer Control

The software for the computer control system was originally written *in house* by Mr. J. Higgins and later up-dated by Dr. A.D. Morse. Computer control can be divided into two separate elements. The first part is the control and manipulation of the mass spectrometer and the data collection, which was done entirely by computer control. The user had limited power over this aspect of the software, only being able to change certain parameters. These are discussed in detail later. The second aspect of computer control is the manipulation of the valves on the inlet system, which could be controlled manually, or automatically by the computer.

Computer control eliminates human error in timing, allowing much better reproduction of experiments, and thus hopefully better precision in results (Prosser, 1993). The software was designed to allow the user to create automated experiments using a 'script' consisting of a variety of commands, in any appropriate order. The commands and their uses are summarised below, in bold type. Some of these commands could be activated from the pull down menus, as could other commands which are described in the following section.

i. Automated Experiments

Experiments could be run as a single analysis, or as automatic repeat analyses. In the latter case the computer put the **Run Again** command at the end of the script, allowing repeat analysis of reference gas aliquots *ad infinitum.*

Load Script: There were several template scripts designed for particular tasks, *e.g.* zero enrichments or analysis of samples of a particular CH_4 concentration. These could be loaded by the user into a new script which would be given the users preferred name. The new script could then be tailored to meet the users own needs. This also kept the original script intact. As data were saved under the name of the

script, this allowed easy data retrieval. For example, work on peatbog samples were called pbog, whereas scripts for ice core work were called ice. Also, calibration scripts were usually given the current date. Load script was also useful for building up a new script comprising a number of earlier scripts.

Open Valve/Close Valve: When valves were switched to computer control, the manual setting was over-ridden. Under computer control, valves could only be operated as part of a script , or *via* the on-screen valve control panel. Valves used for routine sample analysis would normally be operated automatically, leaving valves not involved in that particular script off computer control.

Wait: The computer would wait for a given number of seconds, before carrying out the next command.

Message: This allowed a message to be displayed in the run status bar. This helped the user know exactly what point the analysis had reached, and allowed instructional prompts to be shown. For example, 'sample on the getters, note the new baseline'.

Centre Peaks: This command caused a small range of accelerating voltage to be scanned, to set the optimum value between the major and minor peak centres. The value determined ensured that simultaneous detection of ion beams was carried out (at constant accelerating voltage and magnetic field) at the flat portions of the peaks.

Data Collection: The data acquisition routine switched rapidly between the beams signals to produce a number of beam intensity measurements. The number of points per measurement could be varied in a parameters dialogue box. A summary window showed the results of the data collection. "Beam Decays" and "Ratios" windows could be viewed when the data collection was complete.

Background Scan: This command caused a specified range of accelerator voltage to be scanned, using one collector at a specified gain. The parameters were set using a dialogue box from the main menu, or from within the scan window.

ii. Menu Commands

Peak centring, data collection and background scans could all be generated from the appropriate pull-down menu. The following commands were also activated in that manner.

Zero Amplifiers: The amplifiers were zeroed by measuring the ion beam signal with no sample in the mass spectrometer, to correct for amplifier offset. It was important that the peaks were centred properly prior to this. Although the amplifiers could be zeroed at any point at the present accelerator voltage, in practice it only needed to be done at the start of each day.

Monitor Beams: This command had two uses. It could be used to scan across a given range of accelerating voltage and show up to four beam intensities, or to plot beam intensity against time for a given voltage. This was particularly useful for looking at changes in a particular peak, for example when argon leak testing.

Data Recall: Data from previous experiments could be brought up on the screen using this command. The data summary, beam decays and the ratios windows were retrieved.

Parameters: Adjustment of the parameters of any computer controlled operation could be made under this command. For example, the user might want to alter the accelerating voltage or the amplifier gains.

2.3.3 Sample Analysis

The isotopic analysis of air samples is a protracted and complex procedure. A step by step guide to running an air sample through the instrument is given in this section. This would usually be performed with the valves under computer control, but could, if necessary, also be achieved manually. Valve numbers match those given in Figure 2.8.

In preparation to run a sample, the sample flask was attached to the sample inlet *via* a Swagelok® union (Figure 2.9). The inlet was pumped on the rotary pump,

while the sample flask remained closed. Once sufficient vacuum had been achieved the inlet was isolated from the pump, and the sample flask opened for 30 seconds, allowing the sample to equilibrate in the inlet. The pressure in the GC inlet was noted and room temperature recorded. The sample was then injected onto the GC and the stopwatch activated. Comprehensive details of the analysis are given in Table 2.1. Once the sample had been analysed, two aliquots of reference gas would also be measured, as described in a previous section. This was all part of the computer controlled programme.

Samples which contained a higher concentration of methane than ambient air were split *prior* to being exposed to the getters. There were two reasons for this: firstly, the getters could only absorb a finite amount of nitrogen before requiring reactivation; secondly, it was difficult to calculate the precise amount of CH_4 entering the mass spectrometer, if the baratron pressure was recorded after the sample had been gettered. The split was achieved by incorporating the commands into the computer controlled experiment script, for improved reproducibility. Details of the various splitting options are given in Table 2.2. If necessary, other combinations of split could also be used.

Table 2.1 Details of actions involved in analysing the isotopic composition of an air sample on MIRANDA.

Time (mins)	Action	Dura-tion	Significance
0	Sample injected onto GC manually	11.5 mins	Methane was separated from other components of air.
11.5	Started run on computer		Valves were now under computer control.
	Closed 3C Opened 5C	180 s	Heater off, N_2 (l) placed on molecular sieve trap. Cryotrap was frozen down and filled with He.
14.5	Closed 5C Opened 3C	60s	Cryotrap at -192 °C, He was purging trap. The 'purge' flow rate was measured.
15.5	4-way valve switched GC flow through the cryotrap	360s	Methane eluting from the GC was trapped on the molecular sieve. The carrier gas flow rate was measured by the operator.
21.5	4-way valve switched back		GC was now venting to waste.
	Closed 3C, 1C and 4C Open 5C		Cryotrap isolated. Prevented backflush of air to 3C.
	Opened 2C	120s	He pumped away on rotary pump.
23.5	Closed 2C		
	Closed 3D		Closed off getters to prevent contamination.
	Opened 2A	150s	Cryotrap pumped by turbo pump.
26.0	Closed 3A	450s	N_2 (l) removed from mol. sieve trap, heated to 150 °C. N_2 (l) placed on 'baratron finger' trap, heater switched off. Methane transferred from cryotrap to baratron finger.
33.5	Closed 2A Opened 3A	60s	The methane was now all transferred to the finger. Remaining non-condensables were pumped away. The baseline pressure in the baratron was recorded by theoperator.
34.5	Closed 3A Opened 2C, 1C	225s	N_2 (l) removed from 'baratron finger,' heated to 150 °C. Meanwhile the cryotrap is pumped out.
38.25	Opened 2C, 4C	10s	Valves reset, cryotrap filled with He.
	Closed 5C Opened 3C		Valves reset.
	Wait	10s	Baratron pressure recorded by the operator. Sample was divided at this point if too large for mass spectrometer.
38.6	Opened 3D	100s	Sample gettered.
40.25	Closed 3D		
	Closed 1A		Inlet isolated from the pump.
40.5	Opened 3A	15s	Sample expanded into mass spectrometer inlet.
	Closed 6D		Mass spectrometer isolated from its pump.
	Opened 5D	15s	Sample entered mass spectrometer.
40.75	Closed 5D		Sample inside mass spectrometer.
	Opened 1A		Inlet pumped again.
	Centre Peaks Collect Data Background Scan		Isotope Ratio of the sample was determined.
	Opened 6D		Mass spectrometer pumped out.
45	Opened 3A		Getters pumped out.

Table 2.2 Scripts for samples with elevated levels of methane.

Script Name	Methane Concentration	Size of Split (% entering ms)	Manner of Split
airsmple	up to 2 ppmV	60%	None
3-4ppmGC	2-4 ppmV	43%	Expand into expansion volume, then close.
6-8ppmGC	5-8 ppmV	21.5%	Expand into expansion volume and close. Pump Baratron section, then expand sample back into Baratron section.
bigsmple	9-11 ppmV	9%	Expand sample into inlet section, close Baratron section. Pump inlet.

2.3.4 Mass Spectrometer Performance

a) Interference

Two things cause interference in the mass spectrometer. The main cause of isobaric interference on the sensitive minor collector was water. This directly affected the measured isotope ratio, hence the need for the water trap on the mass spectrometer inlet.

The presence of nitrogen in the mass spectrometer can also affect isotope ratio measurements, by colliding with the ions and deflecting the ion beam from its path.

b) Reference Gas

Mass spectrometer systems do not yield true isotope ratios, because they possess inherent mass discrimination. In order to compare results from different laboratories, it is therefore necessary to make mass spectrometric measurements against an international standard. However, international standards are expensive, so it is usual to have a working standard which is employed each time a sample analysis is made. The working standard is regularly calibrated against the international standard.

To avoid any memory effect the sample was evacuated from the source for five minutes before the reference gas was admitted. The size of the sample and reference gas must be closely matched to maximise precision, so that they may be assumed to behave in a similar fashion in the source. The two gases entered the mass spectrometer in the same manner and were subject to identical data acquisition protocols.

To collect an aliquot of reference gas, valve B3 was closed and methane was allowed to bleed into the small volume between B1, B2 and B3 (Figure 2.10). The size of the aliquot was determined by the bleed time. B2 was then closed to shut off the capillary flow and the gas was expanded into the inlet by opening B1 for 20 seconds. The reference gas was then admitted into the mass spectrometer. By adjusting the crimp, the bleed rate for the aliquoter was set at approximately 1 pmol per second. The size of the aliquot was calculated to the nearest 0.1 second, thus the sample and reference could theoretically be matched to within 0.1 pmol.

c) Calibrations

In MIRANDA's case the international standard used was NGS#3. It was stored in a 2 L Pyrex® bulb, which was attached to the high vacuum inlet *via* a glass line, (see Figure 2.8) and a variable aliquoter (Figure 2.11). The working reference gas standard (Al-CH_4) was calibrated against the international standard NGS#3 every month.

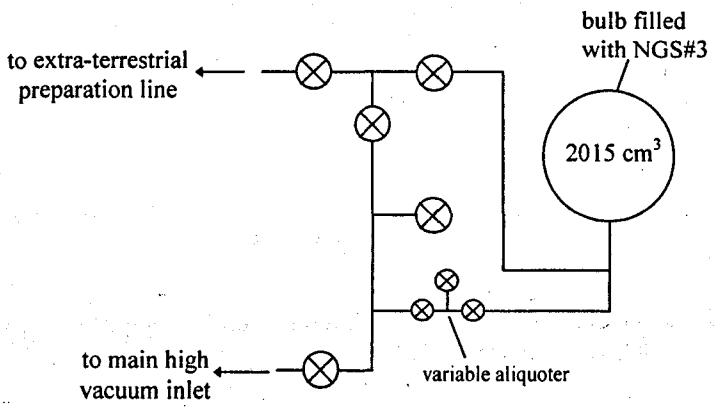

Figure 2.11 Schematic diagram to show the NGS#3 gas inlet.

2.3.5 Performance of MIRANDA

Tests run by Anna Butterworth (1997) showed MIRANDA to have measured the m/e 17/16 isotope ratio of methane gas with a precision of better than 0.2‰, for a sample sizes ranging from 0.1 to 0.6 nmol.

a) Zero Enrichments

To determine the precision of the mass spectrometer *zero enrichment* analyses were regularly made. The mass spectrometer was left to automatically analyse many replicate samples, typically 300 seconds of laboratory reference gas, A1-CH_4. Figure 2.12 shows a typical example of a zero enrichment plot. Sometimes these experiments were left running unattended overnight in which case the inlet water trap was not immersed in N_2 (l) , but rather was at 85°C. The delta value of each sample, measured against the next, should be 0‰. The spread of the values about the mean were quoted as a 1σ standard deviation. Mass spectrometer precision was found to be ± 0.21‰ (n=83).

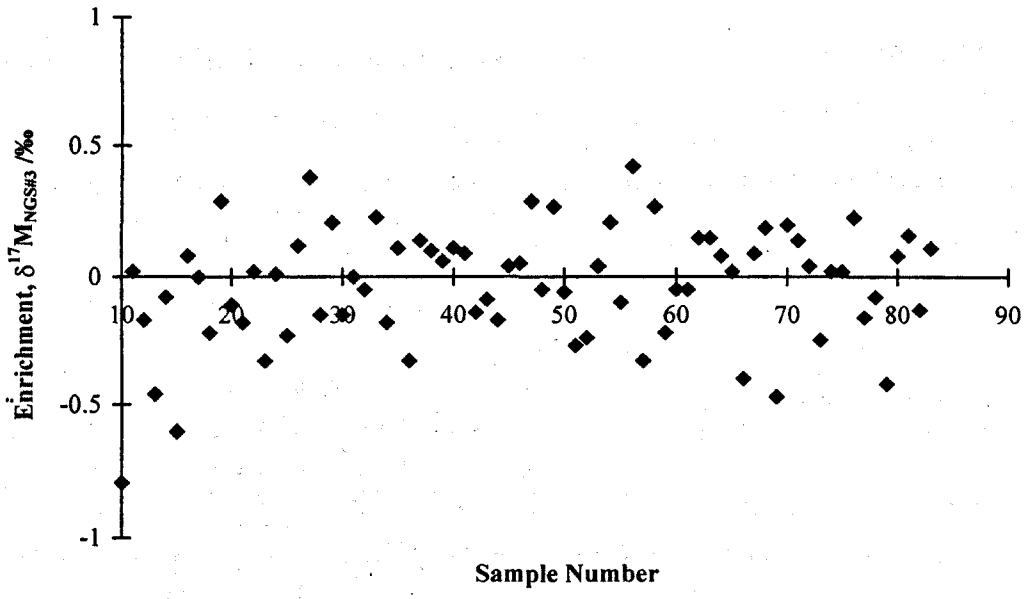

Figure 2.12 Zero enrichment plot acquired overnight on 29th July 1997 (n=83, 1σ std dev = ±0.21‰).

b) Reproducibility

To check that there were no problems with the isotope ratio measurements made via the whole analytical system, a 2L Pyrex® bulb was filled with 2 ppmV CH_4 in N_2 standard (CK Gas Products Ltd.) and the $\delta^{17}M$ was measured as + 35.61 ±0.31‰ (n=4). Each time samples were analysed, a sample from the bulb would be measured to ensure the reproducibility of the system. Each time the bulb was re-filled, the repeat analyses of the isotopic composition were made, and the variation was calculated. Two data sets are shown in Figure 2.13, arising from two re-fillings of the standard bulb. If the $\delta^{17}M$ value for the standard bulb differed from the mean by more than the 2σ variation, sample analysis was abandoned until the cause of the problem was ascertained, and rectified.

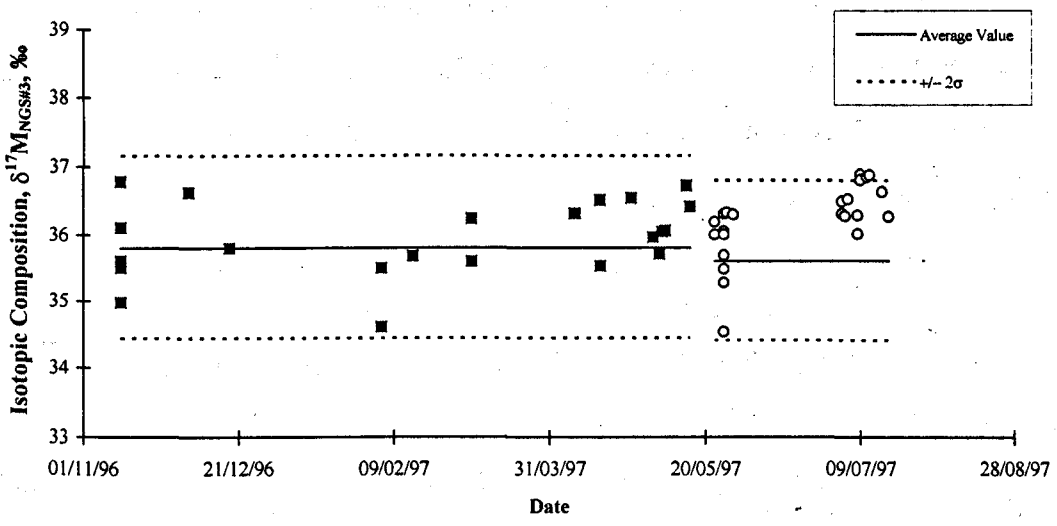

Figure 2.13 Reproducibility of the combined isotopic composition of methane from a 2 ppmV standard bulb, as measured on MIRANDA. Two sets of data arise from re-filling the glass bulb.

c) Accuracy

Tests have shown that the accuracy of the mass spectrometer in determining $\delta^{17}M$ of three international standards, NGS#1, NGS#2 and NGS#3 is within ± 0.4‰ (Butterworth, 1997). The data are given in Table 2.3.

Table 2.3 Measured and calculated $\delta^{17}M_{NGS\#3}$ values for three international methane standards (Butterworth, 1997).

Sample	Measured $\delta^{17}M$ *v* NGS#3	Calculated $\delta^{17}M$ *v* NGS#3
NGS#1	+48.38 ± 0.18	+47.13 ± 0.37
NGS#2	+29.76 ± 0.13	+28.90 ± 0.35
NGS#3	-24.89 ± 0.09	0.00 (defined)

d) Precision

Replicate analysis of samples allows some measure of the precision of MIRANDA as a whole to be determined. For example, repeat same day analyses of the 2 ppmV standard bulb previously mentioned gave a $\delta^{17}M$ value of +35.61 ± 0.31‰ (n=4). Repeat analyses of an air sample from Snowdonia gave a measurement of $\delta^{17}M$ = +31.78 ±0.52‰ (n=4).

e) Concentration

It was important that all the methane from the sample inlet reached the mass spectrometer and was analysed for its isotope composition. Loss of methane in the system could result in isotopic fractionation. The concentration of CH_4 in the sample was determined, using the ideal gas equation, PV = nRT, to calculate the total amount of gas that was present in the sample loop, and calculating the amount of methane reaching the mass spectrometer from the ion beam intensity and the reference gas bleed rate.

Figure 2.14 shows the concentration of the 2 ppmV standard bulb as measured on MIRANDA over a number of months. The average value is 2.05 ±0.9 ppm (n=50). Sample pressure ranged from ~ 350 to 1040 mbar. A further check on the accuracy of the concentration of the methane measured by MIRANDA was a comparison of the concentration of CH_4 in samples as measured on the GC compared

to that measured by MIRANDA. This comparison is shown for samples taken in June 1997 in Figure 2.15. This particular set of samples was analysed on MIRANDA using five different scripts to allow for the range of concentrations.

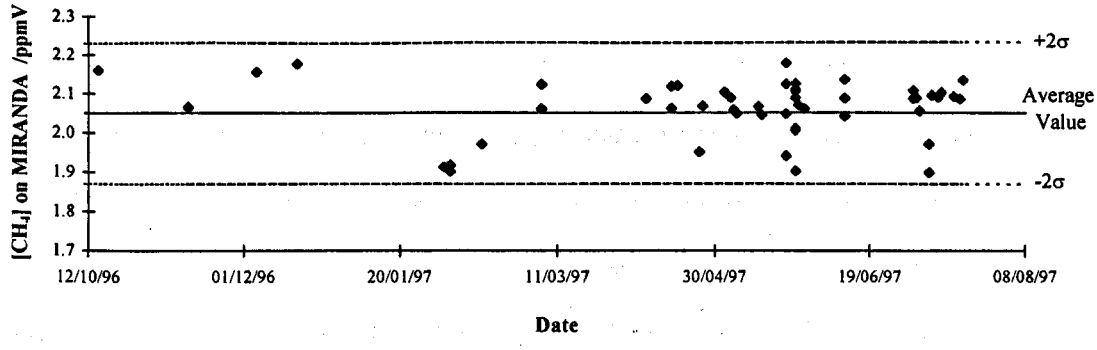

Figure 2.14 Concentration of methane in a 2 ppmV standard bulb as measured on MIRANDA (n=50).

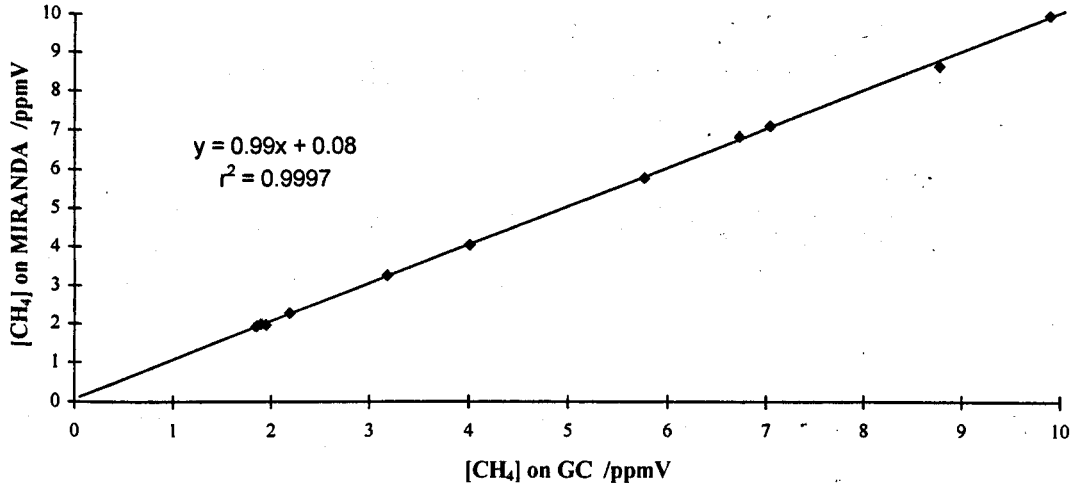

Figure 2.15 Comparison of CH4 concentration measured by MIRANDA and the GC for samples collected in June 1997.

2.4 D/H analysis

Water samples taken from the peat bog (see Section 3.2.1 for full experimental procedure) were isotopically analysed for both δD and $\delta^{18}O$. This analysis was kindly conducted by Professor Tony Fallick and Dr. Susan Waldron at the Scottish

Universities Research and Reactor Centre in East Kilbride. δD was analysed by reaction with hot uranium (Friedman and Smith, 1958), to a precision of ± 2‰. $\delta^{18}O$ was analysed by Epstein-Mayeda equilibration, to an overall precision of ± 0.2‰.

2.5 Summary

Standard techniques for measuring the methane concentration in air samples using gas chromatography, and for determining the isotopic composition of water by mass spectrometry have been briefly outlined.

A novel technique for determining the combined stable isotopic composition of methane by static vacuum mass spectrometry had been described in detail.

Combined Isotopic Composition of Methane Emissions from an Ombrotrophic Mire

3. Introduction

The main aim of this project was to characterise methane emissions from an ombrotrophic mire in terms of the isotopic composition of the CH_4 flux, and to evaluate the effect of the main environmental factors on the isotopic composition. There has been a systematic and concerted effort in the UK to constrain the methane budget for the UK over the past five years, mostly funded by the Natural Environment Research Council (NERC) *via* the Terrestrial Initiative in Global Environmental Research (TIGER) programme (Section 1.5). The research undertaken for this study comprises the main isotope work on methane in the TIGER

programme, however there has been a great deal of work conducted on methane flux measurements (TIGER II Progress Meeting Reports, 1995, 1996, 1997).

An extensive programme of field work was carried out from the autumn of 1995 through to the summer of 1997, in a peat bog in Snowdonia, North Wales. Using headspace chamber techniques for sample collection, methane emissions from the peat bog were characterised isotopically, and the size of the methane flux measured. Both the amount and the isotopic composition of the emitted methane were correlated with environmental variables such as peat temperature and water table depth. The effect of adding a nitrogen source to the peat was also studied.

This chapter details the experimental procedures and summarises the results obtained in the field study. Chapter 4 provides details of laboratory experiments designed to constrain some of the environmental variables, and summarises the results. Chapter 5 is a case study giving a snapshot picture of methane emissions from a peat bog in Finland, which had very different topography from the ombrotrophic mire in Snowdonia. The effect of the main environmental variables: temperature, water table depth and vegetation on the CH_4 flux and its isotopic composition is discussed in detail in Chapter 6, comparing data from the field study in Snowdonia with data from the laboratory study and including data from Finland where appropriate.

3.1 Field Site Description

The field site is located at the Migneint in Snowdonia, North Wales (53°0'N, 3°45'W). The area is an extensive ombrotrophic (rain-fed) mire at an altitude of 450m, with a rainfall of 2169 mm yr^{-1} (thirty-two year average, Environment Agency, 1997). It is remote from sources of atmospheric pollution (Parsons, 1991).

The site consists of a *Sphagnum*-dominated lawn, the angiosperm vegetation is mainly *Eriophorum vaginatum* with a some *E. angustifolium* and ericaceous species.

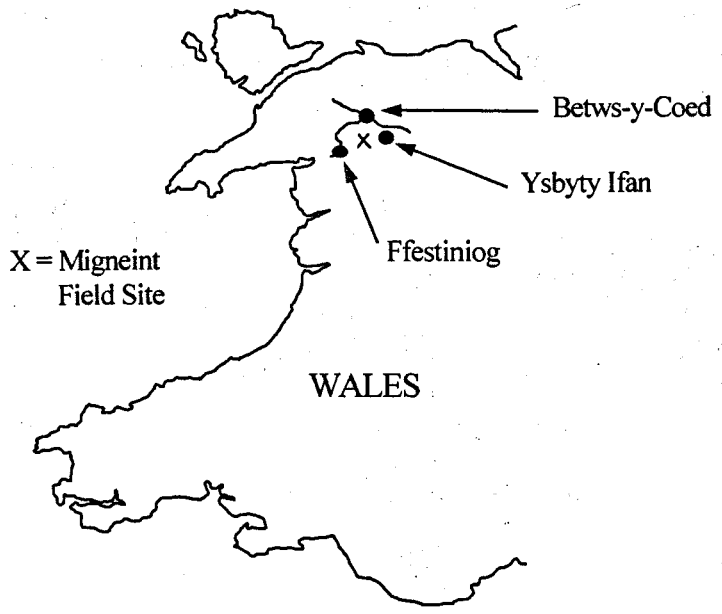

Figure 3.1 Diagram to show the location of the Migneint field site.

The field site was established over a decade ago by the Department of Animal and Plant Sciences of the University of Sheffield, and has been used by other TIGER II (Section 1.5) colleagues. The site consists of four blocks of ten plots each. The plots are 2 x 2m and are separated by a 0.5 m gap to minimise hydrological movement between treatments. Within the blocks the plots are randomised. Treatments applied by other researchers in the past included sulphur and nitrogen (Parsons, 1991; Hutchin *et al.*, 1996). For this study only the three nitrogen treatments were maintained: nitrogen was applied as ammonium, nitrate, and both together.

Treatments were applied in solution using 5 L water. However, adding 5 L water to a plot may potentially affect the methane flux, particularly at times of low rainfall; thus, each block also contained a plot (W), which had received 5 L water. Previous work at this site indicated that there was no significant difference between methane fluxes from watered plots and the control plots (Hutchin *et al.*, 1996). It was therefore decided that the main study would concentrate on the control plots

rather than the watered plots, in order to reduce the volume of water carried to the site. These plots were assumed to be representative of the natural environment.

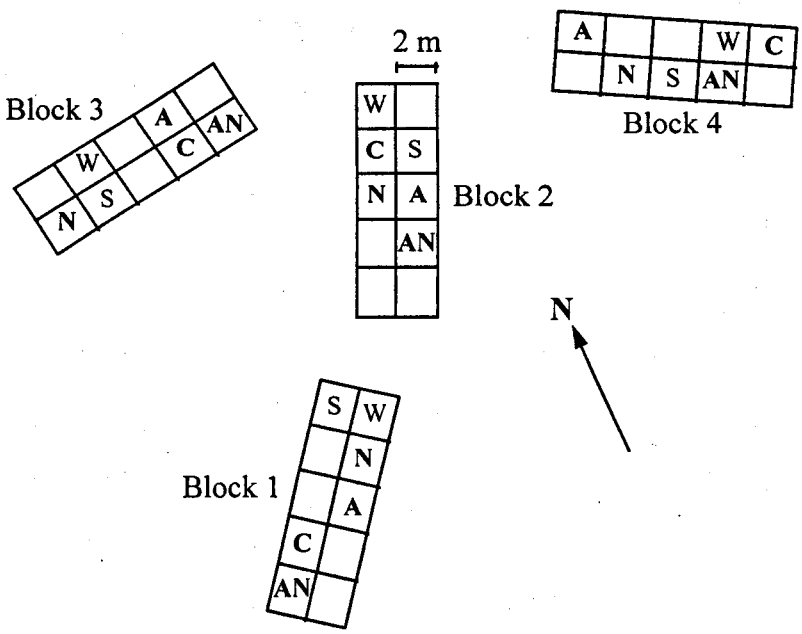

Figure 3.2 Schematic diagram to show the field site layout and treatments, A= ammonium, AN = ammonium and nitrate, C = control (no treatment), N = nitrate, S = sulphate and W = water.

A smaller study was made, to examine the effect of nitrogen fertilisers on the methane flux, and its isotopic composition. Nitrogen in the form of sodium nitrate and ammonium chloride had previously been applied to some of the plots (Hutchin *et al.*, 1996) at fortnightly intervals over a period of two and a half years (Figure 3.2). The application rates were 100 kg N ha^{-1} yr^{-1} in total; approximately 4 times the background deposition rate. In this study, the same total annual amount of N was applied, but at monthly intervals. Stock solutions of sodium nitrate and ammonium chloride (378g L^{-1} and 233g L^{-1} respectively) were made up in the laboratory. These were diluted in the field at a rate of 50 ml stock solution in 5 L water per plot for the single forms of nitrogen, giving a total application rate of 8.3 kg N m^{-2} each month. For the plots receiving both nitrate and ammonium 25 ml each stock solution were diluted together in 5 L water, giving an application rate of 8.3 kg N m^{-2} each month.

The water was carried from the nearby Llyn Conwy Reservoir (Welsh Water). The solutions were evenly applied using a garden watering can fitted with a rose nozzle.

pH Measurements

Peat samples collected in April 1997 (Section 3.3) were subsampled for pH determination. Fresh peat (10 g) was placed in a small beaker and 25 ml 0.01M $CaCl_2$ was added. The pH of the resulting solution was determined electrometrically using a digital pH meter (Model 320, Mettler-Toledo). Calibration was achieved using buffer solutions (4.0 and 7.0) created from pH buffer tablets (Aldrich Chemical Co.).

The pH of the peat ranged from 2.9 to 3.2 (n=11). The peat bog is therefore characterised as an acidic ombrotrophic mire.

3.1.1 Air Sampling Equipment

a) Sample Vessels

100 ml round bottom flasks, fitted with a Teflon®-barrelled high vacuum tap and a side arm (6 mm diameter, 10 cm long), were specially manufactured for this work by J. Young Scientific Glassware Ltd. Previous work had shown that the vessels maintain a 1 x 10^{-5} mbar vacuum for several months, and contribute no measurable blank (Butterworth, 1997). Tedlar bags were not used because Okada and Tezuka (1989) had shown that the carbon isotopic composition of methane could be fractionated by 7.2‰ in less than a month. Hungate® vials fitted with butyl rubber septa were also known to be unsuitable, as a number of vessels failed to maintain a vacuum, even over a week (Brooks *et al.*, 1993; Butterworth, 1997).

b) Chambers

A non-vented, non-steady state chamber technique (Livingston and Hutchinson, 1995) adapted from Christensen (1993) was used to determine methane emissions. The chambers were constructed at the University of Sheffield from transparent

perspex, and the dimensions were 30 cm diameter and 30 cm high. The headspace chambers fitted onto plastic collars (30 cm diameter, 10 cm deep) permanently inserted into the ground. Three collars were randomly distributed in each plot. The area of peat bog enclosed by a collar is described as a core. The bottom rim of the chamber was pushed into a Plasticine-filled groove in the top of the collar. Water was also added to the groove to obtain an air-tight seal (Whalen and Reeburgh, 1988). Initially samples were obtained *via* a septum arrangement that was designed for syringe sampling. However the method was found to be inappropriate for isotopic analysis. Samples became contaminated with indeterminate amounts of background air when the vacuum tap of the sample vessel was opened. The headspace chambers were adapted by the Open University workshop to take glass sampling vessels directly by fitting bulkhead unions (Swagelok SS-400-61, North London Valves and Fittings) through the top of the chambers. An air-tight seal with the glass side arm of the sample vessel was achieved with a 6 mm Teflon® ferrule.

3.2 Measurement of Methane Emissions

3.2.1 Sampling Procedures

Samples were collected at monthly intervals, over a period of 2 years (October 1995 to September 1997), from the control plots of blocks 2 and 3. Air was collected from six headspace chambers at the start of the experiment and after a measured time interval. The sampling period was usually about two hours, and was determined by the approximate flux of methane. It was important to allow sufficient build-up of methane for constructing isotope dilution plots in the data analysis (Section 3.5.2).

Using a chamber fitted with five bulkhead unions, five samples were taken from one core at known time intervals (approximately 20 minutes), to ensure that methane accumulation was linear with time. A non-linear flux would imply there was a problem with the sampling method or that the sampling procedure disturbed

the ecosystem. Ambient air samples were also taken at the start and end of each experiment.

a) Temperature

Duplicate temperature profiles were taken in each plot that had been sampled for methane emission. The peat temperature was measured at 5 cm intervals from the surface to a depth of 30 cm, and then at 40 and 50 cm, using a digital electronic stem thermometer (ATP Instrumentation Ltd.). The ambient air temperature was also recorded in the shade and with the thermometer sheltered from the prevailing wind.

b) Water Table Depth

The water table depth was measured in each plot using a dipstick and a ruler, from a dipwell consisting of a permeable plastic tube (2.5 cm diam) permanently inserted into the peat.

c) Water Samples

Water samples were removed from each plot at a depth of approximately 15 cm using a 16 gauge needle (length 30 cm), and a 20 ml syringe. The water samples were stored in plastic vials in a refrigerator for later δD analysis, as described in Section 2.4. Daily rainfall data for Ysbyty Ifan were supplied by the Environment Agency Welsh Region, (see Appendix C). Ysbyty Ifan is 5 miles to the East of the field site, National Grid Reference SH 81084557, at an altitude of 390 m.

3.2.2 Air Sample Analysis

In the laboratory, air samples were analysed for methane concentration using a gas chromatograph fitted with a flame ionisation detector, and the isotopic composition of each sample was determined using MIRANDA. These methods are described in detail in Chapter 2. Both instruments required far less than a 100 ml sample, but vessels of this size allow multiple analyses if necessary.

Methane fluxes were calculated from the increase in methane concentration and the dimensions of the headspace chamber (Section 3.4.3). The isotopic composition of methane actually emitted from the peat bog was determined from isotope dilution plots, which were constructed using the data obtained from isotopic analysis of the samples (Section 3.5.2).

3.2.3 Diurnal Sampling

Six air samples were collected from one core, six times over a 24 hour period in July 1996, to determine if there was a diurnal pattern in the methane flux. This was done using the sampling technique described in Section 3.2.1. Samples were collected from core 3 in the control plot of block three (Figure 3.2). The headspace chamber was removed from the core between sampling periods. Temperature profiles were measured during each sampling period.

In addition, Dr. Phil Ineson and Mr. Dylan Williams (Institute of Terrestrial Ecology (ITE), Merlewood) also brought their mobile laboratory into the site and methane fluxes were measured continuously for 4 days. A detailed description of the mobile laboratory is given in Chapter 4. Narrow headspace chambers (diameter 12 cm, height 35 cm) were pushed 5 cm into the peat surface to ensure an airtight seal. As several hours elapsed between positioning the headspace chambers and the start of measuring the flux rates, any disturbance caused by this action would have been over by the time measurement commenced. The dynamic sampling system worked in an identical manner to that set up in the laboratory at Merlewood (Chapter 4), except for the following differences:

- the air inlet on each headspace chamber was open direct to atmosphere (no manifold as in the laboratory experiment),
- the outlet from each headspace chamber was connected to the GC in the mobile laboratory *via* 100 m of PTFE tubing; and

- the sample of ambient air for measuring the CH_4 concentration was taken from near the mobile laboratory.

This experiment was conducted in block two (Figure 3.2). Three headspace chambers were placed in the control plot, and three in the plot which had received nitrogen as both sodium nitrate and ammonium chloride (Section 3.3). These headspace chambers stayed in position for the whole duration of the experiment. The GC in the mobile laboratory was able to measure both methane and nitrous oxide fluxes simultaneously.

3.2.4 The Role of Vegetation in the Flux of Methane

In September 1997, a small experiment was conducted to investigate the effect of vegetation on methane emission from the mire. Three of the smaller headspace chambers described in the previous section were used in conjunction with collars permanently sunk into the peat in the control plot in block three (Figure 3.2). The sampling period was 45 minutes. An air sample was taken from the headspace chamber at the start and the end of the sampling period, using pre-evacuated sampling vessels (Section 3.1.1). Then the vegetation (*Eriophorum* spp.) was clipped back to 2 cm above the peat surface, and the sampling procedure repeated.

3.3 Nitrogen Applications

Nitrogen fertilisation has been linked to declining CH_4-oxidising activity in areas where natural ecosystems have been brought into agricultural production (Steudler *et al.*, 1989; Crill *et al.*, 1994). In addition, concern about the effect of nitrogen on peat bogs arises from increased nitrogen deposition from industrial atmospheric pollution. It is thought that nitrogen may effect methane emissions through long-term changes in microbial populations and ecological interactions. The controlling factor may be nitrogen turnover rate rather than the absolute level of nitrogen (Mosier *et al.*, 1991; Hütsch *et al.*, 1993).

Certain forms of nitrogen may also inhibit methane oxidation directly, and consequently affect the overall methane emission rate (Steudler *et al.*, 1989). There is evidence that ammonium in particular can be utilised by methane-oxidising bacteria, methanotrophs (O'Neill and Wilkinson, 1977). The enzyme responsible for the initial step in CH_4 oxidation is methane monooxygenase (MMO), which generally requires molecular oxygen to function. NH_4^+ probably inhibits CH_4 oxidation through competition with CH_4 for the active site of MMO, presumably because the two substrates are very similar in shape and size (Schimel *et al.*, 1993).

Methane emissions from plots receiving nitrogen additions were measured and isotopically analysed in July and November 1996 and April 1997. The sampling procedure used was that described in Section 3.2.1. Air samples were taken from one core in each plot receiving a nitrogen treatment in each block (Figure 3.2). Thus, there were 4 replicate air samples for each nitrogen treatment.

3.3.1 Extractable Nitrate and Ammonium

In July 1996 and April 1997, peat samples (0-20 cm) were taken for determination of extractable nitrate and ammonium from all 12 plots which had received a nitrogen application and the two control plots. At least 6 samples were taken from each plot, and bulked together to provide sufficient material for extraction with potassium chloride.

Extraction of available nitrogen was carried out using a method adapted from Allen (1989). About 100 ml 6% KCl was added to 25 g of fresh peat in a Pyrex® beaker. The mixture was stirred, left to stand for about 10 minutes, and the supernatant liquid was poured through filter paper (No. 44) into a dry vessel. All the filtrate was retained. The peat on the filter was washed with a further 50 ml 6% KCl and allowed to filter. Successive small additions of 6% KCl were leached through the peat until 250 ml leachate was obtained. Two blanks were also run using extractant only. Leachates were frozen until they could be analysed for ammonium

and nitrate content. The moisture content of the fresh peat was determined at the same time by drying overnight at 80 °C.

Analysis for ammonium and nitrate content of the leachate was kindly carried out by Dr. Andrew Bristow, Laboratory Supervisor at the Institute of Grassland and Environmental Research, North Wyke Research Station, using a conventional auto-analyser (Skalar, Utrecht, The Netherlands). The analyses are colorimeteric determinations; nitrate is reduced to nitrite in a cadmium column, then diazotized with sulphanilamide to give a highly coloured (pink) complex absorbing at 540 nm (Navone, 1964). Ammonium determination is based on the modified Bertholot reaction: following chlorination to monochloramine the addition of sodium salicylate converts it to 5-aminosalicylate which is then oxidised and coupled to form a green complex that absorbs at 600 nm (Verdouw *et al.*, 1977).

3.4 Results

3.4.1 Temperature Profiles

The temperature at the surface occasionally showed great variability, particularly in areas with poor vegetation cover on days when the sun was coming in and out of the clouds. To estimate the variation in temperature within the plots, the temperature profile was measured in seven different spots in one particular plot (control, block 3 in December 1995). The results are summarised in Table 3.1.

Peat temperature varied with a standard deviation of about ± 0.2-0.3 °C near the surface, decreasing with depth. It was therefore decided to measure the temperature at two points near to the cores in the two control plots under consideration in the main study (blocks 2 and 3 in Figure 3.2), and take an average of these readings.

Table 3.1 A profile of temperature (°C) at various depths in the peat at 7 points in the control plot in block 3 (Figure 3.2).

Depth /cm	#1	#2	#3	#4	#5	#6	#7	Average	std dev
5	1.3	0.7	0.8	0.7	0.8	0.6	1.2	0.9	0.3
10	1.6	1.4	1.6	2.0	1.4	1.6	1.9	1.6	0.2
15	2.7	2.2	2.5	2.7	2.2	2.4	2.7	2.5	0.2
20	3.3	3.1	3.2	3.4	3.1	3.1	3.0	3.2	0.1
25	3.8	3.9	3.9	4.0	3.9	4.0	4.0	3.9	0.1
30	4.4	4.5	4.4	4.8	4.7	5.0	4.7	4.6	0.2
40	5.4	5.4	5.4	5.4	5.4	5.5	5.6	5.5	0.1
50	6.1	6.1	6.0	6.0	6.1	6.1	6.1	6.1	0.05

It was necessary to ensure that this protocol for recording temperature would provide sufficiently representative measurements during the summer months. This was done in the following manner: in July 1996 a temperature profile was taken in all control plots (four blocks) and each plot receiving a nitrogen treatment (three treatments, four blocks), giving a total of 16 temperature profiles. The average peat temperature and the standard deviation was calculated for each depth; the results are shown in Table 3.2. The peat temperature again showed great variation near the surface (std dev = ±1.9 °C at a depth of 5 cm), but the variation decreased with depth. From 15 cm below the surface the peat temperature varied with a standard deviation of ± 0.5 °C or less. Since the zone of maximum methane production is known to be between 10 and 20 cm below the surface of the water table (Nedwell & Watson, 1995; Daulat & Clymo, 1998) the accuracy of measurement of the peat temperature above that depth, although important, was not critical for this study. It was concluded that even in the summer months, recording two temperature profiles in each control plot in blocks 2 and 3 (Figure 3.2) and taking an average would be representative of the peat temperature.

Table 3.2 Temperature profile for July 1996 (°C, n=16).

Depth /cm	Average Temperature	std dev
5	16.7	1.9
10	14.9	1.0
15	14.0	0.5
20	13.6	0.3
25	13.3	0.2
30	13.1	0.2
40	12.7	0.3
50	12.1	0.3

Temperature profiles constructed for each sampling date are shown in Figure 3.3. It can be seen that the peat temperature ranges between -0.6 and 21.5 °C. Generally the peat temperature remains at 10 °C or below, except for the summer months - June, July and August.

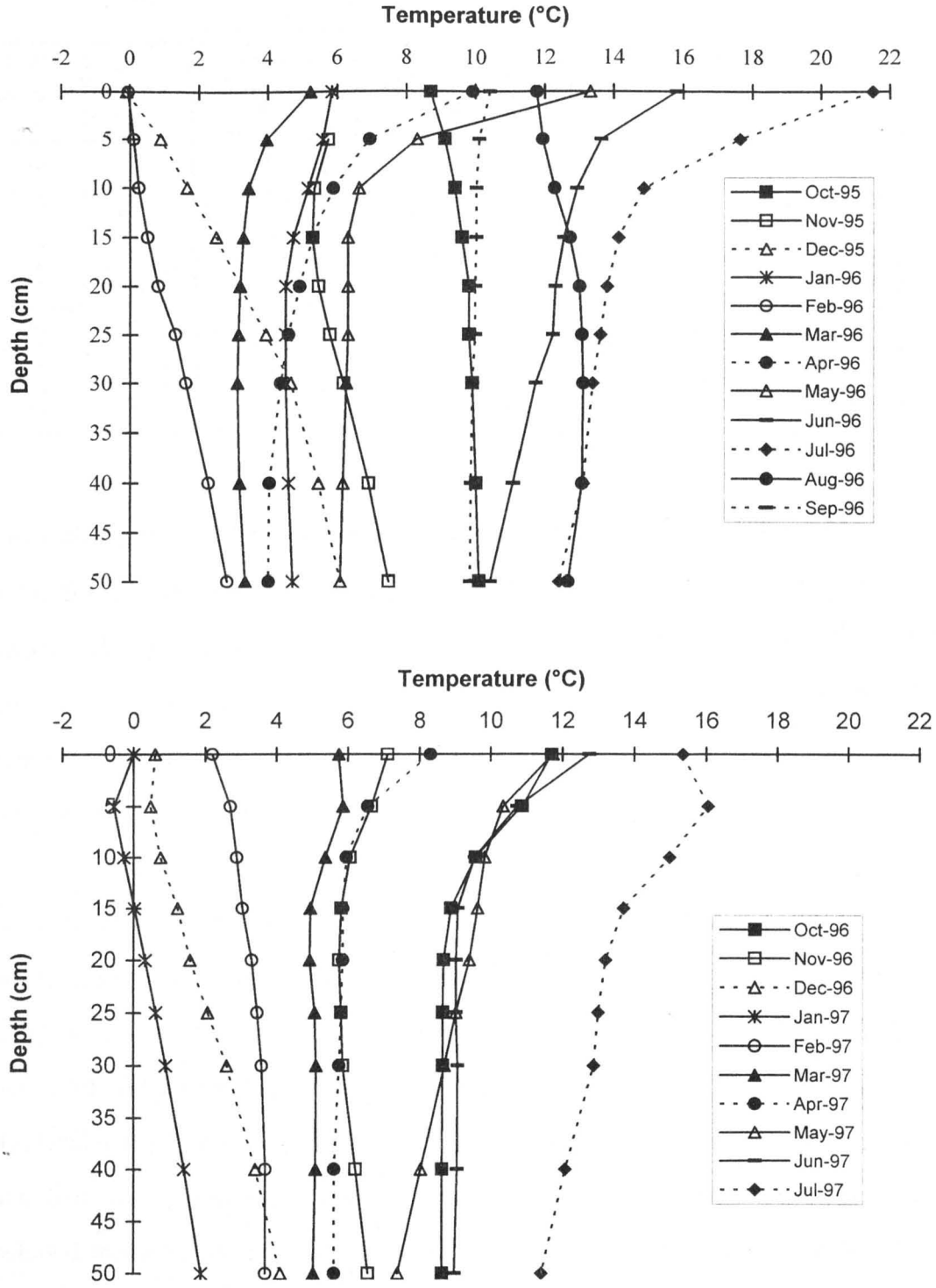

Figure 3.3 Temperature profiles down the peat in the control plots of blocks 2 and 3 (n=4).

3.4.2 Water Table Depth and Rainfall Data

The water table depths for each sampling date are shown in Figure 3.4, these are the average for the control plots in blocks 2 and 3 (Figure 3.2). Corresponding data for the nitrogen addition plots is given in Appendix D. Water table depth ranged from being at the surface of the peat to 132.5 mm below the surface. The water table was at the surface of the peat on nine out of 21 sampling dates. There was no obvious seasonal pattern to the water table depth data.

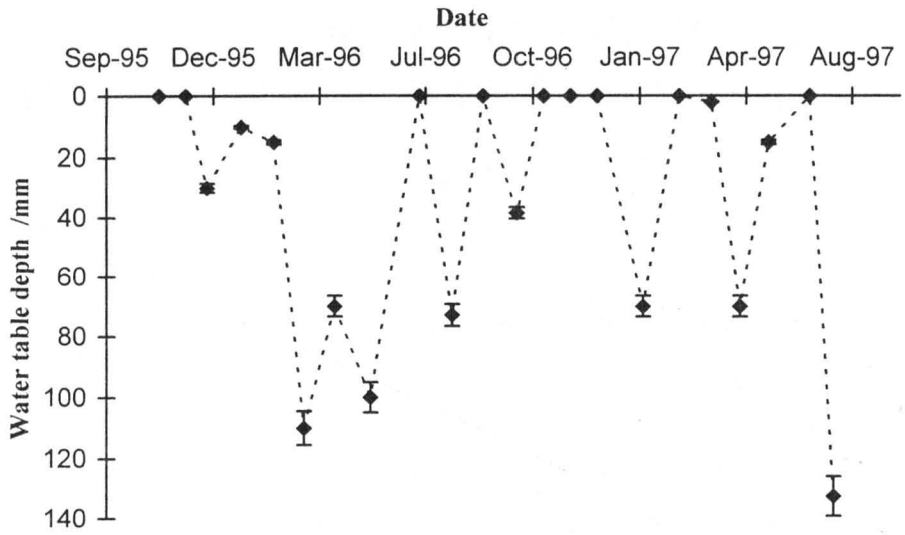

Figure 3.4 Water Table Depth, in mm (n=2).

3.4.3 Flux Measurements

In order to develop mass balance calculations for the global methane budget, it is necessary not only to measure the isotopic composition of each methane source but also to have a good approximation of the rate of methane emissions to the atmosphere.

Methane flux is the amount of CH_4 emitted per unit area per unit time:

$$\text{Flux} = \frac{n}{A.t} \qquad \text{Equation 3.1}$$

where: n is the increase in the number of moles of methane in the headspace,

A is the area of peat bog covered by the headspace chamber, and

t is the time over which the methane was emitted.

The flux for each core was calculated from the accumulation of methane in the headspace chamber, using the Ideal Gas Equation:

$$n = \frac{p.V.c}{R.T} \qquad \text{Equation 3.2}$$

where p is the pressure in the headspace chamber, in Pa,

V is the volume of the headspace chamber, in m^3,

R is the Gas Constant, 8.31 J mol^{-1} K^{-1},

T is the air temperature in the headspace chamber, in K, and

c is the increase in concentration of methane in the headspace chamber.

It therefore follows that

$$\text{Flux} = \frac{p.V.c}{R.T.A.t} \qquad \text{Equation 3.3}$$

The volume of the headspace chambers is given by: $V = \pi r^2 h$

and the surface area is given by: $A = \pi r^2$

where: $\pi \approx 3.1416$,

r is the radius of the chamber, in m, and

h is the height of the chamber, in m.

Substituting V and A:

$$\text{Flux} = \frac{p.h.c}{R.T.t} \qquad \text{Equation 3.4}$$

The pressure in the headspace could be calculated from the pressure of the sample in the vessel in the laboratory, using the pressure law for an ideal gas:

$$p_1/p_2 = T_1/T_2 \qquad \text{Equation 3.5}$$

(the pressure of the sample in the vessel was determined by back-calculating from the drop in pressure as the sample was expanded into the sample loop of the GC.).

The increase in the concentration of methane in the headspace chamber, c, is the difference in concentration between the sample taken at the start and the sample taken at the end of the experiment.

The height from the peat surface to the roof of the chamber was 30 ± 0.5 cm for all cores. The level of the peat surface did not appear to change with season. The accuracy of the flux measurements would be ±1.7% due to this variation.

3.4.4 Methane Accumulation in the Headspace Chambers

At each sampling date, five air samples were taken from a single headspace chamber at known time intervals (Section 3.2.1). The accumulation of methane in the headspace chamber above the control plot in block 2 over two hours in October 1996 is shown in Figure 3.5. As the increase in concentration was linear with time, there was increased confidence that there was no loss of sample associated with the sampling technique and that the experimental procedure did not cause any enhanced methane flux to the atmosphere. It also shows that flux rates were generally constant over time. This example is representative; similar graphs have been constructed for each sampling date.

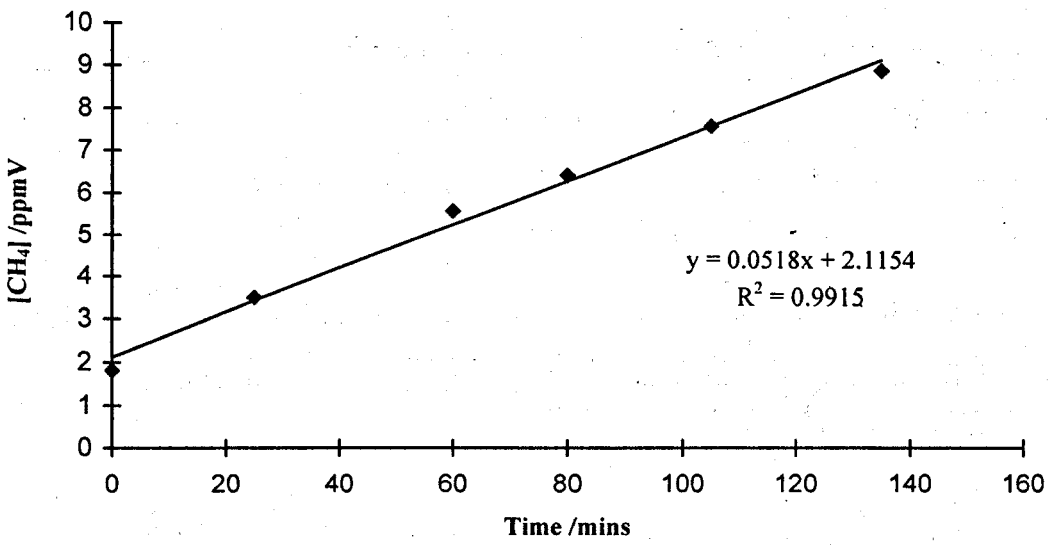

Figure 3.5 Methane accumulation in the headspace chamber, October 1996. Flux rate = 43 μmol CH_4 m^{-2} hr^{-1} (std dev = ±4.4).

3.4.5 Seasonal Flux Rates and Variability

a) Variability Between Cores

The methane fluxes from the three replicate cores in the control plots in blocks 2 and 3 (Figure 3.2) are given in Table 3.4. The maximum flux rate measured was 132 μmol m^{-2} hr^{-1}, in August 1996. There was as much as an order of magnitude variability between the fluxes coming from replicate cores. The effect was more pronounced in the warmer months when the flux was large. This variability was caused by a number of factors such as spatial variability in water content of the peat and the water table depth; variability in the vegetation type and the plant density; spatial variability in the peat structure; and in the summer months, sheep grazed the site. This may have given rise to urine or faeces patches which may cause spatial variability in microbial processes in soils.

b) Seasonal Flux

The average methane flux rates from the ombrotrophic mire in Snowdonia are shown in Figure 3.6. There are several things to notice. Firstly, there was no measurable flux over a one hour sampling period in February 1996. The most likely reason for this was the very cold temperatures of the preceding week; or it may have been because the methane was trapped under a 6.5 cm deep layer of freshly fallen snow. The second scenario, however, was deemed to be unlikely (Dise, 1992).

Average flux rates range from 0 to 70.9 μmol m^{-2} hr^{-1}, the mean value being 17.1 (± 3.4) μmol m^{-2} hr^{-1}. Generally the flux increases with increasing temperature. August 1996 and July 1997 show particularly high flux rates. The former can be explained by warm temperatures and recent torrential rain which had saturated the peat. However although the latter occurs with a relatively warm temperature, the rainfall had been very low for several weeks and the water table had dropped to more than 100mm below the peat surface. In these conditions methane oxidation would be occurring and so the methane *production* rate must have been even greater than the measured flux rate.

Table 3.3 Methane flux from each core in μmol m^{-2} hr^{-1}. Normally six flux measurements were taken. Where only 5 are available, it is due to destruction of sample vessel side arm during analysis (n.m.). n.d.= no flux detected.

	Methane Flux (μmol m^{-2} hr^{-1})							
	Block 2			Block 3				
Date	1	2	3	1	2	3	Average	std error
Oct-95	23.7	53.4	18.6	39.1	70.0	25.2	38.3	8.2
Nov-95	1.3	15.4	22.5	20.1	45.5	13.6	19.7	6.0
Dec-95	4.8	15.2	2.7	11.5	24.3	15.3	12.3	3.2
Jan-96	0.9	1.3	11.5	7.0	16.5	1.0	6.3	2.7
Feb-96	n.d.	n.d.	n.d.	n.d.	n.d.	n.d.	n.d.	
Mar-96	n.m.	4.2	10.4	5.7	13.0	6.7	8.0	1.6
Apr-96	3.8	3.7	21.4	11.1	15.2	2.4	9.6	3.1
May-96	1.6	7.2	12.0	13.6	21.3	18.8	12.4	3.0
Jun-96	56.1	30.1	30.1	25.4	35.7	48.0	37.6	4.9
Jul-96	63.9	23.1	5.8	29.9	27.1	16.8	27.7	8.0
Aug-96	11.6	45.7	132.4	59.7	30.6	97.6	63.0	18.3
Sep-96	2.8	28.6	17.1	27.7	2.9	30.7	18.3	5.2
Oct-96	3.7	38.2	4.0	36.2	21.2	6.4	18.3	6.5
Nov-96	7.6	26.2	53.5	11.2	27.1	30.4	26.0	6.7
Dec-96	4.2	4.3	11.4	7.7	2.1	5.1	5.8	1.3
Jan-97	0.9	0.6	n.m.	9.6	0.1	4.5	3.1	1.8
Feb-97	n.m.	2.3	3.6	2.0	1.1	4.2	2.6	0.6
Mar-97	0.2	7.6	8.9	7.3	10.8	3.7	6.4	1.6
Apr-97	2.0	0.6	2.1	1.1	0.2	0.8	1.1	0.3
May-97	3.3	9.4	26.1	23.4	6.0	15.1	13.8	3.8
Jun-97	13.1	55.9	50.6	31.5	1.5	13.4	27.6	9.0
Jul-97	111.4	74.8	59.1	46.2	40.7	93.0	70.9	11.3

In April 1997, the temperature was beginning to increase, which should have increased methane production. However, this April was also a very dry month, with only 9 mm of rain in the preceding 21 days (32 year average for April = 128 mm) causing the water table to drop to 135 mm below the peat surface. The low methane emission suggests that substantial methane oxidation was occurring as the CH_4 moved up through the peat profile. It has been reported that methane oxidation

occurs more rapidly at lower temperatures than methane production (Dunfield *et al.*, 1993), which is tentatively supported by these data.

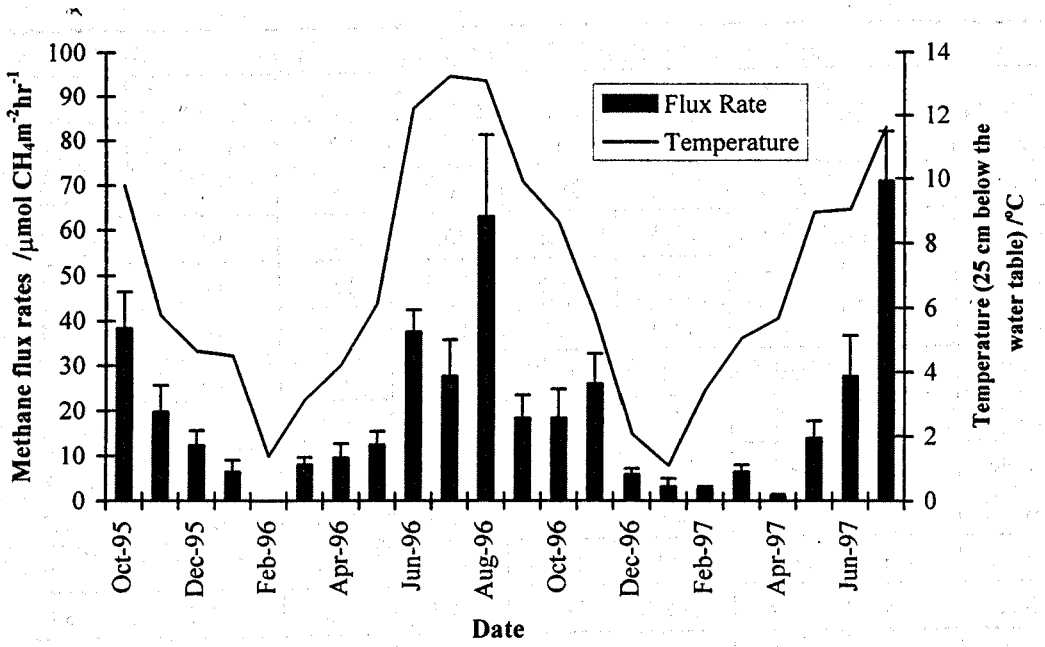

Figure 3.6 Average methane flux rates (n=5 or 6, error bars represent 1σ std error).

The CH_4 fluxes recorded at the Migneint (up to 132 µmol CH_4 m^{-2} hr^{-1}) are in good agreement with the results of Nedwell and Watson (1995) and Fowler *et al.* (1995a) who report summer methane emissions of up to 95.83 µmol m^{-2} hr^{-1} and 170 µmol CH_4 m^{-2} hr^{-1} respectively, from peat bogs in Scotland. The results also agree with the findings of MacDonald *et al.* (1998) who report a summer flux of 128.8 µmol m^{-2} hr^{-1} in a Caithness peat mire. However, the maximum average methane fluxes measured in 1996 and 1997 are four or five times those reported by Hutchin *et al.* (1996) who measured maximum summer fluxes of 14 to 16 µmol m^{-2} hr^{-1} over the previous three years, at the same site. One reason for the discrepancy may be that the summers of 1993 to 1995 were much drier than 1996 and 1997, (Environment Agency Welsh Region).

c) Diurnal Flux Pattern

The results of the diurnal sampling experiment are shown in Figure 3.7a. Due to the constraints of time for sample analysis and the availability of sampling vessels, there was no sample replication. Nevertheless, it is clear that methane emissions from this core reached a maximum at around midnight, and dropped to a minimum at around dawn (6 am). The midnight maximum is also seen in the results from the mobile laboratory (Figure 3.7b), although the minimum appeared to be later in the day.

The magnitude of the fluxes measured by conventional static chamber techniques are less than those measured by the dynamic technique. The mostly likely cause of this discrepancy is spatial variability in the peat bog. Nevertheless, the same pattern of diurnal flux can be seen in both sets of measurements. The pattern is most pronounced from the cores which had received nitrogen inputs. One possible cause for this is that for this particular block (block 2, Figure 3.2) visual assessment revealed that the plots which had received a nitrogen application had a greater plant density than the control plot. Increased plant density may result in increased methane flux. This is an area for further investigation. This diurnal pattern of flux is probably due to the role of the plants in the production and transport of methane in the ecosystem.

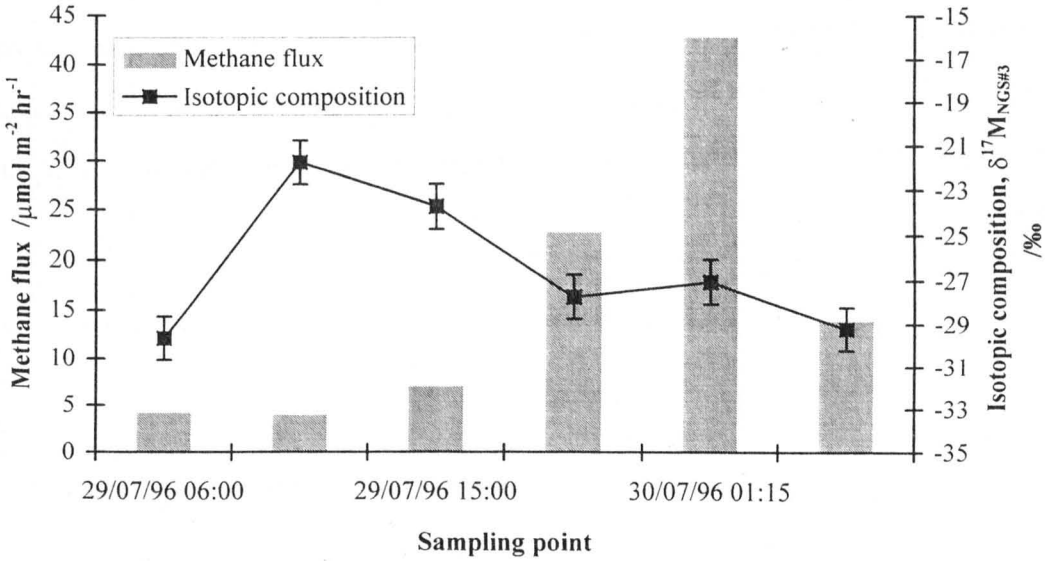

Figure 3.7a Diurnal methane flux rates, 29 to 30 July 1996, from headspace measurements.

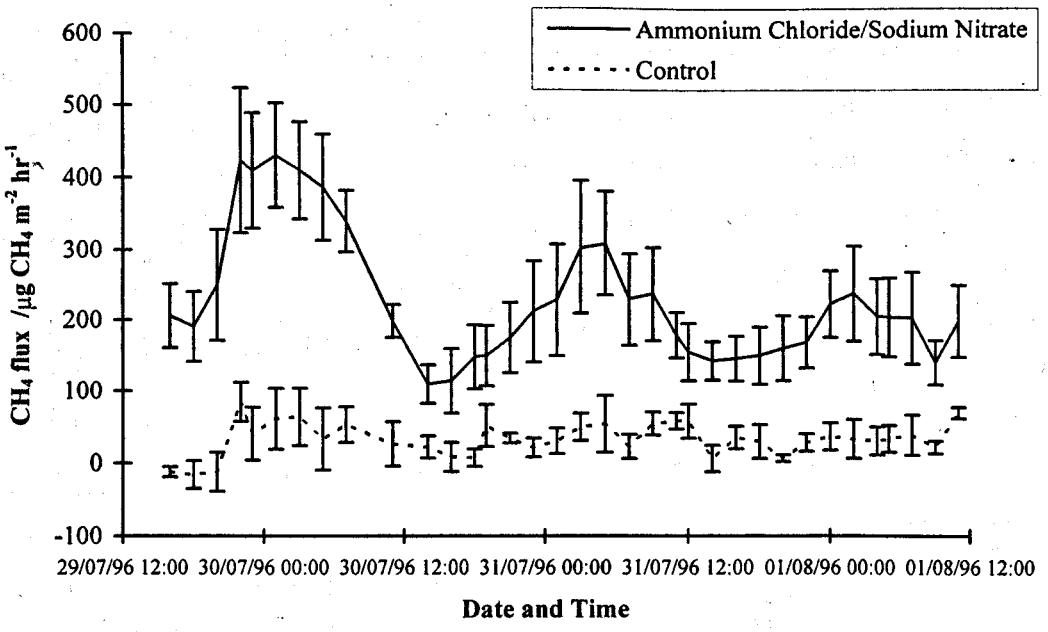

Figure 3.7b Continuous methane fluxes measure by the mobile laboratory, 29 July to 1 August 1996 (n=3, error bars are 1σ std error).

d) Role of Vegetation

Clipping back the vegetation to just above the surface of the peat dramatically reduced the methane flux from the cores to less than 40% of the initial flux. The result is shown in Figure 3.8. As the effect of removing the vegetation was immediate, it would suggest that the plants play a significant role in the transport of methane in the peat, not just its production. There was greater variation in flux rates before removing the vegetation, which may be associated with differences in plant density.

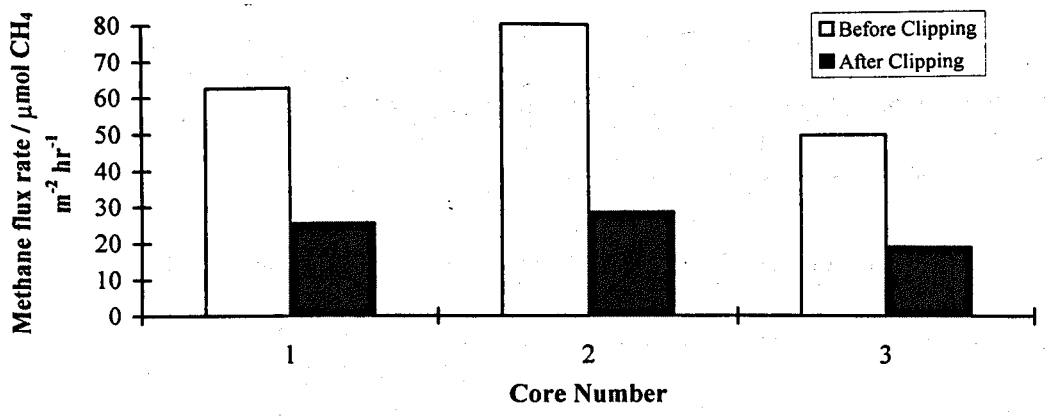

Figure 3.8 The effect of clipping the vegetation. Core 1 to 3 are replicates.

3.5 Isotopic Composition of Methane

3.5.1 Air Samples

To ensure that the techniques used for collecting and analysing the samples are appropriate, it is useful to compare the results for ambient air samples collected during this fieldwork with published data. The concentration of methane in the air samples ranged from 1.72 to 2.08 ppm, the average being 1.84 ppm. There was no correlation between the CH_4 concentration and the isotopic composition (Figure 3.9).

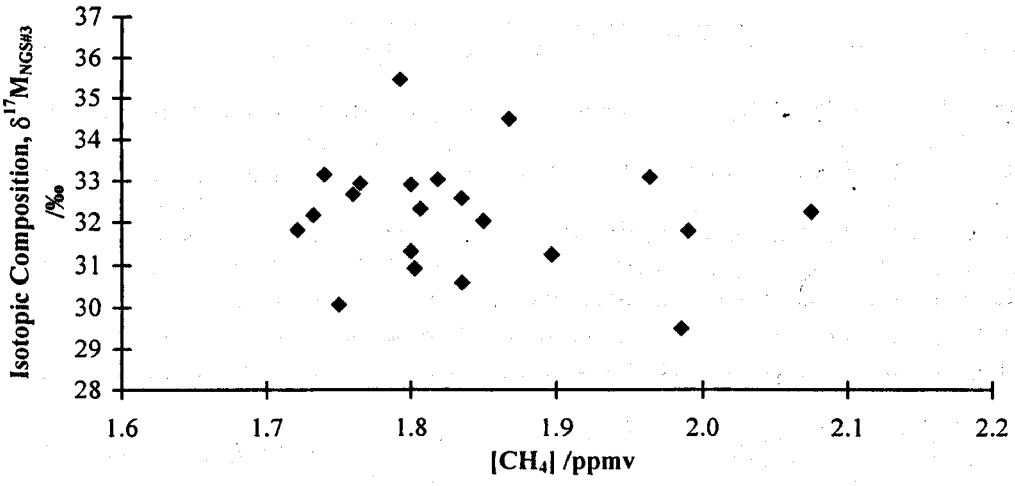

Figure 3.9 Combined isotopic composition against methane concentration in ambient air samples.

$\delta^{17}M$ values for methane in air samples collected at the Migneint between October 1995 and June 1997 ranged from 29.5 to 35.5‰, with an average value of 32.2‰ (Figure 3.10). Using Equation 2.8 (Chapter 2):

$$\delta^{17}M = (1.02893 \times \delta^{13}C) + (0.0569929 \times \delta D) + 84.9405 \quad \text{Equation 2.8}$$

and substituting in $\delta^{13}C$ and δD values for methane in clean air samples from the literature:

- $\delta^{13}C$ = -47.8 to -46.2‰ (Stevens and Rust, 1982; Wahlen *et al.*, 1987; Stevens and Engelkemeir, 1988; Tyler, 1989; Lowe and Brenninkmeijer, 1991; Wahlen, 1994; Conny and Currie, 1996; Sugawara *et al.*, 1996)
- δD = -83‰ (Wahlen, 1994)

gives $\delta^{17}M$ = 31.0 to 32.7‰. The average $\delta^{17}M$ from this field work (32.32 ±0.3‰) falls within this range. As the site at the Migneint receives air from different sources, some more polluted than others, ambient air samples collected over 21 months show a rather wide range of $\delta^{17}M$ values. Linear-circular correlation analysis (Mardia, 1976) shows a statistically significant relationship between the $\delta^{17}M$ values measured at the Migneint and the wind direction on the date of sampling, $p < 0.01$, $r^2 = 0.71$ (Table 3.4). With the exception of October 1996 (no wind), the ten heaviest isotopic compositions (> 32.25‰) occurred when the wind was from a westerly direction. Also, at the remaining eleven sampling dates, on only two occasions is the wind from a westerly direction (October and November 1995).

These data suggest that wind coming over the ocean carries with it methane which is isotopically enriched compared to the wind coming from over mainland Europe. Unlike $\delta^{17}M$, the CH_4 concentration did not show any correlation with wind speed and direction. Thus isotopic analysis provides a clearer picture of differences between sources of CH_4 than CH_4 concentration measurements alone.

Table 3.4 Average $\delta^{17}M$ of methane in ambient air in descending order, and prevailing wind direction.

Date	Average $\delta^{17}M$	Wind Direction
09/04/96	35.45	WSW
12/02/96	34.48	WSW
28/06/96	33.14	WSW
11/03/96	33.08	WSW
26/02/97	33.02	WSW
22/10/96	32.93	calm
27/09/96	32.90	WSW
29/07/96	32.66	WSW
24/04/97	32.57	W
28/03/97	32.31	WNW
11/12/96	32.25	ESE
12/01/96	32.17	SSE
29/06/97	32.03	ENE
27/10/95	31.82	W
16/11/96	31.81	calm
13/05/96	31.33	calm
21/05/97	31.26	ENE
21/11/95	30.94	SSW
27/08/96	30.60	NNE
11/12/95	30.08	calm
23/01/97	29.50	calm

There was no *seasonal* variability in the methane concentration of ambient air samples taken at the Migneint over the period studied (Figure 3.10). Other researchers (Quay *et al.*, 1991; Thom *et al.*, 1993; Lowe *et al.*, 1994) have seen a seasonal cycle in the $\delta^{13}C$ of atmospheric methane, being enriched in the summer and depleted in the winter. The amplitude of the cycle is about 0.5‰. This would translate into an amplitude of about 0.5‰ in a seasonal cycle in $\delta^{17}M$, if there were no change in δD. A corresponding cycle occurs in δD (Conny and Currie, 1996). So, although there may be a seasonal cycle in the two isotopic components in the samples studied here, it appears to be masked either by pollution events, by the infrequency of sampling or the limits in precision of the analysis.

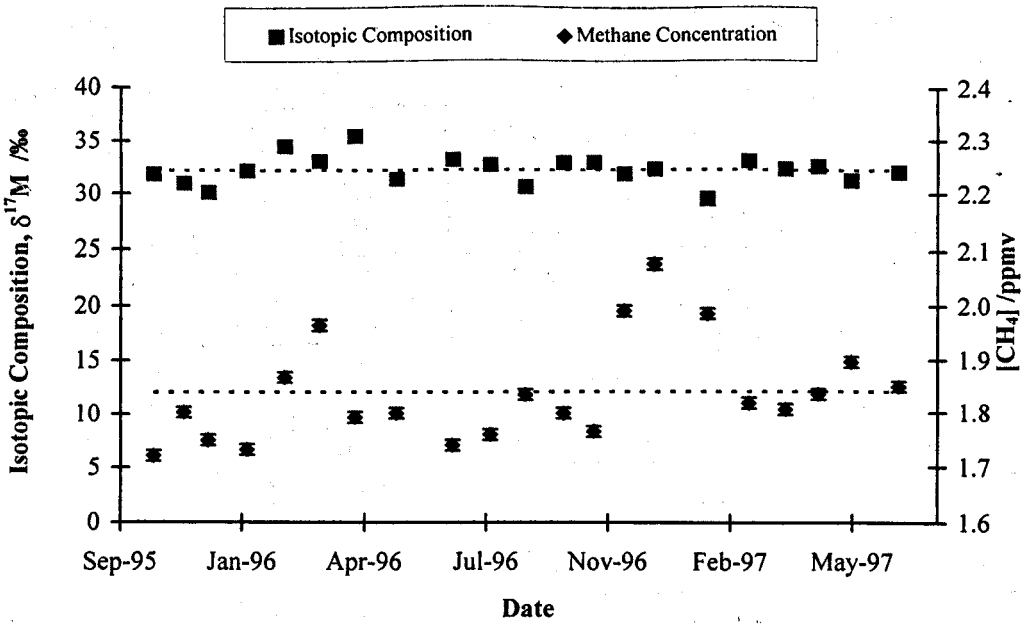

Figure 3.10 Isotopic composition and concentration of methane in air samples collected at the Migneint, October 1995 to June 1997. (Error bars for the isotopic composition are smaller than the marker).

These $\delta^{17}M$ data for ambient air samples have been used by Dr. R.G. Derwent at the United Kingdom Meteorological Office in the evaluation of a general circulation model, in conjunction with Dr. G.H. Morgan (Open University).

3.5.2 Isotope Dilution Plots

The methane present in the headspace at the end of a sampling period was a mixture of ambient air and the methane emitted from the peat bog. The mean combined isotopic signature of the methane emission can be determined using the two-component mixing approach (Thom *et al.*, 1993; Kuhlmann *et al.*, 1998):

$$c_{obs} = c_{bgd} + c_{source} \qquad \text{Equation 3.6}$$

similarly:

$$\delta_{obs} \times c_{obs} = \delta_{bgd} \times c_{bgd} + \delta_{source} \times c_{source} \qquad \text{Equation 3.7}$$

where: c = methane concentration
δ = isotopic composition
obs = observed CH_4 concentration or isotopic composition

source = of the source (peat bog)
bgd = of background or ambient air

(Equation 3.7 is an approximation. However, the difference between $\delta^{17}M_{source}$ and $\delta^{17}M_{bgd}$ in this context is sufficiently small (~65‰) that the accuracy of the method is ±0.02‰, which is less than the precision of the isotopic analysis).

Re-arranging Equation 3.6 and substituting it into Equation 3.7 gives:

$$\delta_{obs} = 1/c_{obs} \times (\delta_{bgd} \times c_{bgd} - \delta_{source} \times c_{bgd}) + \delta_{source} \qquad \text{Equation 3.8}$$

This equates to the equation of a straight line, y= mx + c. Thus by plotting the isotopic composition of the methane against the reciprocal of the methane concentration in the air samples, the isotopic composition of the methane emitted by the peat bog is given by the intercept of the line produced.

Figure 3.11 gives an example of a dilution plot, for samples collected in July 1996. The intercept of the line is -26.4, thus the isotopic composition of the methane emitted from the peat bog in July 1996 was determined to be -26.4‰. Dilution plots were constructed using samples collected each month; the sample analysis data used are given in Appendix E.

In the dilution plot, the isotopes of the methane fluxes all lie very close to the line, indicating that the isotopes of the methane produced by each core are very similar. This suggests that the methane emissions from the cores have all undergone the same biochemical processes en route from the site of production to the surface, regardless of the magnitude of the individual flux. This is in contrast to the great spatial variability of the methane fluxes from the cores (Section 4.4.6).

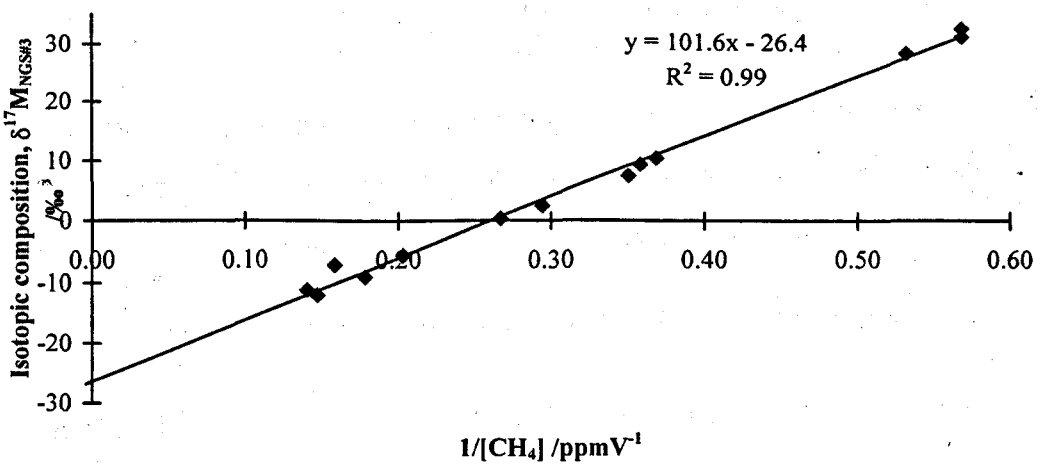

Figure 3.11 Isotope dilution plot for July 1996 (n=13).

3.5.3 Methane Emissions

Using isotope dilution plots constructed from approximately 10 samples , the isotopic composition of the methane emitted from the ombrotrophic mire at each sampling date was determined (Figure 3.12).

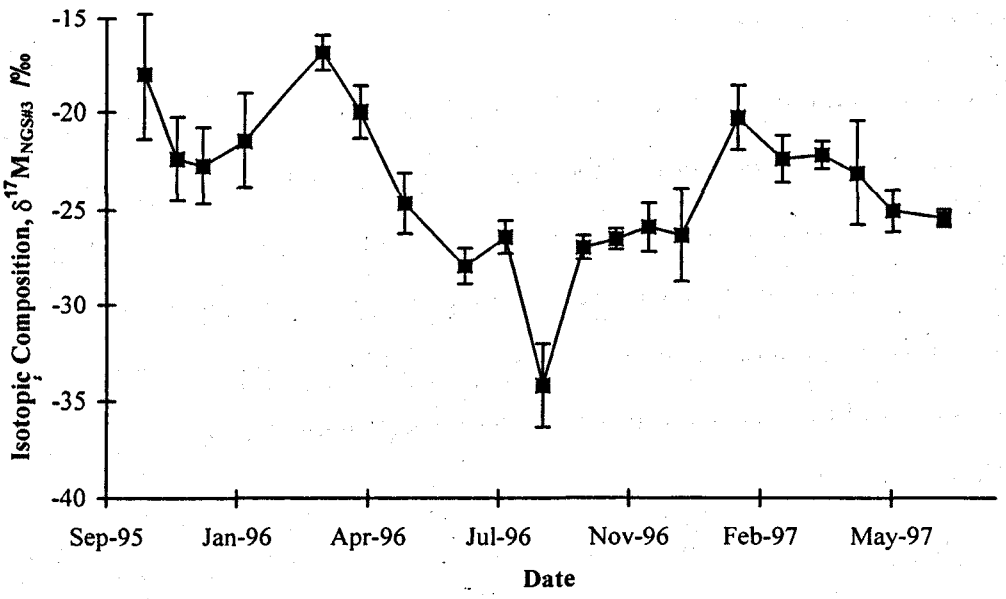

Figure 3.12 Combined isotopic composition of methane emissions from the Migneint, October 1995 to June 1997.

$\delta^{17}M$ values range from -34 to -17‰. These are much lighter than values derived from $\delta^{13}C$ and δD values published in the literature. Figure 2.7 shows the $\delta^{17}M$ values for various sources of methane calculated from $\delta^{13}C$ and δD values reported by Wahlen (1994). These range from +5 to +15‰, for emissions from peat bogs, although no experimental detail is given. Lansdown *et al.* (1992) report $\delta^{13}C$ and δD values which correspond to $\delta^{17}M$ values of -15.3 to -0.3‰, for methane ebullition in a peat bog in Washington State between June 1990 and January 1991. Kuhlmann *et al.* (1998) also report $\delta^{13}C$ and δD values which correspond to $\delta^{17}M$ = -14 to +10‰ from the Hudson Bay Lowlands. As $\delta^{17}M$ is a combination of $\delta^{13}C$ and δD, the differences can be due to either differences in $\delta^{13}C$, differences in δD or a combination of the two. An isotopic shift of 10‰ in $\delta^{17}M$ can arise from individual shifts of 10‰ in $\delta^{13}C$, or 179‰ in δD. The differences may arise from a number of factors:

- The kinetic isotope effect of CO_2 reduction causes much greater depletion in ^{13}C than acetate fermentation (up to 30 - 40‰). Thus, the relative importance of the metabolic pathway partially determines the $\delta^{13}C$ of the methane emitted.
- The $\delta^{13}C$ of the precursor plant material will have an effect on the $\delta^{13}C$ of the methane produced. Plants using a C-3 photosynthetic pathway have a $\delta^{13}C$ value of around -28‰, while in C-4 plants $\delta^{13}C$ is about -14‰.
- It is thought that there may be a latitudinal variation of up to 10‰ in $\delta^{13}C$ of methane from wetlands (Stevens and Engelkemeir, 1988; Quay *et al.*, 1991).
- Reported values for $\delta^{13}C$ of methane emitted from peat bogs and wetlands range from -86 to -50‰ (Lansdown *et al.*, 1992). This range could certainly account for the difference between the heaviest $\delta^{17}M$ value measured in the Migneint (-16.9‰) and the lightest value (+5‰) reported by Wahlen (1994); and incorporate the range of $\delta^{17}M$ values calculated from $\delta^{13}C$ and δD data reported by Lansdown *et al.* (1992).

- There is a latitudinal variation in the isotopic composition of rainfall. The further from the equator, the more depleted δD. This is due to mass transport effects (evaporation is greatest near the equator, the heavier isotopes fall out as rain first, leaving isotopically lighter water behind). For example, the average δD for peat bog water in the ombrotrophic mire at the Migneint is -37.1‰. Sixteen degrees further north (in the north of Finland) δD of the water in a palsa mire pool is -91‰.

That the lightest isotopes should occur in the warmer summer months is surprising. Purely from a kinetic perspective, one would expect the methane to become isotopically enriched with increasing temperature. Also, it might generally be expected that the water table would drop below the surface of the peat in the summer months, increasing the potential for methane oxidation to occur as the methane travels from the point of production to the surface. This process is known to result in enrichment of the isotopic signature (Section 1.2.3). At the Migneint field site, however, there is no correlation between water table depth and season.

It can therefore been seen that although the isotopic composition ($\delta^{17}M$) of the methane measured in this study is lighter than reported values, they are not sufficiently different as to pose serious questions about their validity. It should also be noted that thus far, there are no other published data regarding the isotopic composition of methane in the U.K.

3.5.4 Relationship Between δD of the Peat Bog Water and δD of the Methane

A change in the isotopic composition of the water in the surrounding peat may affect the isotopic composition of the methane produced. The isotopic composition of the water was determined at the Scottish Universities Research and Reactor Centre as described in Chapter 2. The results are shown in Table 3.5. The δD values of the water in the peat bog at the Migneint range from -51 to -24‰, the average being -36‰.

It is not easy to compare δD_{H2O} directly with $\delta^{17}M_{CH4}$ because there is a large isotopic shift associated with the transfer of hydrogen from the water to the methane molecule, as much as 300‰ (Sugimoto and Wada, 1995). There is no statistically significant correlation between the two in this study. The variation in δD_{H2O} measured at the Migneint field site could account for no more than a 2‰ change in $\delta^{17}M$, assuming that the isotopic shift associated with the incorporation of the hydrogen into the methane molecule remained constant.

Table 3.5 Isotopic composition of the water in the surrounding peat (average of two numbers, bracket indicate std dev).

Date	δD (‰)	$\delta^{18}O$ (‰)
Aug-96	-51 (±6)	-7.5 (±1)
Sep-96	-33 (±1)	-4.8 (±0)
Oct-96	-33 (±2)	-5.4 (±0)
Nov-96	-35 (±2)	-5.5 (±0)
Dec-96	-42 (±7)	-6.5 (±2)
Jan-97	-36 (±3)	-5.8 (±0)
Feb-97	-39 (±1)	-5.9 (±0)
Mar-97	-24 (±5)	-4.3 (±1)
Apr-97	-31 (±5)	-5.3 (±1)
May-97	-36 (±0)	-5.2 (±0)
Jun-97	-48 (±7)	-7.2 (±1)
Jul-97	-35 (±0)	-5.6 (±0)
Aug-97	-25 (±0)	-3.7 (±0)

3.6 Effect of Nitrogen Deposition

3.6.1 Extractable Nitrogen

Peat samples for determining extractable nitrogen were collected from block 2, (Figure 3.2) in July 1996, from 4 different depths: 0-5 cm, 5-10 cm, 10-15 cm and 15-20 cm (Table 3.6). The amount of extractable nitrate-N is much lower than the

ammonium-N. This is because anaerobic conditions are not optimal for the process of nitrification; that is the oxidation of ammonium to nitrate. However, nitrate is readily converted to nitrous oxide and molecular nitrogen *via* denitrification. Hence there is an imbalance in the processes of the soil nitrogen cycle.

Table 3.6 Extractable nitrogen measured in block 2 at different depths down the peat profile, July 1996 (n=2).

Treatment	Nitrate	Ammonium	Both	Control
	mg extractable NH_4^+-N 100 g^{-1} dry peat			
0-5 cm	5.95	5.77	6.45	3.85
5-10 cm	3.32	3.73	4.64	4.25
10-15 cm	3.39	3.45	4.25	3.50
15-20 cm	4.20	4.19	4.37	3.37
	mg extractable NO_3^--N 100 g^{-1} dry peat			
0-5 cm	0.27	0.19	0.25	0.25
5-10 cm	0.14	0.22	0.25	0.27
10-15 cm	0.20	0.22	0.16	0.14
15-20 cm	0.22	0.22	0.16	0.16

Using two-way analysis of variance there is no difference between treatments in either form of extractable N in the peat. For extractable nitrate-N there is no significant difference down the profile. However, the 0-5 cm depth does have significantly more ammonium-N than the other depths ($p<0.01$).

In April 1997 peat samples for determining extractable N were taken from 0-20 cm from all blocks (Table 3.7). Two-way analysis of variance shows there is again no difference between treatments and blocks for the extractable nitrate-N. For the extractable ammonium-N, there is no difference between the blocks. However, the control plots have significantly less extractable ammonium-N than the other treatments ($p<0.01$).

Table 3.7 Extractable nitrogen sampled by block, 0-20 cm, April 1997 (n=2).

Treatment	mg extractable NH_4^+-N 100 g^{-1} dry peat	mg extractable NO_3^--N 100 g^{-1} dry peat
Nitrate	1.63	0.92
Ammonium	2.24	0.32
Both	2.41	0.57
Control	1.23	0.68

The results suggest that, despite applying nitrate or ammonium or both, at a rate of 100 kg N ha^{-1} yr^{-1} over 5 years, there are no measurable differences in the extractable nitrogen in the peat between the treated plots. One reason for this may be that the mire, being ombrotrophic, is so nutrient deficient that the applied nitrogen is readily utilised by the vegetation and the microbial population. Generally, the extractable nitrogen for April 1997 is about half that of July 1996. This is probably due to natural seasonal variations in the amount of extractable nitrogen, which would depend upon, for example, the rainfall and subsequent drainage, and the growth stage of the vegetation.

3.6.2 Methane Flux from Nitrogen-Treated Plots

The methane flux from the nitrogen-treated plots was calculated for July and November 1996 and April 1997 (Figure 3.13).

Two-way analysis of variance shows that there is no significant difference in methane flux between the blocks or arising from the treatments. Flux rates were generally lower than expected in April 1997 (Section 3.4.5), probably due to methane oxidation resulting from a low water table. Linear regression analysis on methane flux data from April 1997 shows that there is no correlation between flux rate and extractable NH_4^+ - N, or extractable NO_3^- - N.

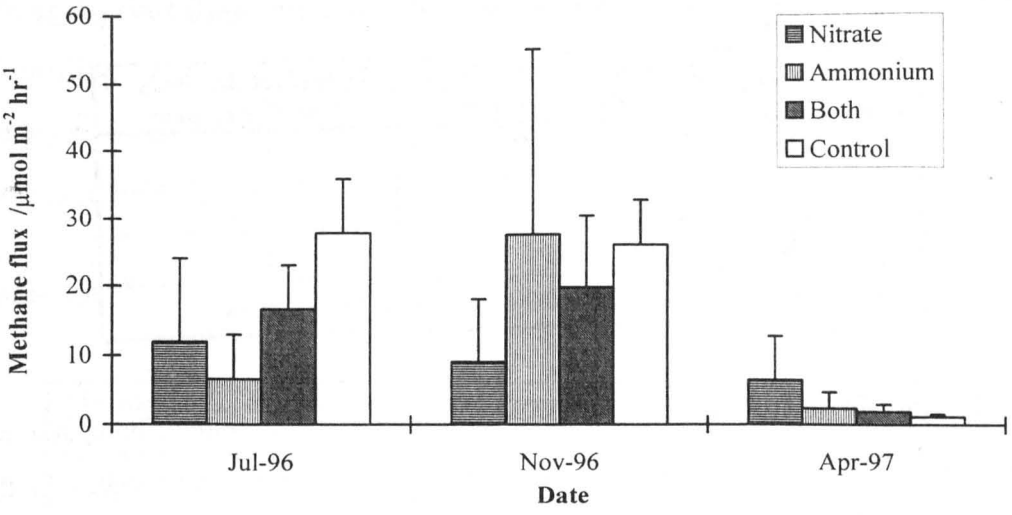

Figure 3.13 Methane fluxes from nitrogen treated plots (n=4).

Preliminary investigations by other TIGER researchers indicated that nitrate may inhibit methane oxidation, (Watson & Nedwell, 1998), which could explain the results from April 1997. If nitrate is inhibiting methane oxidation, there would be evidence in the isotopic analysis: the emitted methane would be isotopically enriched in $\delta^{17}M$. An alternative explanation could arise from a indirect effect. The nitrogen treatments may affect the vegetation, producing conditions which are more favourable to one species over another. The results from the mobile laboratory (Figure 3.7b) suggested that a higher CH_4 flux occurred as the result of nitrogen application, which increased plant density. Visual inspection of all the cores in all the treated plots indicated that long-term (5 years) nitrate applications resulted in a lower plant density compared to those receiving ammonium or ammonium and nitrate together (Chapter 6).

3.6.3 Effect of Nitrogen Applications on the Isotopic Composition of Methane

The isotopic signatures of methane emissions from plots receiving nitrogen applications were determined using standard isotope dilution plots (Section 3.5.2) (Table 3.8).

Two-way analysis of variance shows that there is no difference in isotopic composition due to the treatments applied.

Table 3.8 Isotopic composition of methane from plots applied with nitrogen, $\delta^{17}M_{NGS\#3}$ /‰

Date	Nitrate	Ammonium	Both	Control
Jul-96	-20.65	-24.18	-25.65	-26.39
Nov-96	-28.49	-21.87	-26.63	-25.89
Apr-97	-17.56	-25.60	-18.50	-23.05

Ammonium is likely to inhibit methane oxidation (Bédard and Knowles, 1989; Steudler *et al.*, 1989; Willison *et al.*, 1995) and as previously mentioned, it is possible that nitrate may as well. In July 1996 and April 1997 the water table was more than 120 mm below the surface of the peat, so methane oxidation was occurring. Methane oxidation would result in the lighter isotopes being preferentially removed from the methane, (Barker and Fritz, 1981) and thus the methane emission would have a relatively heavier isotopic signature. If, however, the oxidation was inhibited, the methane would pass through, and the isotopic signature would be lighter than if oxidation was occurring. If it is assumed that oxidation took place in the control plots, then a lighter isotopic signature from the treated plots would indicate that inhibition had occurred. As there was no difference between the isotopic signature due to treatments, it seems unlikely that in this experiment inhibition of methane oxidation took place.

The potential problem with the experimental procedure is that the plots were sampled approximately four weeks after nitrogen was applied to them. Immediately after sampling, the next nitrogen application was made. The highest concentration of available N is in the 0-5 cm depth. It is likely that immediately following application of nitrogen, the concentration of extractable N is at its maximum and declines over time. How fast nitrogen is lost by the system, or incorporated by the plants is unknown. It may be that the isotopic signature is changed immediately after the nitrogen application, or within an hour or a day. Therefore one explanation for the lack of any relationship is that the levels of nitrate and ammonium are too low at the time of sampling to produce measurable inhibition of methane oxidation. Another explanation is that there may be some critical level of ammonium or nitrate which is required before inhibition of methane oxidation starts.

3.7 Summary

Methane fluxes measured at the Migneint field site were consistent with fluxes measured from similar sites in the UK. The flux showed seasonal variation.

The isotopic composition of methane in the air was related in part to wind direction. The isotopic composition of the methane emitted by the ombrotrophic mire ranged from -34 to -17‰ and showed seasonal variation.

From the available results it is difficult to determine the effect of nitrogen applications to the peat bog. The nitrogen treatments in this experiment did not cause any change in the flux rate or the isotopic composition. However, the levels of extractable nitrogen in the peat may have been too low to cause any effect. Any effects that might be seen with higher levels of nitrogen in the peat could arise from vegetation effects.

Controlled Environment Experiments

4. Introduction

The main aim of this project was to characterise methane emissions from an ombrotrophic mire in terms of the isotopic composition of the CH_4 flux, and to evaluate the effect of the main environmental factors on the isotopic composition.

Clearly, in the field there is a very complex ecosystem of inter-dependent factors which affect the total methane flux and thus potentially affect the isotopic composition of the flux. In an attempt to constrain the variables in the system, a series of laboratory experiments were designed, in collaboration with Dr. Phil Ineson and Mr. Dylan Williams at Institute of Terrestrial Ecology (ITE), Merlewood, in Grange-over-Sands.

Early results from several groups of researchers in the TIGER II programme (Section 1.5) found that temperature had an exponential effect on the methane flux from peat wetlands in the UK. They also found that water table depth has an effect

on the amount of methane emitted from the mire, TIGER II Progress Meeting Reports 1995 and references therein.

It was therefore decided initially to examine the effect of changing temperature on the isotopic composition of the methane emitted by the peat, while keeping all other environmental variables constant. The temperature would then be kept constant while the water table was changed. By lowering the water table, the upper layers of the peat would become aerated and there would be potential for methane oxidation to occur. It has been shown in other ecosystems that methane oxidation results in the residual methane being enriched in the heavier isotopes (Barker and Fritz, 1981).

4.1 Experimental Set up.

4.1.1 Materials and Method

Peat cores were collected from the field site at the Migneint in the following manner: Hollow tubes of household soil pipe, 35 cm long and 15 cm diameter were pushed into the peat until the upper rim was about level with the peat surface. Using a garden spade, a hole was cut in the peat down the outside of the tube and the peat cut away underneath the tube. The core was then levered out of the bog, still intact.

Six cores were taken in this manner and transported to the laboratory at ITE Merlewood. Practical considerations made it necessary to reduce the depth of the cores to 25 cm, but the soil pipe remained 35 cm long, thus increasing the volume of the headspace. Clear perspex headspace lids (depth 30 mm) were fitted to the cores, an air-tight seal being provided by a large rubber band seal. The lids had inlet and outlet fittings to allow attachment of the cores to the GC in the mobile laboratory. The cores were placed in "buckets" which had been made by cutting off the tops of cylindrical polyethylene water carriers (10 L). The buckets were then filled with de-ionised water until it was level with the peat surface (Figure 4.1). A sample of the de-ionised water was taken for D/H analysis. Five cores (in the buckets) were then

placed inside a temperature-controlled incubator. The sixth was left on the bench as a control to ensure that there was no isotopic shift caused by the addition of the de-ionised water. As the laboratory was in a windowless cellar, room temperature remained at a constant 15 °C.

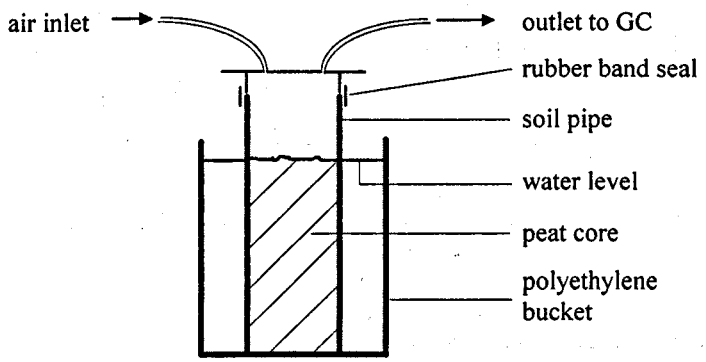

Figure 4.1 Schematic diagram to show core and headspace lid.

Air was drawn through PTFE tubing from outside the building (at a height of 15 m) to a manifold in the laboratory, where the air was split to flow across all the cores. The outlets from the headspace chambers were connected by PTFE tubing ($^1/_4$" o.d.) to the mobile laboratory which was situated outside the building (Figure 4.2). A sample vessel was connected in the outlet tubing from each core headspace and on the inlet of the manifold (a description of the vessels is given in the next section). This allowed a sample of air to be taken by simply closing off both the taps.

This whole system of cores, headspace lids and PTFE tubing coming into the laboratory, passing over the cores and out to the GC had previously been tested for leak-tightness by detection of CO_2 using the GC in the mobile laboratory. The CO_2 was in the form of dry ice.

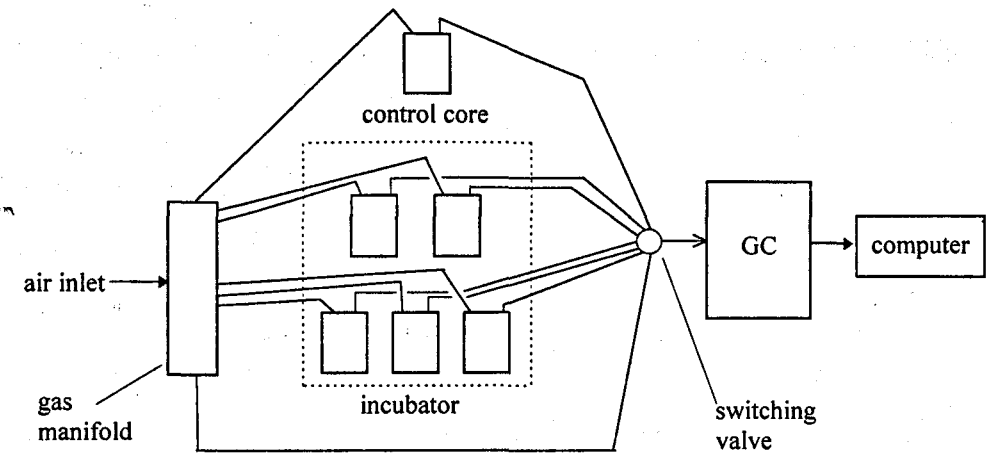

Figure 4.2 Schematic diagram to show the set up of the cores in the laboratory.

4.1.2 Description of the Sample Vessels

A glass sampling vessel was specially designed for this flow-through work by Dr. G.H. Morgan, and made up by J.Young (Scientific Glassware) Ltd. It was loosely based on the design of the 1 L sampling vessels used by the Commonwealth Scientific and Industrial Research Organisation (CSIRO) in their global sampling network. The vessel had a volume of 200 ml (Figure 4.3). The taps are standard Teflon®-barrelled Young's vacuum taps, as used in the sample vessels for field work (Section 3.1.1). There were practical reasons for having the taps at each end configured in different ways. The position of the sample inlet systems on the gas chromatograph (GC) and MIRANDA required different alignments of a long vessel, although both could receive a round vessel easily.

4.1.3 Mobile Laboratory Set up

The mobile laboratory was housed in a twin-axle tow-a-van (trailer), fitted with temperature-controlled heaters and wall extraction fans to maintain constant laboratory temperature for optimum GC operation. It contained a standard GC that was capable of monitoring nitrous oxide (N_2O), carbon dioxide (CO_2), and CH_4 *via* twelve sequentially scanned input ports. All the associated equipment such as the

computer, carrier gas, standard calibration gases and mass flow controllers were also kept inside the mobile laboratory.

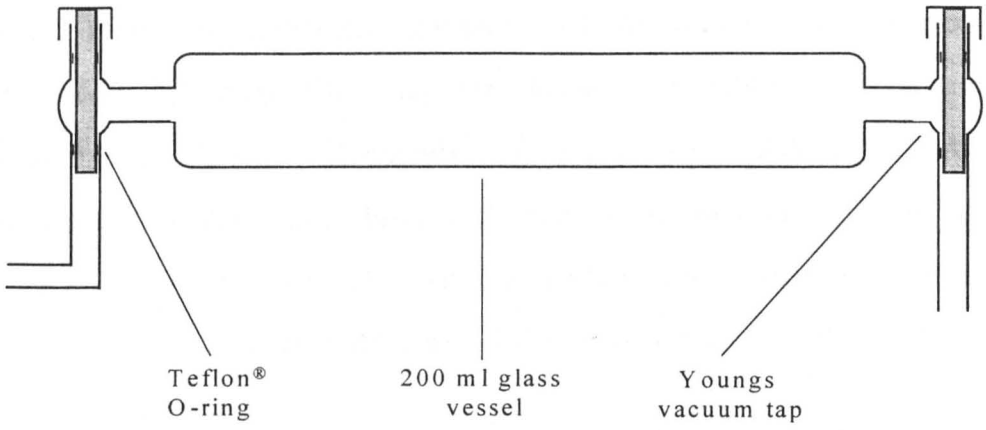

Figure 4.3 Glass sampling vessel for flow-through applications.

A Perkin Elmer 8500 GC was used with a flame ionisation detector for methane determinations. It was also fitted with a ^{63}Ni electron capture detector to allow for N_2O determinations, and a methaniser to analyse for CO_2 (after conversion to CH_4). The sample inlet mechanism consisted of a Valco 2-way pneumatic auto injection valve fitted with a 5 ml sample loop. The column was a stainless steel column packed with Poropak Q (50-80 mesh), 4 m long and $^1/_8$" diameter. The column output had a 2-way silica microbore splitter to feed the two detectors.

Operating conditions: The GC oven operated isothermally at 40 °C. The N_2 carrier gas has a flow rate of 32 ml min^{-1}. Retention times were typically 1.7 minutes for CH_4, and 3.0 & 4.0 minutes for CO_2 & N_2O respectively; but 15 minutes were normally allowed between samples to allow for data processing, storage and plotting.

A Valco 12-way pneumatic valve allowed one of the twelve gas inputs to be fed to the GC. For this work the valve was programmed to sample through eight of the twelve inputs (*via* a Valco Stream Selection Module and a Valco Multiposition Control Module) in a cyclical manner under control from the GC. This valve and the

2-way valve at the sample inlet were driven by an independent compressed air source (Jun-Air Model 3 Minor) set at 350 kPa. The eight output ports were fed from flow regulators set to 25 ml min^{-1}.

One of the gas inputs was linked to the air line entering the cores and six inputs were connected to the outlets from the core headspace lids (Figure 4.2). The eighth input to the GC was linked to a reference gas cylinder *via* a solenoid valve powered from a purpose built sequence timer under GC control. Dual analogue GC outputs were fed to a PE 1020 integrator for processing. The integrator used PE 1020 software and a BASIC programme written in house at Merlewood.

4.2 Experimental Parameters for Investigating the Effect of Temperature

For the investigation into the effect of temperature, the water table was maintained at the surface of the peat, by topping up with de-ionised water as necessary. The required temperature was set on the incubator. This was verified by means of a mercury thermometer inside the incubator. The temperatures studied were 20 °C, 15 °C, 10 °C and 7 °C, in that order. The fluxes of methane from the headspaces were monitored continuously, using the GC in the mobile laboratory, over several days. When the fluxes from the cores reached a constant rate, headspace samples were collected by simply closing off the vacuum taps on the sampling vessels. Once a set of samples had been collected, the temperature was adjusted for the next experiment.

The sample vessels were returned to the Open University for isotopic analysis on MIRANDA. Dilution plots were constructed for each temperature (Section 3.5.2), and the effect of temperature on the isotopic composition of methane emitted from the cores was determined. The effect of temperature on the methane flux was also considered and the activation energy of the net process (flux = production - oxidation) was calculated.

4.3 Experimental Parameters for Investigating the Effect of Water Table Depth

An experiment was performed whereby the water table was dropped to a depth of 25 cm below the surface of the peat, while the temperature was maintained at 15 °C. Again, the methane flux from the cores was monitored by means of the GC in the mobile laboratory. When the flux had stabilised, samples for isotopic analysis were collected from the outlet of each headspace and from the air inlet.

4.4 Results

4.4.1 Control Core

There are a number of reasons why $\delta^{17}M$ may change during the course of this experiment including:

- change in δD of the associated water,
- change in CO_2 in background air, or
- the plants in the cores are dying over time due to the lack of light.

The δD for water supplied to the peat core is known to have an effect on the isotopic composition of the methane produced by the microbial population (Section 6.2 discusses the relationship between δD of water in the peat and $\delta^{17}M$ of the methane emitted). To ensure that any isotopic shifts produced in these experiments were not an artefact of adding de-ionised water to the peat ecosystem, one core was left on the laboratory bench for the total duration of these experiments. The isotopic composition of the methane in the outlet of the headspace is given in Figure 4.4. The $\delta^{17}M$ values for the air inlets at each sampling point is also given. It is difficult to make a comparison, because for each experiment there was a different air inlet sample. Despite this, the $\delta^{17}M$ values all lie fairly well on the line shown, even though the samples were taken over a period of several months. This seems to suggest that any shift in isotopes seen in the main experiments were a result of changing the temperature or water table, and not due to the water used. This is not surprising, as the de-ionised water from ITE, Merlewood had an isotopic

composition, δD, of -43.5‰ which is within the range of δD values for water collected from the field site (Section 3.5.4).

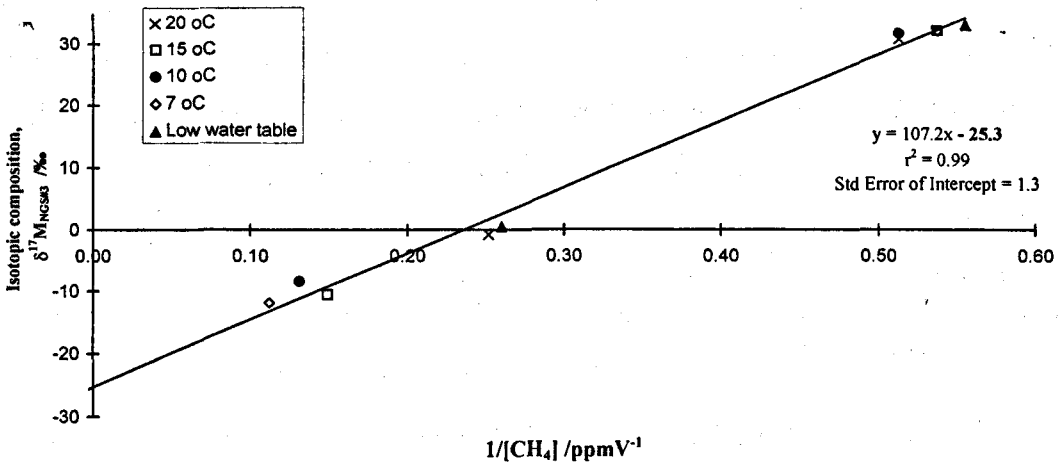

Figure 4.4 Dilution plot showing the isotopic composition of the methane produced by the control core during the controlled environment experiments (n=10).

4.4.2 Effect of Temperature

a) Methane Flux

The flux measurements were made from the cores by comparing the methane concentration in the headspace outlets to the methane concentration in the air inlet. The increase in CH_4 concentration, the flow rate and the core dimensions were used to calculate the methane flux. The results are given in Table 4.1. There was an increase of methane flux rate with increasing temperature. Average CH_4 flux rates range from 11 ±1.4 to 36 ±3.4 μmol m^{-2} hr^{-1} over a temperature range of 7 to 20 °C. The flux rates in the laboratory study were lower than flux rates at comparable temperatures in the field study. This may arise from the cores being kept in the dark in the laboratory study, thus inhibiting photosynthesis and normal plant growth. Vascular plants are known to play an important rôle in methane production and transport in peat bogs (Shannon *et al.*, 1996; Waddington *et al.*, 1996). Photosynthates leaving the plant as root exudates provide a labile carbon source for the methanogenic population to utilise in methane production. Plants also act as a

conduit for methane transport to the atmosphere, either passively or actively. This idea is expanded in Chapter 6.

Table 4.1 Results of the temperature experiments conducted in the laboratory (n=5).

Temperature (oC)	Methane Flux (μmol CH_4 m^{-2} hr^{-1})	1σ std error
7	10.8	1.4
10	15.1	2.0
15	27.9	3.4
20	35.6	3.4

The effect of temperature on methane flux in this experiment is discussed in detail in Chapter 6 along with data from the field study at the Migneint.

b) Isotopic Composition

Dilution plots were constructed for each temperature (Figure 4.5). The intercepts of the dilution plots give the isotopic composition of the methane emitted by the cores (Section 3.5.2). The results are summarised in Table 4.2. $\delta^{17}M$ ranges from -28 (±1.2) to -25 (±1.4)‰ over a temperature range of 7 to 20 °C. This was within the range of $\delta^{17}M$ measured in the field at the Migneint, which ranged from -34 to -17‰.

There was no correlation between peat temperature and the isotopic composition of emitted methane in this experiment. This was in complete contrast to the results from the field experiments (Section 6.1.1). The most likely explanation is that as a consequence of the cores being kept in the dark in the laboratory experiments, there was no photosynthesis and no active plant growth occurring. This suggests that the presence of vascular vegetation in the peat ecosystem is a significant

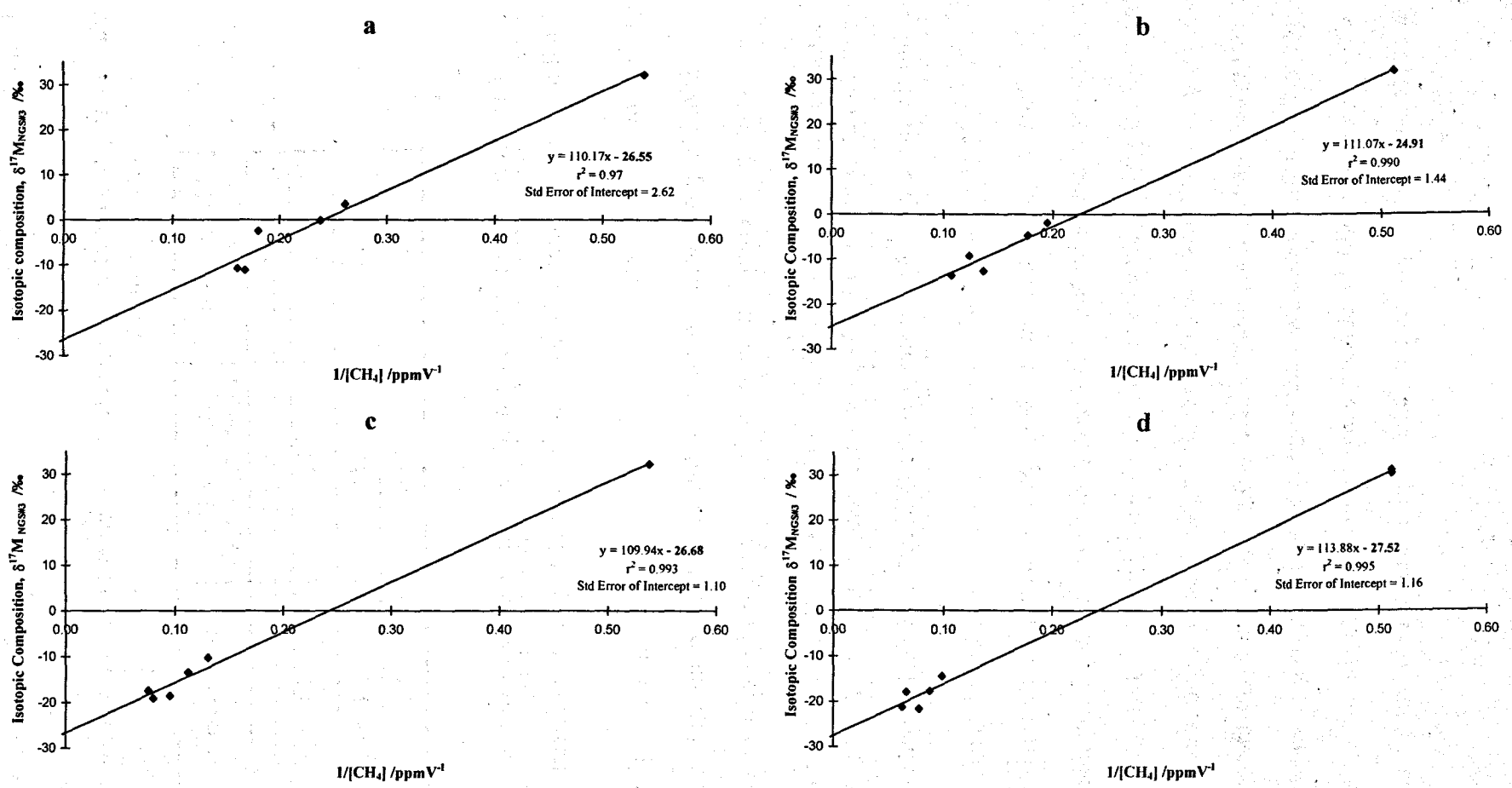

Figure 4.5 Isotope dilution plots for methane emitted from cores in a controlled environment: a = 7, b = 10, c = 15 and d= 20 °C, (water table at the surface).

factor when considering the isotopic composition of methane emissions from wetlands. This idea is discussed in detail in Chapter 6, in a comparison of data from the laboratory experiments and data from the field study.

Table 4.2 Effect of temperature on isotopic composition of methane emitted by cores with water table at the surface (n=6).

Temperature (°C)	Isotopic Composition ($\delta^{17}M_{NGS\#3}$, ‰)	standard error of the dilution plot intercept
7	- 26.6	2.6
10	- 24.9	1.4
15	- 26.7	1.1
20	- 27.5	1.2

4.4.3 Effect of Water Table Depth

Taking the water table down to 25 cm below the surface of the peat (temperature = 15°C) resulted in a decrease in methane concentration as the air was pumped across the cores. This was because atmospheric methane in the headspaces was oxidised by the methanotrophs in the cores. The whole depth of the core was aerated and methane oxidation could occur throughout the core. It was assumed that methanogenesis was inhibited by the presence of oxygen. Once the methane in the cores was used up, methane from the ambient air would diffuse into the cores due to the concentration gradient and be consumed. As air was constantly pumped across the cores, they remained aerobic throughout this experiment. The dilution plot is given in Figure 4.6, which also shows the dilution plot for cores with the water table at the surface of the peat for comparison.

It is assumed that in this experiment the cores were not producing methane and that only atmospheric methane was consumed by the microbes. For methane consumption, or methane oxidation, the intercept of the dilution plot gives the isotopic composition of the methane utilised by the microbial population. It can be

seen in Figure 4.6 that the isotopic composition of the methane consumed, $\delta^{17}M$, is +10.3‰. This indicates that the microbes have preferentially utilised the lighter isotopes of the methane in the air, leaving the residual methane higher in $\delta^{17}M$. Full results are given in Table 4.3.

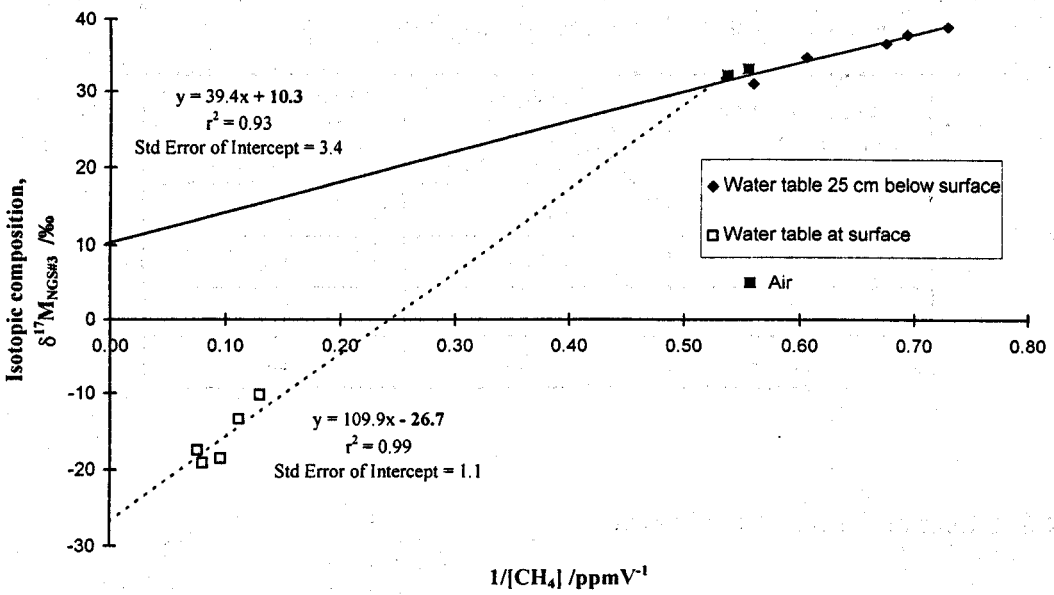

Figure 4.6 Dilution plot for cores with lowered water table (n=6).

Table 4.3 Results for the replicate cores with lowered water table.

Core	$[CH_4]$ /ppmV	Headspace $\delta^{17}M_{NGS\#3}$, ‰	Decrease in $[CH_4]$ /ppmV	Isotopic Composition of CH_4 consumed, $\delta^{17}M_{NGS\#3}$ /‰
inlet	1.80	33.1		
1	1.37	38.9	0.43	14.6
2	1.48	36.6	0.32	16.8
3	1.78	31.1	0.02	214.9
4	1.65	34.7	0.15	15.7
5	1.44	37.9	0.36	14.0
6 (control)	3.84	0.5	2.04 increase	-28.3 produced

Atmospheric methane was oxidised at a rate of ~ 0.8 μmol m^{-2} hr^{-1} (±0.3 1σ std error). This rate is much lower than the rate of methane flux (Table 4.1). Generally,

as the amount of methane consumed by the methanotrophs in the cores increased, the isotopic composition of the residual CH_4 in the headspace also increased.

The isotopic composition of the methane consumed by core 3 appeared to be much higher in $\delta^{17}M$. This is because the actual decrease in CH_4 concentration in the air as it passes over core 3 was very small; it was at the limits of measurement on the GC. Thus, the uncertainty of the calculated isotopic composition of the methane consumed was very high: ±200‰. However, it can be seen that by plotting all the data on a dilution plot overcomes this problem. Taking the intercept of the regression line evens out the uncertainties associated with individual cores.

It can also been seen from Table 4.3 that the core on the bench, at 15 °C with water still at the surface, was producing methane at a rate of approximately 8 μmol m^{-2} hr^{-1}. The isotopic composition of methane being emitted from this core was $\delta^{17}M$ = - 28.3‰, which is consistent with other results where the water table was at the surface, indicating that there had been no significant degeneration of the cores.

4.5 Summary

Methane flux rates ranged from 11 to 36 μmol m^{-2} hr^{-1} over temperature range of 7 to 20 °C. Flux rates increased with increasing temperature while water table was held at the peat surface. The isotopic composition of emitted methane was between -28 and -25‰ over a temperature range of 7 to 20 °C. Comparison of these results with those from the field suggest that plants play an important rôle in methane emissions and the isotopic composition of the methane flux.

Lowering the water table caused oxidation of atmospheric methane. The $\delta^{17}M$ of the methane consumed was +10‰. Atmospheric methane was oxidised at a rate of ~0.8 μmol m^{-2} hr^{-1}.

A full discussion of these results, and a comparison with data from the field study is given in Chapter 6.

Combined Isotopic Composition of Methane Emissions from a Palsa Mire in Finland

5. Introduction

This work was intended as a case study to complement the field work conducted at the Migneint site in Snowdonia (Chapter 3), and the larger programme, "Understanding the Land Surface Physical Processes in the Arctic". The programme was a collaborative initiative between the Institute of Hydrology (IH), the Finnish Meteorological Institute (FMI), and the Institute of Terrestrial Ecology (ITE). The aim of the programme was to gain a better understanding of the basic processes underlying the balance of water, energy, carbon dioxide and methane for arctic land surfaces through a programme of measurements and modelling.

Global climate change model scenarios suggest that the tundra biome will be very sensitive to changes of climate (Christensen, 1991). It is estimated that in the boreal region temperatures might increase by as much as 2 to 4 °C (Dickenson, 1986) and there may be a reduction in summer soil moisture (Manabe and Wetherald, 1986; Mitchell, 1989). However, to date there has been very little research in this area and the factors currently controlling methane emissions are not fully understood. In fact, methane fluxes from tussock tundra sites may be over-estimated by as much as 20 Tg yr^{-1} (Torn and Chapin, 1993), leading to a substantial discrepancy in current global methane budgets.

Much of the Arctic region (north of latitude 66°32'N) is underlain by permafrost. Permafrost is defined as the condition existing below the ground surface, irrespective of its texture, water content or geological character, in which the temperature of the material has remained below 0 °C continuously for more than two years (Muller, 1947). Continuous permafrost covers ~21×10^6 km^2 of the Earth's surface; where it breaks up into patches as it merges with seasonally frozen ground it is known as discontinuous permafrost. Warming of the permafrost region may cause the layer of ground that thaws during the summer (the active layer) to increase in depth, thus providing the potential for greatly enhanced methane emissions (Christensen *et al.*, 1995). Alternatively, if the tundra becomes drier, it could potentially turn the tundra soils into CH_4 sinks because potential for methanogenesis would be decreased and the potential for methane oxidation in the surface layers would be increased. Thus, it is crucial to determine the balance between methane production and consumption in this area, and the environmental factors that control these processes.

The field work in Finland took place in June 1997. One aim of this field work was to use $\delta^{17}M$ measurements of methane to allow a comparison between the CH_4 budgets estimated from micrometeorological methods and those extrapolated from chamber measurements. Unfortunately, this was not possible due to a fatal power

failure for the micrometeorological equipment. However, methane emissions were measured from hollows, hummocks and a lake using static chamber techniques, and their isotopic composition determined. Air samples were also taken manually from the micrometeorological mast. Results from the chamber samples were compared to the results from the micrometeorological measurements on the previous day, which had comparable meteorological conditions.

The micrometeorological and climatic data reported in this chapter were collected and interpreted by Dr Ken Hargreaves and Prof. David Fowler (ITE, Edinburgh). They are reported here for comparison and discussion.

5.1 Field Site Description

A substantial part of northern Finland is covered by palsa mire. Palsa is defined as a mound or ridge of peat or peaty earth containing perennial ice lenses and a core of permafrost (Whittow, 1984). The surface is usually criss-crossed with open fissures caused by frost cracking, dilation cracking (due to doming) or desiccation. It is thought that palsa are formed by differential frost heaving linked to the thermal conductivity of the peat. The site chosen was typical of palsa mires and was situated 10km NNE of Kaamanen in northern Finland close to Lake Inari, 69°8'25"N 27°16'10"E (Figure 5.1). Known locally as Jänkäjärvi, the site consisted of a mixture of pool and hummock areas in a ratio of 2:1 (Hargreaves, *pers. comm.*). The hummocks were up to 1m in height, 2-3m wide and up to 25m in length. The fetch for the micrometeorological masts was between 300 and 800m in most directions, although there was a forest in the 240-320° sector (Section 5.2.1 describes the micrometeorological methodology in detail). In addition there was a small lake to the south-west (Figure 5.2).

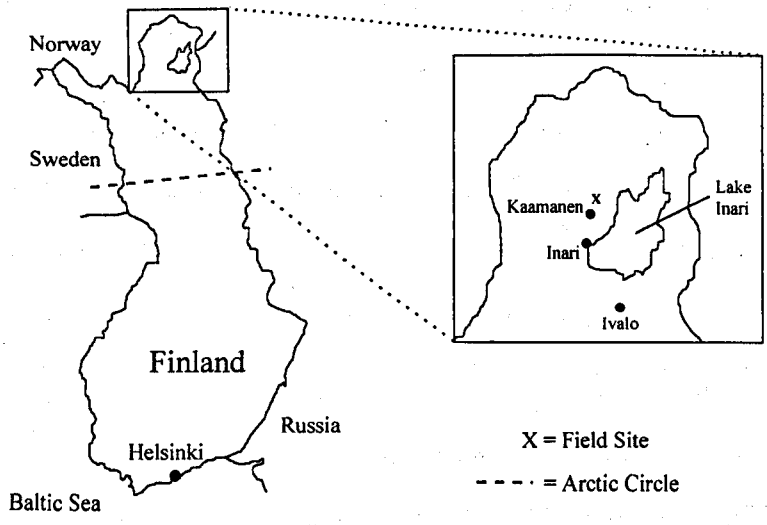

Figure 5.1 Diagram to show the location of the Jänkäjärvi Field Site in Finland. Finland has many lakes (10% of its area is covered by water) but only Lake Inari is shown.

At the time of sampling the pools contained a depth of about 2 cm water, over sediment which appeared to be at least 60 cm deep. Immediately following the snow melt (23-27 May 1997) the water table had been much higher (50 cm), peaking on 30 May 1997 and gradually declining. The vegetation was *Sphagnum* spp., *Menyanthes trifoliata, Eriophorum* spp., *Equisetum* spp. and *Carex* spp.. In contrast the hummocks had vegetation which was predominantly more woody, *Betula nana, Vaccinium vitis-idaea, Vaccinium uliginosum, Empetrum nigrum* and *Ledum palustre* (Hargreaves, *pers. comm.*). At the time of sampling the hummocks were already dried out at the surface. The lake was approximately 35 cm deep and possessed a sandy sediment bottom.

5.2 Experimental Details

All the samples were collected on the same day: 21 June 1997. Sampling was performed in a similar fashion to the field work in Snowdonia, using the same design of glass sample vessel (Chapter 3). Sample vessels were pre-evacuated in the laboratory at the Open University. The total number of samples taken at the field site

was 29; this was limited by the number of sample vessels that could reasonably be carried as hand-luggage on a commercial aircraft.

Two ambient air samples were taken in the manner described in Section 3.2.1. Two of the perspex headspace chambers used in Snowdonia were used for sampling methane emissions. One chamber was fitted with a stainless steel manifold to allow four samples to be taken at timed intervals (including time = 0), in order to ensure that the rate of methane accumulation inside the headspace was constant over the sampling period. With the second chamber one sample was taken at the start of the experiment and one after a known time interval. The time allowed for methane accumulation was noted. Six air samples were collected using the chambers from each of the following areas: a pool, a hummock, over open water on the lake and over vegetation in the lake.

The temperature down the peat profile was measured at 5 cm intervals from 0 to 30 cm, and then at depths of 40 and 50 cm. Two temperature profiles were recorded for each sampling point, at the time of sampling. The air temperature was also recorded.

To estimate CH_4 emission from the pools, a representative pool was selected about 25 m to the NE of the micrometeorological mast. Selection criteria included ease of access; many of the hummocks possessed high vertical sides. The head space chamber was gently placed onto the bottom of the pool to ensure there was no disturbance of the sediment and that no methane was forced out as bubbles into the chamber. Sampling time was one hour.

A hummock adjacent to the pool was also sampled. It was necessary to cut a groove 2 cm into the peat surface using a garden spade to ensure a good seal between the hummock surface and the chamber. This was done 24 hours prior to sampling, to ensure that the system had returned to equilibrium. When the headspace chamber was in place wet *Sphagnum* moss was packed around the base of the chamber (Crill *et al.*, 1988), to assist the seal. Sampling time was two hours.

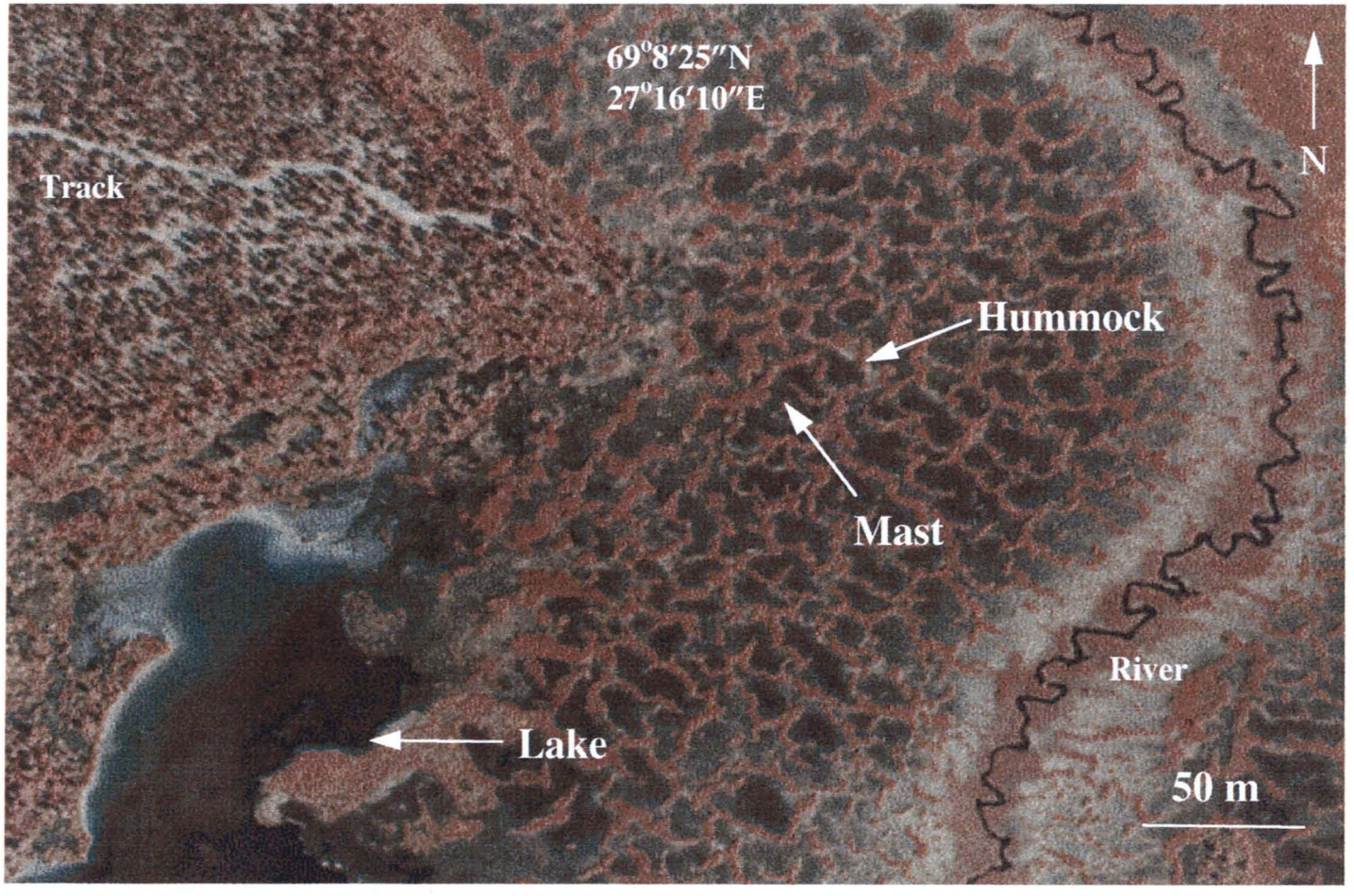

Figure 5.2 Aerial infrared photograph of the Jänkäjärvi field site. Lighter colours indicate higher temperatures, dark colours indicate colder temperatures. The distinct pattern of pools and hummocks is clearly seen down the centre of the picture: the cool pools are dark and the hummocks are red, due to their relatively warmer temperature.

A flotation device was made for the chambers to allow sampling of CH_4 emission from the lake. This consisted of a polystyrene ring about 4 cm in depth, internal diameter 28 cm, external diameter 34 cm, with a groove cut into it to hold the chamber (Figure 5.3). The groove was filled with water to ensure an air-tight seal. Lengths of string were attached to each side to prevent the chamber floating out of reach. The sampling location was again chosen for ease of access as well as being representative. Samples were taken from open water in the absence of vegetation, and over emergent vegetation (*Equisetum fluviatile* and *Menyanthes trifoliata*) in the lake. Sampling time was one hour in both cases.

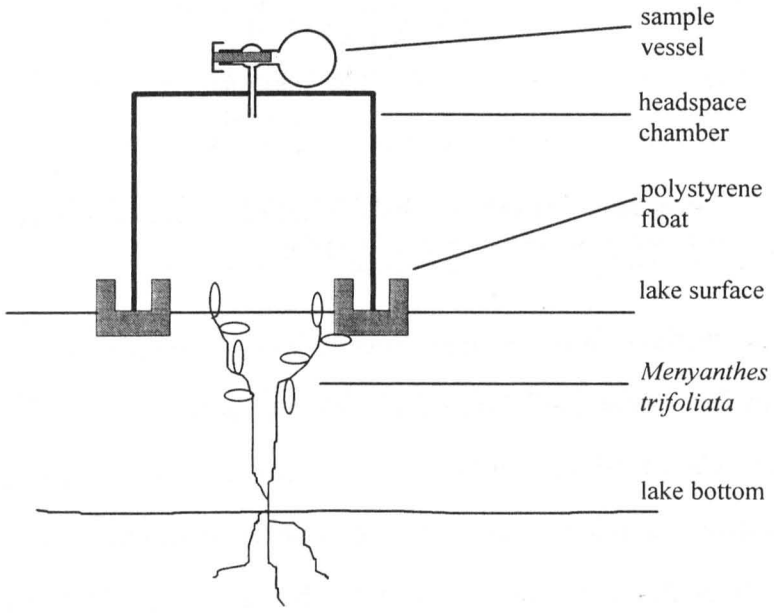

Figure 5.3 Cross-sectional diagram of flotation device for sampling methane emissions from the surface of the lake.

Two samples were also taken *via* the micrometeorological mast. The line carrying the air from the mast to the instrumentation was disconnected near the inlet to the tunable diode laser (TDL). A 1 L syringe was used draw the 'old' air (which was discarded) through the line. By means of a plastic 3-way tap and a plastic T-piece, the syringe was connected to a glass sample vessel (Figure 5.4). Then the syringe was filled from the line. The air in the syringe was steadily expelled through the vent line. The tap of the sample vessel was opened after 250 ml air had been

expelled and closed before the syringe was empty. In this manner, air from the mast inlet was transferred from the syringe into an evacuated vessel with minimum contamination from air at ground level. This was performed while the wind was in an easterly direction and was therefore passing over the field area *en route* to the mast.

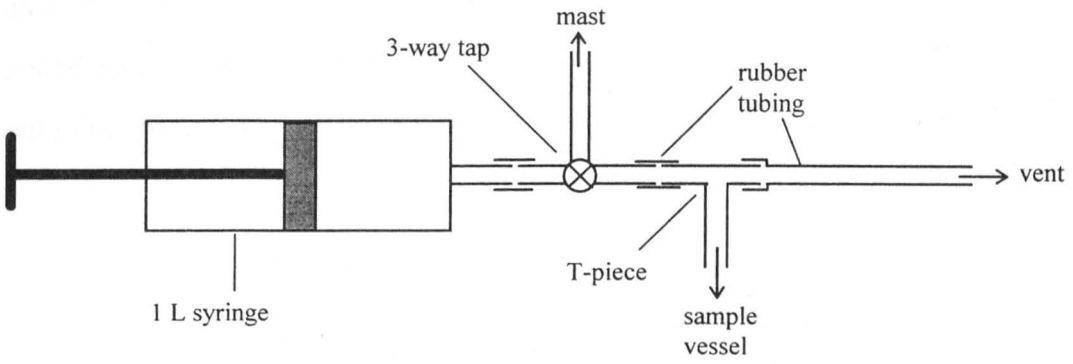

Figure 5.4 Arrangement for transferring air from the micrometeorological mast inlet to a glass sample vessel by way of a 1 L syringe.

A sample of methane was collected directly from bubbles in the submerged peat in the following manner: The headspace chambers used by ITE, Edinburgh possessed a removable lid, which consists of a solid ring or flange (diameter 30 cm, width 4 cm), the centre of which was covered by polythene sheeting. The sheeting had an air-tight seal to the ring, and was flaccid rather than taut. One such lid was used. The polythene sheeting was held below the level of the ring and the ring was carefully lowered into the water so as to exclude any air bubbles. The ring was held submerged while the sediment at the bottom of the pool was disturbed, thus releasing bubbles. The released bubble air was trapped under the polythene sheeting (Figure 5.5). When a sufficient amount had been trapped, a glass sample vessel was gently pushed under the edge of the ring (avoiding the introduction of ambient air) so that the side-arm inlet was in the bubble air. The tap on the sample vessel was then opened and the bubble air was observed to enter the vessel. It was noted that the side-arm inlet would have contained a small amount of ambient air. This was

unavoidable but represents only a very small level of contamination: < 2ml @ 1.8 ppmV in 100ml of potentially pure methane.

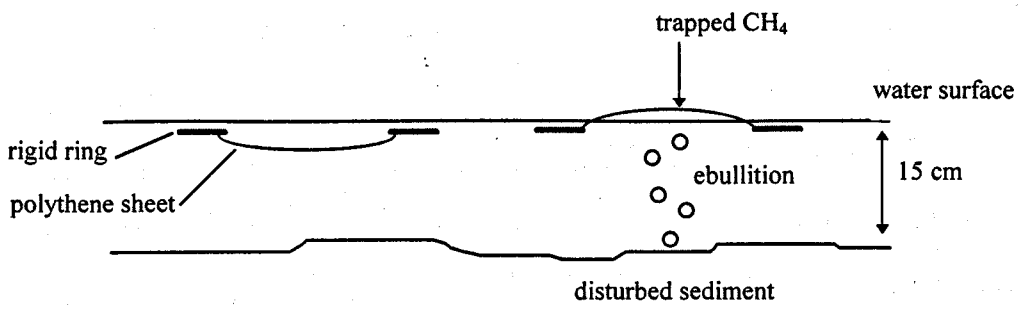

Figure 5.5 Trapping bubbles directly from the sediment at the bottom of a pool.

The samples collected at the Jänkäjärvi field site were returned to the laboratory at the Open University within 2 days, for analysis using gas chromatography to determine the methane concentration, and MIRANDA to determine the combined isotopic composition of the methane as described in Chapter 2. The methane flux was also calculated as described in Section 3.4.3. A total of 29 samples were taken: 2 ambient air, 2 *via* the micrometeorological mast, one from a sediment bubble, 6 from a pool, 6 from a hummock, 6 from over open water and 6 from over vegetation in the lake.

A sample of water was taken from the pool, and from the lake. The isotopic composition of the water (δD and $\delta^{18}O$) was determined by Prof. Tony Fallick at Scottish Universities Research and Reactor Centre as described in Chapter 2.

5.2.1 Micrometeorological Methods

Micrometeorological techniques have a number of advantages over conventional chamber techniques. Firstly, fluxes are averaged over a large area (10^2 to 10^5 m^2) and are thus not subject to sampling problems associated with chamber methods. Secondly, the measurements do not disturb the soil or vegetation in the area under examination as the equipment and disturbance is located downwind of the place where the gaseous exchange is occurring. Lastly, the shorter sampling times

associated with micrometeorological measurements allow studies of the changes in rates of trace gas exchange with changing atmospheric conditions. However, there are also disadvantages, such as equipment costs, transport requirements and the need for specialist training for operators.

The simplest micrometeorological technique is eddy covariance or eddy correlation. In eddy covariance the flux F is given by the product of w', the instantaneous deviation of the vertical wind speed from the mean (ms^{-1}) and χ', the instantaneous deviation of the gas concentration from the mean ($\mu g\ m^{-3}$) (Fowler and Duyzer, 1989; Fowler *et al.*, 1995b):

$$F_\chi = W'\chi' \qquad \text{Equation 5.1}$$

To sample the spectrum of turbulent eddies transporting the methane flux, the instrument must be able to detect the high frequency structure in vertical wind velocity and concentration of gas, which requires a response time of 0.1s or better. It is also necessary to detect differences in CH_4 concentration of 1-10 ppbV. Ultrasonic anemometers can measure the three components of the turbulence, and the rapid measurement of CO_2 and water vapour has also been possible for sometime. However, it is only recently with the development of a tunable diode laser spectrometer (TDL) that the rapid measurement of methane (and N_2O) concentration has become possible. In addition to determining the flux of a trace gas, micrometeorological data can also be used to model the cumulative flux and to predict the flux footprint, *i.e.* the relative contribution to the flux made per unit distance from the mast. Details of the mathematical derivations for this can be found in Leclerc and Thurtell (1990) and Schuepp *et al.* (1990).

There were four micrometeorological masts in the field site. The ITE mast, marked on Figure 5.2, measured methane flux. Eddy covariance measurements of CH_4 and other trace gas fluxes were made on a continuous basis from mid-May to mid-June 1997 over the period of the snow melt. Air was sampled from the top of

the 5 m mast and pumped through nylon tubing ($^3/_{16}$" internal diameter, 25 m long) at a flow rate of 10 L min^{-1} into the TDL, which was housed in a tent on a neighbouring hummock. Power was supplied by a generator located about 200m to the west, at the end of the forest track and generally downwind of the mast. The laser, operating at liquid nitrogen temperatures (75 to 100K) was tuned to an absorption line centred on 3017.46 cm^{-1}. The root mean square (rms) noise was approximately 1% for ambient CH_4 measurements sampled at 20Hz. As described previously, this rapid sampling is a requirement of eddy covariance methods.

A sonic anemometer, also mounted at the top of the mast as close to the gas inlet system as possible without obstruction, provided the three-component wind velocity and air temperature. The flux measurements were calculated from the covariance of the vertical wind and concentrations, with the co-ordinate system rotated to provide the fluctuating component perpendicular to the streamlines of the flow as described by McMillen (1986), using the software 'Eddysol' (Moncrieff *et al.*, 1997). The fluxes were calculated following the subtraction of a 20-minute running mean from the 20 Hz measurements of W and χ to provide 10-minute mean fluxes.

A detailed account of the instrumentation for eddy covariance may be found in Hargreaves *et al.* (1996) and for the TDL in Zahniser *et al.* (1995).

5.3 Results

5.3.1 Temperature Profiles

Temperature profiles for the pools, hummocks and lake sediment are given in Table 5.1. The air temperature ranged from 8.4 to 15.2 °C; the minimum being in the morning, and rising with increased solar radiation. The lake sediment temperature could only be measured to a depth of 10 cm, being constrained by the length of the temperature probe. The water temperature in the lake was 11.6 °C at all depths, and

in the shallower pools it was 14.0 °C. All temperatures were recorded near a headspace chamber at the time of sampling.

The temperature of the hummocks was measured to a depth of 20 to 25 cm; below this depth was a permanent ice lens, and the temperature probe was unable to penetrate this layer.

Table 5.1 Peat temperature profiles for pools, hummocks and lake sediment, at Jänkäjärvi on 21 June 1997.

	Temperature /°C		
Depth /cm	**Pools**	**Hummocks**	**Lake Sediment**
0	14.0	14.2	11.6
5	8.4	10.2	9.8
10	6.8	5.9	8.4
15	6.1	2.3	
20	5.5	0.4	
25	4.9	-0.2	
30	4.2		
40	3.1		
50	2.3		

It is interesting to compare these temperature profiles with those of the Migneint field site (Section 3.4.1). During the winter months the Migneint site has low temperatures such as those found at depth here in Finland. The peat under the pools and in the hummocks in Finland has a temperature drop of 12 and 14 °C from the surface to 50 cm and 25 cm depth respectively. A similar difference is also seen at the Migneint site, but only in the warmest months, and the temperatures are generally about 10 °C higher all the way down the profile compared to Finland. For 50% of the year the temperature down the peat profile changes by less than 5 °C at the Migneint site. In Finland it is not known how the temperature profile of the peat changes in winter but is probably not much different to the Migneint.

5.3.2 Air Samples

The methane concentration in the air samples taken at ground level (1.5 m) was 1.82 (± 0.02, n=3) ppmV and the methane concentration of the samples taken *via* the micrometeorological mast (5 m) was also 1.82 (±0.01, n=2) ppmV.

5.3.3 Methane Fluxes

Methane fluxes were calculated from the increase in methane concentration in the headspace chamber over the course of the experiment, as described in Section 3.4.3. The results are given in Table 5.2.

Table 5.2 Methane fluxes from various terrains in the Jänkäjärvi field site, 21 June 1997 (numbers in brackets are the range, n=4).

Terrain	CH_4 flux ($\mu mol\ m^{-2}\ hr^{-1}$)	1σ std error
Pools	41 (29-54)	±5.3
Hummocks	1 (0.9-2)	±0.2
Lake (no vegetation)	24 (18-34)	±3.7
Lake and vegetation	368 (284-456)	±46

The methane emission from the hummocks was small (Table 5.2). In August 1995 other researchers measured no CH_4 flux or even determined the hummocks to be a CH_4 sink at this site (Hargreaves, *pers. comm.*). One possible explanation for this difference is that the hummocks may have been drier in 1995, than on this occasion.

It is interesting to note that methane fluxes from the pools were about 25% of the fluxes measured at other sites in Finland in 1991 and 1992 (Martikainen *et al.*, 1995; Nykanen *et al.*, 1995). Since those sites were further south than Jänkäjärvi (61'N and 62'N respectively), it is not unreasonable to assume they would be warmer

for much of the year, especially during the growing season. Also, climatic conditions differ from year to year, making comparisons difficult.

It is possible to combine the fluxes from both the pools and the hummocks in this experiment:

The ratio of pool: hummock is 2:1

$$\frac{(2 \times 41) + (1 \times 1)}{3} = 28$$

giving a total flux of 28 (±3.2) μmol CH_4 m^{-2} hr^{-1} across the whole site. In comparison, the micrometeorological data for several days prior to the experiment described here gave an average total methane flux of 47 (±15.7) μmol m^{-2} hr^{-1} (Hargreaves, *pers. comm.*). The contribution of the lake to the total CH_4 flux is omitted from this calculation because it was not within the micrometeorological fetch at this time.

Within experimental error, spatial and temporal variability, the methane flux measured using headspace chambers agrees with the methane flux measured by micrometeorological methods. Micrometeorology integrates over the whole area of palsa mire so the slightly higher fluxes may arise for a number of reasons:

- methane flux is enhanced by vegetation: some pools may have a greater plant density than the one sampled from using headspace chamber,
- there may be a larger flux coming from another source, for example near the river the topography of the mire was slightly different, comprising of many small hummocks less than 30 cm diameter and 30 cm high.

It is clear that the lake is also a significant source of methane, with a flux of 24 (±3.7) μmol CH_4 m^{-2} hr^{-1}, which is more than half the methane emission of the pools. As shallow lakes of this nature are common in northern wetlands and in the Arctic tundra, they should not be neglected in determining methane budgets on the global scale.

Areas of the lake containing vegetation exhibited methane emissions that were ten times greater than lake containing no vegetation, during June 1997. This is in line with research in various locations (*e.g.* Whalen and Reeburgh, 1988; Schütz *et al.*, 1991; Morrisey and Livingston, 1992; Schimel, 1995; MacDonald *et al.*, 1998). The two species under investigation here, *Equisetum fluviatile* and *Menyanthes trifoliata,* are hollow-stemmed and are believed to act in a similar manner to a drinking straw, providing an open conduit to the surface, from deep in the lake sediment.

5.3.4 Isotopic Composition of Methane Emissions From The Palsa Mire

δD for the water sample from the lake was determined as -99‰ and from the pool it was -91‰. Both are much reduced in compared to the average δD value of -37‰ at the Migneint field site (Section 3.5.4), but could only account for a maximum difference of 4‰ in $\delta^{17}M$ between the two sites. The lighter δD values in Finland are presumably a consequence of the fact that the isotopic composition of rain water becomes depleted in δD with increasing latitude (Wahlen, 1994).

Ground-level ambient air samples gave an average $\delta^{17}M$ value of 32.4 (±0.3)‰ (n=2), very close to the average value measured at the Migneint of 32.2‰, indicating rapid mixing of CH_4 emissions into the background air, and the absence of a major source of methane pollution. Only one sample taken *via* the micrometeorological mast was isotopically analysed, and had a $\delta^{17}M$ value of 32.6‰.

Isotope dilution plots constructed (as described in Section 3.5.2) for the various terrains are shown in Figure 5.6. The different terrains have quite different methane isotopic signatures (Table 5.3). Methane emissions from the pools had a $\delta^{17}M$ value of -3.9%. This is heavier than the isotopic composition of the CH_4 emissions from the Migneint site, which ranged from -34.2 to -16.9‰ and in June 1997 were -25.4‰.

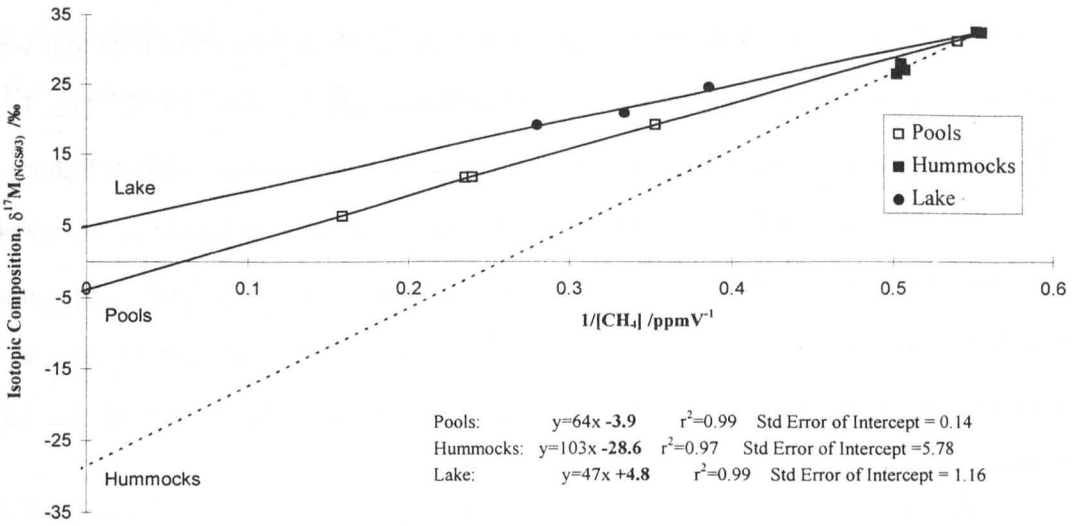

Figure 5.6 Isotope dilution plots for the various terrains in a palsa mire in the arctic region of Finland. Each line is constructed using data from 6 samples.

Table 5.3 Isotopic composition of methane emitted by different parts of a palsa mire in arctic Finland.

Terrain	$\delta^{17}M_{NGS\#3}$ (‰)
Pools	-3.9 (±0.14)
Hummocks	-28.6 (±5.78)
Lake	+4.8 (±1.16)
Forced ebullition	0.0 (±0.12)

Methane emission from the hummocks was small, and thus a large extrapolation is necessary when constructing the isotope dilution plot (Figure 5.6). This is reflected in the large standard error of the intercept. Although there is a large uncertainty in the exact $\delta^{17}M$ value for the hummocks, the data points on the dilution plot clearly lie below the dilution plot line for the pools. So we can be reasonably confident that methane emitted from the hummocks is isotopically lighter than that from the neighbouring pools.

The methane emitted from the lake surface has an isotopic composition of $\delta^{17}M$ = +4.8 (±1.16)‰. This is isotopically heavier than that emitted from both pools and

hummocks. Unfortunately the samples taken from over emergent vegetation in the lake were not analysed for $\delta^{17}M$, due to a failure of the laboratory equipment. This is an important area of future study since plant-mediated methane transport through the sediment is an important part of the total emission from wetlands and the isotopic implications of this transport need to be understood in so far as isotopic data are to be used in determining global methane budgets. At the time of this study (June 1997) the vegetation seen in the lake margins (*Equisetum fluviatile* and *Menyanthes trifoliata*) had not yet become prominent in the pools, but there was evidence that they would soon be re-colonising the pools. This obviously has implications for calculating methane budgets from this area and highlights the need for data on CH_4 flux over a complete growing season.

The isotopic composition of methane from bubbles forced out of the mire was 0.0 (±0.12)‰, mid-way between that emitted from the pools and from the lake.

5.4 Discussion

This study involved limited sampling from several different terrains in the palsa mire. In the light of the seasonal variations in the combined stable isotopic composition of methane emissions from the Migneint, and those reported from the U.S.A. (Martens *et al.*, 1986; Burke Jr *et al.*, 1988b; Chanton and Martens, 1988; Martens *et al.*, 1992), these data provide only a snapshot image of a highly dynamic system. There is much scope for further work before definitive conclusions can be drawn. However, the current data allow useful comparisons to be made between the different ecosystems within the palsa mire.

The fact that the different terrains in the palsa emitted methane of distinct isotopic composition has implications for using micrometeorological methods to obtain isotope data. For example Kuhlmann *et al.* (1998) reported methane emissions from the Hudson Bay Lowlands to have a $\delta^{13}C$ value of -60 (±3.2)‰ and δD of -442 (±142)‰. These figures equate to a $\delta^{17}M$ of -2 (±11)‰ (Equation 2.8).

These data were collected using micrometeorological methods during a strong nocturnal inversion and so the methane measured is a combination of that emitted by pools, hollows and hummocks etc. Clearly, isotope data must be used with care in global methane budgets and general circulation models.

5.4.1 Pools

The isotopic composition of the methane emitted from pools in Jänkäjärvi, -3.9‰, is slightly lighter than the values of +5 to +15‰ determined by Wahlen (1994), but it does fall within the range of -15.3 to -0.3‰ reported by Lansdown *et al.* (1992) for a temperate peat bog.

It is interesting that the methane from the pools in the palsa mire has a greater $\delta^{17}M$ value (-3.9‰) than that emitted from the water-logged ombrotrophic mire at the Migneint only a week later (-25.4‰). As $\delta^{17}M$ is a combination of $\delta^{13}C$ and δD, the differences may arise from differences in either $\delta^{13}C$, δD or a combination of both. The differences in $\delta^{13}C$ and δD, and the reasons for them have been discussed in Section 3.4. In this case, the δD value of the water in Finland was much lighter than that at the Migneint, suggesting that the heavier isotopes in Finland arise from heavier $\delta^{13}C$ values in that ecosystem. Alternatively, the relationship between the δD_{H_2O} and δD_{CH_4} may be different in a palsa mire compared to an ombrotrophic mire (Section 6.2). The two different metabolic pathways, CO_2 reduction and acetate fermentation, exhibit different relationships between δD_{H_2O} and δD_{CH_4}, partly because in CO_2 reduction all 4 hydrogen atoms come from the surrounding water, while in acetate fermentation a methyl group is transferred intact and only one hydrogen comes from the surrounding water, and also because the two reactions have different rate coefficients (Section 1.2.3).

5.4.2 Hummocks

It is surprising that the methane emission from the hummocks has a lower $\delta^{17}M$ value than that from neighbouring pools because it might be assumed that much of the methane produced at depth in the hummocks would be oxidised as it travelled to the atmosphere, due to the well aerated nature of the hummock surface. Since methane oxidation is known to enrich in the heavier isotopes of the methane flux (Barker & Fritz, 1981), the $\delta^{17}M$ value of the CH_4 from the hummocks should be greater than that from the pools, not less (assuming that the formation mechanisms are the same in pools and hummocks). If methane oxidation is occurring in the hummocks, then the $\delta^{17}M$ of the methane produced at depth in the hummock must be even lighter than that of the methane emission from the surface.

The differences in the combined stable isotopic composition of the methane emitted by hummocks (-28.6‰) versus that of pools (-3.9‰) may arise in part because different ecosystems favour different dominant methanogenic pathways: either carbon dioxide reduction or acetate fermentation. Whiticar *et al.* (1986) reported that CO_2 reduction and acetate fermentation may be distinguished isotopically: for CO_2 reduction $\delta^{13}C$ is -110 to -60‰ and δD is -250 to -170‰, while for acetate reduction $\delta^{13}C$ is -65 to -50‰ and δD is -400 to -250‰. Substituting these $\delta^{13}C$ and δD values into Equation 2.8 gives $\delta^{17}M$ values of -43 to 14‰ for CO_2 reduction and -5 to 19‰ for acetate fermentation. Whiticar *et al.* (1986) also reported that acetate fermentation was the predominant pathway in freshwater sediments. It is therefore possible that the difference in the isotopic composition of methane emitted from hummocks and pools arises because the methane was produced by CO_2 reduction in the hummocks and by acetate fermentation in the pools. A definitive conclusion will not be possible until such time as it is possible to determine $\delta^{13}C$ and thus calculate δD for these samples.

It is also possible that the methanogenic precursors in the pools and the hummocks may have different $\delta^{13}C$ values. The nutrient poor hummocks support a

vegetation which is much more woody in nature, compared to the softer grass-like vegetation in the pools. The former would contain a greater percentage of complex compounds such as lignins. In the pools the vegetation is such that the roots would die off each year, causing faster turnover of organic matter and resulting in a greater proportion of labile carbon. Thus, the substrate availability supports the suggestion that the metabolic pathway for methanogenesis in the hummocks is CO_2 reduction, and in the pools the pathway is acetate reduction (Hornibrook *et al.*, 1997).

It is also important to consider the δD component of the $\delta^{17}M$ when looking at differences in the isotopes of the methane emitted by the pools and the hummocks. Only the water in the pool was isotopically analysed. This water presumably came from recent rain water and snow melt. In the hummocks, the hydrogen being incorporated into the methane may come from water which originates from the ice lens as it melts around its perimeter. This may have a different δD value from the water in the pool, although to account for the difference in $\delta^{17}M$, between hummocks and pools, δD for hummock water would have to be ~500‰, assuming $\delta^{13}C$ remained constant.

5.4.3 Ebullition

The isotopic composition of the methane bubbles that were forced out of the mire sediment (0‰) may shed some light on methane transport mechanisms from the point of production to the surface of the pools. It can be assumed that at the point of production in the pool the isotopic composition of the CH_4 was 0.0‰, because stirred bubbles are known to be representative of naturally released bubbles and ebullition does not fractionate the carbon isotopes of methane (Chanton and Martens, 1988). It is known that vegetation is implicated in the transport of methane from the point of production to the surface. Plant transport may result in an isotopic shift in the methane towards isotopically lighter values. However, it should be noted that some

of the methane emitted from the pools was clearly seen to be by ebullition. Methane emitted by this method would be isotopically unchanged.

5.5 Implications for Global Methane Budgets and Climate Change

Tundra is thought to account for between 5 and 10% of the total global methane flux (Christensen, 1991). It is difficult to predict how the fluxes will respond to physical changes in the environment because there is disagreement over which are the most significant environmental factors. Some studies have shown that temperature is more important (Crill *et al.*, 1988; Lansdown *et al.*, 1992; Dise *et al.*, 1993; Edwards *et al.*, 1994), while others report that water table is more significant (Bubier *et al.*, 1993; Vourlitis *et al.*, 1993; Moore *et al.*, 1994). Reasons for these differences in opinion are discussed in Section 6.1.3. The presence of actively growing vegetation also plays a significant rôle in methane emissions in a number of ways (Schimel *et al.*, 1993; Shannon *et al.*, 1996; Waddington *et al.*, 1996). This is discussed in detail in Section 6.4.

Using isotopes as a tool in determining global methane budgets should give a clearer picture of the relative contributions of the different sources of methane. It is important to understand the individual sources and the environmental factors controlling them if we are to predict the impact of climate change. This study highlights the importance of obtaining appropriate isotopic data for use in global climate models.

Although micrometeorological methods can integrate the methane flux over a large area, they can tell us nothing about the relative contribution of the individual components of the area. However, isotopic analysis of individual sources can distinguish between methane emitted from pools, hollows, hummocks and lakes.

The relative contributions of each part of the mire become important in considering the implications of climate change because for example, if the tundra became warmer and drier then the pools could dry out and may become a net sink of

CH_4. However, warming could also melt the permafrost lens of the hummocks and convert them to thermokarsts. Thermokarsts are ground-surface depressions which are created by the thawing of ground ice in the periglacial zone; only thermal processes are involved in the subsidence. The area under pools would be extended. This would obviously increase the CH_4 production. An increase in temperature would generally increase substrate availability and microbial activity, and hence potentially increase methane emissions.

5.6 Further Work in the Palsa Mire

The most important area of further work is to separate out the carbon and hydrogen stable isotopes of the methane emissions in order to test the hypothesis that the differences in isotopic composition of CH_4 emitted from pools and hummocks are due to different metabolic pathways: CO_2 reduction or acetate fermentation.

As the vegetation associated with the lake, *Equisetum fluviatile* and *Menyanthes trifoliata*, had such an impact on CH_4 flux, it would be good to determine the effect the plant has on the isotopic composition of the methane. The relative contributions of the various transport mechanisms and their effect on the isotopic composition of the CH_4 emission should be investigated.

It would be interesting to determine the seasonal variation in the isotopic composition of the methane emissions from each terrain, and to determine if temperature or water table were significant environmental variables. There was a pulse of methane emitted by the palsa mire as the thaw occurred in 1997 (Hargreaves, *pers. comm.*). The isotopic composition of this pulse also needs to be determined. Further investigation is required to determine if the metabolic pathway used remains constant throughout the year.

Differences in $\delta^{13}C$ of the plant materials associated with the different terrains, and $\delta^{13}C$ of the peat in each terrain need to be examined, to establish if this could

account for the differences in the isotopic composition of the methane emissions from the different terrains.

The δD of water in the hummocks needs to be determined. Seasonal variations in δD of water associated with the different terrains need to be monitored and related to $\delta^{17}M$ or the δD of the methane produced.

5.7 Summary

Methane fluxes measured from the pool areas during this study (41 μmol m^{-2} hr^{-1}) are lower than fluxes reported in the literature, possibly due to cooler temperatures. The methane flux from the hummocks (1 μmol m^{-2} hr^{-1}) is greater than those measured by other TIGER researchers in 1995. This was possibly due to a higher water table or lower temperature in 1997 as measurements were made 2 months earlier than in 1995. Combined fluxes (28 μmol CH_4 m^{-2} hr^{-1}) are the same (within experimental error) as the flux measured by micrometeorological methods over the same area (47 μmol CH_4 m^{-2} hr^{-1}). Vegetation is strongly implicated in the transport of methane to the surface, increasing emissions from the lake tenfold in places where actively growing vegetation is present.

Isotopic analysis distinguishes between methane emissions from the pools, the hummocks and the lake. The isotopic composition ($\delta^{17}M$) of methane emissions from the pool was -3.9‰, from the hummocks -28.6‰ and +4.8‰ from the lake. It is speculated that these differences arise because, in the pool and lake sediments methane is formed *via* acetate fermentation, and in the hummocks it is produced *via* CO_2 reduction. Methane from the pools and the lake is isotopically heavier than methane emissions from the Migneint field site, again possibly due to differences in metabolic pathway. However, the methane emission from the hummocks had a $\delta^{17}M$ value similar to that at the Migneint, suggesting the same production process.

There is scope for further research in this area to gain a better understanding of the fluxes of methane from Arctic tundra, its isotopic composition, and the implications for, and of climate change.

Comparison of Field and Laboratory Data, Discussion

6. Introduction

In this chapter two important environmental variables, temperature and water table, are considered. Their effect on the size of the methane flux, and its isotopic composition is discussed. The relationship between δD of the peat water and $\delta^{17}M$ of the emitted methane is also considered. The rôle of vegetation in methane production and emission is also discussed, and its effect on methane isotopes is considered.

6.1 Environmental Variables And Methane Emissions

6.1.1 Effect Of Temperature On Methane Flux Rates

To simplify the problem of inter-dependent environmental variables, initial data analysis was carried out on only the data from sampling dates when the water table was at the surface of the peat. This eliminates the water table depth as a variable, allowing the effect of temperature alone to be determined. As the data

subset consists of 10 sampling dates spread across the various seasons it is sufficiently representative for statistical analysis.

Regression analyses were performed comparing flux rate with temperature, the air temperature and for each individual depth in the peat. There was no significant correlation between flux rate and air temperature. However, there was a statistically significant correlation between flux and the temperature of the peat for every depth. The results are summarised in Table 6.1.

Table 6.1 Summary of regression analyses between flux rates and peat temperature. n=10, significance set at $p<0.05$ level.

Depth /cm	r^2	p
Air	0.37	n.s.
0	0.49	< 0.05
5	0.58	< 0.01
10	0.68	< 0.01
15	0.76	< 0.01
20	0.79	< 0.01
25	0.81	< 0.01
30	0.83	< 0.01
40	0.87	< 0.01
50	0.89	< 0.01

a) Activation Energy

The temperature dependence of any reaction can be described by the Arrhenius Equation:

$$k = Ae^{-E_a/RT} \qquad \text{Equation 6.1}$$

where k = the Rate Constant

A = the Arrhenius factor

E_a = the Activation Energy

R = the Gas Constant

and T = the absolute temperature.

Taking the natural log, we have:

$$\ln k = \ln A - (E_a/RT) \qquad \text{Equation 6.2}$$

Thus, if the natural log of the rate constant is plotted against the reciprocal of RT, the slope of the line will give the Activation Energy.

Methane emissions are the result of more than one biochemical reaction. Thus, any Activation Energy term quoted is merely an apparent E_a. Nevertheless, it provides a useful approximate index of temperature in relation to flux.

In Figure 6.1, the methane flux rate is used in place of the rate constant (Equation 6.2). Since flux = production - oxidation, it is important to eliminate data where oxidation may be occurring; thus, for the field measurements only fluxes where the water table was at the surface have been used. The temperature used in the calculation is that at 25 cm depth, in order to be able to make a comparison with the data from the laboratory study where the cores were 25 cm deep. The Arrhenius plot is shown in Figure 6.1.

It can be seen from Figure 6.1 that the "activation energy" for methanogenesis in the mire was 156 kJ mol^{-1}, while in the laboratory study it was less than half that, 66 kJ mol^{-1}. These values both fall within the range of 32 to 269 kJ mol^{-1} from a variety of wetlands, cited by Dunfield *et al.* (1993). The E_a for the field study is similar to the value of 205 (±43) kJ mol^{-1} determined by Nedwell and Watson (1995) for peat monoliths.

The E_a for the laboratory study is in good agreement with the values reported by some researchers (Bridgham and Richardson, 1992; Prieme, 1994) from laboratory studies on incubated peat (dried & sieved and slurried respectively). There is some evidence that some of the discrepancy in apparent Ea values may be

due to the presence or absence of actively growing plants in the ecosystem. Other reasons for the differences in apparent E_a include:

- methanogenesis occurs *via* two metabolic pathways: CO_2 reduction and acetate fermentation. In some ecosystems the former may be the predominant pathway, in others the latter may be more important,
- different transport mechanisms result in different flux rates at similar temperatures,
- there may be seasonal lags and
- there may be differences in the microbial populations.

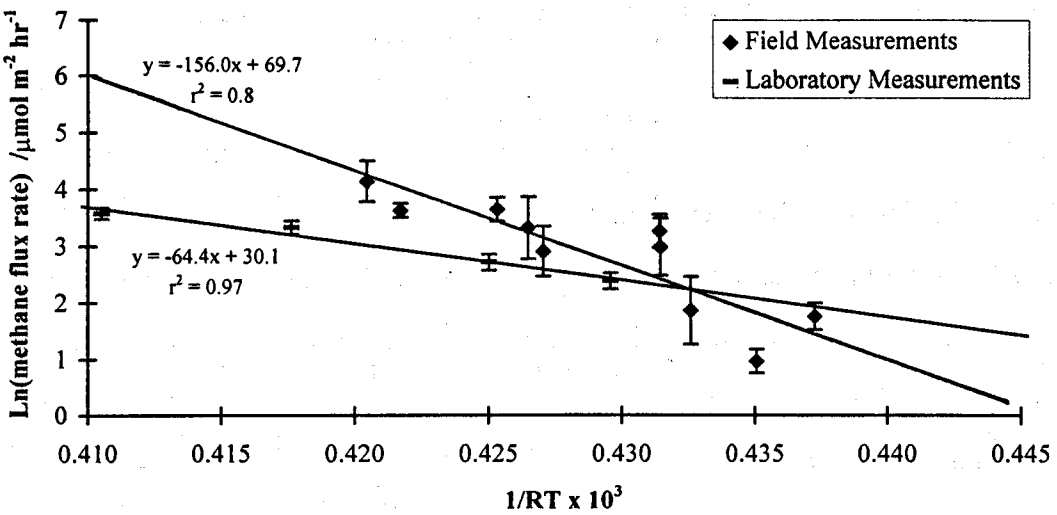

Figure 6.1 "Arrhenius plot" for methane emissions from cores in the field (each point is the average of 6 replicate cores), and cores in the laboratory (5 replicate cores, error bars represent 1σ std error).

b) Effect of Temperature on Reaction Rates

From the field study, the relationship between CH_4 flux and peat temperature at 25 cm below the surface (water table at the surface) is linear between 2 and 14 °C, with a temperature response of 4.6 µmol m^{-2} hr^{-1} $°C^{-1}$ (Figure 6.2). The relationship between CH_4 and temperature in the laboratory study is also linear between 7 and 20 °C. However, in the laboratory the temperature response of flux rate is 2.0 µmol m^{-2} hr^{-1} $°C^{-1}$ (Figure 6.2), half that seen in the field, supporting the argument that the

presence of actively growing plants in the ecosystem affects the methane emissions. The results from the field study are in good agreement with the findings of Hargreaves and Fowler (1998) who reported a temperature response rate of 5 μmol m^{-2} hr^{-1} $°C^{-1}$ over a temperature range of 7 to 11 °C, for a peat bog in Scotland. They also indicated that this is close to the response obtained in controlled conditions.

The temperature response seen in this laboratory study is lower than temperature response rates reported from other laboratory studies for example MacDonald *et al.* (1998). This may be because reported studies kept cores in light conditions, not in the dark.

Comparison of flux rates measured in the field at the Migneint with those measured from cores in the laboratory study at comparable temperatures suggest that the presence of actively growing vascular plants causes enhancement of the methane flux.

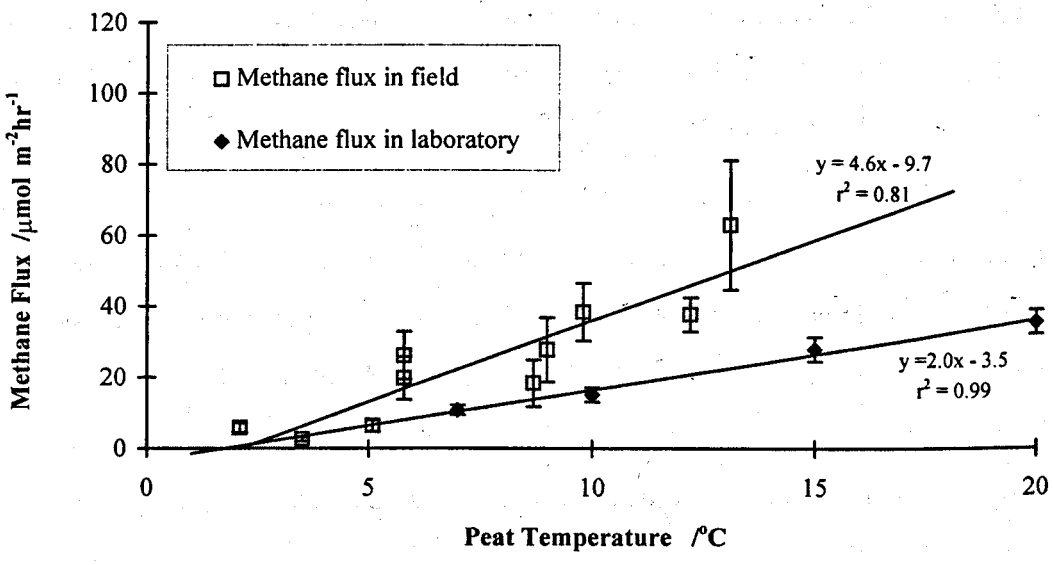

Figure 6.2 The effect of temperature on flux rate, (water table at the surface, average of 6 measurements for field results, average of 5 measurements for laboratory results, error bars represent 1σ std error).

The ratio of the reaction rates for two identical reactions 10 K apart is called the Q_{10} of a reaction. Over the range of temperatures recorded in the field, the

methane flux responds in a linear fashion to temperature. Increasing the temperature from, for example, 5 to 15 °C will result in the flux rate to increase from 8.2 μmol m^{-2} hr^{-1} to 67.3 μmol m^{-2} hr^{-1}, a Q_{10} of 8.2. A Q_{10} of 4.5 was calculated for the laboratory experiment.

These Q_{10} values fall within the values reported by Whiting and Chanton (1993), of 4 to 13; however, Q_{10} for this field study is double that reported by Dise *et al.* (1993) for peatlands in Northern Minnesota, and more than three times those reported by MacDonald *et al.* (1998), Lloyd *et al.* (1998), (both peat cores in the laboratory) Valentine *et al.* (1994) and Prieme (1994) (laboratory studies of methane production potential on slurried peat samples). This discrepancy may well arise because of any combination of the factors mentioned in relation to E_a in the previous section.

Methanogenesis occurs by two metabolic pathways, but in the field only the overall flux rate is measured. It is not possible to determine the predominant pathway from flux measurements; nor if changes in peat temperature affect the ratio of methane produced by each pathway. It seems likely that the processes of carbon dioxide reduction and acetate fermentation will have different activation energies and different Q_{10} values. Also, it should be noted that methanogenesis is the terminal step in a complex decomposition process and may be substrate limited (Watson and Nedwell, 1998). It is possible that the rate determining step in methane emission is actually earlier in the decomposition chain, particularly at low temperatures. So although Q_{10} values are widely reported, it may not be an appropriate measurement for methane flux rates and should be used with caution (Arah and Stephen, 1998).

6.1.2 Effect of Water Table Depth on Methane Fluxes in the Field

In order to determine the appropriate criterion to use in the statistical analysis of the effect of rainfall or water table depth on CH_4 flux rate in the field, stepwise multiple regression analyses were performed using data from all sampling dates, taking into account the effect of temperature. The temperature used here for the first

independent variable was that at 30cm below the water table. Other TIGER collaborators had shown that the zone of methane production moves with the water table (Daulat and Clymo, 1998), thus the temperature at a depth below the water table was a realistic criterion. The actual depth chosen was arbitrary, as there was a strong correlation between flux and peat temperature at all depths from 15 to 50 cm below the water table (Table 6.1). The variables examined were:

- water table depth
- total rainfall in the 7 days prior to sampling
- total rainfall in the month of sampling
- total rainfall in the previous month

The greatest multiple regression coefficient was achieved using water table depth as the second independent variable. A summary is given in Table 6.2.

Table 6.2 Summary of multiple regression analysis of the effect of temperature and water table or rainfall on flux rate (n=22, significance set $p<0.05$ level, $p_{(temp)} \ll 0.01$).

Variable	R^2	$p_{(H_2O)}$
water table depth	0.67	<0.02
last 7 days rainfall	0.54	n.s.
rainfall this month	0.53	n.s.
rainfall last month	0.52	n.s.

Further stepwise multiple regression analyses were performed using data from all sampling dates to determine the relationship between flux rate, peat temperature, and water table depth. Analyses were performed for the temperature at each depth below the surface of the peat, and at each depth below the water table. In all cases, there was a statistically significant correlation between flux, water table depth and peat temperature, ($p_{temp} < 0.05$). Water table depth showed greatest significance

when the temperature at 25 cm below the water table was used, and this also provided the greatest multiple regression coefficient: $R^2 = 0.68$, $p_{H20} < 0.02$, $p_{temp} \ll 0.02$. The temperature at 25 cm below the water table is shown in Figure 3.6, along with the average flux rates.

6.1.3 Discussion on the Effect of Temperature and Water Table Depth on Methane Flux.

A number of researchers have found that in peat bogs and wetlands, temperature is the more significant environmental variable. For example, Crill *et al.* (1988) showed that increased temperature results in increased methane production. Edwards *et al.* (1994) saw a strong relationship between flux rate and peat temperature at 20 cm, while Lansdown *et al.* (1992) reported a linear relationship between flux and temperature at 30 cm. These findings also support the work of Dise *et al.* (1993) who showed that temperature was the controlling factor in flux variation.

However, Moore *et al.* (1994), Bubier *et al.* (1993) and Vourlitis *et al.* (1993) all agree that water table position was the most important environmental variable. This difference of opinion may arise because the relative importance of the hydrology of the ecosystem may depend upon the topography of the mire. There may also be other factors involved in methane emissions, such as vegetation which need to be considered (Section 6.4).

The magnitude of the emissions of methane from the ombrotrophic mire at the Migneint is related to both the water table depth and the peat temperature, with the peat temperature showing the stronger statistical relationship. In this study these variables account for 68% of the annual variability in flux rate.

6.2 Relationship between δD of the Peat Bog Water and δD of the Methane

A number of researchers have determined a relationship between δD_{H_2O} and δD_{CH_4} for various biogenic sources of methane, none of which is a peat bog

ecosystem. As different ecosystems have different microbial, vegetation and physical characteristics, the relationship will vary between ecosystems. For example peat bogs and wetlands possess vegetation, which is generally absent in deep water lake sediments. Nevertheless, it is useful to look at the relationships reported, because they can be used as an approximate guide to what might be happening in the Migneint.

Schoell (1980) looked at methane associated with geological formations, gas of a great age; unlike CH_4 from a peat bog which is much younger or more recent. He found the following relationship:

$$\delta D_{CH_4} = \delta D_{H_2O} - 160\ (\pm 10) \qquad \text{Equation 6.3}$$

Since the slope of the line was 1, he concluded that all the hydrogen in the methane must have come from the water, and therefore the natural gases in his study were predominantly formed by CO_2 reduction. As the data came from world-wide occurrences it was concluded that the relationship was characteristic for all natural biogenic gases. He also conducted D_2O tracer experiments in the laboratory, producing methane from municipal sewage sludge. This resulted in the following relationship:

$$\delta D_{CH_4} = 0.4\delta D_{H_2O} - 323 \qquad \text{Equation 6.4}$$

from which it was assumed that methane was produced by both metabolic pathways.

Later work by Schoell and others (1988) involved culture experiments on sediments from a deep lake on the East African Rift system and adjacent to an active volcano, Lake Kivu. These were carried in the laboratory at elevated temperatures (60 °C). Conditions were selected to ensure that methane was only produced by acetate-fermenting methanogens. The relationship between the D/H ratio of the methane and that of the water was found to be:

$$\delta D_{CH_4} = 0.15\delta D_{H_2O} - 318 \qquad \text{Equation 6.5}$$

Jenden and Kaplan (1986) calculated a similar relationship for sewage sludge fermentation, based on the assumption that 70% of methane was produced from acetate fermentation and 30% from CO_2 reduction:

$$\delta D_{CH_4} = 0.143\delta D_{H_2O} - 393 \qquad \text{Equation 6.6}$$

Working with marine sediments Whiticar *et al.* (1986) suggest the relationship for the carbon dioxide reduction pathway is:

$$\delta D_{CH_4} = \delta D_{H_2O} - 180\ (\pm 20) \qquad \text{Equation 6.7}$$

They also report a clear distinction between the δD_{CH_4} values for marine and freshwater sediments; in the former δD = -250 to -170‰ and in the latter δD = -400 to -250‰. This arises because in marine environments CO_2 reduction is the dominant pathway, and in freshwater sediments acetate fermentation prevails.

From incubation studies with rice paddy soil (at 30 °C), Sugimoto and Wada (1995) determined a relationship for each metabolic pathway:

CO_2 reduction: $\delta D_{CH_4} = (0.683 \pm 0.020)\ \delta D_{H_2O} - (317 \pm 20)$ Equation 6.8

Acetate fermentation: $\delta D_{CH_4} = (0.437 \pm 0.045)\ \delta D_{H_2O} - (302 \pm 15)$ Equation 6.9

δD values for the water samples at the Migneint ranged from -51 to -24‰. Each measured δD value was substituted into each of the above equations, to estimate the range of δD for the methane. The resulting estimated δD_{CH_4} was then substituted into the equation for $\delta^{17}M$:

$$\delta^{17}M = (1.02893 \times \delta^{13}C) + (0.0569929 \times \delta D) + 84.9205 \qquad \text{Equation 2.8}$$

so that the range of $\delta^{13}C$ could be calculated. The $\delta^{17}M$ values used in this calculation corresponded to each δD_{H_2O} value. A summary of the results of these calculations are given in Table 6.3.

From the available data it is not possible to be sure which of the two methanogenic pathways is predominant in the peat at the Migneint. Almost all the

estimated values for δD_{CH_4} fall within the range of values reported in the literature, -442‰ for wetlands (Kuhlmann *et al.*, 1998) and -400‰ for freshwater sediments (Lansdown *et al.*, 1992) to -222‰ for marine sediments (Burke Jr *et al.*, 1988b).

Table 6.3 Estimated values for δD and $\delta^{13}C$ of methane at the Migneint, calculated from δD_{H_2O}.

Reference	estimated δD_{CH_4}	estimated $\delta^{13}C$	Comment
Sugimoto and Wada (1995)	-324 to -318	-98 to -85	acetate fermentation
Schoell *et al.* (1988)	-326 to -323	-98 to -84	acetate fermentation
Schoell (1980)	-211 to -196	-104 to -105	CO_2 reduction
Whiticar *et al.* (1986)	-231 to -216	-103 to -90	CO_2 reduction
Sugimoto and Wada (1995)	-352 to -341	-96 to -83	CO_2 reduction
Schoell (1980)	-343 to -337	-97 to -97	sewage sludge
Jenden and Kaplan (1986)	-400 to -398	-94 to -80	sewage sludge

However, the $\delta^{13}C$ values calculated for methane emissions at the Migneint are lower than literature values, regardless of which methanogenic pathway is assumed to be occurring. They range from -105 to -80‰. The lowest *reported* value of $\delta^{13}C$ for methane from a peat bog was measured in Minnesota, and is -86‰ (Quay *et al.*, 1988). Generally, $\delta^{13}C$ is reported to range from -90 to -40‰ for bacterial sources (Conny and Currie, 1996).

There are two possible reasons why the estimated $\delta^{13}C$ values for CH_4 emitted from the Migneint are lower than published data:

- there is a very different methanogenic pathway involved
- $\delta^{13}C$ really is indeed lower here.

The first suggestion is highly unlikely, the second is more probable. However, measured $\delta^{13}C$ for methane emitted in U.K. peat bogs are clearly needed in order to evaluate this conclusion.

6.3 Effect of Environmental Variables on the Isotopic Composition of Methane

It is likely that peat temperature and water table depth affect the isotopic composition of methane emission as these environmental variables are known to influence methane flux. As discussed in the previous section, the isotopic composition of the water in the peat bog will also have some bearing on the isotopic composition of the methane produced.

To eliminate water table depth as a variable, initial data analysis of results from the field study was again conducted using data from the sampling dates when the water was at the surface. This also allows a direct comparison of data from the field with data from the laboratory study. The effect of δD of the water was assumed to be negligible for this analysis.

Regression analyses were performed comparing isotopic composition of the CH_4 flux with peat temperature at each depth. There was no correlation between isotopic composition and peat temperature for depths of 20 cm and above. However, there was a statistically significant correlation between isotopic composition and peat temperature at depths of 25 cm and below ($p<0.05$). The results are summarised in Table 6.4.

A comparison of the relationship between isotopic composition of CH_4 flux and peat temperature (at a depth of 25 cm) determined in the field study, and in the laboratory study is shown in Figure 6.3. In the field study there was a statistically significant negative correlation between isotopic composition and peat temperature, $r^2 = 0.58$, $p<0.05$. However, in the laboratory study there was no correlation between the two. This indicates that any correlation seen between isotopic composition of methane flux and peat temperature in the field is only a indirect effect, presumably caused by the presence of actively growing plants in the field. The laboratory study was conducted in the dark and so there was no active plant growth.

Table 6.4 Summary of regression analyses between isotopic composition of CH_4 emissions and peat temperature. (n=10, significance set at $p<0.05$ level).

Depth /cm	r^2	p
Air	0.20	n.s.
0	0.25	n.s.
5	0.30	n.s.
10	0.41	n.s.
15	0.51	n.s.
20	0.55	n.s.
25	0.58	<0.05
30	0.61	<0.05
40	0.66	<0.05
50	0.71	<0.02

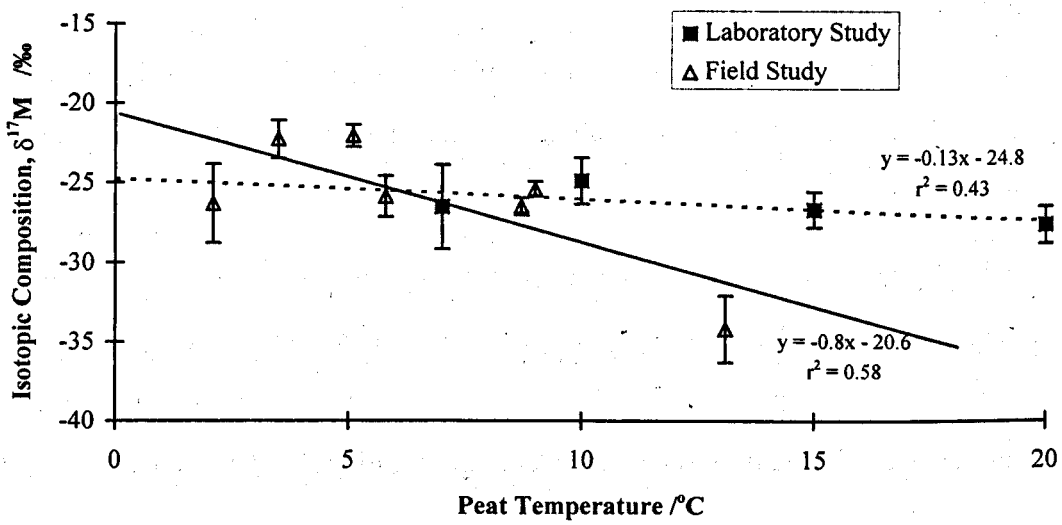

Figure 6.3 Effect of temperature on the combined isotopic composition of methane emissions from peat cores in the field at the Migneint, and from peat cores in the laboratory (water table at the surface).

Seasonal variations in methane isotopic ratio and peat temperature are shown in Figure 6.4a. There was no obvious link between methane isotopic ratio and water table depth (Figure 6.4b). Using Equation 2.8, it was calculated that the seasonal

variation in δD_{H_2O}, from -51 to -24‰, was unlikely to account for more than a 2‰ shift in $\delta^{17}M$.

Stepwise multiple regression analyses were performed between $\delta^{17}M$ and δD_{H_2O}, water table depth and peat temperature at each depth below the surface and below the water table. The contribution of δD_{H_2O} and water table depth to the variation in $\delta^{17}M$ is not significant at the $p<0.05$ level, regardless of which temperature criterion is used. The results for temperatures below the water table gave better regression coefficients and are summarised in Table 6.5. The greatest multiple regression coefficient was achieved using temperature measurements at 50 cm below the water table, $R^2 = 0.83$, $p_{temp} < 0.01$.

These environmental variables therefore account for 83% of the seasonal variation in $\delta^{17}M$, and temperature is the most significant factor. This is surprising in view of the results of the laboratory experiments which indicated no relationship between temperature and $\delta^{17}M$ (Section 4.4.2). This implies that temperature is a indirect effect which may arise because of the presence of actively growing vegetation in the field, which was absent in the laboratory study. This idea is discussed further in Section 6.4.

Clearly more work is needed in order to tease out the complex inter-relationships between the environmental variables and the isotopic composition of the methane. For example, if the $\delta^{13}C$ of the methane emissions at the Migneint had been measured, δD could be calculated and the relationship between δD_{CH_4} and δD_{H_2O} determined.

Table 6.5 Summary of multiple regression analyses between $\delta^{17}M$, δD_{H_2O}, water table depth and temperature at each depth below the water table (n=11).

Depth /cm	R^2	p_{temp}	$p_{\delta D}$	$p_{water\ table}$
0	0.62	n.s.	n.s.	n.s.
5	0.67	n.s.	n.s.	n.s.
10	0.71	<0.05	n.s.	n.s.
15	0.74	<0.05	n.s.	n.s.
20	0.75	<0.05	n.s.	n.s.
25	0.76	<0.02	n.s.	n.s.
30	0.78	<0.02	n.s.	n.s.
40	0.81	<0.01	n.s.	n.s.
50	0.83	<0.01	n.s.	n.s.

One important thing to note however, is that the isotopic composition of methane emissions at the Migneint do change through the year (by 17‰), although the exact reasons are not yet fully understood.

Other researchers have reported seasonal variations in $\delta^{13}C$ of methane at sites in North Carolina and Alaska, U.S.A., which have been attributed to changes in metabolic pathway or substrates used in CH_4 production (Martens *et al.*, 1986; Burke Jr *et al.*, 1988b; Chanton and Martens, 1988; Martens *et al.*, 1992). In contrast, Lansdown *et al.* (1992) found no seasonal variation in $\delta^{13}C$ but determined that CO_2 reduction accounted for 100% of the methane flux.

There are implications for using isotopic data in climate change models. Had this study only carried out field measurements on a two monthly basis instead of monthly, the lightest isotopes in August 1996 could easily have been missed.

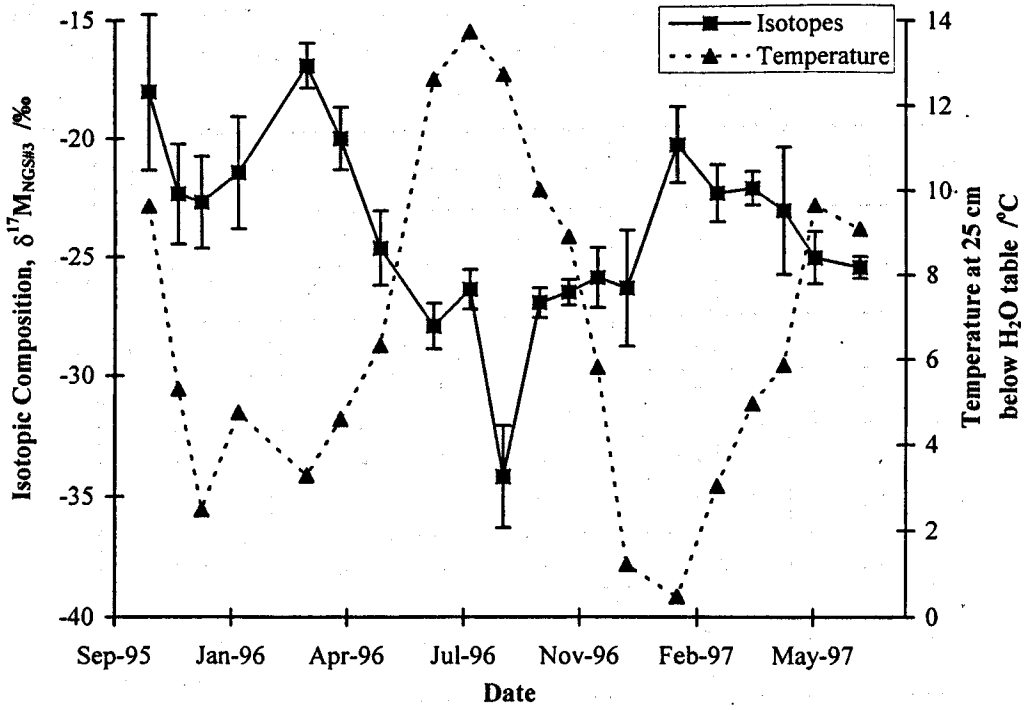

Figure 6.4a Variations in the combined isotopic composition of methane and peat temperature at 25 cm below the water table. Error bars are the standard error of the intercept from the dilution plots, n=4 for temperature measurements.

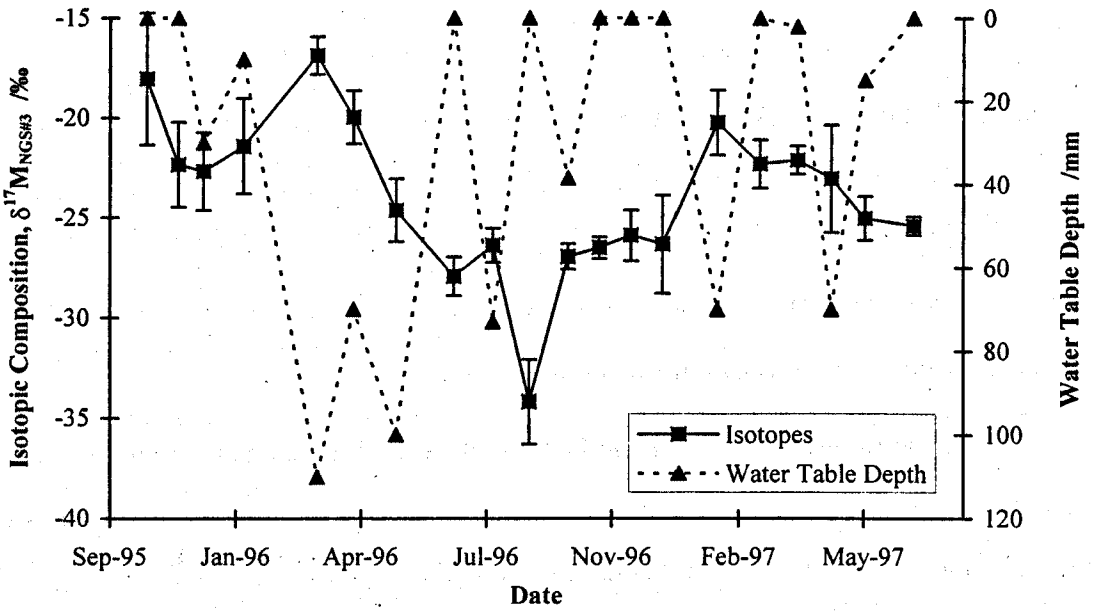

Figure 6.4b Combined isotopic composition of the methane and the water table depth. Error bars are the standard error of the intercept from the dilution plots, n=2 for water table depth.

6.4 Effect Of Vegetation On Methane Flux And Its Isotopic Composition

Vegetation plays an important rôle in the processes of methane production, oxidation and transport in peat. In this section, the rôle of plants in each of these aspects of methane emissions is reviewed. Methane flux and isotope data from the Migneint and from Finland are discussed with respect to the rôle of plants in the ecosystem.

The processes of methane production, oxidation and transport in peat are shown in Figure 6.5. As the bryophyte flora such as *Sphagnum* spp. lack root systems, it is the tracheophytes (vascular plants) which can be assumed to have a rôle in the conduction of gases and soluble carbon sources to depth in the peat. Oxygen and photosynthates are carried downwards and pass out into the rhizosphere via the roots while methane is taken up by the roots and carried up to be emitted out into the atmosphere. The enhancement of methane flux by vascular plants in wetlands, has been reported by a number of workers, (*e.g.* Morrissey *et al.*, 1993; Harden and Chanton, 1994; Boon and Sorrell, 1995; Mikkela *et al.*, 1995; Shannon *et al.*, 1996 Waddington, 1996).

The type of vegetation present may also be a significant factor because of structural differences. For example monocotyledons (plants with one seed leaf) differ fundamentally from dicotyledons (plants with two seed leaves) in root growth and morphology (Mengel and Kirkby, 1987). In dicotyledons a tap root is formed at an early stage which extends deep into the soil, lateral roots develop later. In monocotyledons lateral roots develop from the seminal roots a few days after germination and generally form a dense root system with numerous slender roots. Thus, monocotyledons have a greater root surface area which is the interface for exudation of photosynthates, and the uptake of the methane for transport to the atmosphere. On the other hand, release of O_2 into the rhizosphere will also be increased.

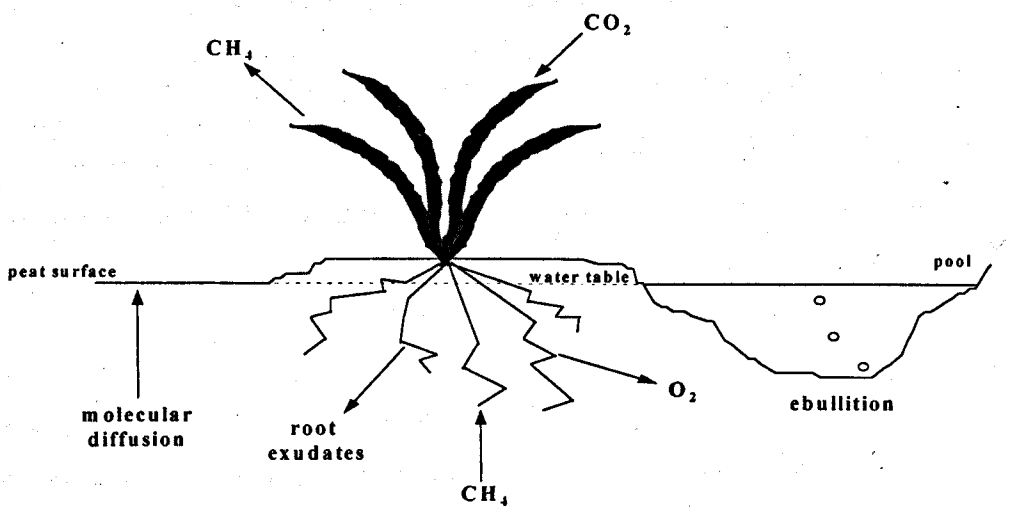

Figure 6.5 Schematic diagram to show the rôle of vascular plants in the processes of methane production, consumption and transport in a peat bog.

This morphological difference will also have implications when the water table drops below the surface of the peat. There may be a point when the root system of monocotyledon plants are fully in the aerobic zone, but the roots of dicotyledons are still able to penetrate the water-logged anaerobic zone (Figure 6.6). Differences in vegetation type may explain why some researchers found water table to be the more significant environmental factor while others did not (Section 6.1.3).

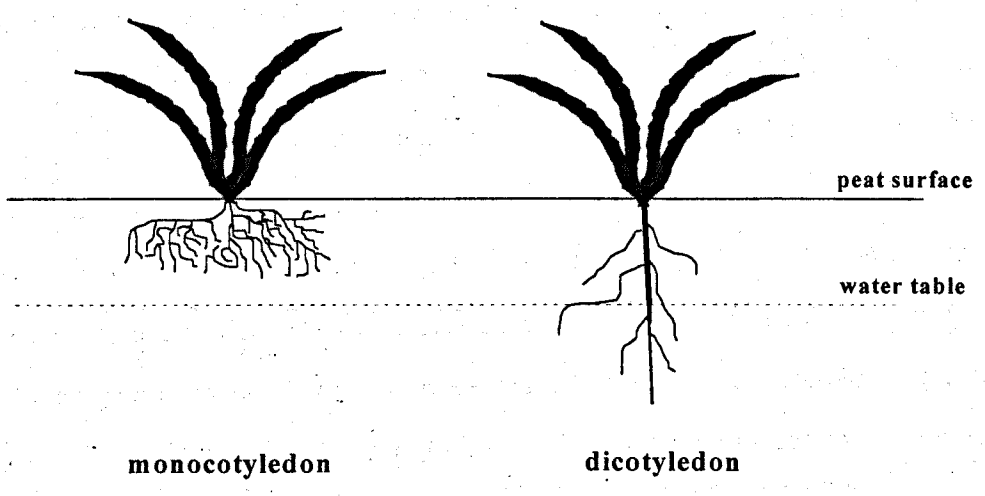

Figure 6.6 Schematic diagram to show the difference in root morphology between monocotyledons and dicotyledons.

6.4.1 Rôle of Plants in Methane Production, Oxidation and Transport

a) Production of methane

As the plant photosynthesises, it supplies both oxygen and root exudates to the rhizosphere. The root exudates represent a source of labile carbon and other nutrients for microbial growth. Thomas *et al.* (1996) suggested that the effects of photosynthate provision are important in CH_4 production. Chanton *et al.* (1997) reported ^{14}C evidence that a significant proportion of methane emitted is derived from recently-fixed organic compounds, and Waddington and Roulet (1996) reported that sites with greater CO_2 fixation also had higher CH_4 fluxes, probably due to enhanced methanogenesis and transport.

When the water table is below the peat surface, the production zone is decreased and the oxidation zone is increased; both potentially reducing the overall production of methane. In addition, less of the plant root lies in the anaerobic zone and therefore proportionally less root exudates are being released into the zone of methane production. Thus, a lowered water table not only results in an oxic layer where methane will be consumed, but also the overall amount of methane produced may be less.

The photosynthetic pathway by which organic matter is fixed determines its isotopic composition. In general C-3 pathway plants have a $\delta^{13}C$ value of about -28‰, while C-4 plants have a $\delta^{13}C$ of around -14‰ (Chanton and Dacey, 1991 and references therein). Although all the plants at the Migneint and the field area in Finland were as identified C-3 plants, the differences between the isotopic signatures of C-3 and C-4 plants has implications for the use of isotopic signatures from this study in global methane budgets.

Kinetic isotopic fractionation occurs during organic matter degradation, resulting in the production of methane which is very depleted in $\delta^{13}C$ (typically -50 to -110‰ (Schoell, 1980)). In fact, Burke *et al.* (1988a) suggest that the isotopic fractionation associated with methane formation from complex organic matter

outweighs the isotopic composition of the starting organic mater in determining the isotopic composition of the CH_4 produced.

b) Methane Oxidation in the Rhizosphere

The O_2 respired by the plants may cause inhibition of methanogenesis, which is a strictly anaerobic process (Conrad, 1989; Knowles, 1993), in the rhizosphere. Oxygen may also be used by methanotrophs in the root zone to consume methane. Burke *et al.* (1988a) reported that emergent aquatic plants appear to affect the stable isotopes by stimulating methane oxidation by root aeration. Chanton *et al.* (1992), however, found no evidence for CH_4 oxidation in the rhizosphere (or within the plant) of *Peltandra virginica*, although the plant was found to transport methane; and Thomas *et al.* (1996) indicated that the positive effects of the presence of *Eriophorum angustifolium* on methane flux outweigh the effects of increases oxygen in the root zone.

c) Transport of Methane through Plants

The methane produced in a peat bog can move to the surface by molecular diffusion, ebullition or through the vegetation. Vascular plants rooted in anoxic sediments have to rely on oxygen transported into the root environment through the plant. Associated with this downward movement of air is an upward movement of methane and other gases, using the same pathway.

Sebacher *et al.* (1985) noted differences in CH_4 emissions through different plant types. Large emissions were associated with freshwater plants which were characterised by soft epidermal layers in the submerged plant parts and parenchyma which develops elongated tubular structures in the rhizome, roots and shoots. Plants with hard outer epidermal structures exhibited low CH_4 emissions because the apparently impermeable root and rhizome cortex tissue presented a strong influx restriction. Thomas *et al.* (1996) reported similar findings: monocotyledons such as *Carex echinata* and *Eriophorum angustifolium* develop large air spaces (lacunae) in

the cortex of the rhizome and the root, and in the case of sedges, also in the leaves. This lacunar system is continuous through the plant. In contrast, *Calluna vulgaris* and *Erica tetralix*, both dicotyledons, lack a lacunar system. In addition their medullary and secondary rays (parenchyma between the pith and the cortex) are often only one cell wide so they are thought less likely to contribute significantly to gas transport processes.

There are two possible paths of transport: i) passive diffusion through the plant and ii) active transport due to partial pressure differences or thermo-osmosis of gases. A brief explanation of these mechanisms is given below; a detailed discussion can be found in for example (Schütz *et al.*, 1991).

i. Diffusion

Methane produced in the peat enters the aerenchyma of the root system; this influx of CH_4 may be facilitated by a diffusion gradient between the peat and the atmosphere. Once methane has entered the root aerenchyma, it will diffuse, due to concentration differences, through the lacunar system to the shoots. For many wetland plants these shoots are porous and permeable. In woody species gases are able to escape from the intercellular spaces inside stems through the lenticels of the bark.

Shannon *et al.* (1996) concluded that methane flux through *Scheuchzeria palustris* was due to molecular diffusion, and was not affected by pressurisation or changes in stomatal aperture.

ii. Active Gas Transport

Pressure-induced flow of methane occurs by heating and pressurisation of green, emergent leaves which drives methane into the roots and through old, brittle leaves to the atmosphere. The pressures generated can be very high, for example, Boon and Sorrell (1995) reported that *Eleocharis* shoots were able to generate pressures of up to 550 Pa during summer days.

The importance of stomatal control and a clear diurnal pattern in methane emission has been reported by some workers (*e.g.* Morrissey *et al.*, 1993; Yavitt and Knapp, 1995; Thomas *et al.*, 1996). However, there are as many reports indicating that stomatal control is not a significant factor in methane transport (*e.g.* Holzapfel-Pschorn *et al.*, 1985; Harden and Chanton, 1994; Whiting and Chanton, 1996). The conclusion to be drawn from these studies is that different plants transport methane in different ways, according to their morphology and adaptation to living in a water-logged environment. This is confirmed by Schimel (1995) who reported that *Eriophorum angustifolium* transported more methane than *Carex aquatilis* due to differences in the size and structure of the two species. An interesting phenomenon reported by MacDonald *et al.* (1998) is that in *Menyanthes trifoliata* efflux of the methane was through the stems.

d) Effect of Transport Mechanism on Methane Isotopic Composition

There is a distinct isotopic fractionation associated with each of the mechanisms used to transport CH_4 from the peat to the atmosphere: ebullition, molecular diffusion or plant transport.

Chanton and Martens (1988) found that ebullition did not fractionate the carbon isotopes of methane as there was no systematic difference between the $\delta^{13}C$ in naturally released bubbles and bubbles released by stirring the sediment. It was thus concluded that stirred bubbles are representative of naturally released bubbles.

Chanton and Martens (1988) also suggested that ebullition resulted in methane that was depleted in ^{13}C compared to methane transported through plants or by molecular diffusion because the zones of microbial methane oxidation are by-passed during ebullition. Isotopic fractionation across the air-water interface has also been reported (Zyakun *et al.*, 1979).

Transport through plants has different effects on the isotopic composition of the methane due to factors such as the diversity of plant species structure, and the

different mechanisms of gas transport used by plants. Chanton *et al.* (1988) found CH_4 in the stems of emergent macrophytes to be enriched *or* depleted in $\delta^{13}C$ by as much as 12‰ compared to sediment methane, depending on plant species. Later work by Chanton and co-workers (1992) shows that for emergent macrophytes characterised by molecular diffusion of gas, the isotopic composition of methane in the plant stem is not a good indicator of the isotopic composition of the methane efflux from the plant. They report that *Peltandra virginica* emitted methane that was depleted in ^{13}C by 10 and 15‰ compared to the CH_4 within the stems and in the sediment bubbles respectively.

Harden and Chanton (1994) reported that methane emitted by two other macrophytes being depleted in ^{13}C by 10‰ compared to methane in the sediment. They suggest that there is a mass-dependent fractionation associated with molecular diffusion through plants, and speculate that there would be less fractionation associated with transport in plants using pressurised through-flow ventilation. A further hypothesis they make is that since plants persistently preferentially mobilise the lighter isotopes of methane over the growing season, the methane remaining in the peat becomes increasingly enriched in the heavier isotopes.

The isotopic enrichment of methane in the plant stem may be caused by several factors:

- oxidation in the rhizosphere,
- isotopic fractionation may occur as methane exits the leaf, *via* preferential loss of lighter isotopes, leaving the methane in the stem isotopically enriched or
- methane taken up by plants may not be from the main area of bubble formation or the methane in the bulk sediment is not representative of the methane entering the plants.

6.4.2 Experimental Evidence from the Migneint and Jänkäjärvi for the Rôle of Vascular Plants in Methane Emissions

a) Vegetation Types

The vascular plant vegetation at the Migneint field site consists of *Eriophorum* spp. which are monocotyledons, and ericaceous species which are dicotyledons. There were no hollow-stemmed plants such as *Menyanthes trifoliata* (bog bean) and *Equisetum* spp. (horsetails) present.

There was a greater variety of plant species present in the Finnish field site. The vascular plant vegetation in the lake comprised of hollow-stemmed plants *Menyanthes trifoliata*, a dicotyledon and *Equisetum* spp. which are not angiosperms (flowering plants) but rather belong to the Pteridophyta division of the plant kingdom. The pools contained *Eriophorum* spp. and *Carex* spp., both monocotyledons, and *Menyanthes trifoliata*, a hollow-stemmed dicotyledon However, the sampling was only carried out over the monocotyledons. In contrast, the woody plants of the hummocks are all dicotyledons. The hypothesis that the difference in isotopic composition of methane emissions between pools and hummocks, -4‰ compared to -29‰, is due in part to differences in plant species is pure speculation but is a potential area for further work.

b) Production and Oxidation

A comparison between field and laboratory results in this study indicates that plants are significantly implicated in methane emissions. The response of methane flux rate to temperature between 4 and 14 °C is 5.9 μmol m^{-2} hr^{-1} $°C^{-1}$ in the field at the Migneint, compared to 2.0 μmol m^{-2} hr^{-1} $°C^{-1}$ in laboratory studies (Section 6.1.1).

In addition, in the laboratory there was no correlation between temperature and the isotopic composition of the methane from 7 to 20 °C (Section 6.3). In the field however, there was a strong statistically significant correlation between the isotopes and the temperature, although the temperature range was different: 2 to 14 °C (Section 6.3). The main difference between the ecosystem of the peat cores in the

laboratory and the peat in the field was that the peat cores in the laboratory were kept in the dark, so there was no photosynthesis and no plant growth occurring. A further difference between laboratory and field conditions is that in the field the temperature sometimes varied down the peat core by as much as 5°C, while in the laboratory the temperature remained constant throughout the core.

The effect of temperature on the isotopic composition of methane emissions from this ombrotrophic mire is probably a indirect effect, due to the presence of vascular plants. The peat bog was about 50% covered with vascular plants, with only one or two small patches of bare mud. Plant growth and also the rate of photosynthesis are correlated with temperature. Thus, the seasonal variation of methane isotopes is likely to be caused by changes in the plant growth cycle. This conclusion is supported by the findings of Bergamaschi (1997) who reported that the seasonal variation in $\delta^{13}C$ of the methane flux in a Chinese rice paddy may be due to systematic changes relative to the production, transport and oxidation during the vegetation cycle.

Methane emissions studied over a 24 hour period at the Migneint site, using headspace chambers, clearly show a diurnal flux pattern (Section 3.4.5). This pattern cannot be explained by changes in peat temperature or variations in peat temperature down the core. The flux rate started to increase in the afternoon and the maximum methane flux occurred about one to two hours after dark. Waddington *et al.* (1996) suggest that the lag in methanogenesis response behind daytime CO_2 uptake by the plant may be between 6 to 12 hours. This could explain the diurnal flux pattern seen at the Migneint.

Further evidence that the flux is related to photosynthesis or root respiration is that continuous monitoring of the flux rates in the laboratory experiments (Chapter 4) showed no diurnal pattern over a peat temperature range of 7 to 20 °C; in contrast the traces from continuous monitoring by the mobile laboratory in the field show a diurnal range of ~90 $\mu g\ CH_4\ m^{-2}\ hr^{-1}$ at a peat temperature of 14 °C (Section 3.4.5).

The isotopic composition of the samples taken at intervals over a 24 hour period using headspace chambers also show an interesting pattern (Section 3.4.5). The water table was 73 mm below the surface of the peat, presenting potential for methane oxidation. The isotopic composition was enriched in ^{13}C or D, when the flux was at its lowest, and the methane was most isotopically depleted when the flux was at its maximum (Figure 3.7). Since there was no sample replication it would not be appropriate to draw major conclusions from these data. One explanation might be that as the temperature of the peat surface drops, there is a decrease in CH_4 oxidation rate and thus CH_4 emission is increased. However, the temperature changes are small, such that the temperature response of methane oxidation would have to be about 20 $\mu mol\ m^{-2}\ hr^{-1}\ ^{o}C^{-1}$ to account for the differences in methane flux rates. The only recorded change in peat temperature was at 15.00 on 29 July 1996, when the 0-5 cm layer was 5 ^{o}C warmer than at the other sampling times. However, any increase in CH_4 oxidation should show a heavier $\delta^{17}M$, which was not the case.

A more likely explanation is that the rate of oxidation remains constant. When the methane production rate is low, a larger proportion of the methane is oxidised, resulting in a more pronounced isotopic shift. When the rate of production is at a maximum, a smaller percentage of the methane is consumed, and thus the isotopic shift is correspondingly smaller. This is a potential area for further work.

c) Transport Mechanisms

The rate of CH_4 emission from plants using an active gas transport system can be much higher than that of diffusion (Schütz *et al.*, 1991). The effect of clipping the vegetation (*Eriophorum* spp.) at the Migneint field site reduced the methane flux rate by 60% (Figure 3.8). This indicates that 60% of the total methane emission is transported through *Eriophorum* spp. by an active gas transport mechanism, rather than diffusion. (If methane were being transported by passive diffusion, clipping the vegetation would have no effect on the methane flux rate.) This result is in good

agreement with the findings of Waddington *et al.* (1996) who report that removal of *E. vaginatum* by clipping decreased the flux rate by between 55 and 85%.

The methane emitted by the lake in Finland (Chapter 5) was observed to be transported through the water by molecular diffusion, rather than ebullition. The $\delta^{17}M$ of the methane was 5‰ heavier than the methane stirred up from pool sediment (which was thought to be the same as the sediment in the lake). This would support the hypothesis that there is some isotopic enrichment associated with molecular diffusion (Chanton and Martens, 1988).

The methane emitted by the pool area in Finland (Chapter 5) was had a 3‰ lower $\delta^{17}M$ compared to the sediment methane. Very little was observed to be transported by ebullition. Some CH_4 would be transported by molecular diffusion through the water and some through the vegetation. Simple mass balance approximations indicate that if the methane from ebullition is at 0‰, and the CH_4 from molecular diffusion is enriched by up to 5‰ (as was the case at the lake) then the methane passing through the plants must have been even lower in $\delta^{17}M$ than the overall -3‰ measured. It is therefore likely that the vegetation present in the pools depleted the methane transported through it, either in ^{13}C or D. Further work is required to determine the proportion of methane that is transported through the plants, and the exact isotopic depletion.

6.4.3 Implications for Climate Change

The rôle of plants in the production, oxidation and transport of methane is a significant factor in the event of global climate change. A shift in plant species present in an ecosystem due to climatic change could potentially result in greater, or less methane emission.

6.5 Seasonal Variations in Methane Isotopes Explained

The $\delta^{17}M$ of the methane emitted from the ombrotrophic mire ranges from -17 to -34‰ seasonally (Figure 3.12) and is linked to the plant growth cycle. The methane flux is also seasonal, it is strongly correlated with temperature and also associated with the plant growth cycle. The changes in δD of the peat bog water can account for no more than 2‰ of the variation in $\delta^{17}M$. The remaining variation could be due to one, or a combination, of the following:

- A shift in dominant methanogenic pathway: at certain times of the year acetate fermentation may be predominant, at others carbon dioxide reduction may be more important.
- A difference in the isotopic composition of the starting materials. At times when there is minimum plant growth, the methane precursor may be old decaying organic matter. When plant growth is vigorous, much of the methane may be formed from root exudates.
- Transport *via* plants may cause the methane to have lower $\delta^{17}M$ compared to the methane in the peat. Although *Eriophorum* spp. are different to the macrophytes studied by Chanton and his co-workers, the 15‰ lower $\delta^{13}C$ they report would translate into a similar decrease in $\delta^{17}M$, if the water remained constant. However, it would appear that only about 60% of the methane emitted travels through the plants (Section 3.4.5). Assuming for simplicity that the remaining 40% of the methane flux has an isotopic composition of ~ -20‰, (average winter emissions), then a 15‰ shift due to plant transport might account for the lighter isotopic composition of the total methane emission (~ -27‰) in June, July, September, October, November and December 1996.

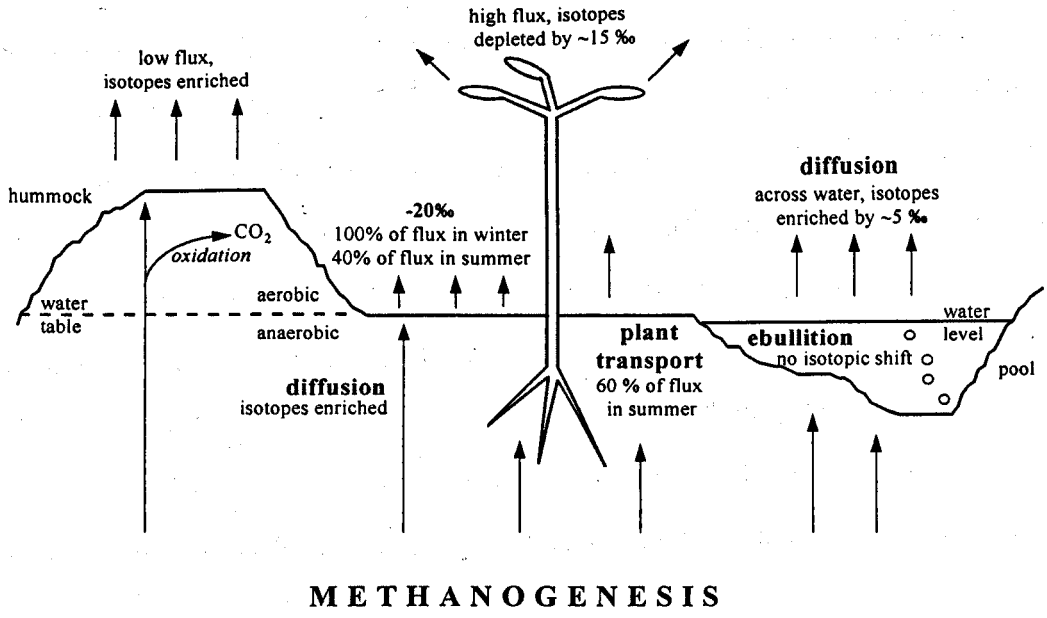

Figure 6.7 Transport mechanisms for the emission of methane from peatbogs, including some indication of size of flux and changes in $\delta^{17}M$.

The methane isotopes for August 1996 are about 7‰ lower in $\delta^{17}M$ than the months preceding and following. A possible explanation for this may be that the proportion of total CH_4 emission that came through the plants was greater than 60%. The overall isotopic composition of -34‰ for total methane emission may be accounted for if ~93% of the methane was transported *via* the plants, with an accompanying depletion of 15‰.

This scenario however, does not take into account that on some occasions, the water table was below the peat surface and so methane oxidation would occur, resulting in the methane that is moving to the surface through the peat being higher in $\delta^{17}M$. It appears however, that at the Migneint the changes in $\delta^{17}M$ caused by changes in water table depth are small and therefore masked by greater changes in $\delta^{17}M$ caused by life cycle changes in plants. It is likely that as the methane flux increases, a greater proportion is transported through the plants and so the amount of CH_4 oxidised is a smaller proportion of the total flux, thus the enrichment would cause a smaller isotopic shift overall.

Whiticar *et al.* (1986) reported that CO_2 reduction and acetate fermentation may be distinguished isotopically: for CO_2 reduction $\delta^{13}C$ is -110 to -60‰ and δD is -250 to -170‰, while for acetate reduction $\delta^{13}C$ is -65 to -50‰ and δD is -400 to -250‰. Substituting these $\delta^{13}C$ and δD values into Equation 2.8 gives $\delta^{17}M$ values of -43 to 14‰ for CO_2 reduction and -5 to 19‰ for acetate fermentation. The $\delta^{17}M$ values recorded at the Migneint (-34 to -17‰) there suggest that the predominant methanogenic pathway in the ombrotrophic mire studied here is CO_2 reduction. This conclusion is supported by the findings of Lansdown *et al.* (1992) who reported that methane production in a peat bog in Washington State was solely by CO_2 reduction.

6.6 Summary

Methane fluxes measured at the Migneint field site are consistent with fluxes measured from similar sites in the U.K.. The flux shows seasonal variation due to primary effects: peat temperature and water table depth. This is entirely in keeping with findings in the literature. Vegetation is shown to enhance methane flux.

The isotopic composition of the methane emitted by the ombrotrophic mire ranged from -17 to -34‰ and showed seasonal variation. A small part of this variation can be accounted for by the change in the isotopic signature of the surrounding water. Although there is a strong correlation between peat temperature and methane isotopic composition in the field, temperature is thought to have a indirect effect on the isotopic composition because in laboratory studies this relationship was entirely absent. It is speculated that as the vegetation has an important rôle in the processes of methane production, oxidation and transport, the seasonal variation in isotopic composition is also linked to the plant growth cycle. It is suggested that in the ombrotrophic mire at the Migneint, the predominant metabolic pathway for methane production is CO_2 reduction. It is also suggested that in the palsa mire at Jänkäjärvi the predominant metabolic pathway may differ with terrain, being acetate fermentation in the pools and CO_2 reduction in the hummocks.

Conclusions

7.1 Summary

A novel static mass spectrometer system, utilising methane as the analyte, has been used to determine the combined isotopic composition ($\delta^{17}M$) of methane emissions from an ombrotrophic mire in Snowdonia, and from a palsa mire in Finland. The technique, which requires small quantities of methane, and thus air, for analysis, combined with simple sampling equipment has allowed $\delta^{17}M$ of methane fluxes to be studied with unprecedented regularity. The $\delta^{17}M$ values of methane were measured to a precision of ± 0.5‰.

Methane fluxes from the ombrotrophic mire have been measured over 2 years (Autumn 1995 to Summer 1997), and the combined stable isotopic composition ($\delta^{17}M$) of the fluxes have been determined. Average CH_4 flux rates ranged from 0 to 63 μmol m^{-2} hr^{-1}. These values compare well with flux rates measured by other researchers, from similar sites in the United Kingdom. The CH_4 flux showed

seasonal variation due to peat temperature and water table depth. This relationship was statistically significant: $R^2 = 0.67$, $p_{temp} = \ll 0.01$, $p_{H20} = < 0.02$, n=22.

The presence of vascular plants in the ombrotrophic mire was shown to enhance methane flux rates. It was calculated that approximately 60% of the total CH_4 emission was transported through *Eriophorum* spp. by an active gas transport mechanism.

The $\delta^{17}M$ of the methane flux from the ombrotrophic mire ranged from -34 to -17‰. This was isotopically lighter than $\delta^{17}M$ values calculated from $\delta^{13}C$ and δD values for peat bogs reported in the literature. However, the isotopic composition of methane emissions from the ombrotrophic mire compared well with $\delta^{17}M$ values calculated from the limited $\delta^{13}C$ and δD values given for sediments in which CO_2 reduction is the main methanogenic pathway. Therefore it is speculated that the predominant metabolic pathway for methanogenesis in the ombrotrophic mire was CO_2 reduction.

The $\delta^{17}M$ of methane emissions from the ombrotrophic mire varied seasonally (-34 to -17‰). The variation in δD of the surrounding water could account for no more than 2‰ of the variation in $\delta^{17}M$, assuming that the relative contributions of the two metabolic pathways remained constant. There was a strong correlation between peat temperature and isotopic composition in the field ($r^2 = 0.58$, $p < 0.05$, n=9) which was not seen in the laboratory study. Therefore, it is concluded that the effect of peat temperature on the isotopic composition of methane flux was a secondary effect. The seasonal variation in isotopic composition of CH_4 emission seen in the field is assumed to be linked to the growth cycle of the vascular plants present in the mire.

Although lowering the water table was shown to result in isotopic enrichment of the residual methane in the laboratory study (at constant temperature), no significant effect of water table on isotopic composition of methane flux was

detected in the field. This may be because the effect was small and masked by the greater effect of peat temperature in the field.

Diurnal CH_4 flux measurements and isotopic analysis of these fluxes indicated that during the summer months flux was linked to diurnal cycles in active plant growth. Using $\delta^{17}M$ it was shown that increased night-time CH_4 fluxes were more likely to have been caused by increased methane production, than decreased methane oxidation.

There was no measured effect of nitrogen applications, in terms of the size or isotopic composition of the methane flux. However, plots which had received long-term treatment with either ammonium or ammonium and nitrate had a greater plant density than plots treated with nitrate, which were dominated by *Sphagnum* spp..

Measurement of methane fluxes in a palsa mire showed that pools emitted 41 μmol m^{-2} hr^{-1}, non-vegetated lakes emitted 24 μmol m^{-2} hr^{-1} and hummocks emitted 1 μmol m^{-2} hr^{-1}. It was also shown that the presence of *Equisetum fluviatile* and *Menyanthes trifoliata* in the lake resulted in a ten-fold increase in CH_4 flux. The overall average flux from the palsa mire was calculated to be 28 ±3.2 μmol m^{-2} hr^{-1}, which compared well (within spatial and temporal variability) with an average flux of 47 ±15.7 μmol m^{-2} hr^{-1} measured at the same site over the previous ten days using micrometeorological methods.

Isotopic analysis of the methane emissions from a palsa mire in Finland showed that different terrains emitted CH_4 of distinct isotopic composition: $\delta^{17}M$ for lakes was +4.8‰, for pools, -3.9‰ and for hummocks, -28.6‰. The isotopic composition of methane from bubbles released from pool sediment was determined to have a $\delta^{17}M$ of 0‰. It is speculated that the differences in isotopic composition of CH_4 flux from different terrains arises due to different methanogenic pathways: in pool and lake sediments the predominant metabolic pathway could be acetate fermentation and in the hummocks CO_2 reduction might prevail.

It was noted that the differences in $\delta^{17}M$ of methane emissions from the various terrains in the palsa mire has implications for the use of isotopic measurements in climate change models. If the relative contributions of the sources change, the aggregate $\delta^{17}M$ value of overall methane flux will shift.

7.2 Further Work

7.2.1 Development of Isotopic Analysis

The novel static mass spectrometer, MIRANDA, has allowed an extensive programme of field work and laboratory studies due to the small sample requirement and the simplicity of sampling equipment. However, the technique is limited to $\delta^{17}M$ measurements, and by a sample through-put time of 1 hr.

Since this project started, continuous flow mass spectrometers suitable for $\delta^{13}C$ determinations on methane in air samples have become commercially available. Conventional techniques for determining δD are time consuming and require large sample sizes and sophisticated sampling equipment. Therefore it is concluded that the best way forward in terms of obtaining $\delta^{13}C$ and δD measurements for small methane samples is to employ the technique of utilising methane as the analyte for determining $\delta^{17}M$, in conjunction with a mass spectrometer dedicated to $\delta^{13}C$ analysis, and then calculate δD.

The optimum use of this technique is probably in laboratory studies to make investigations at the process level, due to the limitations in the number of samples that can be taken in the field. $\delta^{13}C$ measurements could be used for screening purposes, and only selective samples analysed for $\delta^{17}M$ and thus δD.

Clearly, the next stage for this project is to separate out the components of $\delta^{17}M$ into $\delta^{13}C$ and δD. This should allow further constraint of the metabolic pathways used to produce methane in pool and lake sediments, and in hummocks in the palsa mire in Finland It should also enable determination of the predominant metabolic pathway used to produce methane in the ombrotrophic mire in Snowdonia.

It may also be possible to determine whether the seasonal variations in $\delta^{17}M$ of the methane flux are due to changes in the relative contributions of the two metabolic pathways: if the shifts in $\delta^{13}C$ and δD are in the same direction, oxidation may be occurring; if, however, $\delta^{13}C$ and δD shift in opposite directions, then it is probably due to changes in metabolic pathway.

7.2.2 Relationship Between δD_{H20} and δD_{CH4}

The ability to calculate δD for methane emissions will allow the relationship between δD of the surrounding water and δD in methane to be determined. This may also give further clues to the metabolic pathway being used by the microbial population.

It would be interesting to conduct a laboratory study using deuterated water to establish the time it takes for the hydrogen in water to be transferred to methane in the peat, further constraining the relationship between δD_{H20} and δD_{CH4}.

7.2.3 Environmental Factors

In the laboratory study the effect of temperature was investigated by keeping replicate cores in the dark. This work could be repeated, keeping the cores under controlled lighting conditions. The investigation could be extended to include lower temperatures and even examine the effect of freeze-thaw cycles on methanogenesis and the isotopic composition of the CH_4 flux.

A detailed laboratory study should be conducted to constrain the effect of water table on the isotopic composition of methane. Experiments should include several water table heights and be performed at different temperatures because methane oxidation has a different temperature response to methanogenesis. It would also be interesting to maintain the anaerobic and the aerobic zones at different temperatures.

7.2.4 Effect of Plants

This study concluded that the seasonal variation in the isotopic composition of methane flux from an ombrotrophic mire could not be accounted for solely by

changes in peat temperature and water table. It was, however, linked to the growth cycle of the plants. This may be due to the relative importance of plant transport mechanisms compared to ebullition and molecular diffusion in bringing methane to the surface. Alternatively it may be that during the growing season the relative contributions of the two metabolic pathways change, possibly due to the availability of the labile carbon source provided by photosynthates exuded into the rhizosphere. Investigations leading to a more definitive cause of the seasonal variation in the isotopic composition of methane emission are clearly required.

A comparison of methane flux (and its isotopic composition) from mires characterised by different species of vegetation should be made. A detailed study of the effect of clipping vegetation above and below water levels could also be conducted. It may be possible to determine the relative contributions of fluxes from mire dominated by *Sphagnum* mosses, fluxes through *Eriophorum* spp. and ericaceous species. Plant transport mechanisms and their effects on the isotopic composition of the CH_4 flux may then be established.

In the field solar radiation is variable. Using isotopic data in a laboratory study that varies incident radiation for the plants while maintaining constant temperature and water table may provide a further insight into the rôle of plants in methane production.

7.2.5 Diurnal variability

In this study the diurnal variations of the methane flux and its isotopic composition was only investigated over one 24-hour period, without sample replication. Clearly, further work is required to verify the results obtained. The investigation needs to be broadened to examine the diurnal patterns when the water table is at the surface, and throughout the year. As active plant growth has an effect on the isotopic composition of CH_4 emission, the diurnal pattern may also show seasonal variability.

7.2.6 Nitrogen Applications

Due to limitations of sample through-put time, and therefore the total number of samples it was possible to analyse, the investigation of the effect of nitrogen applications in this study proved inconclusive. Further study should sample the CH_4 fluxes immediately before and at regular intervals immediately after the nitrogen applications, to determine if there is an instantaneous but short-lived effect.

7.2.7 Palsa Mires

As the research conducted in the palsa mire in Finland provided only a snapshot image of that ecosystem there is much scope for further study. Seasonal variations in the isotopic composition of CH_4 flux, and the effects of environmental variables could be investigated. The effects of *Equisetum fluviatile* and *Menyanthes trifoliata* on the isotopic composition also need to be determined.

7.2.8 Broader Applications

The technique used in this project has applications in investigations of methane fluxes from agricultural ecosystems, *e.g.* ruminant emissions and rice paddies. It would also be useful for investigating other sources of methane such as landfill sites and vehicle emissions.

There is also potential for adapting static mass spectrometer techniques to determine the combined isotopic composition of nitrous oxide, N_2O. This could then be used to investigate the processes of denitrification and nitrification in agricultural ecosystems.

7.3 Implications for the Future

The beauty of the technique described is its application at many levels. It is ideal for investigations at the process level, looking at the mechanisms involved in methane production and emissions. It is also an excellent tool for determining the importance of environmental factors. The use of the technique in a palsa mire in

Finland has shown its suitability at the landscape scale, investigating a varied topography. Use of atmospheric methane $\delta^{17}M$ data collected using MIRANDA in the evaluation of general circulation models proves the versatility of the technique.

It is concluded that, due to the wide range of potential applications coupled with the facile nature of the sampling technique, MIRANDA will make a major contribution to our understanding of the global methane budget in the future.

References

Allen S.E. 1989. Chemical Analysis of Ecological Materials. Blackwell Scientific Publications, Oxford.

Alperin M.J., Blair N.E., Alberts D.B., Hoehler T.M. & Martens C.S. 1992. Factors that control the stable carbon isotopic composition of methane produced in an anoxic marine sediment. *Global Biogeochemical Cycles,* **6**(3), 271-291.

Alperin M.J., Reeburgh W.S. & Whiticar M.J. 1988. Carbon and hydrogen isotope fractionation resulting from anaerobic methane oxidation. *Global Biogeochemical Cycles,* **2**(3), 279-288.

Arah J.R.M. & Stephen K.D. 1998. A model of the processes leading to methane emission from peat land. *Atmospheric Environment,* **32**(19), 3257-3264.

Aselmann I. 1989. Global-scale extrapolation: a critical assessment. In: *Exchange of Trace Gases between Terrestrial Ecosystems and the Atmosphere* (ed. M.O. Andreae & D.S. Schimel), pp. 119-133. J.Wiley & Sons, Chichester.

Aselmann I. & Crutzen P.J. 1989. Global distribution of natural wetlands and rice paddies, their net primary productivity, seasonality and possible methane emissions. *Journal of Atmospheric Chemistry,* **8**, 307-358.

Badr O., Probert S.D. & O'Callaghan P.W. 1991a. Atmospheric methane: Its contribution to global warming. *Applied Energy,* **40**, 273-313.

Badr O., Probert S.D. & O'Callaghan P.W. 1991b. Origins of Atmospheric methane. *Applied Energy,* **40**, 189-231.

Badr O., Probert S.D. & O'Callaghan P.W. 1992a. Methane: A greenhouse gas in the earth's atmosphere. *Applied Energy,* **41**, 95-113.

Badr O., Probert S.D. & O'Callaghan P.W. 1992b. Sinks for atmospheric methane. *Applied Energy,* **41**, 137-147.

Barker J.F. & Fritz P. 1981. Carbon isotope fractionation during microbial methane oxidation. *Nature,* **293**, 289-291.

Barrie A. 1991. New methodologies in stable isotope analysis. In: *Stable Isotopes in plant nutrition, soil fertility, and environmental studies.* Proceedings of an international symposium on the use of stable isotopes in plant nutrition, soil fertility and environmental studies jointly organised by the IAEA & FAO of the UN, held in Vienna, October 1990. International Atomic Energy Agency, Vienna.

Bates T.S., Kelly K.C., Johnson J.E. & Gammon R.H. 1996. A re-evaluation of the open ocean source of methane to the atmosphere. *Journal of Geophysical Research,* **101**(D3), 6953-6961.

Bédard C. & Knowles R. 1989. Physiology, biochemistry and specific inhibitors of CH_4, NH_4 and CO oxidation by methanotrophs and nitrifiers. *Microbiological Reviews,* **53**, 68-84.

Bekki S., Law K.S. & Pyle J.A. 1994. Effect of ozone depletion on atmospheric CH_4 and CO concentrations. *Nature,* **371**, 595-597.

Bender M. & Conrad R. 1993. Kinetics of methane oxidation in oxic soils. *Chemosphere,* **26**, 687-696.

Benstead J. & Lloyd D. 1996. Spatial and temporal variations of dissolved gasses (CH_4, CO_2 and O_2) in peat cores. *Microbial Ecology,* **31**, 57-66.

Bergamaschi P. 1997. Seasonal variations of stable hydrogen and carbon isotope ratios in methane from a Chinese rice paddy. *Journal of Geophysical Research,* **102**(D21), 25383-25393.

Bergamaschi P., Schupp M. & Harris G.W. 1994. High-precision direct measurements of $^{13}CH_4/^{12}CH_4$ and $^{12}CH_3D/^{12}CH_4$ ratios in atmospheric methane sources by means of a long path tunable diode laser absorption spectrometer. *Applied Optics,* **33**(33), 7704-7716.

Beswick K.M., Simpson T.W., Fowler D., Choularton T.W., Gallagher M.W., Hargreaves K.J., Sutton M.A. & Kayes A. 1998. Methane emissions on large scales. *Atmospheric Environment,* **32**(19), 3283-3291.

Blair N.E. & Carter Jr W.D. 1992. The carbon isotope biogeochemistry of acetate from a methanogenic marine sediment. *Geochimica et Cosmochimica Acta,* **56**, 1247-1258.

Blake D.R. & Rowland F.S. 1986. World-wide increase in tropospheric methane 78-83. *Journal of Atmospheric Chemistry,* **4**, 43-62.

Blake D.R. & Rowland F.S. 1988. Continuing worldwide increase in tropospheric methane, 1978 to 1987. *Science,* **239**, 1129-1131.

Blake D.R., Mayer E.W., Tyler S.C., Makide Y., Montague D.C. & Rowland F.S. 1982. Global increase in atmospheric methane concentrations between 1978 and 1980. *Geophysical Research Letters,* **9**(4), 477-480.

Boeckx P. & Van Cleemput O. 1996. Methane Oxidation in a neutral landfill cover soil: influence of moisture content, temperature and nitrogen turnover. Journal of Environmental Quality, **25**, 178-183.

Boon P.I. & Sorrell B.K. 1995. Methane fluxes from an Australian floodplain wetland: the importance of emergent macrophytes. *Journal of the North American Benthological Society,* **14**, 582-598.

Bouwman A.F. 1990. Introduction. In: *Soils and the Greenhouse Effect* (ed. A.F. Bouwman), pp. 25-32. J.Wiley & Sons, Chichester.

Bridgham S.D. & Richardson C.J. 1992. Mechanisms controlling soil respiration (CO_2 and CH_4) in southern peatlands. *Soil Biology Biochemistry,* **24**(11), 1089-1099.

Bridgham S.D., Johnston C.A., Pastor J. & Updegraff K. 1995. Potential feedbacks of Northern wetlands on climate change. *Bioscience,* **45**, 262-274.

Brooks P.D., Atkins G.J., Herman D.J., Prosser S.J. & Barrie A. 1993. Rapid isotopic analysis of selected soil gases at atmospheric concentrations. In: *Agricultural Ecosystem Effects on Trace Gases and Global Climate Change* (ed. L.A. Harper, *et al.*), pp. 193-202. Vol. ASA Special Publication Number 55. American Society of Agronomy, Madison, WI, USA.

Bubier J.L., Moore T.R. & Roulet N.T. 1993. Methane emissions from wetlands in the midboreal region of Northern Ontario, Canada. *Ecology,* **74**, 2240-2254.

Burke Jr R.A. 1993. Possible influence of [H] on microbial CH_4 stable hydrogen isotope composition. *Chemosphere,* **29**, 55-67.

Burke Jr R.A., Barber T.R. & Sackett W.M. 1988a. Methane flux and stable hydrogen and carbon isotope composition of sedimentary methane from the Florida Everglades. *Global Biogeochemical Cycles,* **2**(4), 329-340.

Burke Jr R.A., Martens C.S. & Sackett W.M. 1988b. Seasonal variations of D/H and $^{13}C/^{12}C$ ratios of microbial CH_4 in surface sediments. *Nature,* **332**, 829-831.

Butterworth A.L. 1997. Determination of the Combined Isotopic Composition of Atmospheric Methane. PhD thesis, The Open University, Milton Keynes.

Cantrell C.A., Shetter R.E., McDaniel A.H., Galvert J.G., Davidson J.A., Lowe D.C., Tyler S.C., Cicerone R.J. & Greenberg J.P. 1990. Carbon kinetic isotope effect in the oxidation of methane by the hydroxyl radical. *Journal of Geophysical Research,* **95**, 22455-22462.

Cao M., Marshall S. & Gregson K. 1996. Global carbon exchange and methane emissions from natural wetlands: Application of a process-based model. *Journal of Geophysical Research,* **101**(D9), 14399-14414".

Carr R.H., Wright I.P., Joines A.W. & Pillinger C.T. 1986. Measurement of carbon stable isotopes at the nanomole level: a static mass spectrometer and sample preparation technique. *Journal of Physics E:Scientific Instruments,* **19**, 798-808.

Chanton J.P. & Dacey W.H. 1991. Effects of vegetation on methane flux, reservoirs and carbon isotopic composition. In: *Trace gas emissions by plants.* (ed. T.D. Sharkey, E.A. Holland & H.A. Mooney), pp. 65-92. Academic Press, Inc., New York.

Chanton J.P. & Martens C.S. 1988. Seasonal variations in ebullitive flux and carbon isotopic composition of CH4 in a tidal freshwater estuary. *Global Biogeochemical Cycles,* **2**(3), 289-298.

Chanton J.P., Pauly G.G., Martens C.S., Blair N.E. & Dacey J.W.H. 1988. Carbon isotopic composition of methane in Florida Everglades soils & fractionation during its transport to the troposphere. *Global Biogeochemical Cycles,* **2**(3), 245-252.

Chanton J.P., Whiting G.J., Blair N.E., Lindau C.W. & Bollich P.K. 1997. Methane emission from rice: stable isotopes, diurnal variations and CO_2 exchange. *Global Biogeochemical Cycles,* **11**, 15-27.

Chanton J.P., Whiting G.J., Showers W.J. & Crill P.M. 1992. Methane flux from Peltandra Virginica: stable isotope tracing and chamber effects. *Global Biogeochemical Cycles,* **6**, 15-31.

Chappellaz J., Barnola J.M., Raynaud D., Korotkevich Y.S. & Lorius C. 1994. Historical CH_4 record from the Vostok ice core. In: *Trends '93: A Compendium of Data on Global Change* (ed. T.A. Boden, *et al.*), pp. 229-232. Carbon Dioxide Information Analysis Center, Oak Ridge National Laboratory, Tennessee, USA.

Christensen T. 1991. Arctic and sub-arctic soil emissions: possible implications for global climate change. *Polar Record,* **27**(162), 205-210.

Christensen T.R. 1993. Methane emission from Arctic tundra. *Biogeochemistry,* **21**, 117-139.

Christensen T.R., Jonasson S., Callaghan T.V. & Havstrom M. 1995. Spatial variation in high-latitude methane flux along a transept across Siberian and European tundra environments. *Journal of Geophysical Research,* **100**(D10), 21035-21045.

Cicerone R.J. & Oremland R.S. 1988. Biogeochemical aspects of atmospheric methane. *Global Biogeochemical Cycles,* **2**(4), 299-327.

Cicerone R.J. & Shetter J.D. 1981. Sources of atmospheric methane: measurements in rice paddies and a discussion. *Journal of Geophysical Research,* **86**(C8), 7203-7209.

Clymo R.S. 1984. The limits of bog growth. *Philosophical Transactions of the Royal Society, London: B,* **303**, 605-654.

Clymo R.S. 1987. The ecology of peatlands. *Science Progress,* **71**, 593-614.

Clymo R.S. 1991. Peat growth. In: *Quaternary Landscapes* (ed. L.C.K. Shane & E.J. Cushing). University of Minnesota Press, Minneapolis, USA.

Clymo R.S. 1992. Models of peat growth. *Suo,* **43**, 127-136.

Clymo R.S. & Pearce D.M.E. 1995. Methane and carbon dioxide production in, transport through and efflux from a peatland. *Philosophical Transactions of the Royal Society, London: A,* **350**, 249-259.

Coleman D.D., Risatti J.B. & Schoell M. 1981. Fractionation of carbon and hydrogen isotopes by methane-oxidizing bacteria. *Geochimica et Cosmochimica Acta,* **45**, 1033-1037.

Conny J.M. & Currie L.A. 1996. The isotopic characterisation of methane, non-methane hydrocarbons and formaldehyde in the troposphere. *Atmospheric Environment,* **30**(4), 621-638.

Conrad R. 1989. Control of methane production in terrestrial ecosystems. In: *Exchange of Trace Gases between Terrestrial Ecosystems and the Atmosphere* (ed. M.O. Andreae & D.S. Schimel), pp. 39-58. J.Wiley & Sons, Chichester.

Conrad R. 1995. Soil microbial processes and the cycling of atmospheric trace gases. *Philosophical Transactions of the Royal Society, London: A,* **351**, 219-230.

Craig H. 1957. Isotopic Standards for carbon and oxygen and correction factors for mass spectrometeric analysis of carbon dioxide. *Geochimica et Cosmochimica Acta,* **12**, 133-149.

Craig H. & Chou C.C. 1982. Methane: the record in polar ice cores. *Geophysical Research Letters,* **9**, 1221-1224.

Craig H., Chou C.C., Welhan J.A., Stevens C.M. & Engelkemeir A. 1988. The isotopic composition of methane in polar ice cores. *Science,* **242**, 1535-1539.

Crill P.M., Bartlett K.B., Harriss R.C., Gorham E., Verry E.S., Sebacher D.I., Madzar L. & Sanner W. 1988. Methane flux from Minnesota peatlands. *Global Biogeochemical Cycles,* **2**(4), 371-384.

Crill P.M., Martikainen P.J., Nykänen H. & Silvola J. 1994. Temperature and N fertilisation effects on methane oxidation in a drained peatland soil. *Soil Biology Biochemistry,* **36**, 1331-1339.

Crutzen P.J. 1993. Global budgets for non-CO_2 greenhouse gases. In: *Non-CO_2 greenhouse gases: why and how to control them?* (ed. J. van Ham, L.J.H.M. Janssen & R.J. Swart). Proceedings of an International Symposium held in Maastricht, December 1993. Kluwer Academic Publishers, London.

Crutzen P.J. 1995. Overview of tropospheric chemistry: developments during the past quarter century and a look ahead. *Faraday Discussions,* **100**, 1-21.

Daniels L., Fulton G., Spencer R.W. & Orme-Johnson W.H. 1980. Origin of hydrogen in methane produced by *Methanobacterium thermoautotrophicum*. *Journal of Bacteriology,* **141**, 694-698.

Daulat W.E. & Clymo R.S. 1998. Effects of temperature and watertable on the efflux of methane from peatland surface cores. *Atmospheric Environment,* **32**(19), 3207-3218.

Davidson J.A., Cantrell C.A., Tyler S.C., Shetter R.E., Cicerone R.J. & Calvert J.G. 1987. Carbon kinetic isotope effect in the reaction of CH_4 with $HO^{\bullet}$. *Journal of Geophysical Research,* **92**(D2), 2195-2199.

DeMore W.B. 1993. Rate constant ratio for the reactions of OH with CH_3D and CH_4. *Journal of Physical Chemistry,* **97**, 8564-8566.

Derwent R. 1994. The estimation of global warming potentials for a range of radiatively active gases. In: *Non-CO_2 greenhouse gases: why and how to control them?* (ed. J. van Ham, L.J.H.M. Janssen & R.J. Swart), pp. 289-299.

Devol A.H., Richey J.E., Forsberg B.R. & Martinelli L.A. 1990. Seasonal dynamics in methane emissions from the Amazon River floodplain to the troposphere. *Journal of Geophysical Research,* **95**(D10), 16417-16426.

Dickenson R.E. 1986. How will the climate change? The climate system and modelling of future climate. In: *The Greenhouse Effect, Climatic Change and Ecosystems* (ed. B. Bolin, *et al.*), pp. 201-270. John Wiley & Sons, Chichester.

DiMarco A.A., Bobik T.A. & Wolfe R.S. 1990. Unusual coenzymes of methanogenesis. *Annual Reviews of Biochemistry,* **59**, 355-394.

Dise N.B. 1992. Winter fluxes of CH4 from Minnesota peatlands. *Biogeochemistry,* **17**, 71-83.

Dise N.B. 1993. Methane emission from Minnesota peatlands: spatial and seasonal variability. *Global Biogeochemical Cycles,* **7**(1), 123-142.

Dise N.B., Gorham E. & Verry E. 1993. Environmental factors controlling methane emissions from peatlands in Northern Minnesota. *Journal of Geophysical Research,* **98**(D6), 10583-10594.

Dlugokencky E.J., Harris J.M., Chung Y.S., Tans P.P. & Fung I. 1993. The relationship between the methane seasonal cycle and regional sources and sinks at Tae-ahn peninsula, Korea. *Atmospheric Environment,* **27A**(14), 2115-2120.

Dlugokencky E.J., Lang P.M., Masarie K.A. & Steele L.P. 1994a. Atmospheric methane records from sites in the NOAA/CMDL air-sampling network. In: *Trends '93: A compendium of data on global change* (ed. T.A. Boden, *et al.*), pp. 274-371.

Dlugokencky E.J., Lang P.M., Masarie K.A. & Steele L.P. 1994b. Global CH4 record from the NOAA/CMDL air sampling network. In: *Trends '93: A compendium of data on global change* (ed. T.A. Boden, *et al.*), pp. 262-266.

Dlugokencky E.J., Masaire K.A., Lang P.M., Tans P.P., Steele L.P. & Nisbet E.G. 1994c. A dramatic decrease in the growth rate of atmospheric methane in the Northern Hemisphere during 1992. *Geophysical Research Letters,* **21**, 45-48.

Dlugokencky E.J., Steele L.P., Lang P.M. & Masarie K.A. 1994d. The growth rate and distribution of atmospheric methane. *Journal of Geophysical Research,* **99**(D7), 17021-17043.

Dlugokencky E.J., Masarie K.A., Lang P.M. & Tans P.P. 1998. Continuing decline in the growth rate of the atmospheric methane burden. *Nature,* **393**, 447-450.

Duenas C., Fernandez M.C., Carretero J., Perez M. & Liger E. 1994. Consumption of methane by soils. *Environmental Monitoring and Assessment*, **31**, 125-130.

Dumke I., Faber E. & Poggenburg J. 1989. Determination of stable carbon and hydrogen isotopes of light hydrocarbons. *Analytical Chemistry,* **61**(19), 2149-2154.

Dunfield P., Knowles R., Dumont R. & Moore T.R. 1993. Methane production and consumption in temperate and sub-arctic peat soils - response to temperature and pH. *Soil Biology Biochemistry,* **25**, 321-326.

Edwards G.C., Neumann H.H., den Hartog G., Thurtell G.W. & Kidd G. 1994. Eddy correlation measurements of methane fluxes using a tunable diode laser at the Kinosheo Lake tower site during the Northern Wetlands Study (NOWES). *Journal of Geophysical Research,* **99**(D1), 1511-1517.

Etheridge D.M., Pearman G.I. & de Silva F. 1988. Atmospheric trace-gas variations as revealed by air trapped in an ice-core from Law Dome, Antarctica. *Annals of Glaciology,* **10**, 28-33.

Fowler D. & Duyzer J.H. 1989. Micrometeorological techniques for the measurement of trace gas exchange. In: *Exchange of Trace Gases between Terrestrial Ecosystems and the Atmosphere* (ed. M.O. Andreae & D.S. Schimel), pp. 189-207. J.Wiley & Sons, Chichester.

Fowler D., Hargreaves K.J., MacDonald J.A. & Gardiner B. 1995a. Methane and CO_2 exchange over peatland and the effects of afforestation. *Forestry,* **68**, 327-334.

Fowler D., Hargreaves K.J., Skiba U., Milne R., Zahniser M.S., Moncrieff J.B., Beverland I.J. & Gallagher M.W. 1995b. Measurements of CH_4 and N_2O fluxes at the landscape scale using micrometeorological methods. *Philosophical Transactions of the Royal Society, London: A,* **351**, 339-356.

Francez A.J. & Vasander H. 1995. Peat accumulation and peat decomposition after human disturbance in French and Finnish mires. *Acta Oecologica,* **16**, 599-608.

Fraser P.J., Khalil M.A.K., Ramussen R.A. & Steele L.P. 1984. Tropospheric methane in the mid-latitudes of the Southern Hemisphere. *Journal of Atmospheric Chemistry,* **1**, 125-135.

Friedli H., Loetscher H., Oeschger H., Siegenthaler U. & Stauffer B. 1986. Ice core record of the $^{13}C/^{12}C$ record of atmospheric CO_2 in the past two centuries. *Nature,* **324**, 237-238.

Fung I., John J. & Lerner J. 1991. Three-dimensional model of synthesis of the global methane cycle. *Journal of Geophysical Research,* **96**, 13033-13065.

Galchenko V.F., Lein A. & Ivanov M. 1989. Biological sinks of methane. In: *Exchange of Trace Gases between Terrestrial Ecosystems and the Atmosphere* (ed. M.O. Andreae & D.S. Schimel), pp. 59-71. J.Wiley & Sons, Chichester.

Gallagher M.W., Choularton T.W., Bower K.N., Stromberg I.M., Beswick K.M., Fowler D. & Hargreaves K.J. 1994. Measurements of methane fluxes on a landscape scale from a wetland area in North Scotland. *Atmospheric Environment,* **28**(15), 2421-2430.

Games L.M. & Hayes J.M. 1976. On the mechanisms of CO_2 and CH_4 production in natural anaerobic environments. In: *Environmental biogeochemistry : Carbon, nitrogen phosphorous, sulfur and selenium cycles* Proceeding of 2nd International Symposium on Environmental Biogeochemistry (ed. J.O. Nriagin), pp. 51-73. Science Press, Ann Arbor, Michigan, USA.

Games L.M., Hayes J.M. & Gunsalus R.P. 1978. Methane-producing bacteria: natural fractionations of the stable C isotopes. *Geochimica et Cosmochimica Acta,* **42**, 1295-1297.

Gardiner L.R. & Pillinger C.T. 1979. Static mass spectrometry for the determination of active gases. *Analytical Chemistry,* **51**, 1230-1236.

Gelwicks J.T., Risatti J.B. & Hayes J.M. 1994. Carbon isotope effects associated with acetoclastic methanogenesis. *Applied and Environmental Microbiology,* **60**, 467-472.

Genthon C. 1994. Antarctic climate modelling with general circulation models of the atmosphere. *Journal of Geophysical Research,* **99**(D6), 12953-12961.

Gleason J.K., Bhartia P.K., Herman J.R., McPeters R., Newman P., Stolarski R.S., Flynn L., Labow G., Larko D., Seftor C., Wellemeyer C., Komhyr W.D., Miller A.J. & Planet W. 1993. Record low global ozone in 1992. *Science,* **260**, 523-526.

Gordon S. & Mulac W.A. 1975. Reaction of the $OH(x^2II)$ radical produced by the pulse radiolysis of water vapor. *International Journal of Chemical Kinetics,*

Proceedings of a Symposium on Chemical Kinetics Data for the Upper and Lower Atmosphere. J. Wiley & Sons, New York, USA.

Graedel T.E., Bates T.S., Bouwman A.F., Cunnold D., Dignon J., Fung I., Jacob D.J., Lamb B.K., Logan J.A., Marland G., Middleton P., Pacyna J.M., Placet M. & Veldt. C. 1993. A complication of inventories of emissions to the atmosphere. *Global Biogeochemical Cycles,* **7**(1), 1-26.

Gupta M., Tyler S. & Cicerone R. 1996. Modelling atmospheric $\delta^{13}CH_4$ and the causes of recent changes of atmospheric CH_4 amounts. *Journal of Geophysical Research,* **101**(D17), 22923-22932.

Hagemann R., Nief G. & Roth E. 1970. Absolute isotopic scale for deuterium analysis of natural waters, absolute D/H ratio of SMOW. *Tellus,* **22**, 712-715.

Hamilton D., Kelly C.A., Rudd J.W.M., Hesslein R.H. & Roulet N.T. 1994. Flux to the atmosphere of methane & carbon dioxide from wetland ponds on the Hudson Bay lowlands. *Journal of Geophysical Research,* **99**(D1), 1495-1510.

Hansen J., Fung I., Lacis A., Rind D., Lebedeff S., R.Ruedy, Russell G. & Stone P. 1988. Global climate changes as forecast by Goddard Institute for Space Studies 3-D model. *Journal of Geophysical Research,* **93**(D8), 9341-9364.

Harden H.S. & Chanton J.P. 1994. Locus of methane release and mass-dependent fractionation from two wetland macrophytes. *Limnology and Oceanography,* **39**(1), 148-154.

Hargreaves K.J. & Fowler D. 1998. Quantifying the effects of water table and soil temperature on the emission of methane from peat wetland at the field scale. *Atmospheric Environment,* **32**(19), 3275-3282.

Hargreaves K.J., Wienhold F., Klemedtsson L., Arah J.R.M., Beverland I.J., Fowler D., Galle B., Griffith D.W.T., Skiba U., Smith K.A., Welling M. & Harris G.W. 1996. Measurements of nitrous oxide from agricultural land using micrometeorological methods. *Atmospheric Environment,* **30**, 1563-1571.

Harriss R., Bartlett K., Frolking S., Crill P. & Oremland R.S. 1993. Methane emissions from Northern high latitude wetlands. In: *Biogeochemistry of global change:radiatively active trace gases*, pp. 449-486. Chapman and Hall, New York, USA.

Harvey L.D.D. 1993. A guide to global warming potentials. *Energy Policy,* **Jan 93**, 24-34.

Holzapfel-Pschorn A., Conrad R. & Seiler W. 1985. Production, oxidation and emission of methane in rice paddies. *FEMS Microbiology Ecology,* **31**, 343-351.

Hornibrook E.R.C., Longstaffe F.J. & Fyfe W.S. 1997. Spatial distribution of microbial methane production pathways in temperate zone wetland soils:

Stable carbon and hydrogen isotope evidence. *Geochimica et Cosmochimica Acta,* **61**, 745-753.

Houghton J. 1994. *Global Warming The Complete Briefing.* Lion Publishing plc.

Hovland M., Judd A.G. & Burke R.A., Jr. 1993. The global flux of methane from shallow submarine sediments. *Chemosphere,* **26**, 559-578.

Hutchin P.R., Press M.C., Lee J.A. & Ashenden T.W. 1995. Elevated concentrations of CO_2 may double methane emissions from mires. *Global Change Biology,* **1**, 125-128.

Hutchin P.R., Press M.C., Lee J.A. & Ashenden T.W. 1996. Methane emission rates from an ombrotrophic mire show marked seasonality which is independent of nitrogen supply and soil temperature. *Atmospheric Environment,* **30**(17), 3011-3015.

Hütsch B.W., Webster C.P. & Powlson D.S. 1993. Long-term effects of nitrogen fertilisation on methane oxidation in soil of the Broadbalk wheat experiment. *Soil Biology Biochemistry,* **25**, 1307-1315.

Ingram H.A.P. 1978. Soil layers in mires: function and terminology. *Journal of Soil Science,* **29**, 224-227.

IPCC. 1992. Climate change 1992. The Supplementary Report to the IPCC Scientific Assessment. Intergovernmental Panel on Climate Change. Cambridge University Press, Cambridge.

IPCC. 1994. Climate change 1994 Radiative Forcing of Climate Change and an Evaluation of the IPCC IS92 Emission Scenarios. Intergovernmental Panel on Climate Change. Cambridge University Press, Cambridge.

IPCC. 1995. Climate change 1995. The Science of Climate Change. Intergovernmental Panel on Climate Change. Cambridge University Press, Cambridge.

Jenden P.D. & Kaplan I.R. 1986. Comparison of microbial gases from the Middle American Trench and Schripps Submarine Canyon: implications for the origin of natural gas. *Applied Geochemistry,* **1**, 631-646.

Johnson E.G. & Nier A.O. 1953. Angular aberrations in sector shaped electromagnetic lenses for focusing beams of charged particles. *Physics Reviews,* **91**, 10-17.

Johnston H.S. 1984. Human effects on the global atmosphere. *Annual Review of Physical Chemistry,* **35**, 481-505.

Jones W.J. 1991. Diversity and physiology of methanogens. In: *Microbial production of greenhouse gases: methane, nitrogen oxides and halomethanes* (ed. J.E. Rogers & W.B. Whitman), pp. 39-55. American Society for Microbiology, Washington D.C., USA.

Kandlikar & McRae. 1995. Inversion of the global methane cycle using chance constrained programming: methodology and results. *Chemosphere,* **30**(6), 1151-1170.

Kaye J. 1987. Mechanisms and observations for isotope fractionation of molecular species in planetary atmospheres. *Reviews of Geophysics,* **25**, 1609-1658.

Keller M., Goreau T.J., Wofsy S.C., Kaplan W.A. & McElroy M.B. 1983. Production of N_2O and consumption of methane by forest soils. *Geophysical Research Letters,* **10**(12), 1156-1159.

Kettunen A., Kaitala V., Alm J., Silvola J., Nykanen H. & Martikanen P.J. 1996. Cross-correlation analysis of the dynamics of methane emissions from a peatland. *Global Biogeochemical Cycles,* **10**(3), 457-471.

Khalil M.A.K. & Rasmussen R.A. 1983. Sources, sinks and seasonal cycles of atmospheric methane. *Journal of Geophysical Research,* **8**(C9), 5131-5144.

Khalil M.A.K. & Rasmussen R.A. 1994. Trends in atmospheric methane. *Pure and Applied Chemistry,* **66**(1), 143-147.

King G.M. 1992. Ecological aspects of methane oxidation, a key determinant of global methane dynamics. In *Advances in Microbial Ecology*, Vol. 12 (ed. K.C. Marshall). Plenum Press, New York, USA.

King S.L., Quay P.D. & Lansdown J.M. 1989. The $^{13}C/^{12}C$ kinetics isotope effect for soil oxidation of methane at ambient atmospheric concentrations. *Journal of Geophysical Research,* **94**(D15), 18273-18277.

Knowles R. 1993. Methane: processes of production and consumption. In: *Agricultural ecosystem effects on trace gases and global climate change* (ed. L.A. Harper, *et al.*), pp. 145-156. American Society of Agronomy, Madison, WI, USA.

Kuhlmann A.J., Worthy D.E.J., Trivett N.B.A. & Levin I. 1998. Methane emissions from a wetland region within the Hudson Bay Lowland: an atmospheric approach. *Journal of Geophysical Research,* **103**(D3), 16,009-16016.

Lacis A., Hansen J., Lee P., Mitchell T. & Lebedeff S. 1981. Greenhouse effect of trace gases, 1970-1980. *Geophysical Research Letters,* **8**, 1035-1038.

Lansdown J.M., Quay P.D. & King S.L. 1992. CH_4 production via CO_2 reduction in a temperate bog: A source of ^{13}C-depleted CH_4. *Geochimica et Cosmochimica Acta,* **56**, 3493-3503.

Lasaga A.C. & Gibbs G.V. 1991. *Ab initio* studies of the kinetic isotope effect of the CH_4 and OH atmospheric reaction. *Geophysical Research Letters,* **18**, 1217-1220.

Lassey K.R., Lowe D.C., Brenninkmeijer C.A.M. & Gomez A.J. 1993. Atmospheric methane and its carbon isotopes in the southern hemisphere: their time series and an instructive model. *Chemosphere,* **26**, 95-109.

Leclerc M.Y. & Thurtell G.W. 1990. Footprint prediction of scalar flux using a Markovian Analysis. *Boundary-Layer Meteorology,* **52**, 247-258.

Lelieveld J. & Crutzen P.J. 1993. Methane emissions into the atmosphere: an overview. In: *Methane and nitrous oxide methods in national emissions inventories and options for control.* Proceedings of an IPCC workshop held at Amersfoort, February 1993. pp 17-25. RIVM, Bilthoven, The Netherlands.

Lelieveld J., Crutzen P.J. & Bruhl C. 1993. Climate effects of atmospheric methane. *Chemosphere,* **26**, 739-768.

Livingston G.P. & Hutchinson G.L. 1995. Enclosure-based measurements of trace gas exchange: applications and sources of error. In: *Biogenic Trace Gases: Measuring Emissions from Soil and Water* (ed. P.A. Matson & R.C. Harriss), pp. 14-51. Blackwell Scientific Publications, Oxford.

Lloyd D., Thomas K.L., Benstead J., Davies K.L., Lloyd S.H., Arah J.R.M. & Stephen K.D. 1998. Methanogenesis and CO_2 exchange in an ombrotrophic peat bog. *Atmospheric Environment,* **32**(19), 3229-3238.

Logan J.A., Prather M.J., Wofsy S.C. & McElroy M.B. 1981. Tropospheric chemistry: a global perspective. *Journal of Geophysical Research,* **86**, 7210-7254.

Lowe D.C. & Brenninkmeijer C.A.M. 1991. Determination of the isotopic composition of atmospheric methane and its application in the Antarctic. *Journal of Geophysical Research,* **96**, 15455-15467.

Lowe D.C., Brenninkmeijer C.A.M., Brailsford G.W., Lassey K.R., Gomez A.J. & Nisbet E.G. 1994. Concentration and ^{13}C records of atmospheric methane in New Zealand and Antarctica: evidence for changes in methane sources. *Journal of Geophysical Research,* **99**(D8), 16913-16925.

MacDonald J.A., Fowler D., Hargreaves K.J., Skiba U., Leith I.D. & Murray M.B. 1998. Methane emission rates from a Northern wetland; response to temperature, water table and transport. *Atmospheric Environment,* **32**(19), 3219-3227.

MacKenzie D. 1994. Carbon targets not tough enough. In *New Scientist*, 17 September 1994, p. 7.

Manabe S. & Wetherald R.T. 1986. Reduction in summer soil wetness induced by an increase in atmospheric carbon dioxide. *Science,* **232**, 626-628.

Mardia K.V. 1976. Linear-circular correlation co-efficients and rhythmometry. *Biometrika,* **63**, 403-405.

Martens C.S., Blair N.E., Green C.D. & Marais D.J.D. 1986. Seasonal variations in the stable carbon isotopic signature of biogenic methane in a coastal sediment. *Science,* **233**, 1300-1303.

Martens C.S., Kelley C.A., Chanton J.P. & Showers W.J. 1992. Carbon and hydrogen isotopic characterisation of methane from wetlands and lakes of the Yukon-Kuskokwim Delta, Western Alaska. *Journal of Geophysical Research,* **97**(D15), 16689-16701.

Martikainen P.J., Nykanen H., Alm J. & Silvola J. 1995. Change in fluxes of carbon dioxide, methane and nitrous oxide due to forest drainage of mire sites of different trophy. *Plant and Soil,* **169**, 571-577.

Matthews E. 1993. Wetlands. In: *Atmospheric Methane: sources, sinks and role in global change* (ed. M.A.K. Khalil), pp. 314-361. Vol. I. NATO ASI.

Matthews E. & Fung I. 1987. Methane emissions from natural wetlands: global distribution area, and environmental characteristics of sources. *Global Biogeochemical Cycles,* **1**, 61-86.

McKinney C.R., McCrea J.M., Epstein S., Allen H.A. & Urey H.C. 1950. Improvements in mass spectrometers for the measurement of small differences in isotope abundance ratios. *Review of Scientific Instruments,* **21**, 724-730.

McMillen R.T. 1986. NOAA Technical Memo: ERL ATRL-147. NOAA.

Melloh R.A. & Crill P.M. 1996. Winter methane dynamics in a temperate peatland. *Global Biogeochemical Cycles,* **10**(2), 247-254.

Mengel K. & Kirkby E.A. 1987. *Principles of Plant Nutrition.* International Potash Institute, Bern, Switzerland.

Merritt, D.A., Hayes J.M. & Marais D.J.D. 1995. Carbon isotopic analysis of atmospheric methane by isotope ratio monitoring gas chromatography-mass spectrometry. *Journal of Geophysical Research,* **100**(D1), 1317-1326.

Michaels P.J. 1990. The greenhouse effect & global change: review and reappraisal. *International Journal of Environmental Studies,* **36**, 55-71.

Migeotte M.V. 1948. Spectroscopic evidence of methane in the Earth's atmosphere. *Physical Review,* **73**, 519-520.

Mikkela C., Sundh I., Svensson B.H. & Nilsson M. 1995. Diurnal variation in methane emission in relation to the water table, soil temperature, climate and vegetation cover in a Swedish acid mire. *Biogeochemistry,* **28**, 93-114.

Minami K. 1994. Methane from rice production. In: *Methane and nitrous oxide methods in national emissions inventories and options for control.* Proceedings of an IPCC workshop held at Amersfoort, February 1993. pp 143-162. RIVM, Bilthoven, The Netherlands.

Mitchell J.F.B. 1989. The greenhouse effect and climate change. *Reviews of Geophysics,* **27**, 115-139.

Moncrieff J.B., Massheder J.M., De Bruin H., Elbers J., Friborg T., Huetzenfeldt B., Kabat P., Scott S., Soogard H. & Verhoef A. 1997. A system to measure surface fluxes of momentum, sensible heat flux, water vapour and carbon dioxide. *Journal of Hydrology,* **189**, 589-611.

Moore T.R. & Knowles R. 1989. The influence of water table levels on methane and carbon dioxide emissions from peatlands soils. *Canadian Journal of Soil Science,* **69**, 33-38.

Moore T.R. & Knowles R. 1990. Methane emissions from fen, bog and swamp peatlands in Quebec. *Biogeochemistry,* **11**, 45-61.

Moore T.R., Heyes A. & Roulet N.T. 1994. Methane emissions from wetlands, Southern Hudson Bay. *Journal of Geophysical Research,* **99**(D9), 1455-1467.

Moosavi S.C., Crill P.M., Pullman E.R., Funk D.W. & Peterson K.M. 1996. Controls on CH_4 flux from an Alaskan boreal wetland. *Global Biogeochemical Cycles,* **10**(2), 287-296.

Moraes F. & Khalil M.A.K. 1993. Permafrost methane content: 2. modelling theory and results. *Chemosphere,* **26**, 595-607.

Morrissey L.A. & Livingston G.P. 1992. Methane emission from Alaskan arctic tundra: an assessment of local spatial variability. *Journal of Geophysical Research,* **97**, 16661-16670.

Morrissey L.A., Zobel D.B. & Livingston G.P. 1993. Significance of stomatal control on methane release from *Carex*-dominated wetlands. *Chemosphere,* **26**, 339-355.

Morse A.D. 1991. Attempts to analyse D/H ratios of sub-micromole quantities of hydrogen: Applications in the study of ordinary chondrites. PhD thesis, The Open University, Milton Keynes.

Morse A.D., Morgan G.H., Butterworth A.L., Wright I.P. & Pillinger C.T. 1996. Combined Isotope Analysis of nanogram quantities of atmospheric methane. *Rapid Communications in Mass Spectrometry,* **10**, 1743-1746.

Mosier A., Schimel D., Valentine D., Bronson K. & Parton W. 1991. Methane and nitrous oxide fluxes in native, fertilised and cultivated grasslands. *Nature,* **350**, 330-332.

Mudge F. & Adger W.N. 1995. Methane fluxes from artificial wetlands: a global appraisal. *Environmental Management,* **19**(1), 39-55.

Muller S.W. 1947. *Permafrost of Permanently Frozen Ground and Related Engineering Problems*. Edwards Brothers, Ann Arbour, Michigan, USA.

Murase J. & Kimura M. 1994. Methane production and its fate in paddy fields VII electron acceptors responsible for anaerobic methane oxidation. *Soil Science and Plant Nutrition,* **40**(4), 647-654.

Navone R. 1964. Proposed method for nitrate in potable waters. *Journal of the American Water Works Association,* **56**, 781-783.

Nedwell D.B. & Watson A. 1995. CH_4 production, oxidation and emission in a UK ombrotrophic peat bog: influence of SO_4^{2-}. *Soil Biology Biochemistry,* **27**, 893-903.

Neftel A., Moor E., Oeschger H. & Stauffer B. 1985. Evidence from polar ice cores for the increase in atmospheric CO_2 in the past two centuries. *Nature,* **315**, 45-47.

Nicolet M. 1964. Reactions and photochemistry of atoms and molecules, I. introduction to chemical aeronomy. *Discussion of the Faraday Society,* **37**, 7-20.

Nier A.O. 1940. A mass spectrometer for routine isotope abundance measurements. *Review of Scientific Instruments,* **11**, 212-216.

Nier A.O. 1947. A mass spectrometer for isotope and gas analysis. *Review of Scientific Instruments,* **18**, 398-411.

Nisbet E.G. 1989. Some northern sources of atmospheric methane: production, history and future implications. *Canadian Journal of Earth Science,* **26**, 1603-1611.

Nykanen H., Alm J., Lang K., Silvola J. & Martikainen P.J. 1995. Emissions of CH_4, N_2O and CO_2 from a virgin fen and a fen drained for grassland in Finland. *Journal of Biogeography,* **22**, 351-357.

Okada S. & Tezuka M. 1989. Some problems of estimation of carbon stable isotope ratio of methane in natural gases. *Journal of the Japanese Association for Petroleum Technology,* **54**(2), 1-6.

O'Neill J.G. & Wilkinson J.F. 1977. Oxidation of ammonia by methane-oxidising bacteria and the effects of ammonia on methane oxidation. *Journal of General Microbiology,* **100**, 407-412.

Oremland R.S. & Marais D.J. 1983. Distribution, abundance and carbon isotopic composition of gaseous hydrocarbons in Big Soda Lake, Nevada: an alkaline, meromictic lake. *Geochimica et Cosmochimica Acta,* **47**, 2107-2114.

Parker D.E., Jones P.D., Folland C.K. & Bevan A. 1994. Interdecadal changes of surface temperature since the late 19th century. *Journal of Geophysical Research,* **99**(D7), 14373-14399.

Parsons A.N. 1991. Critical loads of nitrogen and sulphur from an ombrotrophic mire. PhD thesis, University of Manchester, Manchester.

Pearman G.I. & Fraser P.J. 1988. Sources of increased methane. *Nature,* **332**, 489-490.

Pearman G.I., Etheridge D., de Silva F. & Fraser P.J. 1986. Evidence of changing concentrations of atmospheric CO_2, N_2O and CH_4 from air bubbles in Antarctic ice. *Nature,* **320**, 248-250.

Piccot S.D., Beck L., Srinivasan S. & Kersteter S.L. 1996. Global methane emissions from minor anthropogenic sources and biofuel combustion in residential stoves. *Journal of Geophysical Research,* **101**(D17), 22757-22766.

Pine M. & Barker H.A. 1956. Studies on the methane fermentation. XII. The pathway of hydrogen in the acetate fermentation. *Journal of Bacteriology,* **71**, 644-661.

Pollock W., Heidt L.E., Leub R. & Ehhalt D. 1980. Measurement of stratospheric water vapour by cryogenic collection. *Journal of Geophysical Research,* **85**, 5555-5568.

Prather M., Derwent R., Ehhalt D., Fraser P., Sanhueza E. & Zhou X. 1995. Other trace gases and atmospheric chemistry. In: *Climate change 1994:Radiative forcing of climate change and an evaluation of the IPCC IS92 emission scenarios* (ed. J.T. Houghton, *et al.*), pp. 77-129. Cambridge University Press, Cambridge.

Prieme A. 1994. Production of methane in a brackish and a freshwater wetland. *Soil Biology Biochemistry,* **26**, 7-18.

Prinn R., Cunnold D., Rasmussen R., Simmonds P., Alyea F., Crawford A., Fraser P. & Rosen R. 1987. Atmospheric trends in methylchloroform and the global average for the hydroxyl radical. *Science,* **238**, 945-950.

Prosser S.J. 1993. The development of new and emerging techniques for automated stable-isotope-ratio mass spectrometry. PhD thesis, The Open University, Milton Keynes.

Prosser S.J., Wright I.P. & Pillinger C.T. 1990. A preliminary investigation into the isotopic measurements of carbon at the picomole level using static-vacuum mass spectrometry. *Chemical Geology,* **83**, 71-88.

Quay P.D., King S.L., Lansdown J.M. & Wilbur D.O. 1988. Isotopic composition of methane released from wetlands: implications for the increase in atmospheric methane. *Global Biogeochemical Cycles,* **2**, 385-397.

Quay P.D., King S.L., Stutsman J., Wilbur D.O., Steele L.P., Fung I., Gammon R.H., Brown T.A., Farwell G.W., Grootes P.M. & Schmidt F.H. 1991. Carbon isotopic composition of atmospheric methane: fossil & biomass burning source and strengths. *Global Biogeochemical Cycles,* **5**(1), 25-47.

Ramanathan V. 1988. The greenhouse theory of climate change: a test by an inadvertent global experiment. *Science,* **240**, 293-299.

Rasmussen R.A. & Khalil M.A.K. 1981. Atmospheric methane: trends and seasonal cycles. *Journal of Geophysical Research,* **86**, 9826-9832.

Rasmussen R.A. & Khalil M.A.K. 1984. Atmospheric methane in the recent and ancient atmospheres: concentrations, trends and interhemispheric gradient. *Journal of Geophysical Research,* **89**, 11599-11605.

Reeburgh W.S., Whalen S.C. & Alperin M.J. 1993. The role of methylotrophy in the global methane budget. In: *Microbial growth on C1 compounds* (ed. J. Murrell & D.P. Kelly), pp. 1-14. Intercept, Andover.

Rinsland C.P., Levine J.S. & Miles T. 1985. Concentration of methane in the troposphere deduced from the 1951 infrared solar spectra. *Nature,* **330**, 245-246.

Roulet N., Moore T., Bubier J. & Lafleur B. 1992. Northern fens: methane flux and climate change. *Tellus,* **44B**, 100-105.

Rudolph J. 1994. Anomalous methane. *Nature,* **368**, 19-20.

Russell S. 1992. A carbon and nitrogen isotope study of chondritic diamond and silicon carbide. PhD thesis, The Open University, Milton Keynes.

Rust F.E. & Stevens C.M. 1980. Carbon kinetic isotope effect in the oxidation of methane by hydroxylation. *International Journal of Chemical Kinetics,* **12**, 371-377.

Schimel J.P. 1995. Plant transport and methane production as controls on methane flux from arctic wet meadow tundra. *Biogeochemistry,* **28**, 183-200.

Schimel J.P., Holland E.A. & Valentine D. 1993. Controls on methane flux from terrestrial ecosystems. In: *Agricultural ecosystem effects on trace gases and global climate change* (ed. L.A. Harper, *et al.*), pp. 167-182. American Society of Agronomy, Madison, WI, USA

Schoell M. 1980. The hydrogen and carbon isotopic composition of methane from natural gases of various origins. *Geochimica et Cosmochimica Acta,* **44**, 649-661.

Schoell M. 1988. Multiple origins of methane in the earth. *Chemical Geology,* **71**, 1-10.

Schoell M., Tietze K. & Schoberth S.M. 1988. Origin of methane in Lake Kivu (east-central Africa). *Chemical Geology,* **71**, 257-265.

Schuepp P.H., Leclerc M.Y., MacPherson J.I. & Desjardins R.L. 1990. Footprint prediction of scalar fluxes from analytical solutions of the diffusion equation. *Boundary-Layer Meteorology,* **50**, 355-373.

Schütz H. & Seiler W. 1989. Methane flux measurements: methods and results. In: *Exchange of Trace Gases between Terrestrial Ecosystems and the Atmosphere* (ed. M.O. Andreae & D.S. Schimel), pp. 209-228. J.Wiley & Sons, Chichester.

Schütz H., Holzapfel-Pschorn A. & Renneberg H. 1991. Role of plants in regulating the methane flux to the atmosphere. In: *Trace gas emissions by plants* (ed. T.D. Sharkey, E.A. Holland & H.A. Mooney), pp. 29-63. Academic Press Inc., New York.

Schütz H., Seiler W. & Conrad R. 1990. Processes involved in the formation and emission of methane in rice paddies. *Biogeochemistry,* **7**, 33-53.

Sebacher D.I., Harriss R.C. & Bartlett K.B. 1985. Methane emissions to the atmosphere through aquatic plants. *Journal of Environmental Quality,* **14**, 40-46.

Seiler W.R., Conrad R. & Scharffe D. 1984. Field studies of methane emission from termite nests into the atmosphere and measurements of methane uptake by tropical soils. *Journal of Atmospheric Chemistry,* **1**, 171-186.

Shannon R.D., White J.R., Lawson J.E. & Gilmour B.S. 1996. Methane efflux from emergent vegetation in peatlands. *Journal of Ecology,* **84**, 239-246.

Sheppard J.C., Westberg H., Hopper J.F., Ganesan K. & Zimmerman P. 1982. Inventory of global methane sources and their production rates. *Journal of Geophysical Research,* **87**(C2), 1305-1312.

Simmonds P.G., Derwent R.G., McCulloch A., O'Doherty S. & Gaudry A. 1996. Long term trends in concentrations of halocarbons and radiatively active trace gases in Atlantic and European air masses monitored at Mace Head, Ireland from 1987-1994. *Atmospheric Environment,* **30**(23), 4041-4063.

Slania J., Warneck P., Bazhin N.M., Akmoto H. & Kieskamp W.M. 1994. Assessment of uncertainties in the projected concentrations of methane in the atmosphere. *Pure and Applied Chemistry,* **66**, 137-200.

Smith M.R. & Mah R.A. 1980. Acetate as sole carbon and energy source for growth of Methanosarsina strain 227. *Applied Environmental Microbiology,* **39**, 993-999.

Steele L.P., Dlugokencky E.J., Lang P.M., Tans P.P., Martin R.C. & Masarie K.A. 1992. Slowing down of the global accumulation of atmospheric methane during the 1980s. *Nature,* **358**, 313-316.

Steele L.P., Fraser P.J., Rasmussen R.A., Khalil M.A.K., Conway T.J., Crawford A.J., Gammon R.H., Masarie K.A. & Thoning K.W. 1987. The global distribution of methane in the atmosphere. *Journal of Atmospheric Chemistry,* **5**, 125-171.

Stephen K.D., Arah J.R.M., Daulat W. & Clymo R.S. 1998. Root-mediated gas transport in peat determined by argon diffusion. *Soil Biology Biochemistry,* **30**(4), 501-508.

Steudler P.A., Bowden R.D., Melillo J.M. & Aber J.D. 1989. Influence of nitrogen fertilization on methane uptake in temperate forest soils. *Nature,* **341**, 314-315.

Stevens C.M. & Engelkemeir A. 1988. Stable carbon isotopic composition of methane from some natural and anthropogenic sources. *Journal of Geophysical Research,* **93**(D1), 725-733.

Stevens C.M. & Rust F.E. 1982. The carbon isotopic composition of atmospheric methane. *Journal of Geophysical Research,* **87**(C7), 4879-4882.

Stevens C.M. & Wagner A.F. 1989. The role of isotope fractionation effects in atmospheric chemistry. *Zeitschrift fur Naturforschung,* **44a**, 376-384.

Striegl R.G., McConnaughey T.A., Thostenson D.C., Weeks E.P. & Woodward J.C. 1992. Consumption of atmospheric methane by desert soils. *Nature,* **357**, 145-147.

Sugawara S., Nakazawa T., Inoue G., Machida T., Mukai H., Vinnichenko N.K. & Khattatov V.U. 1996. Aircraft measurements of the stable carbon isotopic ratio of atmospheric methane over Siberia. *Global Biogeochemical Cycles,* **10**(2), 223-231.

Sugimoto A. & Wada E. 1993. Carbon isotopic composition of bacterial methane in a soil incubation experiment: contributions of acetate and CO_2/H_2. *Geochimica et Cosmochimica Acta,* **57**, 4015-4027.

Sugimoto A. & Wada E. 1995. Hydrogen isotopic composition of bacterial methane: CO_2/H_2 reduction and acetate fermentation. *Geochimica et Cosmochimica Acta,* **59**(7), 1329-1337.

Thom M., Bösinger R., Schmidt M. & Levin I. 1993. The regional budget of atmospheric methane of a highly populated area. *Chemosphere,* **26**, 143-160.

Thomas K.L., Benstead J., Davies K.L. & Lloyd D. 1996. Role of wetland plants in the diurnal control of CH_4 and CO_2 fluxes in peat. *Soil Biology Biochemistry,* **28**(1), 17-23.

Thomas K.L., Price D. & Lloyd D. 1995. A comparison of different methods for the measurement of dissolved gas gradients in waterlogged peat cores. *Journal of Microbial Methods,* **24**, 191-198.

Topp E. & Hanson R.S. 1991. Metabolism of radiatively important trace gases by methane-oxidising bacteria. In: *Microbial production and consumption of greenhouse gases: methane, nitrogen oxides, and halomethanes* (ed. J.E. Rogers & W.B. Whitman), pp. 71-90. American Society for Microbiology, Washington D.C., USA.

Torn M.S. & Chapin F.S., III. 1993. Environmental and biotic controls over methane flux from arctic tundra. *Chemosphere,* **26**, 357-368.

Trenberth K.E. 1997. The use and abuse of climate models. *Nature,* **386**, 131-133.

Tyler S.C. 1989. $^{12}C/^{13}C$ ratios in atmospheric methane and some of its sources. In: *Stable Isotopes in Ecological Studies* (ed. P.W. Rundell, J.R. Ehleringer & K.A. Nagy), pp. 395-409. Ecological Studies Vol. 68.

Tyler S.C., Crill P.M. & Brailsford G.W. 1994. $^{13}C/^{12}C$ fractionation of methane during oxidation in a temperate forested soil. *Geochimica et Cosmochimica Acta,* **58**, 1625-1633.

Urey H.C. 1948. Oxygen isotopes in nature and in the laboratory. *Science,* **108**, 489-496.

Vaghjiani G.L. & Ravishankara A.R. 1991. New measurement of the rate coefficient for the reaction of OH with methane. *Nature,* **350**, 406-409.

Valentine D.W., Holland E.A. & Schimel D.S. 1994. Ecosystem and physiological controls over methane production in northern wetlands. *Journal of Geophysical Research,* **99**(D1), 1563-1571.

Verdouw H., Van Echteld C.J.A. & Dekkers E.M.J. 1977. Ammonium determination based on indophenol formation and sodium salicylate. *Water Research,* **12**, 399-402.

Vourlitis G.L., Oechel W.C., Hastings S.J. & Jenkins M.A. 1993. The effect of soil moisture and thaw depth on methane flux from wet coastal tundra ecosystems on the north slope of Alaska. *Chemosphere,* **26**, 329-337.

Waddington J.M. & Roulet N.T. 1996. Atmospheric-wetland carbon exchanges: scale dependency of CO_2 and CH_4 exchange on the developmental topography of a peatland. *Global Biogeochemical Cycles,* **10**(2), 233-245.

Waddington J.M., Roulet N.T. & Swanson R.V. 1996. Water table control of CH_4 emission enhancement by vascular plants in boreal peatlands. *Journal of Geophysical Research,* **101**(D17), 22775-22785.

Wahlen M. 1993. The global methane cycle. *Annual Review of Earth and Planetary Sciences,* **21**, 407-426.

Wahlen M. 1994. Carbon dioxide, carbon monoxide and methane in the atmosphere: abundance and isotopic composition. In: *Methods in Ecology. Stable Isotopes in Ecology & Environmental Science* (ed. K. Lajtha & R.H. Michner). Blackwell Scientific Publications, Oxford.

Wahlen M. *et al.* . 1990. δD in CH_4: additional constraints for a global CH_4 budget. *EOS,* **71**(43), 1249.

Wahlen M., Tanaka N., Henry R., Deck B., Zeglen J., Vogel J.S., Southon J., Shemesh A., Fairbanks R. & Broecker W. 1989. Carbon-14 in methane sources and the atmospheric methane: the contribution from fossil carbon. *Science,* **245**, 286-290.

Wahlen M., Tanaka N., Henry R., Yoshinari T., Fairbanks R.G., Shemesh A. & Broecker W.S. 1987. ^{13}CD and ^{14}C in methane (poster abstract). *EOS,* **68**(44), 1220.

Wassmann R., Thein U.G., Whiticar M.J., Rennenberg H., Seiler W. & Junk W.J. 1992. Methane emissions from the Amazon floodplain: characterisation of production and transport. *Global Biogeochemical Cycles,* **6**, 3-13.

Watson A. & Nedwell D.B. 1998. Methane production and emission from peat: the influence of anions (sulphate and nitrate) from acid rain. *Atmospheric Environment,* **32**(19), 3239-3245.

Watson A., Stephen K.D., Nedwell D.B. & Arah J.R.M. 1997. Oxidation of methane in peat: kinetics of CH_4 and O_2 removal and the role of plant roots. *Soil Biology Biochemistry,* **29**(8), 1257-1267.

Wayne R.P. 1992. Atmospheric chemistry: the evolution of our atmosphere. *Journal of Photochemistry and Photobiology A:Chemistry,* **62**, 379-396.

Whalen S.C. & Reeburgh W.S. 1988. A methane flux time series for tundra environments. *Global Biogeochemical Cycles,* **2**, 388-409.

Whiticar M.J., Faber E. & Schoell M. 1986. Biogenic methane formation in marine and freshwater environments: CO_2 reduction versus acetate fermentation - isotope evidence. *Geochimica et Cosmochimica Acta,* **50**, 693-709.

Whiting G.J. & Chanton J.P. 1993. Primary production control of methane emission from wetlands. *Nature,* **364**, 794-795.

Whiting G.J. & Chanton J.P. 1996. Control of diurnal pattern of CH_4 emission from emergent aquatic macrophytes by gas transport mechanisms. *Aquatic Botany,* **54**, 237-253.

Whittow J.B. 1984. *The Penguin Dictionary of Physical Geography.* Penguin Books, London.

Willison T.W., Webster C.P., Goulding K.W.T. & Powlson D.S. 1995. Methane oxidation in temperate soils: effects of land use and the chemical form of nitrogen fertiliser. *Chemosphere,* **30**(3), 539-546.

Wofsy S.C. 1976. Interactions of CH_4 and CO in the Earth's atmosphere. *Annual Reviews of Earth and Planetary Science,* **4**, 441-469.

World Meteorological Organisation. 1988. Montreal Protocol on substances that deplete the ozone layer report, WMO Bulletin 37 pp. 94-97.

Yagi K., Tsuruta H., Kanda K. & Minami K. 1996. Effect of water management on methane emission from a Japanese rice paddy field: automated methane monitoring. *Global Biogeochemical Cycles,* **10**(2), 255-267.

Yavitt J.B. & Knapp A.K. 1995. Methane emission to the atmosphere through emergent cattail (*Typha latfolia* L.) plants. *Tellus,* **47B**, 521-534.

Yavitt J.B., Lang G.E. & Sexstone A.J. 1990. Methane fluxes in wetland and forest soils, beaver ponds and low-order streams of a temperate forest ecosystem. *Journal of Geophysical Research,* **95**(D13), 22463-22474.

Zahniser M.S., Nelson D.D., McManus J.B. & Kebabian P.L. 1995. Measurement of trace gas fluxes using tunable diode laser spectroscopy. *Proceedings of the Royal Society A,* **351**, 371-382.

Zander R., P. Demoulin, Ehhalt D.H. & Schmidt U. 1989. Secular increases of the vertical abundance of methane derived from IR spectra recorded at the Jungfraujoch Station. *Journal of Geophysical Research,* **94**(D8), 11029-11039.

Zeikus J.G. 1977. The biology of methanogenic bacteria. *Bacteriology Review,* **41**, 514-541.

Zimmerman P.R., Greenberg J.P., Wandiga S.O. & Crutzen P.J. 1982. Termites: a potentially large source of atmospheric methane, carbon dioxide and molecular hydrogen. *Science,* **218**, 563-565.

Zyakun A.M., Bondar V.A. & Namsarayev B.B. 1979. Carbon-isotope fractionation in microbial oxidation of methane. *Geochemistry International,* **16**, 164-169.

Appendix A

Further Definitions of Wetland Types used in the Canadian Wetland Classification System

Fen: "a peatland with the water table usually at or just above the surface. The waters are mainly nutrient rich and minerotrophic from mineral soils. The dominant materials are moderately to well decomposed sedge and/or brown moss peat of variable thickness. The soils are mainly Mesisols, Humisols and Organic Cryosols. The vegetation consists predominantly of sedges, grasses, reeds, and brown mosses with some shrubs, and at times a sparse tree layer."

Marsh: "a mineral wetland or peatland that is periodically inundated by standing or slowly moving water. Surface water levels fluctuate seasonally, with declining levels exposing drawdown zones of matted vegetation of mudflats. The waters are rich in nutrients, varying from fresh to highly saline. The substratum usually consists of mineral material, although occasionally well decomposed peat. The soils are predominantly Gleysols with some Humisol and Mesisols. Marshes characteristically show zonal or mosaic surface patterns composed of pools or channels interspersed with clumps, or emergent sedges, grasses, rushes, and reeds, bordering grassy meadows and peripheral bands of shrubs or trees. Submerged and floating aquatic plants flourish where open water areas occur."

Swamp: "a mineral wetland or peatland with standing water or water gently flowing through pools or channels. The water table is at or near the surface. There is pronounced internal water movement from the margin or other mineral sources: hence the waters are rich in

nutrients. If peat is present, it is mainly well-decomposed wood, underlain at times by sedges peat. The associated soils are Mesisols, Humisols and Gleysols. The vegetation is characterised by a dense cover of deciduous or coniferous tress or shrubs, herbs and some mosses."

Shallow Water: "characteristic in intermittently or permanently flooded or seasonally stable water regimes, featuring open expanses of standing or flowing water which are variously called ponds, pools, shallow lakes, oxbows, reaches, channels, or impoundments. Shallow water is distinguished from deep water by mid-summer water of depths less than 2 m, and from other wetlands by summer open water zones occupying more than 75% of the wetland surface area."

Canadian Soil Classification	**Soil Classification in England and Wales (Avery, 1980)**
Fibrosols	Peat soils: eu-fibrous and oligofibrous soils 10.11, 10.12, 10.21 and 10.22
Mesisols	No intermediate "mesic" category
Humisols	Peat soils: amorphous soils 10.13, 10.14, 10.23 and 10.24
Gleysols	Ground-water soils: humic-alluvial gley soils and humic gley soils 8.5 and 8.7 or Peat soils: oligofibrous soils 10.11
Organic Cyrosols	No equivalent soil type

APPENDIX B

Manufacturers and Suppliers

Air Products PLC (Speciality Gases Group)
Weston Road, Crewe, Cheshire, CW1 1BT.

Aldrich Chemical Company
The Old Brickyard, New Road, Gillingham, Dorset, SP8 4XT.

Alltech Associates Applied Science Ltd.
Unit 6-7, Kellet Road Industrial Estate, Kellet Road,
Carnforth, Lancaster, LA5 9XP.

ATP Instrumentation Ltd.
Tournament Way, Ivanhoe Industrial Estate,
Ashby-de-la-Zouch, Leicestershire, LE65 2UU.

CK Gas Products Ltd.
Unit 5, Marino Way, Hogwood Lane Industrial Estate,
Finchhampstead, Berkshire, RG11 4RF.

Chell Instruments Ltd.
Tudor House, Grammar School Road, North Walsham, Norfolk, NR28 9JH.

Chrompak (UK) Ltd.
Unit 4, Indescon Court, Millharbour, London, E14 9TN.

Edwards High Vacuum International

Manor Royal, Crawley, West Sussex, RH10 2LW.

Mettler Toledo Ltd.

64, Boston Road, Beaumont Leys, Leicester, LE4 1AW.

North London Valve and Fitting Company Ltd.

34, Capitol Way, Capitol Industrial Park, London, NW9 0EQ.

Phase Separations Ltd.

The Boulevard, Blackmoor Lane, Watford, Hertfordshire, WD1 8YW.

SAES Getters (GB) Ltd.

5, Southern Court, South Street, Reading, Berkshire, RG1 4QS.

SMC Pneumatics (UK) Ltd.

Vincent Avenue, Crownhill, Milton Keynes, MK8 0AN.

Scientific Glass Engineering (UK) Ltd. (SGE)

1, Potters Lane, Kiln Farm, Milton Keynes, MK11 3LA.

Vacuum Generators Isotopes Ltd.

Ion Path, Road Three, Winsford, Cheshire, CW7 3BX.

J. Young (Scientific Glassware) Ltd.

11, Colville Road, Acton, London, W3 8BS.

APPENDIX C

Daily Rainfall Data for Ysbyty Ifan, October 1995 to July 1997.

Recorded using a tipping bucket rain gauge, at Ysbyty Ifan (Grid Reference SH8108 4557) by the Environment Agency Welsh Region, in mm.

	Oct 95	Nov 95	Dec 95	Jan 96	Feb 96	Mar 96	Apr 96	May 96	Jun 96	Jul 96	Aug 96	Sept 96
1	9.2	-	1.6	0.2	0.2	-	-	11.0	14.6	2.6	1.4	-
2	9.0	0.2	1.8	0.2	-	-	-	0.2	0.6	12.6	-	0.2
3	17.4	-	4.6	2.2	-	0.4	-	-	4.0	7.2	-	-
4	11.8	-	0.2	2.8	-	0.2	-	0.2	0.2	4.6	-	-
5	9.0	-	0.2	2.2	-	-	-	-	-	1.4	1.6	0.2
6	14.0	1.2	0.2	10.4	2.8	0.2	-	-	0.2	-	20.8	-
7	12.6	0.4	-	8.2	1.4	-	0.8	-	2.0	0.8	0.4	-
8	-	6.0	1.4	16.0	7.4	0.6	2.8	-	-	0.8	3.4	-
9	0.4	0.4	-	6.0	18.2	0.2	1.2	-	6.4	-	4.4	-
10	2.4	3.6	-	2.8	31.4	0.2	1.4	0.6	8.0	-	6.6	-
11	0.8	9.0	-	3.2	23.6	24.4	6.2	-	9.0	3.8	-	1.2
12	-	5.4	-	22.0	10.6	0.2	12.6	-	-	0.2	-	-
13	0.4	0.2	0.2	2.6	-	-	0.6	-	-	1.0	-	-
14	4.8	18.0	0.2	1.4	-	-	1.8	-	-	-	-	-
15	3.4	19.6	-	-	2.2	7.0	1.4	-	-	-	-	-
16	4.6	1.4	-	0.2	1.4	1.0	8.2	-	-	-	-	-
17	8.2	4.6	5.8	-	48.2	0.2	11.0	0.6	-	-	-	-
18	-	0.2	-	0.6	11.4	-	15.2	6.2	-	-	-	-
19	0.2	0.4	1.8	-	0.2	-	2.4	12.8	-	-	3.4	1.2
20	0.2	7.2	1.6	-	-	1.0	2.6	4.4	-	-	0.8	-
21	-	5.2	24.2	-	4.0	0.4	3.8	7.8		-	0.4	-
22	0.8	1.6	10.6	0.2	1.4	1.6	11.4	12.0	-	-	11.4	-
23	0.2	16.0	2.8	-	14.6	6.4	2.4	23.4	-	0.6	12.6	-
24	24.8	13.2	-	-	8.0	0.4	0.4	-	-	-	19.4	7.2
25	2.0	0.8	2.2	-	8.4	7.0	0.4	2.8	2.8	-	13.8	0.6
26	9.6	0.2	3.8	-	0.8	1.6	1.0	18.8	-	1.2	8.6	6.0
27	0.2	0.8	1.2	-	0.2	-	-	-	11.2	0.6	8.6	0.2
28	-	1.6	-	-	-	0.2	-	36.6	7.0	7.6	2.2	88.8
29	0.2	1.2	-	-	-	0.2	5.4	7.0	1.2	1.0	0.4	21.2
30	-	1.0	-	-		-	2.8	1.4	7.4	11.8	-	0.6
31	0.2		2.2	-		-		1.4		3.2	-	
Total	146.6	119.4	66.6	81.2	196.4	53.4	95.9	147.2	74.6	61.0	120.2	127.4

	Oct 96	Nov 96	Dec 96	Jan 97	Feb 97	Mar 97	Apr 97	May 97	Jun 97	Jul 97
1	1.4	43.6	6.6	-	4.0	25.8	-	-	-	1.6
2	3.8	32.6	14.8	1.0	0.2	-	1.2	-	-	3.2
3	22.0	11.2	27.0	0.2	60.0	3.6	0.2	10.0	-	-
4	10.4	16.2	6.4	-	0.8	-	1.6	12.4	-	-
5	2.0	31.8	-	-	0.8	20.6	2.2	21.2	1.0	-
6	-	5.2	-	-	23.4	0.2	-	4.0	3.8	-
7	2.6	5.8	0.4	-	0.2	4.6	-	15.6	12.4	-
8	0.4	1.8	-	-	11.2	-	-	7.0	2.0	-
9	0.6	2.4	0.2	-	30.8	0.8	-	3.2	1.8	-
10	-	-	0.2	1.2	4.8	-	-	20.0	13.6	-
11	-	6.0	-	6.4	49.2	0.4	-	2.6	31.0	-
12	-	0.4	-	1.6	29.2	2.2	-	5.0	6.6	0.2
13	0.2	1.6	-	-	-	19.4	-	1.2	0.6	0.2
14	16.6	0.6	5.8	-	0.2	1.8	-	-	0.4	7.8
15	31.4	0.6	2.6	0.2	3.0	0.6	-	-	0.2	1.8
16	13.4	14.0	-	-	21.8	0.4	-	12.6	-	5.0
17	9.2	2.4	2.8	1.8	44.2	8.8	-	5.4	-	-
18	14.6	2.0	3.2	-	2.8	7.2	-	-	9.4	-
19	7.2	6.0	3.6	-	30.0	-	-	3.8	3.8	-
20	28.6	7.2	-	-	9.2	0.6	-	2.0	12.0	-
21	0.6	29.8	-	0.4	0.6	-	0.4	1.0	22.4	-
22	-	2.8	-	1.0	17.8	16.4	4.6	0.2	1.8	-
23	1.8	2.6	-	0.4	16.4	2.0	-	-	-	10.8
24	6.6	22.4	-	5.2	16.2	1.0	9.6	-	7.4	4.8
25	14.6	5.2	-	-	18.6	10.4	4.0	-	17.6	1.2
26	17.2	-	4.2	-	8.4	5.4	2.6	-	10.0	18.0
27	15.6	-	-	-	24.0	16.0	11.2	-	3.2	0.2
28	17.8	26.4	0.2	-	-	-	23.4	-	1.0	-
29	0.8	5.6	1.2	0.2		-	-	-	0.2	12.6
30	12.0	2.2	-	-		-	-	-	8.0	3.6
31	40.8		-	0.2		-		-		9.2
Total	292.2	288.4	79.2	19.8	427.8	148.2	61.0	127.2	170.2	80.2

Computed monthly averages for 1964 to 1996 inclusive, in mm:

Jan	Feb	Mar	Apr	May	Jun	Jul	Aug	Sept	Oct	Nov	Dec	Total
239	151	198	128	116	125	128	152	188	216	257	271	2169

Annual Rainfall Totals, in mm:

1995	1996	1997
1639.4	1617.0	1795.8

APPENDIX D

Water Table Depth in Nitrogen Application Plots

All depths are in mm.

	Block	Nitrate	Ammonium	Nitrate and ammonium
July 96				
	1	89	70	62
	2	86	117	107
	3	185	72	120
	4	101	105	116
November 96				
	1	0	0	0
	2	0	0	0
	3	0	0	0
	4	0	0	0
April 97				
	1	120	78	80
	2	135	165	135
	3	120	200	135
	4	90	155	170

APPENDIX E

Sample Analysis Data

Core notation: 2.1 refers to core 1 in block 2 (Figure 3.2) and so on. Air refers to ambient air. Sampling time is the length of time of enclosure of the core under a headspace chamber. Date of analysis refers to isotopic analysis on MIRANDA (Chapter 2).

Sample	Date collected	Core	Sampling time	$\delta^{17}M_{NGS\#3}$ /‰	$[CH_4]$ /ppm	Date analysed
1	**27-Oct-95**	air	0	31.8	1.61	23/11/95
2		3.1	60	4.1	4.72	23/11/95
3		3.2	60	-3.0	7.14	23/11/95
4		3.3	60	1.1	3.62	06/12/95
5		2.2	0	27.49	1.77	23/11/95
6		2.2	60	-10.0	6.02	06/12/95
7		2.3	60	5.1	3.09	06/12/95
8	**21-Nov-95**	air	0	31.1	1.81	19/12/95
9		air	60	30.8	1.79	20/12/95
10		3.1	0	28.1	1.98	08/12/95
11		3.2	0	31.7	1.96	08/12/95
12		3.3	0	29.6	1.87	08/12/95
13		3.1	60	5.4	3.6	06/12/95
14		3.2	60	-1.4	5.6	06/12/95
15		3.3	60	12.0	2.96	06/12/95
16		2.1	60	26.8	1.9	08/12/95
17		2.2	0	33.2	1.82	19/12/95
18		2.2	15	20.1	2.35	10/01/96
19		2.2	30	13.7	2.65	10/01/96
20		2.2	45	8.4	2.96	10/01/96
21		2.2	60	7.4	3.05	08/12/95
22		2.3	60	1.7	3.6	08/12/95
23	**11-Dec-95**	air	0	31.8	1.76	21/12/95
24		air	0	32.4	1.74	10/01/96
25		air	60	26.0	1.75	20/12/95
26		3.1	0	31.1	1.76	21/12/95
27		3.2	0	30.1	1.78	21/12/95
28		3.3	0	30.6	1.78	21/12/95
29		3.1	60	13.0	2.63	19/12/95
30		3.2	60	4.7	3.66	10/01/96
31		3.3	60	8.8	2.94	20/12/95
32		2.1	0	31.6	1.74	21/12/95
33		2.2	0	30.9	1.72	20/12/95
34		2.3	0	31.2	1.78	20/12/95

Sample	Date collected	Core	Sampling time	$\delta^{17}M$	$[CH_4]$	Date Analysed
35		2.1	60	20.7	2.11	20/12/95
36		2.2	15	22.6	2.06	19/12/95
37		2.2	30	17.3	2.39	20/12/95
38		2.2	45	12.6	2.66	10/01/96
39		2.2	60	7.0	2.90	20/12/95
40		2.3	60	22.6	1.99	20/12/95
41	**12-Jan-96**	air	0	32.8	1.75	25/01/96
42		air	0	30.8	1.69	23/01/96
43		air	60	32.9	1.75	24/01/96
44		air	60	32.2	1.74	24/01/96
45		3.1	0	32.7	1.75	23/01/96
46		3.2	0	30.2	1.71	24/01/96
47		3.3	0	32.1	1.71	23/01/96
48		3.1	60	16.6	2.33	25/01/96
49		3.2	60	9.8	3.07	25/01/96
50		3.3	60	31.2	1.79	24/01/96
51		2.1	0	32.8	1.75	24/01/96
52		2.2	0	31.6	1.70	23/01/96
53		2.3	0	32.5	1.76	24/01/96
54		2.1	60	30.4	1.82	24/01/96
55		2.2	15	29.0	1.87	25/01/96
56		2.2	30	29.5	1.80	25/01/96
57		2.2	45	29.7	1.77	25/01/96
58		2.2	60	28.9	1.81	25/01/96
59		2.3	60	11.8	2.71	25/01/96
60	**12-Feb-96**	air	0	34.7	1.84	27/02/96
61		air	0	34.3	1.85	27/02/96
62		3.2	0	34.3	1.87	27/02/96
63		3.3	0	32.9	1.87	27/02/96
64		3.2	60	33.1	1.89	27/02/96
65		3.2	60	33.6	1.90	27/02/96
66	**11-Mar-96**	air	120	33.1	1.97	23/04/96
67		air	120	33.8	1.96	24/04/96
68		air	120	32.4	1.96	25/04/96
69		3.1	0	32.2	2.00	23/04/96
70		3.2	0	32.4	1.98	23/04/96
71		3.3	0	32.1	2.00	23/04/96
72		3.1	120	16.5	2.90	04/05/96
73		3.2	120	8.5	4.04	24//4/96
74		3.3	120	14.5	3.09	24/04/96
75		2.1	0	32.5	1.96	23/04/96
76		2.2	0	33.6	1.95	24/04/96
77		2.3	0	33.6	1.95	24/04/96
78		2.2	55	32.2	2.06	24/04/96
79		2.2	80	27.9	2.22	24/04/96
80		2.2	100	23.1	2.45	24/04/96
81		2.2	120	20.5	2.62	23/04/96
82		2.3	60	17.0	2.78	23/04/96

Sample	Date collected	Core	Sampling time	$\delta^{17}M$	$[CH_4]$	Date Analysed
83	**04-Apr-96**	air	0	35.8	1.78	04/05/96
84		air	0	34.4	1.76	07/05/96
85		air	160	35.7	1.83	07/05/96
86		air	160	36.0	1.8	30/04/96
87		3.1	0	34.9	1.82	30/04/96
88		3.2	0	34.5	1.79	04/05/96
89		3.3	0	34.5	1.83	30/04/96
90		3.1	150	4.8	4.04	30/04/96
91		3.2	60	14.5	3.01	26/04/96
92		3.3	150	22.6	2.32	04/05/96
93		2.1	0	32.9	1.82	04/05/96
94		2.2	0	30.2	2.11	30/04/96
95		2.3	0	34.7	1.81	04/05/96
96		2.1	90	22.9	2.28	26/04/96
97		2.2	45	23.9	2.23	04/05/96
98		2.2	75	19.0	2.5	30/04/96
99		2.2	100	15.8	2.71	26/04/96
100		2.2	150	14.3	2.85	04/05/96
101		2.3	60	7.1	3.54	30/04/96
102	**13-May-96**	air	0	31.7	1.80	04/07/96
103		air	0	30.9	1.80	05/07/96
104		air	150	31.3	1.80	04/07/96
105		air	150	31.5	1.80	04/07/96
106		3.1	0	31.6	1.82	05/07/96
107		3.2	0	30.7	1.82	04/07/96
108		3.3	0	31.6	1.85	04/07/96
109		3.1	145	-0.3	4.50	16/07/96
110		3.2	60	7.7	3.55	10/07/96
111		3.3	145	-4.7	5.56	10/07/96
112		2.1	0	30.7	1.84	04/07/96
113		2.2	0	31.7	1.82	04/07/96
114		2.3	0	31.3	1.82	04/07/96
115		2.1	75	26.4	2.00	05/07/96
116		2.2	40	19.3	2.37	05/07/96
117		2.2	60	14.7	2.64	05/07/96
118		2.2	100	2.6	3.02	10/07/96
119		2.2	140	9.1	3.16	16/07/96
120		2.3	140	-3.8	4.08	10/07/96
121	**28-Jun-96**	air	0	33.1	1.74	18/07/96
122		3.2	0	32.1	1.78	18/07/96
123		3.2	0	32.5	1.78	18/07/96
124		3.1	120	-12.6	5.91	16/07/96
125		3.2	120	-10.9	7.6	17/07/96
126		3.3	120	-17.2	9.59	17/796
127		2.2	0	32.8	1.74	18/07/96
128		2.1	120	-18.3	10.78	17/07/96
129		2.2	90	-10.6	5.34	18/07/96
130		2.2	100	-10.8	5.79	18/07/96

Sample	Date collected	Core	Sampling time	$\delta^{17}M$	$[CH_4]$	Date Analysed
131		2.2	110	-9.4	6.16	17/07/96
132		2.2	120	-12.3	6.72	17/07/96
133		2.2	120	-13.9	6.64	18/07/96
134		2.3	120	-7.3	6.61	17/07/96
135	**29-Jul-96**	air	0	32.7	1.76	15/08/96
136		3.1	120	-12.2	6.79	09/08/96
137		3.2	120	-7.2	6.31	09/08/96
138		3.2	66	2.4	3.40	10/08/96
139		2.2	0	31.2	1.76	10/08/96
140		2.3	0	28.4	1.88	10/08/96
141		2.1	60	-11.3	7.11	09/08/96
142		2.2	30	10.5	2.71	08/08/96
143		2.2	45	9.4	2.79	10/08/96
144		2.2	60	0.4	3.75	09/08/96
145		2.2	90	-5.6	4.92	10/08/96
146		2.2	120	-9.2	5.61	09/08/96
147		2.3	120	7.5	2.85	08/08/96
148	**27-Aug-96**	air	0	30.6	1.84	01/10/96
149		3.2	0	30.9	1.84	01/10/96
150		3.1	150	-26.8	13.96	12/09/96
151		3.2	70	-6.8	4.73	03/10/96
152		3.3	150	-40.0	21.60	12/09/96
153		2.2	0	31.2	1.87	01/10/96
154		2.1	135	-0.1	3.97	03/10/96
155		2.2	50	-14.0	7.70	03/10/96
156		2.2	75	-14.4	8.13	03/10/96
157		2.2	105	-17.0	9.18	12/09/96
158		2.2	135	-20.3	10.19	12/09/96
159		2.3	75	-28.7	15.25	12/09/96
160	**27-Sep-96**	air	0	32.9	1.80	10/10/96
161		3.3	0	30.2	1.90	09/10/96
162		3.1	120	-7.1	6.30	05/10/96
163		3.2	120	19.9	2.28	09/10/96
164		3.3	60	-2.6	4.40	09/10/96
165		2.2	0	30.4	1.86	09/10/96
166		2.1	120	19.1	2.34	09/10/96
167		2.2	45	-3.0	4.54	09/10/96
168		2.2	100	-9.9	6.07	05/10/96
169		2.2	112	-10.5	6.28	05/10/96
170		2.2	120	-11.6	6.52	05/10/96
171		2.3	60	6.0	3.18	09/10/96
172	**22-Oct-96**	air	0	32.9	1.76	31/10/96
173		3.2	0	31.7	1.79	29/10/96
174		3.1	75	-7.5	5.5	29/10/96
175		3.2	145	-7.5	5.99	31/10/96
176		3.3	145	7.0	3.03	31/10/96
177		2.3	0	32.1	1.79	29/10/96
178		2.1	67	23.6	2.11	31/10/96
179		2.2	25	5.1	3.49	29/10/96

Sample	Date collected	Core	Sampling time	$\delta^{17}M$	$[CH_4]$	Date Analysed
180		2.2	60	-7.9	5.56	29/10/96
181		2.2	80	-9.8	6.4	29/10/96
182		2.2	105	-14.3	7.56	29/10/96
183		2.2	135	-14.9	8.87	29/10/96
184		2.3	135	14.3	2.53	31/10/96
185	**16-Nov-96**	air	0	31.8	1.99	22/11/96
186		3.2	0	30.2	1.97	22/11/96
187		3.1	60	15.4	3.01	21/11/96
188		3.2	60	4.0	4.17	21/11/96
189		3.3	60	-2.1	4.49	21/11/96
190		2.1	0	29.3	2.13	22/11/96
191		2.2	0	29.2	2.05	21/11/96
192		2.1	40	20.6	2.54	21/11/96
193		2.2	40	5.0	3.44	21/11/96
194		2.2	60	0.4	4.26	21/11/96
195		2.2	80	-1.4	5.07	20/11/96
196		2.2	90	-3.9	5.44	20/11/96
197		2.2	105	-6.1	5.77	20/11/96
198		2.3	105	-16.3	9.83	20/11/96
199	**11-Dec-96**	air	0	32.3	2.06	14/12/96
200		3.3	0	26.3	2.28	14/12/96
201		3.1	100	12.6	3.11	17/12/96
202		3.2	140	22.4	2.50	13/12/96
203		3.3	140	11.4	3.22	13/12/96
204		2.2	0	29.7	2.09	17/12/96
205		2.1	125	18.6	2.72	13/12/97
206		2.2	22	25.6	2.27	14/12/96
207		2.2	65	22.2	2.29	14/12/96
208		2.2	85	25.3	2.34	14/12/96
209		2.2	100	23.1	2.42	14/12/96
210		2.2	125	22.4	2.43	13/12/96
211		2.3	60	2.6	3.86	17/12/96
212	**23-Jan-97**	air	0	29.5	1.99	06/03/97
213		3.3	0	30.3	2.06	06/03/97
214		3.1	205	2.4	4.61	07/03/97
215		3.2	205	28.2	2.06	07/03/97
216		3.3	205	9.7	3.27	05/02/97
217		2.1	0	31.0	2.01	07/03/97
218		2.2	0	31.6	2.04	07/03/97
219		2.1	195	25.7	2.23	07/03/97
220		2.2	60	20.0	2.59	15/02/97
221		2.2	135	24.2	2.28	06/03/97
222		2.2	165	25.6	2.20	07/03/97
223		2.2	195	25.4	2.18	05/02/97

Sample	Date collected	Core	Sampling time	$\delta^{17}M$	$[CH_4]$	Date Analysed
224	**26-Feb-97**	air	0	33.0	1.82	13/03/97
225		3.2	0	31.4	1.88	14/03/97
226		3.1	135	6.1	3.80	13/03/97
227		3.2	135	13.9	3.01	13/03/97
228		3.3	135	-4.3	6.08	14/03/97
229		2.2	0	32.3	1.83	14/03/97
230		2.2	60	10.9	2.91	13/03/97
231		2.2	80	7.9	3.23	13/03/97
232		2.2	90	6.5	3.38	13/03/97
233		2.2	105	5.7	3.46	13/03/97
234		2.2	135	0.5	4.12	13/03/97
235		2.3	135	-4.5	5.37	14/03/97
236	**28-Mar-97**	air	0	32.3	1.79	10/04/97
237		3.1	140	9.0	3.20	12/04/97
238		3.2	140	2.3	3.98	12/04/97
239		3.3	60	24.3	2.14	12/04/97
240		2.2	0	32.2	1.79	10/04/97
241		2.1	130	29.8	1.90	12/497
242		2.2	30	26.2	2.06	12/04/97
243		2.2	70	23.4	2.15	12/04/97
244		2.2	90	16.8	2.51	12/04/97
245		2.3	70	14.2	2.66	12/04/97
246	**24-Apr-97**	air	0	32.6	1.83	05/05/97
247		3.1	150	25.7	2.06	26/04/97
248		3.2	120	30.5	1.9	26/04/97
249		3.3	120	29.5	1.98	03/05/97
250		2.2	0	32.4	1.84	03/05/97
251		2.1	160	22.2	2.26	26/05/97
252		2.2	10	30.8	1.9	03/05/97
253		2.2	35	28.7	1.97	05/05/97
254		2.2	150	29.6	1.97	05/05/97
255		2.2	165	29.0	1.97	03/05/97
256		2.3	95	25.1	2.12	03/05/97
257	**21-May-97**	air	0	31.4	1.91	29/05/97
258		air	0	31.1	1.89	28/05/97
259		3.1	121	-5.9	5.97	29/05/97
260		3.2	121	12.3	3.02	27/05/97
261		3.3	63	6.7	3.30	27/05/97
262		2.2	0	31.3	1.96	27/05/97
263		2.1	120	15.9	2.63	27/05/97
264		2.2	35	11.6	3.16	27/05/97
265		2.2	60	4.1	3.63	27/05/97
266		2.2	90	1.4	3.97	29/05/97
267		2.2	120	4.7	3.59	27/05/97
268		2.3	64	-2.1	4.26	28/05/97

Sample	Date collected	Core	Sampling time	$\delta^{17}M$	$[CH_4]$	Date Analysed
269	**29-Jun-97**	air	0	0.5	32.03	18/07/97
270		3.2	0	0.5	29.62	08/07/97
271		3.3	0	0.5	31.44	19/07/97
272		3.1	115	0.1	-9.74	19/07/97
273		3.2	115	0.5	21.92	18/07/97
274		3.3	70	0.3	6.59	18/07/97
275		2.2	0	0.5	30.75	08/07/97
276		2.1	110	0.2	1.65	19/9797
277		2.2	60	0.1	-9.56	19/07/97
278		2.2	85	0.1	-12.16	19/07/97
279		2.2	100	0.1	-14.32	19/07/97
280		2.2	110	0.1	-16.27	19/07/97
281		2.3	55	0.2	-8.22	19/07/97